Assessment of Tissue Viability in Acute Thermal Injuries Using Near Infrared Point Spectroscopy.

Dr. Karen Michelle Cross

A thesis submitted in conformity with the requirements for the degree of

Doctor of Philosophy

Institute of Medical Science

University of Toronto

Assessment of Tissue Viability in Acute Thermal Injuries Using Near Infrared Point Spectroscopy.

Dr. Karen Michelle Cross

Doctor of Philosophy

Institute of Medical Science

University of Toronto

2010

Abstract

Introduction: Currently, there are no objective techniques to assess burn depth. An early assessment of burn depth would enable accurate management decisions, which would improve patient outcomes. Near infrared (NIR) technology has shown promise as a non-invasive monitor of oxygenation and perfusion, and its potential to assess the depth of burn injuries has been investigated clinically over the past five years. The purpose of the thesis was to determine the capacity of NIR technology to differentiate acute thermal injuries.

Methods: Burn sites (n=5) and control sites (n=5) were created on the dorsum of sixteen animals with brass rods held at constant pressure and heated to 100°C and 37.5°C respectively. NIR data was collected from the burns and control sites pre-burn, immediately post-burn, and 1, 12, 24, 36, 48 and 96 hours after the burn injury. Biopsies of the burn and control sites were acquired at each time point and used to confirm the

depth of injury. NIR data was processed for the content of water, oxy-, deoxy- and methemoglobin.

Results: Oxyhemoglobin and total hemoglobin decreased as burn depth increased. The proportion of oxy- and deoxyhemoglobin to total hemoglobin showed that the ratio of oxy- to deoxyhemoglobin decreased as burn injury increased. Methemoglobin levels as a ratio of total hemoglobin also showed that as the severity of injury increased the proportion of methemoglobin also increased. Finally, superficial partial thickness injuries (3 s and 12 s) showed early peak levels of water, which rapidly declined towards baseline. The deep partial thickness injuries (20 s and 30 s) do not experience peak levels and retain water over the course of the experiment. The full thickness injuries water levels remain close or below baseline levels throughout the experiment.

Conclusion: NIR spectroscopy could distinguish burn depth using water, oxy-, met- and total hemoglobin as separate entities. The presence of methemoglobin in the burn wounds is a novel finding that has not been described previously in burn literature.

Acknowledgements

I am grateful for the mentorship of my thesis committee and collaborators at the University of Toronto:, Drs. Steven Boyce, Chris Forrest, Daniel Ghazarian, Wedad Hana, Miles Johnston, Peter Neligan, Michael Sefton and John Semple. The Division of Plastic Surgery and the Surgeon Scientist Program were instrumental in providing the support and the environment for this research to transpire.

Heartfelt thanks to the entire staff of the Ross Tilley Burn Centre at Sunnybrook Health Science Centre. In particular, sincere gratitude to Dr. Manuel Gomez for his dedication, inspiration and infinite wisdom as well as Sandy Davies for her advocacy, assistance and outstanding ability to make it all happen in the eleventh hour.

I would also like to thank the staff at the Institute of Biodiagnostics at the National Research Council of Canada. Dr. Michael Sowa and his team were integral to the research and I appreciate all of their hard work. Dr. Lorenzo Leonardi deserves special recognition for the countless hours of teaching and academic banter, and for challenging my intellectual boundaries. Thank you for believing in my ability to succeed and helping me find my passion. You embodied the role as my supervisor and are a true inspiration.

Dr. Joel Fish mentored me through one of the greatest academic achievements of my life. The science was a fraction of what I have learned from you. You are and will continue to be one of the most influential people in my career and life. I deeply appreciate having the privilege of your encouragement, guidance and wisdom.

I am forever indebted to my family and friends for the tremendous amount of support they have given me throughout my journey. My father Randy taught me to “shoot for the moon and even if you miss, you’ll land amongst the stars.” My mother Jean instilled in me perseverance, patience and perspective. Darryl, my brother and the loudest cheerleader in my stadium, has always reminded me to “live life and love life.” Daniel, my husband, you lived and breathed the Ph.D. with me. You enlightened me to the “left path” and for this I will be forever grateful.

Two roads diverged in a wood, and I—
I took the one less traveled by,
And that has made all the difference.
Robert Frost

I am indebted to all who have been a part of my journey. This thesis is dedicated to you.

Table of Contents

List of Abbreviations

AMP = adenosine monophosphate

ATP = adenosine triphosphate

CCD = charge coupled device

df = degrees of freedom

F = F-statistic

Fe^{2+} = ferrous iron

Fe^{3+} = ferric iron

H&E = hematoxylin and eosin

LDI = laser Doppler imaging

MDA = malondialdehyde

MPO = myeloperoxidase

NIR = near infrared

NIRS = near infrared spectroscopy

NO = nitric oxide

OCT = optical coherence tomography

ODC = oxygen dissociation curve

PU = perfusion units

RISA = radioiodinated serum albumin

ROS = reactive oxygen species

RNS = reactive nitrogen species

SC = source collector

SD = source detector

P_c and P_{if} = hydrostatic pressure of the capillary and interstitium

π_p and π_{if} = osmotic pressure of the capillary and interstitium.

K_f = fluid filtration coefficient

δ = capillary permeability

List of Tables

List of Figures

Chapter 1: Introduction and Background Information

1.1 The Clinical Dilemma

Burn wound depth assessments are currently clinically based and rely heavily on the experience of the physician. Assessing burn depth is difficult, especially when differentiating indeterminate or partial thickness wounds. In this situation, even experienced burn clinicians make an incorrect diagnosis 30-40% of the time or as Heimbach stated, “it’s like flipping a coin.”[1] The evaluation of burn depth is the critical component on which treatment decisions are based, as inaccuracies can lead to unnecessary surgeries or patients staying for extensive lengths of time. There have been significant improvements in burn care over time yet there have been no reported advances in burn depth determination, nor have there been reductions in diagnostic errors made by burn surgeons.

An inaccurate diagnosis of burn depth means patients do not receive the appropriate treatment. Clinical treatment regimens dictate that superficial burns require little or no treatment and full thickness injuries require an operation. Superficial partial thickness injuries are viable and will heal with vigourous antimicrobial dressings, unlike deep partial thickness wounds, which require surgical excision and grafting for improved functional and cosmetic outcomes. Partial thickness wounds are complicated to treat, as it is difficult to determine if viable structures are present and capable of healing the wound. The inaccuracies associated with diagnosis affect treatment, as it is possible that a superficial burn will receive surgery for a healing wound. In contrast, a deep partial thickness burn designated as viable may remain in hospital with dressings until it is clear

that the burn needs an operation. In Ley's study of 249 hand burns that compares compares early excision to conservative therapy, patients with full thickness injuries had improved functional outcomes compared to deep partial thickness burns. Outcome differences were related to uncertainty in determining the viability which translated to delayed surgical intervention for patients with partial thickness injuries. This lengthened patients hospital stays and delayed when they could return to work.[2] Therefore, a delay in diagnosis has a significant impact on patient outcome, length of stay in the hospital and return to work. The future of burn surgery lies in the capacity of a diagnostic tool to accurately assess wound viability early in the course of the burn injury.

The diagnostic limitations of clinical assessment of burn injury have led many researchers to search for an optimum technique to accurately judge burn depth. A wide range of diagnostic tools has been reported in the literature such as laser Doppler, various dyes, ultrasonography, thermography, nuclear magnetic resonance and optical coherence tomography.[3–15] However, to date none of these technologies have achieved widespread clinical acceptance or utilization.

Experts convened at an international conference in 1987 to discuss the existing and future practices of burn depth assessment and management. What was clear from the round table discussion was that "there is no accurate test for depth…and there is very little work going on to develop such a test." It was also felt that technologies utilized at that time were "experimental...not perfect, but better than our clinical judgment." The conclusion from this summit was that clinical judgment is inadequate and a need exists to develop an objective technology to assess burn depth.[2] Since the 1980s, there are still

very few groups working in this area and there has been no global acceptance of a diagnostic tool for depth assessment.

Burn wounds are challenging problems as they are dynamic and have the capacity to change and progress over time. The term “burn depth” is used to describe the extent of damage to skin layers (epidermis, dermis and fat) but also implies that a burn injury can be classified anatomically or in physical levels within the skin. Burn wounds undergo significant hemodynamic and physiologic changes over the course of injury, making it difficult to classify burn wounds according to anatomy or a clinical description. Therefore, the ideal technology for burn depth assessment would be a device that assesses the changing physiology and not anatomy.

Near infrared (NIR) spectroscopy is well-suited to assess tissue injury occurring after thermal injury. A simple reflectance of light can assess the oxygenation, perfusion and edema that exist within the tissue. These variables are important predictors of tissue viability. A technology that can assess burn depth should be portable, non-invasive and accurate, with fast data acquisition and the ability to perform repeat measurements. NIR technology is light based and poses no risk to the patient. This also means that the device is portable and can be used as a bedside monitor of hemodynamics. Data acquisition is fast and multiple sites can be collected at any time point. Over the past five years, near infrared spectroscopy has been utilized successfully to classify burn injuries in both a laboratory and clinical environment. This thesis is a representation of this work and will focus on the utilization of NIR Point Spectroscopy as a tool to differentiate burn wounds in a porcine burn model.

1.2 Overview of Burn Depth Pathophysiology

1.2.1 Thermal Energy

The duration and temperature of thermal exposure are important determinants of the degree of injury to the tissue. Heat is transferred though tissue via conduction, convention and radiation. Thermal damage will continue even after the heat source has been removed and complete cooling is achieved.[16]

In a classic paper by Moritz and Hedriques in 1942, it was determined in human subjects that as temperature increased the time required to cause a thermal injury decreased.[17] As temperature increased by one degree within the range of 44–51°C, the time required to cause a burn injury in humans was cut in half. At temperatures above 55°C only seconds were required to cause tissue damage. Singer et al. tested the time and temperature dependence of thermal injury in a porcine burn model using histology. As temperature increased so did the damage to the collagen, endothelium and epithelium of the hair follicle. The effect of time was more predominant above 70°C. A 10 s exposure caused endothelial necrosis within the first 30% of the dermis versus a 30 s injury where the physical levels of necrosis was measured at 85% of the dermis.[18]

Thermal injury causes irreversible damage to proteins and membranes. Thermal injury causes direct damage to the lipid bilayer and consequently cell membrane lysis.[19] At high temperatures, proteins will unfold and form insoluble and irreversible aggregates.[20] This can occur at temperatures as low at 40–44°C and it affects various proteins, enzymes and membrane protein pumps.[16] Once the bilayer is damaged the protein ion

pumps cannot keep pace with ion diffusion across the membrane. The metabolic energy of the cell is depleted, resulting in biochemical arrest and necrosis.[19]

1.2.2 Burn Wound Variability and Progression

The effect of heat on tissue affects skin structures differently, producing an injury that is not uniform and has inherent variability. The variability within a burn wound was first described by Jackson in 1953 as the zones of injury. The central region is a zone of coagulation or an area of necrotic tissue and cells. Immediately surrounding the coagulative region is the zone of stasis. The zone of stasis is a mixture of patent and occluded vessels and viable and non-viable cells. This zone has the potential to either regenerate or it can convert to a necrotic region. The zone of hyperemia is a zone of prominent vasodilation and increased blood flow that surrounds the zone of stasis.[21]

The zone of stasis is important as its conversion to a zone of coagulation causes an extension of the burn injury and increases the total body surface area of the burn. The prevention or reversal of the tissue ischemia and necrosis in this region has been a major focus for many investigators. Zawacki demonstrated that the zone of stasis is reversible in a guinea pig small total body surface area (TBSA) burn model. The depth of capillary stasis, as measured with a micrometer from the dermal-epidermal junction, increased up to 16 hours following the burn injury. After this time point, capillary circulation was restored first in the lower portions of the dermis at 24 hours post-injury. By 7 days post-injury, there was no evidence of capillary stasis and the histology of the

wounds was similar to pre-burn.[22] This study was also evidence for the dynamic nature of a burn wound and its inherent variability.

It has been well-documented that burn wounds are dynamic and can progress over time. The changes that occur in a burn wound do not become visually apparent immediately, which makes it hard to classify the healing potential of the injury at early time points. deCamera tried to identify early changes in burn wound morphology using skin biopsies from a 10% TBSA burn in guinea pigs. Morphological changes in the epidermis, dermis, basement membrane and blood vessels were observed to occur up to 8 hours post-injury. There were no morphological changes observed after 8 hours other than superficial collagen necrosis and an infiltration of polymorphonuclear leukocytes at 96 hours post-injury.[23] In this study, light microscopy and electron microscopy did not provide information about the changing physiology of the burn wound until there were visually apparent changes in the skin sample. The results obtained in both the laboratory and clinical environment during this thesis have shown that microscopic changes are apparent in the skin structures as early as 1 hour after injury and changes continue to occur over the course of the injury. Therefore, macroscopic assessments of burn depth are very similar to a visual assessment whereby changes are not apparent for several days after the injury.

Burn wounds of varying depths can be classified as healing or non-healing wounds at varying time points. Papp et al. used a swine model to document the progression of burn injury using histology. Superficial burns showed no changes in depth, full thickness injuries experienced no changes after 24 hours, and partial thickness injuries continued

changing up to 48 hours after injury.[24] Nanney et al. used vimentin immunostaining to document the progression of burn injuries. Positive vimentin immunostaining was found in the upper portions of the dermis at one day post-injury for the majority of burn wounds. Superficial injuries did not show an extension of injury at 3 days post-burn but the deep injuries lacked vimentin staining in the lower portions of the dermis.[25] Boykin found that changes occur within the zone of stasis between 8–48 hours but no new microthombi occluded the vessels after 48 hours.[26] Kloppenberg et al. found that superficial burn wounds have peak perfusion at day 1, partial thickness injuries have peak perfusion at 4 days, and full thickness injuries have low laser Doppler perfusion that does not change over time.[5] Schiller et al. also found that laser Doppler perfusion was high in healing wounds at day 1 and 5 but could not be distinguished at 3 days.[27]

These studies all suggest that there is a critical time point when burn injuries differentiate into viable and non-viable wounds. In all of the studies, it appears that this critical time point is between 12 and 72 hours post-burn. The results from the NIR imaging device also suggest that hemodynamics are altered between day 2 and day 4 as shown in Appendix A.[28] The NIR images for total hemoglobin showed mixed perfusion at post-burn day 2 but increased perfusion by day 4. This suggests that there is a potentially critical event in this time frame that separates a burn injury into a viable and non-viable wound. If the critical hemodynamic event could be identified then it may be possible to find early differences in hemodynamics, which could identify and separate viable and non-viable injuries.

1.2.3 **Cut-off Points for Viability**

Laser Doppler has been able to successfully differentiate burn depth with defined specific cut-off perfusion or flux values for viable and non-viable injuries. Riordan et al. performed a study in 35 extremity burns in 25 adult burn patients with a 10% TBSA burn. Deep dermal injuries were found to have a flux value less than 1.3 and correlated the findings with the reference standard histology.[4] Schiller et al. measured blood flow using a laser Doppler probe in 31 patients with 43 hand burns. The median flow values for a 5-day period were 150mV for non-grafted wounds and 90mV for grafted hands[27]. Park et al. used LDI in 100 burn sites from 44 patients and created cut-off values for superficial partial thickness (>100 PU), deep partial thickness (10–100 PU) and full thickness (<10 PU).[29] Kloppenberg et al. measured wound depth in 22 wounds in 16 patients with 10% TBSA burns. Flux values were measured at 1, 4 and 12 days post-burn for healed burns and 1 and 4 days for surgical wounds. A cut-off value of 2V separated the viable and non-viable injuries.[5]

A cut-off value could be misleading as shown in the Kloppenburg study. At 4 days post-burn injury a cut-off value of less than 2V was used to define deep burn injuries. However, very superficial injuries also have flux values that are below 2V. Park el al. also found that the cut–off value used to distinguish full thickness burn wounds from partial thickness injuries was between 4–9 perfusion units (PU). However, normal skin in this study had a normal basal blood flow of between 3–7 PU.[29] Atiles et al. classified injuries that were above 80 PU as healing wounds and those below 80 PU as non-healing injuries. However, of the 36 wounds with flow less than 80 PU that were classified as non-healing burns on day 0, 33% (12/36) actually increased to healing

ranges by day 1. The other 66% of the wounds remained below 80 PU and did not heal.[30] These injuries likely represent the true sample of “indeterminate” partial thickness injuries where it is difficult to determine the viability at early time points post-burn. The indeterminate burn is described as “the cessation of capillary flow where the signs of necrosis occur but do so only gradually” yet “capillary stasis can be completely reversed and necrosis prevented.”[22] Zawacki’s description of indeterminate wounds is a great summation of the problem that arises with indeterminate burns. The definition emphasizes that these wounds initially can appear to be non-healing but spontaneously change to healing wounds. The inherent variability within the indeterminate burn and the dynamic nature of the wound suggest that cut-off values have to be considered in conjunction with the time point post-burn injury and in conjunction with the clinical diagnosis.

Jeng et al. measured perfusion in 41 wounds from 23 patients with 10% TBSA burns. Wounds were classified into superficial partial (>250 PU), deep partial (150–250 PU) and full thickness (<150 PU) injuries based on perfusion units as the cut-off value. The results from this study were able to highlight the discrepancies that occur between clinical judgment and outcome. The surgeon and LDI agreed 56% of the time but the LDI and histology were in agreement 71% of the time. The performance of the LDI was not perfect and may have performed better if the imaging results were interpreted correctly at the time of data collection. The LDI reported 21 cases as healing wounds but according to pathology 8 of the cases were either deep dermal or full thickness injuries.[6] These 8 cases were reviewed by an experienced LDI user and in hindsight were deep dermal burn wounds. When the laser Doppler images were reviewed by an experienced

device user it was found that the images had been erroneously reported as healing secondary to a surrounding region of hyperemia. This has been one of the largest criticisms of laser Doppler, as the interpretation of the imaging results can be difficult and there is a learning curve.

1.2.4 **Perfusion and Oxygen Delivery**

There is a critical requirement for molecular oxygen in wounds. Oxygen is a fundamental molecule required for energy producing biochemical pathways.[31] Oxidative phosphorylation in the mitochondria is an oxygen-dependent process. Aerobic glycolysis, B-oxidation of fatty acids and the citric acid cycle rely of the ATP produced by oxidative phosphorylation.[31]

Oxygen plays an important role in collagen synthesis as fibroblast proliferative activity relies on oxygen tensions of more than 15mmHg in the wound.[31, 32] The post-translation modification of proline relies on oxygen and this modification is required to produce stable triple helix procollagen molecules. Oxygen concentration impacts the tensile strength of collagen. *In vitro* collagen maturation and cross-linking increases linearly when oxygen concentration increases.[33] Re-epithelialization of the wound is controlled by the oxygen supply and diffusion distance of oxygen. Angiogenesis is affected by oxygen levels with high arterial pO_2 driving new vessel growth into hypoxic regions. Oxidative phagocytic killing in wounds relies on oxygen to generate free radicals for the respiratory burst. Wound oxygen tension correlates with blood oxygen tension and tissue perfusion.[33]

Near infrared spectroscopy utilizes oxy- and deoxyhemoglobin to assess the oxygenation and perfusion of tissue. Oxygen saturation is the ratio of oxyhemoglobin to total hemoglobin and represents oxygenation. Total hemoglobin, the summation of oxy- and deoxyhemoglobin levels, is used to represent blood volume or the perfusion of tissue.[28, 34] The utilization of both oxy- and deoxyhemoglobin can provide information about what is occurring in the tissue in terms of perfusion and oxygenation. Studies performed in human forearms, flaps and the limbs of laboratory animals have indicated that certain patterns of these variables can be used to determine the perfusion to the tissue and the type of vascular compromise. For example, oxyhemoglobin values decline for arterial, venous and total occlusions. The largest changes in oxyhemoglobin occur with arterial and total occlusions as venous occlusion oxyhemoglobin levels can remain unchanged. Deoxyhemoglobin levels experience the highest level of change with total occlusions versus venous occlusion. Deoxyhemoglobin levels represent oxygen utilization by cells and/or impaired venous drainage.[35] If cells are using aerobic metabolism then oxygen is released to the tissue, which means deoxyhemoglobin levels should increase.[36] Finally, total hemoglobin levels decrease with arterial occlusion, increase with venous occlusion and experience no change with both arterial and venous occlusion.[34, 37]

Arterial Occlusion	Venous Occlusion	Total Occlusion
↓Ohb	↓Ohb or no change	↓Ohb
↑Hhb	↑Hhb	↑Hhb
↓ tHb	↑tHb	tHb-no change

Table 1-1: Changes in Oxy-, Deoxy-, and Total Hemoglobin with Arterial, Venous or Total Vascular Occlusions

1.3 Methemoglobin

The presence of methemoglobin in the tissue has never been described in a burn wound and the literature surrounding methemoglobin formation post-burn injury is limited. The only report of high systemic levels of methemoglobin were reported in three patients with smoke inhalation injury after exposure to hydrogen cyanide, a chemical released by burning plastics.[38] Methemoglobin forms when the iron of the hemoglobin is oxidized to its ferric state.[39] With its tense conformation deoxyhemoglobin is ten times more susceptible to oxidation than the relaxed conformation of hemoglobin.[40] The ferric iron of methemoglobin will not bind oxygen but instead binds water or a hydroxyl group, depending on the pH of the tissue. The tetrameric structure of methemoglobin is distorted and the non-oxidized heme molecules will bind O_2 with vigour but will release oxygen much less efficiently.[41]

In healthy individuals only 1% of hemoglobin is methemoglobin, and anything greater is considered to be methemoglobinemia.[39, 41, 42] Methemoglobinemia is uncommon, with only 600 cases reported over the last 40 years.[41] Increased fractions of methemoglobin will affect the oxygen dissociation curve by inhibiting oxygen binding at the heme iron binding sites. In addition, the conformation change of the oxidized Fe^{3+} causes a high affinity for oxygen in the subunits, which shifts the ODC to the left.[41–43] In areas where there is a low partial pressure of oxygen, the hemoglobin will have an affinity for O_2 and hypoxia ensues.[41] Methemoglobinemia leads to cyanosis, impaired aerobic respiration, metabolic acidosis and in severe cases death.[42] No one has specifically described the normal content of methemoglobin in the skin or the level that impacts tissue injury.

1.3.1 **Methemoglobin Formation in Burn Wounds**

The red blood cell is a major target for reactive oxygen species (ROS) and reactive nitrogen species (RNS) because it is bathed in an oxygen- and nitric oxide-rich environment.[44] Methemoglobin participates in redox reactions with free radicals in the tissue and its formation has been described with both ROS and RNS production. An overview of free radical formation and the interaction of iron are shown in Figure 1-1.

Oxyhemoglobin can undergo spontaneous oxidation at the heme iron centre. Oxygen bound to iron creates a superoxo-ferriheme, $Fe^{3+}O^{2-}$, which upon release of oxygen to tissue produces a superoxide free radical ($O^{2\bullet-}$). The free radical actually leaves the iron in a ferric state, forming methemoglobin.[39, 40, 45] This process is called auto-oxidation and occurs normally at a rate of 3% per day.[46]

The auto-oxidation of oxyhemoglobin produces a superoxide radical when oxygen is offloaded to the tissue. The presence of hydrogen peroxide will accelerate this process and increase the formation of methemoglobin.[47] Normally, the red blood cell has reduction mechanisms that keep the levels of methemoglobin low. However, at low oxygen tensions and with partially oxygenated hemoglobin the rate of methemoglobin formation is accelerated.[46] Only 24% of methemoglobin formation occurs from the auto-oxidation process and the remainder occurs from ROS and RNS.[48]

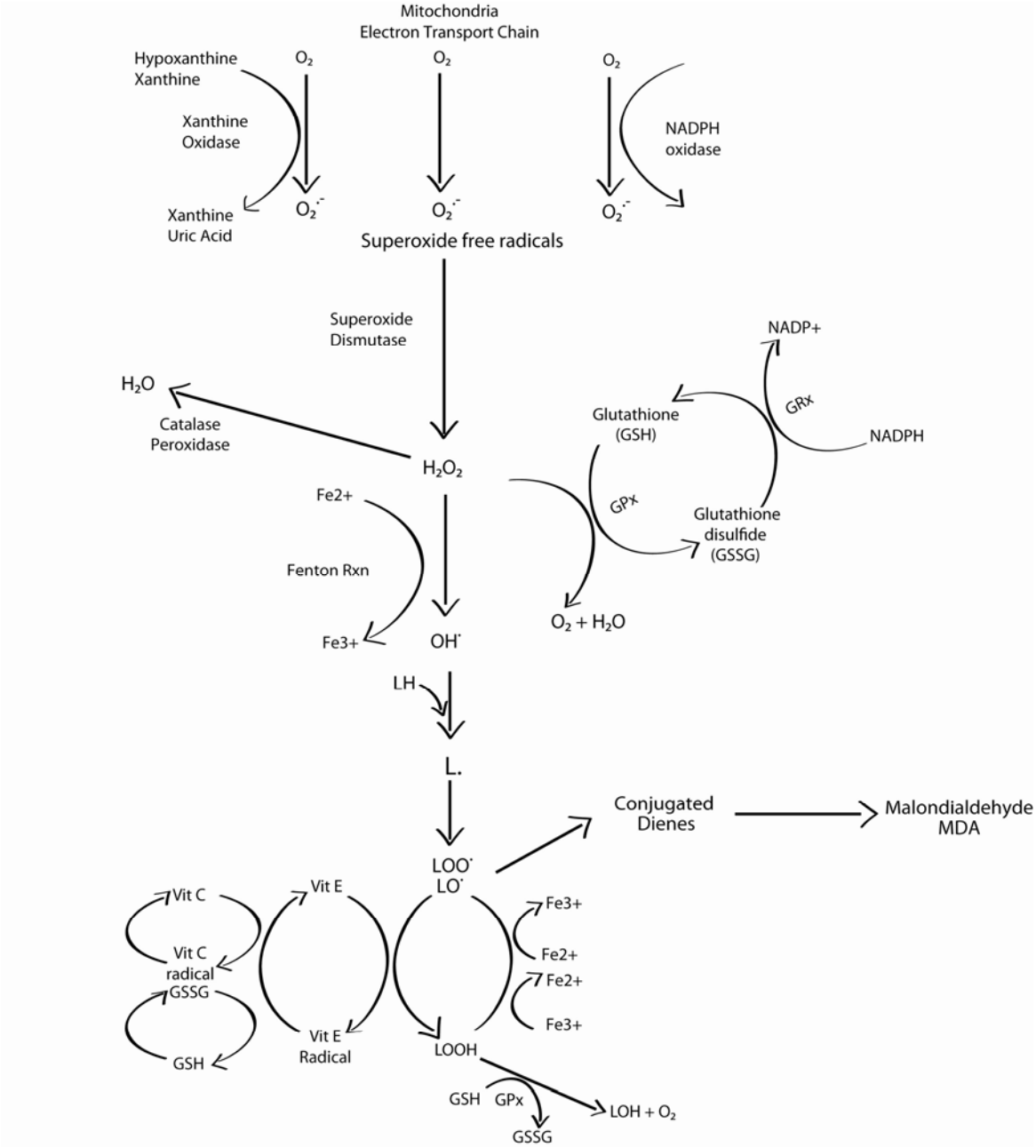

Figure 1-1: Free radical formation and reduction pathways demonstrating the interaction of iron, hemoglobin and methemoglobin (Valko et al.[49])

There are several known sources of free radicals post-thermal injury, including the oxidative bust by phagocytes, xanthine oxidase and nitric oxide.

The oxidative burst by phagocytes (activated macrophages and neutrophils) is responsible for the reactive oxidant species (ROS) that are generated post-burn injury. Neutrophils are present in a burn wound within 4 hours post-injury and remain high for at least 24 hours.[50] NADPH oxidase is located in the cell membrane of activated phagocytes and converts oxygen to $O^{2\bullet-}$ or the superoxide anion.[49, 51] The superoxide anion in the presence of protons and superoxide dismutase will form the oxidant hydrogen peroxide. The superoxide anion is considered to be the "primary" ROS because it interacts with other molecules to form "secondary" ROS (hydrogen peroxide).[49]

Xanthine oxidoreductase produces hydrogen peroxide and a superoxide free radical in ischemia-reperfusion injuries. In the ischemic phase of the injury, oxygen is limited and therefore less ATP is produced. The increased AMP production is catabolized to hypoxanthine. Return of blood flow to the burn results in the conversion of hypoxanthine to xanthine and uric acid by xanthine oxidase. In the process of this conversion, hydrogen peroxide and a superoxide radical are formed.[52] Volume replacement post-burn restores perfusion and oxygenation. The restoration of oxygenation is important for cellular survival but also initiates a cascade of events that results in an exacerbation of ischemia-related free radicals and tissue injury. This ischemia-mediated free radical injury is called the "oxygen paradox."[52] Xanthine oxidase has been shown to be elevated in thermally injured skin.[53] It is believed that upregulation of xanthine oxidase is

secondary to ischemia or mediated by histamine release from mast cells.[53, 54] In 23 burn patients, xanthine oxidase activity increased from 30mmol/l on day 1 to 451 mmol/l by day 6 post-burn injury.[55] Xanthine oxidase upregulation produces two oxidants, superoxide radical and hydrogen peroxide, known to be involved in the oxidation of ferrous to ferric iron.

Hydrogen peroxide reacts with ferrous iron to form ferric iron via the Fenton reaction.[56] The conversion to methemoglobin generates the hydroxyl radical, which is one of the most potent oxidants. Hydrogen peroxide also reacts with methemoglobin and oxyhemoglobin to form a ferrylhemoglobin (Hb^{4+}) intermediate and a reactive globin species.[45, 47, 48, 57, 58] Creating the ferryl intermediate also produces a reactive globin chain radical. This radical is insensitive to catalase reduction and therefore cannot be reduced by the normal mechanisms within the red blood cell.[59] For this reason, the ferryl intermediate is one of the most toxic radicals.

Methemoglobin is also formed by the interaction of hemoglobin with nitric oxide and nitrites. These interactions form a unique system for sensing oxygen tension and altering perfusion. Nitric oxide (NO) is produced by the endothelial cells and controls vascular tone.[46] NO diffuses from the endothelial cells into the vessel lumen and enters the red blood cell. The NO reacts with oxyhemoglobin to form nitrate (NO^{3-}) and in the process oxidizes the Fe^{2+} to Fe^{3+}.[45, 57] Scavenged NO is unable to interact with the blood vessel and the vessel will not dilate.

Deoxyhemoglobin interacts with nitrite (a product from the auto-oxidation of nitric oxide) to reduce deoxyhemoglobin to methemoglobin and free nitric oxide. The free nitric oxide acts to dilate the blood vessels and increase perfusion.[46]

It has been documented that the rate of nitric oxide synthesis occurs at 40-60% oxygen saturation and oxygen tensions between 15–40 mmHg. Therefore, the hemoglobin-methemoglobin couple acts as a sensor of oxygen tension. In low oxygen tensions, there are increased levels of deoxyhemoglobin to interact with the nitrite and produce free nitric oxide. The free nitric oxide will dilate the vessels and increase perfusion to a region with poor oxygenation. At higher oxygen tensions, there will be more oxyhemoglobin present to bind with the nitric oxide and prevent its vasodilatory effects.[46]

Nitric oxide production is elevated post-burn injury with increased levels within the burn wound.[51] The inducible mediated nitric oxide (iNOS) production is upregulated so that NO production far exceeds baseline levels.[52] Nitric oxide interacts with the superoxide anion to form peroxynitrite.

Peroxynitrite can cross cell membranes, has a high diffusion distance and can be found at least 10 μm from its site of formation, which means it can react with molecules at distant sites.[59] Peroxynitrite causes single-strand DNA breakage, lipid peroxidation and a decrease in superoxide dismutase activity.[60, 61] Peroxynitrite has also been shown to react with existing methemoglobin to form a toxic ferryl intermediate.

Finally, it has to be considered that the formation of methemoglobin in burned tissue could be directly related to the thermal injury. Forensic studies looking at the effect of heat on blood have shown that increased temperature causes an immediate conversion of hemoglobin to methemoglobin.[62] Methemoglobin has been shown to shorten T1 relaxation times during MRI thermal ablations of tissue.[63, 64] Heat induces the conversion from ferrous hemoglobin to methemoglobin as measured by a change in T1 time. The presence of hydrogen peroxide was also shown to accelerate the formation of methemoglobin as measured using MRI.[65] In these MRI studies, investigators utilized near infrared spectroscopy to confirm the presence of methemoglobin in the tissue and validate the MRI results.

1.3.2 **Impaired Reduction of Methemoglobin in Burns**

The red blood cell is a source of both oxidants and antioxidants. In normal situations, the red blood cell is an efficient antioxidant and contains many reductive systems within the cell.[44]

There are several enzymatic and non-enzymatic mechanisms that can reduce methemoglobin back to hemoglobin. The NADH cytochrome b5/cytochrome b5 reductase system accounts for 99% of daily methemoglobin reduction. The reconversion rate of methemoglobin hemoglobin in normal individuals is 15% per hour, assuming no ongoing production.[42] The NADH cytochrome b5/cytochrome b5 reductase is responsible for the reduction of methemoglobin to its ferrous state. It operates by

donating an electron from NADH to the cytochrome reductase. This electron is then transferred to the cytochrome, reducing the Fe^{3+} to Fe^{2+}.

If the NADH cytochrome b5/ cytochrome b5 reductase system is overwhelmed then the minor pathways will be upregulated. These minor pathways include the NADPH Methemoglobin Reductase system and the Glutathione Reductase system.[40, 42] The NADPH methemoglobin reductase enzyme reduces a flavin (e.g., Riboflavin) in the presence of NADPH, which can then reduce methemoglobin. This enzyme is also responsible for the reduction of the ferric iron in the presence of methylene blue. Methylene blue, the clinical treatment for methemoglobinemia, accepts an electron from NADPH and subsequently reduces methemoglobin as an electron donor.[40, 42, 48] Normally, this system represents less than 5% of the methemoglobin reduction that occurs in the body.[40]

Reduced glutathione can reduce ferric iron back to ferrous iron. The oxidized glutathione is then converted to its reduced form via glutathione reductase and NADPH as shown in Figure 1-1. Glutathione is one of the major regulators of redox homeostasis.[51] As an antioxidant, glutathione functions as a cofactor for detoxifying enzymes (e.g., Glutathione peroxidase), scavenging the hydroxyl radical and singlet oxygen as well as regenerating ascorbic acid and α-tocopherol back to their active forms.[49] Glutathione also prevents the interaction of ferrous and ferric iron with LOOH to produce LOO• and LO• radicals.[49]

Other secondary defence mechanisms against free radical-induced injury include superoxide dismutase (SOD), catalase (CAT), the thioredoxin system, ascorbic acid, α-tocopherol and plasma membrane oxidoreductases. [48, 66] The role of some of these free radical scavengers is shown in Figure 1-1. Both enzymatic and non-enzymatic defence mechanisms are impaired following a burn injury. The concentration of alpha tocopherol, ascorbic acid and glutathione are depleted.[52, 67] There are also decreased levels of superoxide dismutase (SOD) and catalase (CAT).[68]

All of these findings in combination suggest ongoing production of free radicals in an environment where the defence systems are overwhelmed. It has been well-documented that ferrous hemoglobin can be converted to its ferric form by both ROS and RNS. Therefore, the high concentration of both in the burn wound is a plausible reason for the presence of methemoglobin in a burn wound.

1.3.3 **Methemoglobin and Cellular Injury**

Endothelial cells are the first targets of free hemoglobin and methemoglobin and their breakdown products.[69] Methemoglobin increases the rigidity of the red blood cell, which results in cell lysis. Without the protection of the red cell's reduction system, cell lysis causes the release of methemoglobin. Free methemoglobin has been shown to increase the production of IL-6, IL-8 and E-selectin by the endothelial cells.[69]

Methemoglobin will release heme more freely than the reduced form.[70, 71] Free heme toxicity is related to its hydrophobic nature, which gives it the ability to cross and

intercalate into cell membranes.[70, 72] The presence of free heme causes an increase in vasopermeability, increased adhesion molecule expression (ICAM-1, VCAM-1 and E-selectin) and increases the infiltration of leucocytes.[69] ICAM-1 is involved in the binding of leukocytes and neutrophils to the vascular endothelium, which allows them to migrate into the tissue.[52] Once heme is within the cell, it can release free iron via non-enzymatic oxidative degradation or through enzymatic degradation by heme oxygenase.[70] Free iron will incorporate into the hydrophobic areas of the phospholipid bilayer and oxidize the cell membrane.[70] The presence of iron has been shown to accelerate oxidant damage in endothelial cells.[73]

Endothelial cells exposed to heme of methemoglobin will induce the synthesis of heme oxygenase -1 and ferritin.[69, 72, 74] These proteins are both defence mechanisms that prevent cellular injury by methemoglobin and iron. Heme oxygenase-1 is a heme-degrading enzyme that opens the porphyrin ring to produce biliverdin, carbon monoxide and free iron. Biliverdin reductase catalyzes the conversion of biliverdin to bilirubin.[70] Ferritin will bind the free iron and prevent it from intercalating into the membranes.[70]

Haptoglobin is a circulating protein that binds free methemoglobin to prevent the toxic release of heme.[56, 69, 70] Haptoglobin's binding of hemoglobin is exhausted at free hemoglobin levels above 15 μm.[69] The free heme released from methemoglobin is bound by hemopexin; hemopexin therefore acts to prevent the oxidative damage that free heme can cause when released.[56]

1.4 Burn Wound Pathophysiology – Edema

1.4.1 Burn Edema Pathophysiology

The amount of edema formation following a burn injury is dependent on the depth of the burn, total body surface area involvement, fluid resuscitation and the presence or absence of inhalation injury.[75] Edema forms rapidly in a burn patient with peak edema at 12 hours post injury and resorption dependent on the factors mentioned above. Fluid accumulation occurs in both the burned and non-burned tissue as well as in the organsalong with the organs.[76]

The accumulation of burn edema occurs in a biphasic pattern as there is a rapid increase in interstitial fluid within the first hour post-injury. Approximately 80% of total edema is present at 4 hours post-injury. [53, 77–79] The second phase is marked by a gradual increase in fluid accumulation over the next 12–24 hours. Normally, fluid movement from the capillary to the interstitium is balanced by lymphatic clearance so that excess fluid does not accumulate. However, in burn injuries the movement of fluid and protein into the extravascular space occurs very rapidly and edema ensues because the lymphatics are unable to keep pace with the clearance of fluid and protein. The physical changes responsible for the influx of fluid and protein into the interstitium can be explained by changes to Starling's forces [$J_v = K_f (P_c - P_{if}) – \delta (\pi_p - \pi_{if})$].[75, 76]

The osmotic pressure (π_p) of the capillary decreases within the first hour post-burn injury as a result of protein extravasation into the interstitium.[53, 80, 81] The extra protein in the interstitial space causes an increase in the oncotic pressure (1 g albumin = 4 mmHg

oncotic pressure) of the interstitium, which in turn increases fluid flux into this region.[76] Normally, the oncotic gradient is maintained by the resorption of protein by the lymphatics. In a burn wound, the oncotic pressure of the interstitium does decrease in response to the decrease in capillary osmotic pressure but once it reaches a certain level (3-4mmHg or protein 1.5/dl) the π_{if} cannot decrease any further to compensate for the hypoproteinemia of the plasma.[82] Therefore, the oncotic gradient is maintained in favour of fluid efflux. From animal models, the π_p is decreased within 1 hour post-burn injury but the appropriate compensation by π_{if} lags behind. The π_{if} decreases immediately post-burn with its lowest values at 8 hours post-burn, but it is still not enough to compensate completely for decrease in π_p. However, by 2–3 hours after the initial burn injury the drop in interstitial colloid pressure has almost compensated for the change in the oncotic gradient. By 24 hours the oncotic gradient has been restored back to baseline levels. In fluid resuscitated patients there is an even greater decrease in the π_p secondary to dilution of the plasma volume.[80] The combination of a decrease in capillary osmotic pressure and the increase in the osmotic pressure of the interstitium causes the oncotic gradient (π_p - π_{if}) to approach zero and the P_c becomes the dominant force.[80] In addition, heat denaturation of the tissue also causes a cellular destruction of the tissue and releases proteins into the interstitium, causing an increase in colloid osmotic pressure.

The P_{if} is normally subatmospheric in normal unburned tissue (-2 mmHg). After burn injuries the P_{if} becomes strongly negative and there is nothing to counter the hydrostatic pressure of the capillary (P_c), which results in a net fluid flux into the interstitium. Guyton et al. coined the term “safety factors” to describe the mechanisms that prevent the

accumulation of fluid in the interstitium. Normal hydrostatic buffering is a “safety factor” that counters the increase in P_c by increasing the P_{if} to atmospheric levels. In burn injuries the extremely negative value for P_{if} actually “suctions” fluid out of the capillary and into the interstitium.[83] The strongly negative P_{if} occurs immediately after the burn injury and has been reported to either return to baseline between 50–150 minutes post-burn or, as reported in other studies, is still below control values after 180 minutes.[83–86] The P_{if} is associated with the size of the injury, with a larger TBSA burn creating a more negative P_{if}.[86] The strongly negative P_{if} has been shown to occur in deep partial and full thickness injuries only, as in superficial wounds P_{if} remains around baseline levels.[85] Fluid resuscitation improves the P_{if} as both colloid and non-colloid resuscitations result in a return to baseline more quickly than a non-resuscitated burn in a large TBSA (40%) rat model.[80, 84, 86] Colloid solutions such as plasma produce a greater improvement in the P_{if} than non-colloid solutions. The P_{if} returns to baseline more quickly with colloid solutions.[80] The extreme negative value for the P_{if} and the increase in P_c are believed to create enough pressure for the rapid movement of fluid into the interstitium. Some investigators believe that this is the rationale for the early and rapid influx of fluid into the interstitium post-burn injury.[76, 84–86] There are three proposed explanations for a strongly negative P_{if}[84]:

1) There are new macromolecules or colloids present in the interstitium created from the thermal injury.
2) There is a physicochemical rearrangement of structural elements of the tissue, which causes an expansion of the interstitial fiber matrix.
3) The cells are dehydrated and fluid moves from the interstitium into the cell.

Normally, the interstitial space is composed of two phases, a collagen fiber framework and small pockets of free fluid that contain proteins from the plasma.[87, 88] The collagen fiber framework of the skin is comprised of a gel phase of glycosaminoglycans (GAGs) of which two-thirds are hyaluronan. The random coil organization of hyaluron allows it to occupy a space that is “100–1000 times larger than that occupied by its organic matter.”[88] The hyaluron molecules also form an entangled network with other hyaluron molecules and collagen, which forms high-density units and limits the hyaluron mobility in the interstitial space. The plasma proteins in the interstitium cannot fit into these high-density spaces because of the interactions of hyaluron. This characteristic of the matrix is called the protein exclusion effect.[87, 89] Both the collagen fibrils and the hyaluron have been implicated in the interstitial volume exclusion. Approximately two-thirds of the fractional exclusion of albumin is from collagen intrafibrillar spaces and the other one-third is from glycosaminoglycans (eg.hyaluronan). These small pockets of free fluid created by the collagen matrix or proteoglycans are selectively available to other parts of the extra-cellular matrix.[87, 90] The organization of the matrix is responsible for the regulation of fluid and protein movement throughout the interstitial space.[90, 91] When the hydrostatic pressure of the capillary increases, fluid moves into the interstitium and increases the fluid volume. The interstitial volume expansion causes a decrease in the number of exclusionary domains, which means the protein now distributes into a larger fraction of the interstitial fluid volume.[89] Therefore, there is less protein concentration in the interstitium, which decreases the oncotic pressure (π_{if}) and reduces the oncotic gradient. In addition, a volume expansion 3–5 times above baseline has been shown to double the pore radius and increase protein diffusion to the lymphatics.[88]

Thermal injury could potentially change the fraction of protein normally excluded by the interstitial matrix by physically changing the structural organization of the extracellular matrix.[90] Hyaluron, a glycosaminoglycan of the matrix, has been shown to increase in both the lymph and the plasma post-burn injury. Hyaluron is generally removed from the tissues by lymphatic drainage and can be metabolized in the lymph nodes or liver. Once it reaches the plasma hyaluron is rapidly eliminated by the liver ($t_{1/2}$ = 2–6 minutes), which means an increase represents increased production or reduced clearance.[91] Hyaluron concentrations in the plasma post-thermal injury are increased over control values. The amount of fluid and the type of fluid resuscitation impact the level of hyaluron in the plasma. Doubling the resuscitation formula produces a 50% increase in the level of hyaluron in the plasma.[91] Colloid solutions reduce the level of hyaluron in the plasma compared to saline or no resuscitation. This supports the hypothesis that Ringer's lactate or saline solutions lower the plasma colloid osmotic pressure, increase fluid flux into the interstitium and increase lymph flow as seen by the high levels of hyaluron in the lymph. The increased fluid in the interstitium changes the fractional exclusion of proteins, alters the pore radii and improves diffusion of proteins (hyaluron) to the lymphatics. It could also be hypothesized that the hyaluron detected in the blood is fragmented or denatured, which is why the levels are high. However, the molecular size of hyaluron has been shown to be unchanged post-burn injury, which means that it is not necessarily denatured.[91] The likely mechanism of increased mobility of hyaluron is a change in the charge interactions within hyaluron molecules or between hyaluron molecules and collagen secondary to heat and/or increased volume.

The permeability determinants are affected by a burn injury as K_f increases and δ decreases. The δ determinant is an index of the osmotic pressure generated by proteins that are exerted across the capillary wall. At 1.0 the capillary is impermeable to protein and at 0 there is a free flow of protein. In studies performed in a dog hind limb, the normal value for δ was 0.87, which decreased to 0.45 after burn injury. The decrease in δ indicates a high permeability for proteins. It has been shown that macromolecules as large as 120Å can move through the gaps in the endothelial junctions.[77] Albumin and immunoglobulins represent 80% of the proteins in the plasma and are the major proteins found in the interstitial space.[92] Interestingly, the non-burn tissue shows an increase in δ but the gap junctions are selective and permit the movement of molecules with a molecular size less than 108Å such as fibrinogen. The movement of proteins through the endothelium has been explained by the pore theory. The pore size of the endothelium is divided into small pores (50Å) and large pores (300Å). Post-burn, these pores increase in size to 70 and 400Å respectively. The large pores account for an 18-fold increase in total filtration of water versus the small pores, which account for a 3-fold increase. The large pores also account for 49% of the total filtration of fluid post-burn injury compared to 13% pre-burn.[77] Initially, the increase in permeability of the endothelium was felt to be the major force driving the fluid efflux post-burn injury. In fact, the edema that accumulates in the tissue 12–24 hours post-burn has been attributed to a continued permeability of the endothelium and protein efflux. This has led to significant controversy in the clinical literature about the type of resuscitation fluids (colloid versus non-colloid) and especially surrounding the timing of colloid institution. As the capillary is felt to be “leaky” up to 48 hours post-burn, the practice of early colloid infusion has fallen out of favour with some burn units because colloids were felt to propagate edema formation

through increased albumin into interstitium. Brouchard et al. performed a small partial thickness burn study in rats. They injected radioactively-tagged albumin immediately after the burn injury and found an increase in albumin in the tissue at 6 hours post-injury, with high levels up to 48 hours post-burn. However, in their second set of experiments the rats received the radiolabelled albumin prior to euthanasia at specific time points post-burn. Animals that received the radiolabelled albumin injection within 8 hours of the burn had high levels of albumin in the tissue, whereas injections after 8 hours showed no change from unburned controls.[93] This suggests that in this model albumin does not "leak" into the interstitium after 8 hours. It also suggests that the administration of colloid after this time point may not directly translate into increased albumin in the extravascular spaces.

The K_f is a coefficient used to describe the ease at which fluid can pass through the capillary endothelium and is dependent on two factors: 1) the surface area of the capillaries perfusing the tissue, and 2) hydraulic conductivity of the capillary membrane.[75, 76] This means that increased perfusion through patent blood vessels equals fluid movement into the interstitial space. It also explains why partial thickness injuries experience more burn wound edema, as they have more patent blood vessels. Full thickness injuries experience less edema formation because the blood vessels are thrombosed or coagulated.

The hydraulic conductivity of the capillary membrane is determined by the endothelial function and the capillary basement membrane thickness. However, the compliance, or distensibility, of the interstitial space has a direct impact on the coefficient. The

compliance of the tissue is expressed as the ratio of the change in interstitial fluid volume divided by the corresponding change in interstitial pressure. A low compliance means that a small volume increase will result in a large increase in counter-pressure. Counter-pressure is defined as the pressure exerted by the interstitium, which keeps fluid in the capillary. A high compliance means that a large volume increase will result in a low counter-pressure. Tissues with a high compliance do not provide much counter-pressure despite large fluid fluxes. Compliance varies within the skin layers as the subcutaneous tissue can expand markedly compared to the dermis. The pressure-volume curve for skin was described by Guyton in 1965.[94] There is a linear relationship between volume and pressure when the tissue is dehydrated, at baseline levels or is slightly overhydrated. However, if the fluid volume increases to 30% of the interstitial fluid volume the pressure actually plateaus and stays constant. This means the counter-pressure exerted by the tissue remains the same and the volume of fluid can continue to accumulate without resistance. It has been reported that counter-pressure could not be increased 1–1.5 mmHg in control values, which has lead investigators to speculate that the hydrostatic counter-pressure is incapable of preventing edema formation. Washout and protein dilution are felt to play a larger role in limiting edema formation.[94–96]

Lymph flow also affects the accumulation of edema in a burn wound. Harms et al. showed that there was increased lymph flow immediately after injury, with peak levels occurring at 2.5 hours post-burn. Lymph flow remained high and had still not returned to baseline 72 hours after injury.[81, 92] The increase in lymph flow has been shown to last for several days post-injury.[82, 92] There are also fewer lymphatics in the subdermal space, which means fluid and protein accumulation in this region will resorb more slowly. Using

a small TBSA rat model, Brouhard et al. found that the RISA-labelled albumin injected immediately following the injury was present in the tissue 48 hours later.[93] The fact that RISA-labelled albumin did not show an increase in tissue when injected 8 hours after the injury suggests that the increase in albumin in the tissue at 48 hours is related more to poor lymphatic clearance than continued permeability of the capillary. Non-burn tissue also experiences a 2–3-fold increase in lymph flow with a peak at 6–18 hours and a return to baseline by 48 hours.[81] The non-burn tissue shows a selective permeability to albumin and gamma globulin but not larger molecules such as fibrinogen.[92] The permeability of the endothelium to albumin and gamma globulins was also transient and resolved by 12 hours post-burn.[81]

1.4.2 **Burn Wound Edema Biochemical Factors**

The formation of burn wound edema is attributed to more than the physical forces within the tissue, as it is mediated by various biochemical factors. Neutrophils, lymphocytes, oxidants, histamine, kinins and prostaglandins have all been implicated in edema formation within burn wounds. Neutrophils are a major source of oxidants in the tissue and the pattern of neutrophil migration is different in a superficial and deep burn. Neutrophils arrive early in a superficial burn wound, peak at 24 hours and are almost absent by 72 hours post-burn. Neutrophils take longer to arrive in a deep wound and will persist for longer periods of time. However, the direct presence of neutrophils in the wound is not required for edema formation.[53]

In the first hour post-burn, there are large quantities of oxidants produced in the burn tissue. The oxidants are likely generated by the activation of neutrophils (myeloperoxidase activity), from endothelium (xanthine oxidase activity) or as a byproduct of arachidonic acid metabolism. Malondialdehyde and conjugated dienes, markers of the lipid peroxidation processes, are present and increased in the venous system within 3 hours post-injury and return to baseline by 12 hours. They appear to have a second phase of increase around 3 days after the burn injury, which may reflect the inflammatory processes rather than a direct injury to tissue in the early phase.[97] The production of oxidants is uninhibited as there is impaired scavenging and oxidant neutralization. Oxidants are responsible for the cellular injury to endothelium and the extracellular matrix denaturation and fragmentation. The production of xanthine oxidase is a source of oxidants in ischemia-reperfusion injuries and plasma levels in burn wounds peak before a corresponding increase in edema formation.[53] Shimizu et al. found that levels of xanthine oxidase in rats were higher in a superficial burn than in deeper burns[85]. The source of the xanthine oxidase in burn tissue is unknown but histamine is felt to modulate its activity post-burn injury.

Mast cells produce and release large quantities of histamine immediately post-burn injury. Histamine is associated with the increase of fluid leakage and protein permeability in capillaries and venules, although the direct mechanism is unknown. Investigators have tried to use histamine antagonists to decrease the effects described above on capillary permeability. There is considerable debate in the literature about which histamine receptors to block.[98] H_2 antagonists have been shown to decrease edema formation in some studies but there has been no benefit in others. The recently

discovered H_3 receptor showed no benefit with an antagonist but the utilization of an agonist actually improved blood flow to the burn wounds.[98] Therefore, histamine bound to the H_3 receptor appears to be an important mediator of perfusion. This would explain the associated edema with rising histamine levels, as the K_f coefficient increase is secondary to an increased surface area of perfusion. Histamine production also varies according to the depth of the burn injury.[85 99] In a small contact TBSA burn in swine, Papp found that a full thickness injury had the highest levels of histamine produced at 1–2 hours post-injury, which continued up to 6 hours post-injury. At 12–24 hours the histamine levels were comparable between the superficial, partial and full thickness injury.[99] In rats with a 20% TBSA scald burn, Shimizu et al. found that a superficial burn had the highest histamine levels measured at 15 minutes intervals up to 1 hour post-burn. The deep injury histamine levels were higher than control but less than the superficial burn. Histamine values had returned to baseline within an hour after the injury.[85] Therefore, the effect of burn depth on the levels of histamine is still controversial, but these two studies suggest that histamine accumulation differs with the depth of injury.

The presence of known oxidants post-burn injury has lead to studies utilizing antioxidants or free radical scavengers as mediators of edema formation. Antioxidants trialed include vitamin C, vitamin E, glutathione, N-acetyl cysteine, allopurinol, ibuprofen, platelet activity factor inhibitor and lazaroids.[76]

The only antioxidant that has shown promise is the utilization of vitamin C during resuscitation. In a rat with a 10% TBSA scald burn, vitamin C has been shown to limit

the initial decrease in the negative P_{if} and bring the values of the interstitial hydrostatic pressure back to baseline more quickly than rats treated with saline alone.[100] In addition, the total tissue water content is decreased in burns treated with vitamin C compared to animals not treated with the antioxidant.[100, 101] Dubick et al. showed that in a 40% TBSA flame burn in sheep that a vitamin C infusion decreased fluid requirements and the net fluid balance by 30% at 6 hours post-injury. This volume-sparing effect of vitamin C continued for 48 hours post-burn.[102] Tanaka et al. performed a randomized control trial in 37 patients with TBSA burns greater than 30%. The addition of vitamin C to the fluid resuscitation routines decreased the fluid requirements by 45% when compared to a Ringer's lactate resuscitation. This translated to a net fluid accumulation and body weight that was significantly less in the vitamin C group.[103] There have only been a handful of studies that examine the use of vitamin C in burn injuries, so its direct mechanism of action to reduce fluid volumes and edema formation is still unknown. It has been hypothesized that vitamin C is a free radical scavenger in the burn wound by reducing vitamin E free radicals and the hydroxyl and superoxide radicals. Burn wounds treated with vitamin C show less malondialdehyde (MDA) in the wounds than non-treated wounds.[103]

Prostaglandins, such as thromboxane and prostacyclin, are present in burn edema and plasma.[104] Injury to the cellular membrane would activate the hydrolysis of arachidonic acid from phospholipids and produce prostaglandins.[104] High levels of thromboxane B2 and prostaglandin in the lymphatics have been shown to be high 3 hours post-injury. These values are elevated for 12 hours after the burn before returning to baseline.[97] Thromboxane is a potent vasoconstrictor, which decreases blood flow to the wound,

increases membrane permeability, and enhances platelet aggregation and neutrophil margination.[105] Inhibition of thromboxane has been shown to improve blood flow and reduce edema. However, these results are controversial as other studies have been unable to replicate the findings.[106] Overall, others have felt that improving the prostacyclin to thromboxane (PGI2:TXA2) ratio is beneficial for the survival of ischemic tissue. PGI2 is a vasodilator and inhibitor of platelet aggregation.[107]

Kinins such as bradykinin have been found in burn wound edema fluid and are potent mediators of pain, increased vascular permeability and vasodilation.[76, 108] Bradykinin has a short half-life, making it very difficult to measure its levels directly. Consequently, bradykinin antagonists have been used prove its presence in tissue. In animal models, bradykinin antagonists have been shown to improve blood flow in deep or full thickness burns. However, the bradykinin antagonists have to be given pre-injury in order to show any beneficial effects. A recent study by Jonkam et al. suggested that specific bradykinin receptors, B_2 receptors, have to be blocked in order to reduce lymph flow and fluid accumulation.[109] Bradykinin likely plays a role in burn wound edema physiology, though the exact nature or its mechanism of action in is still unknown. In the future, as more becomes known about the role of the mediators in burn injury, the pathophysiology of edema will become clearer.

1.4.3 **Burn Edema Non-Invasive Devices**

One of the difficulties in assessing burn wound edema and the impact of treatments on edema is the fact that there are very few methods for non-invasively measuring water

content. Several technologies other than near infrared technology have been used to assess edema or the hydration of skin non-invasively. They include electrical impedance methods, ultrasound and magnetic resonance imaging, and spectroscopy. Other than NIR spectroscopy, the only technology utilized to assess burn edema is an electrical impedance technology.

Electrical techniques utilize the impedance (Z), or total opposition to electrical alternating current, to assess the water content of the skin. Impedance depends on the resistance, capacitance and frequency of the applied alternating current as shown.[110–112] There are several commercial technologies that utilize impedance measurements to assess hydration in skin. The commercial devices measure different aspects of skin impedance but the designs are all based on the same basic principles of circuits. An alternating current or an electromagnetic wave is applied and travels through the skin. The skin acts as a resistor and capacitor that shifts the phase of the current returning to the detectors. The coaxial probe, which measures the electrical properties of the skin, is designed as a series of concentric rings. One ring will transmit a high-frequency electromagnetic incident wave and the other rings or detectors collect the reflected waves.[113–115] The probe geometry is important as the ring distance determines the depth of penetration into the tissue.

Impedance technologies are designed to detect hydration changes in the stratum corneum or the epidermis. They are mainly used by dermatologists and industry to assess skin lesions, therapeutics or moisturizers. In the area of burns, surface capacitance has been used to evaluate the epidermal barrier development in skin

substitutes such as cultured epidermal autograft.[111, 116] The only technology that has been redesigned to assess water in the deeper portions of the skin is the MoistureMeter from Delphin Technologies. The MoistureMeter technology is a capacitance-only technology that relies on changes in the tissue dielectric constant. If there is a high content of water then the electromagnetic radiation will be absorbed and the energy of the reflected wave is reduced. From the reflected wave, the dielectric constant is calculated and is considered to be a direct measure of tissue water content.[114]

Electrical impedance technologies have shown promise in the investigation of the hydration of skin. The impedance technology of interest in burn depth (MoistureMeter-D) has also been used to assess fluid changes following cardiac surgery, cerebral edema, irradiated skin after a mastectomy and burn tissue edema content.[115, 117–119]

1.5 Reference Standard for Burn Depth Determination

Clinical assessment is still considered to be the most reliable way to assess the viability of the wound despite its 60-70% accuracy rate, or as Heimbach stated, “it is like flipping a coin.”[1] Over the last 10–20 years, innovative tools have been designed to assess burn depth. The reason some of these technologies have not been overwhelmingly successful is partially related to the poorly defined reference standard for burn depth determination histology.

Over the past five years, the capacity of near infrared spectroscopy has been tested as a non-invasive tool to assess the progression of injury. It was evident early in the course of

this work that the reference standard was subjective and lacked clear consensus criteria. Determining the accuracy of any new diagnostic tool requires the use of a validated reference standard. This is in concordance with the FDA's STARD (Standards for Reporting of Diagnostic Accuracy) guidelines and is important to recognize for all future work in the area.[120]

The reference standard for burn depth determination has not been revised in over 50 years. Compared to other areas of medicine, the standards used in burn depth determination have lagged behind. For example, staging systems in oncology have undergone multiple revisions in the last decade alone.[121] Clearly, a need exists to establish clear criteria to measure the severity of tissue injury.

The criteria for histological burn depth determination lacks consensus in the literature with respect to which staining techniques yield accurate results or even how to interpret the findings. Investigators infrequently report the criteria used to define burn wound depth and rarely is it stated that the pathologist was blinded to the clinical diagnosis. Histology is dependent on observer reliability, and the final report is a professional opinion based on an individual's experience and judgment. Also, a pathological diagnosis is not always clear-cut and differentiation may be based on minor morphological features.[122] Therefore, it is imperative that histopathological criteria be defined to aid pathologists in the diagnosis of burn wound depth and that standards are created that define the various levels of burn injury. With increasing reliance on pathology as the reference standard for burn depth diagnosis, it is crucial that accurate histology grading criteria are established.

1.5.1 **Vimentin Immunostaining as an Adjunctive Staining Technique**

Histopathology has made major advancements over the past 30 years with the advent of immunohistochemistry. Vimentin immunostaining has shown promise as an immunohistochemical technique to assess burn depth. A pillar paper published by Nanney et al. in 1996 used vimentin successfully to document the progression of burn injuries and distinguish burn depth.[25] The findings from this paper were impressive and quickly adopted by the burn community as a new reference standard for burn depth determination. Diagnostic tools trialed to assess burn depth have received scrutiny, if not validation, through the use of vimentin immunostaining as the reference standard. Currently, there are no published guidelines on the utilization and interpretation of vimentin immunostaining in burn wounds.

The publication of the vimentin immunostaining paper represents a paradigm shift in histology. Monoclonal antibodies were identified in the early 1980s and provided pathologists with a new tool for tumour and cell differentiation.[123] The availability of intermediate filament protein antibodies allowed pathologists to identify the same antigens in different types of tissue or in diseased tissue. Intermediate filaments became useful in pathology because they have a “stable expression even after transformation to pathological states.”[123] This permits specific cell type staining and has aided pathologists to make more concise diagnosis of specific diseases.

Vimentin is a class III intermediate filament protein that is part of the eukaryotic cytoskeleton. Vimentin is a 52kDa protein that is found in cells of mesenchymal origin and has structural similarities to GFAP and desmin but is immunologically distinct from these class III intermediate filaments.[124, 125] The role of vimentin in the cytoskeleton is still largely unknown. The vimentin knockout mouse (vim -/-) does not yield a specific phenotype and instead appears to be completely normal.[126, 127] However, upon closer inspection vim -/- fibroblasts have decreased motility, which is related to impaired wound healing in these mice.[124]

Vimentin has been shown to be useful in the delineation of viable from non-viable tissue in thermal injuries. Vimentin is the most ubiquitous intermediate filament expressed during cell differentiation. It is expressed by mesenchymal cells such as fibroblasts, endothelial cells, macrophages, neutrophils, and lymphocytes, as well as myoepithelial cells such as eccrine glands.[128] Fibroblasts, endothelial cells and eccrine glands play an important role in the viability of the burn wound, as they represent the regenerative capacity of the tissue. Vimentin immunostaining, therefore, is a marker of cell differentiation in structures important to burn wound healing. Consequently, the viable portions of a burn wound should show positive vimentin immunostaining and the non-viable regions should show negative immunostaining.[25] It is felt that the absence of staining is an indication of non-viability of the tissue and could be used as a marker of burn wound progression in acute wounds.

1.6 Modalities for Assessing Burn Depth

1.6.1 Thermography

Thermography use was first reported as a technology to assess burn depth by Lawson in 1964. Thermography uses an infrared camera to determine the surface temperature or the emitted infrared radiation from burn wounds. Deep injuries have a decrease in temperature in comparison to superficial injuries, with a reported accuracy of 90% in terms of burn depth determination.[129]Thermography has not been widely accepted as it is greatly affected by environmental temperatures.[130] The information obtained using thermography is also not clinically useful in predicting outcome for patients.

1.6.2 Vital Dyes

Indocyanine green (ICG) and fluorescein fluorescence have been used to assess blood flow to the burn injury. Once the dye is injected, either an ultraviolet or near infrared light is used to excite the dye. The excited dye will emit photons that can be detected by a photon detector and transformed into an image. Peak ratio times for the dye to enter the tissue are decreased for full thickness injuries compared to partial thickness injuries.[131]

The injection of vital dyes has fallen out of favour due to the invasiveness of the technique. Also, once the dye is injected it requires hours in order to be fully washed out of the tissue and multiple measures cannot be acquired. The lack of washout is also affected by the leaky endothelium post-burn injury and the dye is transported into the interstitium. Finally, the results from the dye tests are affected by ointments, creams and burn eschar. All of these features make vital dyes impractical in the clinical environment.

1.6.3 **Ultrasound**

High-frequency ultrasound detects echoes or reflected sound waves, which are a property of the acoustic impedance of the tissue. In burn wounds, the acoustic interface is created by the division between necrotic tissue and viable tissue. This interface is the physical division line that separates healthy and non-healthy tissue. An acoustic interface in burn tissue suggests that there is a certain cut-off level within the skin, and everything above the level is non-viable and everything below is viable. This concept is difficult to apply to burn wounds as they are dynamic in nature and there is significant variability within all levels of the tissue. Also, the deep signals are believed to represent patent deep dermal blood flow but others have countered that these echoes are from the dermal fat interface. Finally, the ultrasound probe requires contact and pressure with the tissue, which can be painful.[10, 132]

1.6.4 **Optical Coherence Tomography (OCT)**

Optical coherence tomography is based on the propagation and reflection of polarized light in burn tissue. Thermal injury causes collagen to change from a rod-like alpha helix to a random coil conformation. The inter- and intramolecular bonds are lost, which leads to a measurable loss of bifringence.[133, 134]

OCT has been criticized as patient movement, breathing and any inadvertent perturbation of the sensor are serious confounding factors leading to variation in measurements from different sites in the same subject and from one site in a single

individual at intervals of minutes, hours and days. OCT also does not have a deep penetration depth and is limited to the epidermis and upper portions of the dermis. Although collagen is one of the variables utilized to determine burn wound viability, the vasculature and presence of viable epithelium are also important and are not measured with this device.

1.6.5 **Magnetic Resonance Imaging**

Magnetic resonance imaging has used the physical state of water in the tissue to assess the degree of thermal injury according to T1 and T2 relaxation times. Partial thickness and full thickness injuries could be distinguished at 48 hours post-burn based on water content.[13] However, in this particular study by Koruda et al., the burn tissue of the rat had to be excised and placed in optical density tubes for T1 and T2 time determinations. Nettlblad used magnetic resonance imaging to assess electrical burns in a few patients. T2-weighted images could localize the muscle necrosis not seen visually on the surface of the skin.[135] Schweizer used ^{31}P-NMR spectroscopy to assess 4% TBSA burns in rats.[136]

Magnetic resonance imaging is not practical in the clinical burn environment as the study period takes too long and there are specific ferromagnetic requirements to ensure the safety of the patients in the imaging suite. Typically, skin grafts are secured to a wound bed using hundreds of staples, which is an automatic exclusion for MR imaging. Large TBSA burns are hemodynamically unstable, making repeated transports to an imaging modality difficult. Spatial distortion is a problem with MRI, as any involuntary movements

decrease the signal to noise ratio. MRI is expensive and may not be cost-effective in an already expensive burn wound environment. Finally, the visualization of skin requires a specific skin gradient coil that currently has only been used to assess peripheral limbs.

MRI is not practical for burn skin assessments but it is an accepted medical technology in which the physics and mathematics have been well-delineated. There are multiple research groups working in the area to make advances in the capabilities of MR technology. MRI technology relies on the protons of water to create images, therefore it is an accurate measurement of water content. This means that MR could play an important role in the research environment when trying to validate new devices for edema assessment.

1.6.6 **Laser Doppler**

Laser Doppler is a valuable non-invasive tool to assess burn depth. The technology relies on a frequency shift between stationary and moving blood cells within a sample of tissue. These results are then converted to an arbitrary measurement that reflects the movement of the red blood cells. The results for laser Doppler are usually reported as either perfusion units (PU) or a flux value that represents blood flow within the tissue. The units of perfusion are determined by the type of commercial device used in the studies.

Laser Doppler was popularized by Pape et al. in a study published in the *Burns* journal in 2001. In this study, laser Doppler was used in a prospective fashion to determine the

treatment for burn wounds of indeterminate depth. Laser Doppler divided the patients into wounds requiring surgery (non-viable) and wounds (viable) that would heal in less than 21 days. The non-viable wounds as predicted by LDI had 100% correlation with histology findings. This was unlike the clinical diagnosis where the agreement with histology was 81%. LDI was able to predict viable wounds in 95% of the cases whereas the clinician was accurate for 70% of the wounds.[137] The Pape et al. study was based on a previous paper by Niazi et al. in which 13 patients with wounds of indeterminate depth were evaluated with LDI. The laser Doppler and histology had 100% correlation while clinical judgment only correlated with histology in 41% of cases.[138] These studies prove that the clinical prediction of outcome for indeterminate injuries can be inaccurate. They also support the need to develop and utilize objective technologies that can accurately predict the burn wound outcome.

Laser Doppler has also been used to document the progression of burn injuries. Kloppenberg showed that perfusion remains low and does not change over time for burn wounds requiring surgery. Very superficial injuries show an initial increase in perfusion but overall decreases in a 12-day period. Wounds that heal in less than 2 weeks have increased perfusion that peaks at 4 days post-burn before declining towards baseline. Finally, wounds that heal in less than 3 weeks have increased perfusion that remains high for 12 days post-burn injury.[5] Schiller also monitored perfusion over time and found that healing wounds had high perfusion at 1 and 5 days post-burn compared to wounds requiring surgery. However, there were no differences between burn depths at 3 days post-burn.[27]

Laser Doppler is the only technology in the assessment of burn depth determination that has achieved success at differentiating viable and non-viable injuries. Laser Doppler does have some inherent limitations that have impeded its widespread application for burn depth determination. Studies performed using laser Doppler are difficult to compare as they report different values for perfusion (PU versus volts) and the cut-off values to define burn depth categories vary from study to study. Eschar and interstitial edema can interfere with laser Doppler measurement's assessment of blood flow.[4] Silver-based dressings, such as silver sulfadiazine and acticoat, utilized in burn wound treatment impede the laser Doppler signal and display the image pixels as areas of low perfusion.[6] Finally, the laser Doppler images can be difficult to interpret as they are based on a colour palette and there is a learning curve associated with the interpretation of the results.

1.7 Near Infrared Spectroscopy Technology

1.7.1 General Overview

The discovery of NIR light occurred over 200 years ago when Herschel determined that there was a temperature increase in the region next to the red region of the visible spectrum. Herschel coined the term "infrared" radiation, or light above the red. The application of NIR light did not become practical until the mid 1960s when Karl Norris used the device industrially.[139] NIR technology became popular as a medical tool to assess oxygenation after a publication by Jobsis in 1977 that showed its potential to monitor cerebral oxygenation.[140] Since this time, NIR has been used as an investigative tool to assess cerebral and muscle perfusion along with the determination of end points

of resuscitation in trauma patients.[141–146] Its capacity to accurately determine blood volume and oxygenation has been well-documented in the literature. Near infrared-based technologies can accurately monitor altered tissue hemodynamics and hydration that occurs deep within the tissue as a result of impaired circulation or ischemia.

The near infrared range within the electromagnetic spectrum is between 600–2500 nm. Light in this region poses no risk to the patient or the investigators use this type of electromagnetic radiation. Near infrared technology's ability to assess chromophores in tissue is related to the absorption and scattering of light at specific wavelengths. Chromophores that can be measured in the NIR region include water, methemoglobin, cytochrome aa_3, deoxy- and oxy-hemoglobin and myoglobin.[147, 148] The basic principles of NIR spectroscopy, device design and the utilization of the technology for medical applications are discussed in this section.

1.7.2 **NIR Point Device Design**

Near infrared spectroscopy devices consist of the following basic components.

1) Electromagnetic Energy Source
2) Light Delivery and Collection system
3) Wavelength Selection
4) Detector

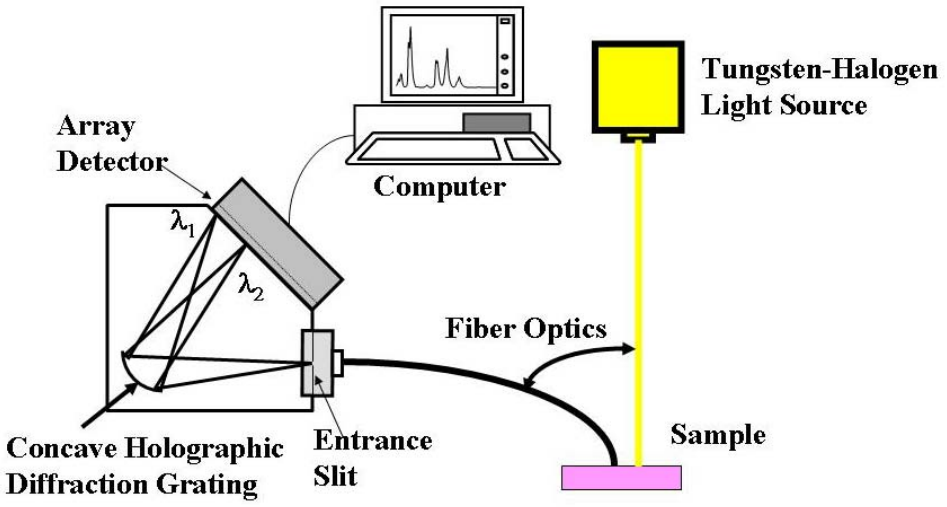

Figure 1-2: NIR Point Spectroscopy Device Design Schematic

The NIR Point device utilized for this thesis is shown in Figure 1-2. The light source is a tungsten filament lamp that provides radiation from 400–2500 nm. Light is delivered and collected from the tissue via a multi-optical fiber probe. The multi-optical fiber probe consists of one light deliver fiber and four detection fibers that are housed in one unit. The diameter of the probe head that rests on the skin is 1.5 cm. Light from the tissue is collected by the four optical fibers and delivered to the entrance of the wavelength selection-detection system. The wavelength dispersion element utilizes a diffraction grating to spatially divide the light into selected wavelengths. These selected wavelengths of light are detected by a charge coupled device or CCD. The CCD is an array of closely packed mini photoelectric semiconductors. The CCD converts the light signal to an electrical signal, which is recorded on the computer. A digital photo of the device is shown in Figure 1-3.

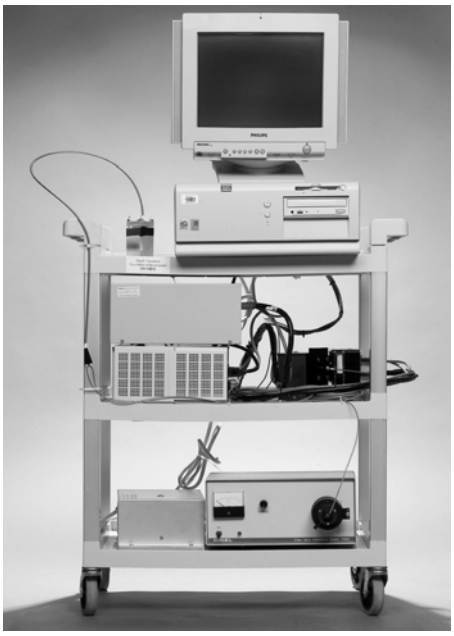

Figure 1-3: NIR Point Spectroscopy Device

NIR devices can be classified in many different ways based on their technical design. However, it is hard to place NIR devices into discrete categories based on the components incorporated in the devices. A better classification method uses the capacity of the NIR technology to measure absolute or relative concentrations of the devices. Devices that assess the relative concentration of chromophores do not require an exact light pathlength determination, while devices that assess the absolute concentration of chromophores in tissue are able to calculate the pathlength of light through the tissue.

The best examples of NIR spectroscopy devices that calculate the relative concentration change in the chromophore include pulse oximetry and the NIR device used for the thesis experimental work. Pulse oximetry is a clinically-accepted technology for assessing oxygenation and was the first application of NIR in the clinical environment.

Pulse oximetry is a non-invasive near infrared measure of oxygen saturation based on the ratio of oxyhemoglobin to total hemoglobin. There are only two wavelengths utilized for oxyhemoglobin (940 nm) and deoxyhemoglobin (660 nm). These wavelengths are based on the absorption coefficients of oxy- and deoxyhemoglobin.[149, 150] Pulse oximetry is unable to detect the presence of other hemoglobin species in the tissue because of its limited wavelength selection and consequently is not accurate in the presence of dyshemoglobinemias.

The NIR Point device used for the work in thesis measures the relative concentration of the chromophore. It is also known as a broadband spectroscopy device. The term broadband refers to the large range of wavelengths within the electromagnetic spectrum that can be utilized to measure the absorbance characteristics of the sample. The overall NIR device design was described in Figure 1-2. The major differences between NIR devices that measure relative concentrations are related to the differences in wavelength selection and the detection systems.[150]

The absolute determination of chromophore concentrations is possible with NIR devices that can accurately determine the pathlength of light in tissue. There are currently two types of systems that are able to measure the optical pathlength. The first device is a “time of flight” method that utilizes small pulses of light. A beam splitter divides the light into two directions, with one beam directed at tissue and the other beam to a reference detector. The pathlength is calculated by the time difference between the reference and response detectors (light collected from tissue).[151] The second method is a frequency-modulated technique that detects a phase shift of light.[151] In this design the incident light

is comprised of lasers oscillating at specific frequencies. The detected light will be out of phase from the incident light and this change can be used to calculate the pathlength of light through the tissue.

1.7.3 **NIR Point Device Calibration**

Calibration of an *in vivo* NIR Point Spectroscopy device occurs in two stages; the first phase is a system calibration and the second phase a variable calibration. The system calibration occurs in three stages (filter, dark reference count) in which the probe is place in a prefabricated calibration box. The calibration box consists of one slot containing a didymium filter and one slot containing Spectralon® (Labsphere, NH). The filter count is measured by placing the probe within the didymium filter slot and turning the light source on. Didymium has three distinct peaks at 575 nm, 730 nm, 800 nm. These characteristic peaks are used to ensure the device is functioning correctly and that all four detection fibers are collecting data. The dark count is obtained by placing the probe within the didymium filter slot with the light source off. The dark count measures the inherent noise within the system and has to be subtracted from the spectrum that is collected. Finally, a reference count is measured with the probe placed in the Spectralon® slot with the light source on. Spectralon® has the highest diffuse reflectance of any known substance (95-99%) and is spectrally flat in the NIR region.[152] The reference measurement of light reflectance is called the raw reflectance and it occurs over the same series of wavelengths utilized for the sample (unknown) reflectance. The sample or unknown in this research study is porcine skin (burn or control).

The computer records a signal representing the actual wavelength used for measurement with the raw reflectance and the sample. The spectrum becomes the difference between the raw reflectance measurement of the sample and the raw reflectance measurement of the reference material (Spectralon®). The CCD of the NIR Point device does not measure absorbance directly and instead records the level of incident light and measured light. The log (measured light/incident light) is the absorbance, which is measured in optical density units or OD. To account for the inherent noise in the system and to convert the measured values to absorbance units, the following equation is utilized:

$$\log(sample - darkcount) \div (referencecount - darkcount)$$

Absorbance will be described in further detail in Sections 1.7.4 and 1.7.5. The second phase of calibration, variable calibrations, will be discussed in Section 1.7.5.

1.7.4 **Beer-Lambert Relationship**

The basic principles of NIR spectroscopy are based on the Beer-Lambert law, which states that light transmitted through a material containing chromophores will be absorbed and the emitted light will have a reduced intensity.[148] The attenuation of light can then be used to determine the concentration of the chromophore in the tissue.

The basic principles of laboratory spectrophotometers can be used to illustrate the Beer-Lambert relationship. It also serves as a foundation for the more complex extraction of

chromophores from tissue spectra. Figure 1-4 is a pictorial illustration of light propagation and attenuation for a spectrophotometer. Spectrophotometers are designed such that incident light of a specific intensity (I_o) passes through the cuvette wall, through the sample and out through the cuvette wall to a detector. The light that exits from the cuvette is attenuated or reduced and this is measured as the reduced light intensity (I).

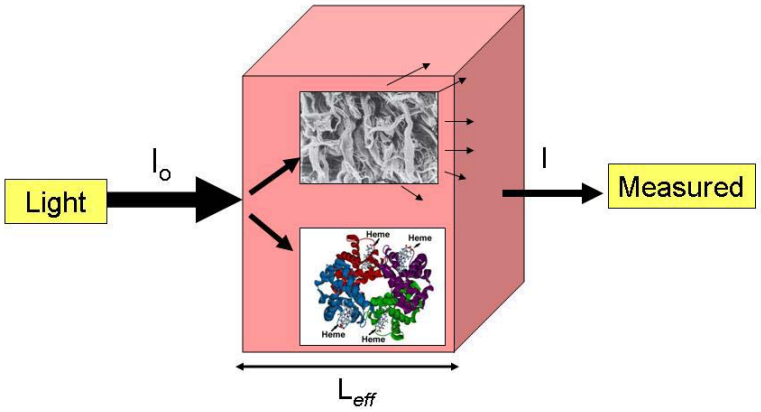

Figure 1-4: Light Propagation and Attenuation in Tissue

Transmittance is the ratio of the reduced intensity to the incident intensity of light (I/I_o). The logarithm of the inverse of the transmittance is called absorbance. The absorbance of light, in optical density units, is explained by the Beer-Lambert law:

$$A_\lambda = \log (I/I_0) = \varepsilon\, c\, L$$

which states that the absorbance (A_λ) of light is proportional to the concentration (C) of the chromophore, where ε_λ [$cm^{-1}mM^{-1}$] is the wavelength-dependent absorption

coefficient, C [mM] the concentration of the chromophore and L [cm] the path length of light.[147, 148, 153] Therefore, by knowing the extinction coefficients, the pathlength of light and the attenuation of light, the concentration of the chromophore can be calculated using the Beer-Lambert relationship. The absorption coefficient is a measure of how strongly a molecule absorbs light at a particular wavelength of light. The extinction coefficient is a calculated constant acquired from the literature.

In tissue, the analysis of the chromophores is more complicated as there is more than one absorbing compound in the sample. The measured absorptions (A_m) are assumed to be linear functions of the extinction coefficients and the concentration of the chromophores present ($A_m = A_{Hb}+A_{HbO2} + A_{H20}$). The extinction coefficients are wavelength-dependent and therefore the equations have to be solved at each wavelength as shown by the equations below:

$$A_{\lambda 1} = (\varepsilon_{1,\lambda 1}\,[C]_1 + \varepsilon_{2,\lambda 1}\,[C]_2 + \varepsilon_{3,\lambda 1}\,[C]_3\,L)$$

$$A_{\lambda 2} = (\varepsilon_{1,\lambda 2}\,[C]_1 + \varepsilon_{2,\lambda 2}\,[C]_2 + \varepsilon_{3,\lambda 2}\,[C]_3\,L)$$

$$A_{\lambda 3b} = (\varepsilon_{1,\lambda 3}\,[C]_1 + \varepsilon_{2,\lambda 3}\,[C]_2 + \varepsilon_{3,\lambda 3}\,[C]_3\,L)$$

1.7.5 **Pathlength of Light**

The pathlength of light is a known entity in laboratory spectrophotometers but this is not always the case for *in vivo* spectroscopy devices. The determination of pathlength has been one of the greatest challenges when utilizing the Beer-Lambert law to extract the concentration of the chromophore from light attenuation in tissue.[153]The pathlength of

light is dependent on both the scattering and absorption properties of the tissue. Light intensity is lost secondary to scattering and absorption by one order of magnitude per centimeter of tissue traversed (one optical density per centimeter).[151]

Incident light that enters the tissue is scattered in many directions. The photons will either be forward- or backward-scattered. Forward scattering occurs when the light traverses in the same direction as incident light. Backward scattering occurs when scattered light changes its direction from the incident light by 180°.[153] Scattering is a product of the refractive index of the structures that reside within the tissue. Cell walls, blood vessels and the matrix of collagen all have a refractive index that changes depending on the cell density, size and shape of particles.[150, 151, 153]

Near infrared light experiences tissue-scattering that is two orders of magnitude greater than absorption. It is this combination of low absorption and high scattering that imparts near infrared light's deep penetration into the tissue.[150] Penetration depth has been reported from as low as 1 cm to as high as 10 cm into the tissue.[150] The deep penetration depth gives NIR light distinct advantages over other optical technologies. For example, visible light cannot penetrate greater than 1 cm into the skin due to its attenuation by scattering and absorption.[147]

NIR spectroscopy's reliance on the scattering of light for forward propagation is also one of its limitations. Forward scattering of light changes the path that light traverses through the tissue. Therefore, pathlength *in vivo* is both a property of the physical or geometric pathlength (L) and the optical pathlength (L_o). The optical pathlength, or differential

pathlength factor, is the actual distance that scattered light takes through the tissue and can be difficult to quantify.[147, 153] The differential pathlength factor in a normal adult head is 6.3, which means light travels 6.3 times further than a straight line path. The differential pathlength factor is also wavelength-dependent.[147] This has direct implications to the Beer-Lambert relationship, as the pathlength has to be known in order to calculate the concentration of the chromophore.

In the mathematical algorithms used in this thesis to extract the concentration of the chromophores from the measured spectrum, a linear scatter term is added to the Beer-Lambert relationship:

$$A_\lambda = \log (I/I_0) = \varepsilon_\lambda C_\lambda L + m\lambda + \text{offset}$$

The linear scatter term is an assumption that the scattering coefficient is large but constant over the wavelengths of interest. The term $m\lambda$ is added to the Beer-Lambert law to account for the light attenuation by scattering in the tissue.

Light is absorbed by the chromophore if the wavelength of incident light has the correct energy to interact with the molecule. The photon raises the energy of the molecule and excites it to a higher energy state, resulting in molecular vibrations. Absorption bands in the near infrared region are related to the overtones and combinations of fundamental vibrations of O-H, C-H, N-H bonds.[139, 150] In the NIR region, the strongest absorbers of light are oxy- and deoxyhemoglobin, methemoglobin and water. These chromophores produce distinct spectra that can be used as a fingerprint for the molecule.

The region between 600–1050 nm is utilized with the NIR Point device to extract the variables of interest. The region between 600–850 nm is generally used to determine the *in vivo* measurement of tissue hemoglobin. There are other chromophores in this region, including melanin, oxy- and deoxy-myoglobin, cytochrome oxidase and methemoglobin. The region between 900–1050 nm is used to determine the water content in tissue and within this region fat has a distinct absorption spectrum. Extinction coefficients are used to deconvolute the overlapping spectra of major chromophores in the region.

1.7.5.1 **Hemoglobin Spectrum**

In the visible portion of the spectrum, oxyhemoglobin has two peaks at 540 nm and 576 nm (bright red colour) and deoxyhemoglobin has one peak at 555 nm (dark red colour). The visible region is generally not utilized secondary to the attenuation of light by melanin in the epidermis and the depth limitations of this light.[150] In the near infrared region the spectra for oxy- and deoxyhemoglobin look featureless, unlike the visible region. Extracting deoxy and oxyhemoglobin occurs over the range of 700–900 nm because scattering remains fairly constant within this range. Light absorbance is equal for oxy- and deoxyhemoglobin at 800 nm or the isosbestic point. Deoxyhemoglobin light absorbance predominates below the isosbestic point with an absorption maximum at 760 nm. Oxyhemoglobin light absorbance is higher than deoxyhemoglobin at wavelengths greater than the isosbestic point.[37, 154] Therefore, at particular wavelengths the light absorption by oxy- or deoxyhemoglobin will predominate, although the entire region of 680–820 nm is used to extract oxy- and deoxyhemoglobin content. The absorption coefficients for oxy- and deoxyhemoglobin utilized to generate the reference

spectrum were acquired from Scott Prahl's compilations of W.B. Gratzer (Medical Research Council Labs, Holly Hill, London) and N. Kollias (Wellman Laboratories, Harvard Medical School, Boston) studies.

Methemoglobin has a prominent Soret band at 411 nm with a weaker absorption peak at 630 nm. The 630 nm peak is within the visible near infrared region and is the preferred wavelength for deep penetration into the tissue.[155, 156] The absorption coefficients for methemoglobin used to generate the reference spectrum were acquired from Zijlstra.[157] Absorption spectra for Oxy-, Deoxy-, Carboxy- and Methemoglobin are shown in Figure 1-5.

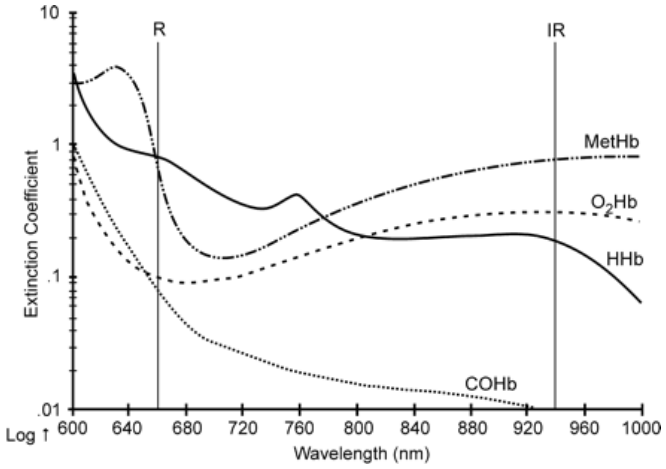

Figure 1-5: Absorption Spectra of Oxy-, Deoxy-, Carboxy- and Methemoglobin[43]

1.7.5.2 **Water Spectrum**

One of the strongest absorbers of light in the near infrared region is water.[147] In the near infrared region, there are several absorption bands that represent the large amplitude

stretching vibrations between oxygen and hydrogen (O-H bond of water). The first overtone, symmetric and asymmetric OH stretching, as well as an OH-stretch-stretch combination, occur at 1440 nm. The second overtone is at 980 nm and the third overtone is located at 740 nm, as shown in Figure 1-6. There are also combination bands at 1940 nm and 1200 nm. Combination bands are the product of a symmetric and asymmetric OH stretching mode plus an HOH bend.[158] Light absorption by tissue in these spectral regions is mainly due to water, which enables NIR technology to directly measure the water content.[159] The intensity of the absorption bands are proportional to the amount of water in the tissue and NIR technology can be used to quantitate water in tissue.[160] The absorption coefficients for water used to generate the reference spectrum were acquired from Scott Prahl and are centred around the 980 nm overtone.[156]

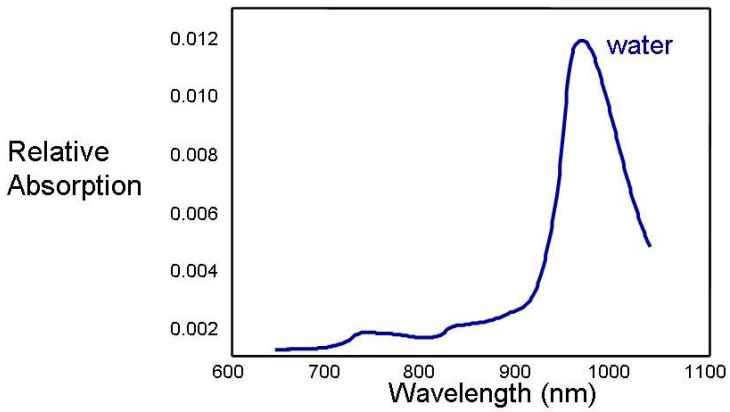

Figure 1-6: Absorption Spectra for Water

1.7.5.3 **Myoglobin Spectrum**

Myoglobin and hemoglobin have similar absorption spectra for their deoxygenated and oxygenated forms. Investigators working in the area of skeletal muscle physiology actually report the results from their studies as a combination of hemoglobin and myoglobin. In the fiber geometry, or the separation distance between the source collectors utilized in this study, the contribution of myoglobin to the spectra of skin should be minimal, as myoglobin is exclusively located in muscle. However, it is possible that the deep source collector 4 could be interrogating a portion of the muscle. Theoretically, if myoglobin was contributing to the spectra in the deep collectors there should be an elevation in the amount of both oxy- and deoxyhemoglobin content in this source collector.

The majority of the NIR signal in the 680–900 nm region is secondary to hemoglobin, not myoglobin. Mancini et al. performed a study using ^{1}H-proton spectroscopy to measure deoxy-myoglobin in humans during exercise. Proton spectroscopy and NIR spectroscopy were coupled to collect measurements simultaneously. They found that the major signal in this wavelength region was from deoxyhemoglobin, not myoglobin. In the same study, the veins of the forearm muscle were cannulated and blood gases acquired to monitor oxygenation. There was a linear correlation between the 760–800 nm absorption and changes in venous saturation (correlation coefficients between 0.82–0.97). A similar study was repeated in dog gracilis muscle and there was a linear relationship (correlation coefficient 0.97–0.98) between venous oxygen saturation and changes in NIR absorption in this region.[161] Finally, ethyl hydrogen peroxide was injected into the venous system of a dog to convert myoglobin to its ferrous form so it would stay

oxygenated. This ensured that myoglobin did not contribute to the 760–800 nm absorption region. NIR measurements were acquired before and after the ethyl hydrogen peroxide injection and there was no change in the absorbance spectra. If myoglobin was contributing to the spectra in this region then there should have been large changes in the absorption spectra for deoxyhemoglobin. The fact that there was no change indicates that hemoglobin is the main contributor to the spectra in this region. The region between 740–820 nm is generally used to determine the *in vivo* measurement of tissue hemoglobin.

1.7.5.4 **Melanin Spectrum**

The melanin content of skin affects the absorbance of light. Melanin content varies between races, anatomic location and has seasonal variations (summer versus winter). Because light has to first pass through the epidermis (where melanin resides), it will be absorbed by melanin before it can reach the deeper tissue layers. This impacts photon migration into the deeper tissues and light absorbed by the other chromophores.[162, 163]

There have been several attempts to develop a melanin index for skin that would account for the changes in the absorbance spectrum that occur in highly pigmented individuals. Some techniques employ methods that use the slope of a portion of the collected spectrum to determine melanin content.[164, 165] Other methods compare a melanin spectrum (bloodless spectrum) to a whole spectrum (blood spectrum) and apply a pigmentation factor.[166] These techniques all require the exertion of pressure onto the tissue. This is not practical *in vivo,* as applying pressure impairs the microcirculation, impacts the results of oxy- and deoxyhemoglobin and changes the spectrum collected.

Pigmentation varies within an individual and measurements using the above techniques would have to be made at every new site. This increases the time required to collect data and limits the ability to automate the data processing algorithms, which limits the practicality of the device in a clinical setting.

Our group has developed mathematical algorithms to deal with the impact of melanin on the absorption spectra of hemoglobin. A modified Beer-Lambert equation is used to fit the observed attenuation spectrum to the number of known chromophores. Essentially, to account for pigmentation melanin is added as one of the chromophores in the univariate regression model. Comparing the results of the regression equation both with and without melanin as a variable showed that the addition of melanin as a chromophore improved the spectra of light- and dark-skinned individuals. The regression equation without melanin in dark-skinned individuals showed that deoxyhemoglobin values were underestimated by 1 order of magnitude, oxyhemoglobin was underestimated by 3 orders of magnitude and water was overestimated by 2 orders of magnitude. These results suggest that melanin should be included in all near infrared spectroscopy fitting routines used to assess hemoglobin in tissue.[163]

Accounting for melanin or skin pigmentation is important when brining a technology like near infrared spectroscopy (NIRS) into a diverse patient population. Crookes and Cohn have published a series of papers about the capacity of NIRS to assess the endpoints of resuscitation in trauma patients. As part of one of their studies, the normal values for regional oxygen saturation of the thenar eminence were assessed. They found that the regional oxygen saturation values they measured differed between Caucasians (82%),

Native Americans (83%), Hispanics (85%), and African Americans (90%). These results are likely related to the increasing melanin content of the racial groups. The InSpectra $St0_2$ (Hutchinson Technology) uses four wavelengths, 680, 720, 760 and 800 nm, to assess the oxy- and deoxyhemoglobin content of tissue.[143] It is not clear from the manufacturer's website or other publications how they process their data or even if melanin is included in their algorithms. Assuming they use the percentage of oxyhemoglobin to total hemoglobin as the $St0_2$ value and no melanin in the fitting routines, the fact that the saturation value increased in African Americans does not make sense in terms of what we know about the attenuation of light by melanin. In fact, the oxyhemoglobin levels should have declined in darkly pigmented individuals. Our studies have shown that oxy- and deoxyhemoglobin are actually underestimated without melanin within the fitting routines.

1.7.5.5 **Cytochrome Oxidase Spectrum**

Cytochrome oxidase (CtOx) is found in the mitochondrial membrane and is the terminal enzyme of the respiratory chain. The cytochrome enzyme catalyzes more than 90% oxygen saturation.[167] The enzyme has four metal centres but it is the copper (CU_A) centre that absorbs weakly in the near infrared region.[168] In its oxidized form, cytochrome oxidase has a broad absorption band at 830 nm and as the enzyme is reduced the absorption band disappears in this region.[169] Cytochrome oxidase is very difficult to measure *in vivo* as CtOx exists in very small concentrations compared to hemoglobin.[168, 169] The concentration of cytochrome oxidase is approximately 1/10 that of hemoglobin in most tissue.[169] In addition, the redox state of CtOx changes very slowly and a baseline measure is generally required, with results presented as a change from

baseline.[168] Finally, CU_A changes are only measured once extensive hemoglobin desaturation occurs, therefore it contributes little to the region used for hemoglobin extraction.

1.7.5.6 **Fat Spectrum**

There is very little published information about the absorption spectra for mammalian fat. The major peak for mammalian fat is located at 930 nm and the absorption spectrum is shown in Figure 1-7 [170]. This peak is distinct from the water peak located at 970 nm and also shown in Figure 1-7.

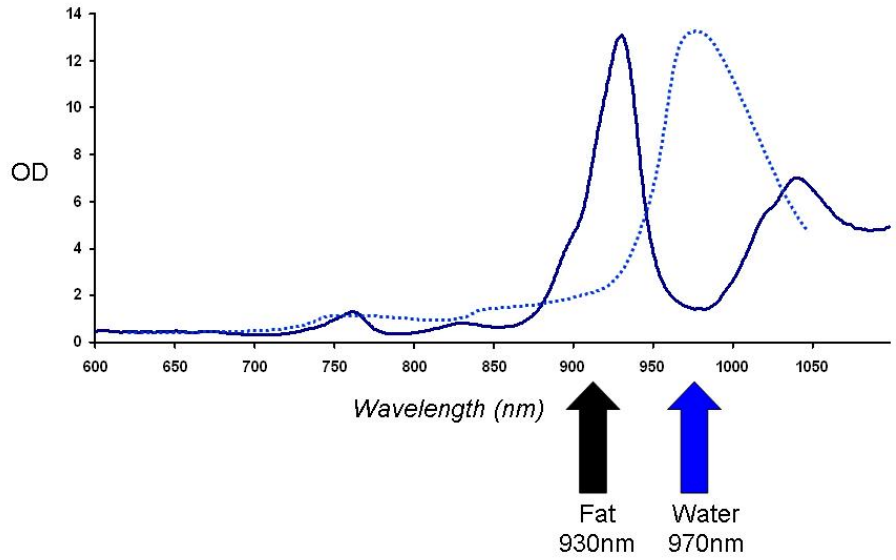

Figure 1-7: Spectrum of Fat and Water

1.7.6 NIR Device – Sources of Variability

There are several sources of variability associated with NIR Point Spectroscopy. These factors are related to instrument validation, the environment, subject factors, tissue factors and data management.

1.7.6.1 Instrument Validation

Instrument validation refers to the system and variable calibrations that are utilized for the NIR Point device. Calibration was discussed in Sections 1.7.3 and 1.7.5. Sources of variability for instrument validation are related to the constants or absorption coefficients used for the extraction of variables from the spectrum.

1.7.6.2 Environmental Conditions

1. **Temperature**

Conditions such as temperature can affect blood flow or perfusion to the skin. One of the primary functions of the skin is thermoregulation. Therefore, the body's response to increased temperature is to increase blood flow through dilated capillaries. Sweat glands are stimulated and dissipate heat through the surface evaporation of water. In the process, the hydration state of the stratum corneum increases. Humidity also increases the hydration of the stratum corneum by preventing evaporative heat losses.[171]

Studies by Hampson et al. and Mancini et al. showed that temperature increases in blood flow had minimal contribution to the NIR spectroscopy's measurement of oxygen saturation in human subjects. However, their studies had flawed study designs as they

did not specifically measure blood flow, nor did they utilize a method that could sustain a local or systemic change in temperature.[36, 172] Davis et al. rectified the methodology limitations of the previous two studies by specifically controlling temperature changes, and measuring changes in blood flow with a laser Doppler probe. From this study, temperature increases caused an increase in blood flow along with a corresponding change in oxygen saturation as measured with NIR spectroscopy. These changes were found both with local heating of the skin and systemic changes in temperature.[173] Therefore, temperature plays an important role in the perfusion of the skin and could be a confounding variable with NIR spectroscopy measurements in human skin.

2. Lighting

NIR spectroscopy data has to be collected in a dark environment. The lights produced by conventional fluorescent lighting or the heat lamps used in the burn centre produce additional noise in the spectrum. To improve the signal to noise ratio, all lighting has to be turned off when data is collected. Figure 1-8 shows the effect of the heat lamps on the spectrum of human skin versus the spectrum collected in a dark room. The top panel (dark room) represents a normal spectrum of human skin. However, collecting data with the heat lamps on (bottom panel) changes the absorbance of the NIR light as shown by the negative absorbance on the y-axis. The negative numbers mean that the skin is reflecting more than the reference sample and the spectrum is featureless.

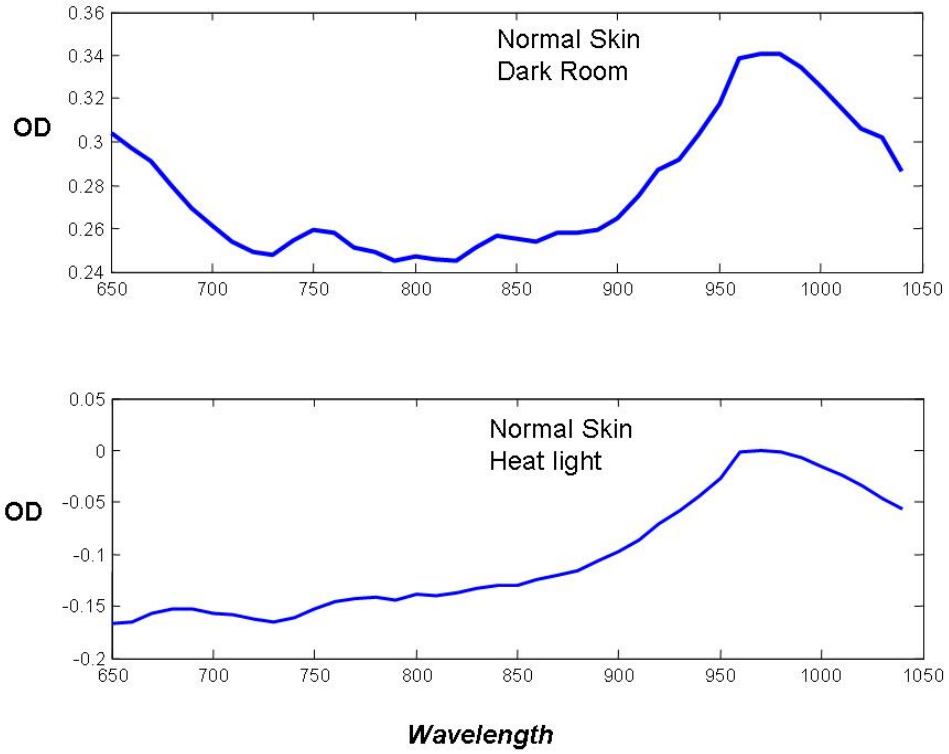

Figure 1-8: The Effects of Lighting on the Spectrum of Human Caucasian Skin

1.7.6.3 **Subject Factors**

Subject factors such as skin thickness, body position and medical therapeutics could impact the measurements acquired with NIR spectroscopy. There are several limitations when measuring blood flow and edema in skin and using a device that is designed to interrogate the various layers of the tissue. The biggest challenge for any device utilized to assess skin is the non-uniformity of skin and the variability of skin thickness. Skin thickness varies with anatomic location and age, and there are even racial variations. Skin thickness is dynamic and affected by the degree of hydration. Hydration states are

known to vary with age, gender, time of day, body position and disease states. The various hydration states influence skin thickness, which could potentially alter the tissue layer being assessed.

Skin thickness decreases with increasing age, as individuals experience a 6% loss of epidermal thickness and a 6% loss of dermal thickness per decade.[174–177] This means that the dermis of a 60-year-old will experience a 24% reduction in skin thickness compared to the average 20-year-old. This decrease in skin thickness with age is attributed to a reorganization of proteins and collagen along with a reduction in water content.[176] Skin thickness also varies with anatomic location. Skin is thicker on the back (2.2 mm) than on the eyelid (0.5 mm).[176, 178] There are racial variations in skin thickness between Caucasians and Asians.[178] There are also proportional epidermal differences, as Koreans have 8% epidermis and Caucasians have a 4% ratio of epidermis to the thickness of the skin.[178] In this animal study there was very little concern about skin thickness changes associated with age, as all the swine were the equivalent of late teenagers. Anatomic regional thickness was controlled by keeping all of the experimental sites on the dorsum of the animal. However, the effect of skin thickness on the measurement of skin hydration is a real challenge in the clinical environment and has not been resolved by this study. Electrical impedance technologies have been used to show the impact of age on the measurement of water content in the skin.[179, 180] Investigators have also used ultrasound to determine the hydration status based on the changing thickness of skin.[175, 176, 181]

There are variations in skin thickness between males and females, as females tend to have thinner skin.[174, 176, 178] These variations between the sexes become more predominant after 50 years of age.[174] In addition, female sex hormones influence skin thickness, as estrogen and progesterone in the second phase of the menstrual cycle increase water retention in the dermis.[182] Eisenbeiss performed a study in healthy menstruating women and found that skin thickness corresponds to changing estradiol levels during the menstrual cycle. Estradiol upregulates the rennin-angiotensin system and in turn aldosterone levels. Aldosterone is responsible for the reabsorption and retention of sodium and water by the kidneys. Estradiol also leads to systemic arterial vasodilation and increased capillary permeability, which produces an efflux of water into the interstitium. Finally, estradiol increases hyaluronic acid retention of water in the tissue. All of these features of estradiol serve to enhance the efflux of water from the intravascular space and cause swelling of the interstitial space. Pregnancy is the perfect example of extremely high estradiol levels and pregnant women experience a 10% increase in skin thickness in the third trimester, which is attributed to water retention.[182] Although the issue of gender is not critical in the current study, it is important to consider in the clinical environment.

There are diurnal variations in water content and skin thickness. The lower limb shows increased skin thickness from morning to night in elderly patients.[181] Positional changes also influence skin thickness. Changing the head position alone from baseline head up to head down position increased the water content in the forehead by 16%.[177] Kusano et al. also showed that in 12 healthy subjects that positional changes from supine to lateral as measured with NIR spectroscopy caused changes in regional perfusion.[183]

Our own group has investigated the changes in water content and hemodynamics that occur over time in 10 healthy subjects. NIR Point measurements were collected every 12 hours for a total of 5 days from various anatomic regions. From this study, water content, total hemoglobin and oxygen saturation did not vary over time if the location was kept constant. Figure 1-9 shows no changes in oxygen saturation of the proximal forearm over time. However, anatomic regions did differ over time with respect to water content, oxygen saturation and total hemoglobin. Figure 1-10 shows the differences in water content between all the anatomic regions investigated. Oxygenation, perfusion and water content are different from region to region and the impact of skin thickness on NIR results has still yet to be resolved.

The dielectric constant, ultrasound, MRI and MR spectroscopy and near infrared spectroscopy are all devices utilized to measure the hydration or water content of skin. Skin thickness has been a challenge for all of these technologies and one that the scientific community still needs to resolve before new technologies are fully incorporated into the clinical environment. This is not an easy problem to resolve, as the skin is dynamic and contains a variety of structures and cells that affect electromagnetic radiation.

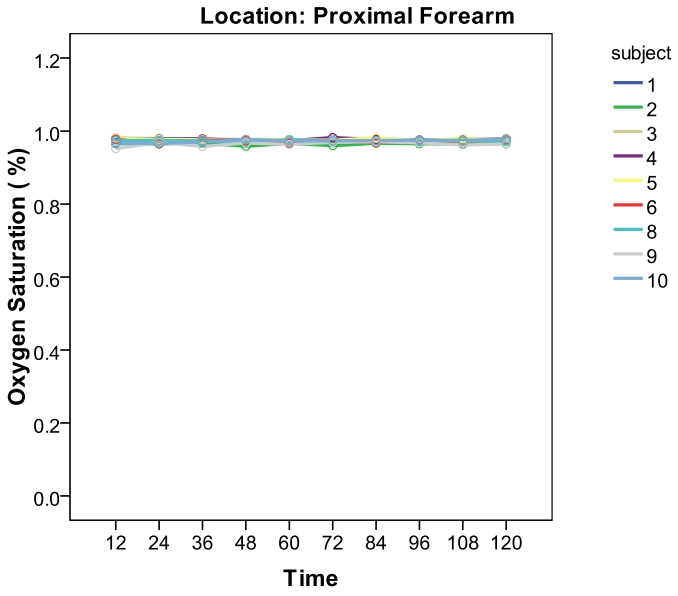

Figure 1-9: Oxygen Saturation Measurement from the Proximal Forearm of Ten Healthy Human Subjects

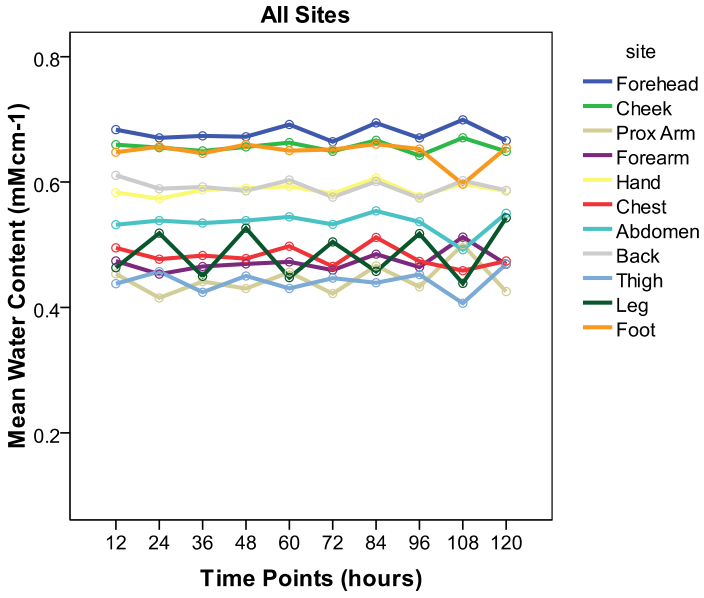

Figure 1-10: Water Content over Time at Various Anatomic Sites for Ten Healthy Human Subjects

Finally, the various creams and ointments used to treat burn wounds can impact the NIR spectrum. Silver sulfadiazine, polysporin, and skin substitutes all impact the amount of light entering the tissue and change the absorption properties of the skin. In Figure 1-11, a spectrum was collected from a finger and then again from the same finger after polysporin was applied. The spectrum collected from the finger with polysporin shows a decrease in overall absorption compared to the finger alone. Therefore, all creams and ointments have to be removed from the wounds prior to NIR spectroscopy measurements.

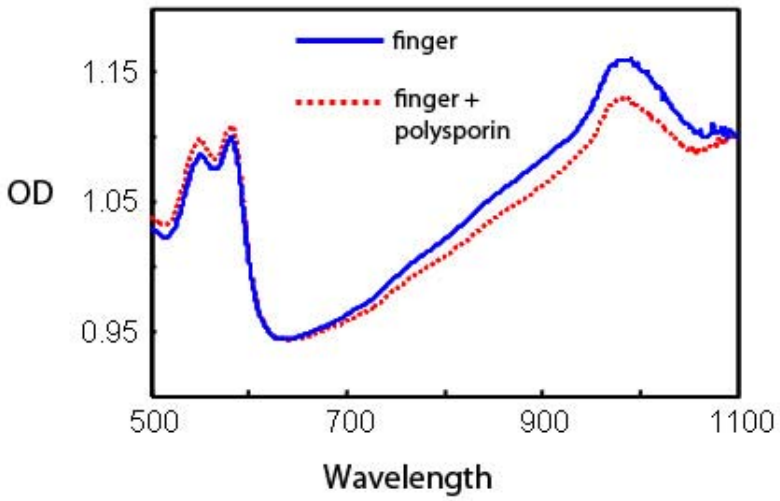

Figure 1-11: Impact of Polysporin Ointment on the Near Infrared Spectrum of Normal Human Skin

1.7.6.4 **Data Management**

The current prototype NIR Point Spectroscopy device does not provide instantaneous results when assessing wounds but instead relies on delayed data processing. This means that the data is first collected and then analyzed at a later date. Both the laboratory and clinical studies were designed specifically to develop and test the mathematical algorithms for the spectral extraction and analysis of burn wounds. In time and with future work, this will eventually be an automated process.

1.8 NIR Spectroscopy Assessment of Burn Depth

The advantages of near infrared technology far outweigh any of the current limitations of the device. NIR can penetrate deep into the tissue and in transmission mode can reach depths up to 10 cm. The devices in this study are designed to use reflectance mode and have a penetration of 2–3 cm, which is appropriate for the interrogation of skin.[150] The utilization of near infrared light also means that there is no risk to the patient or technician, as the light exposure is less than a person receives under normal room lighting situations over the same period of time. NIR spectroscopy is portable, non-invasive and can be used for any anatomical location. Data collection is fast, as one site takes approximately 16 seconds. The devices are comfortable for the majority of patients and contact occurs only with gentle placement of the probe on the burn wound. The technology was easily incorporated into routine dressing changes and did not interfere with nursing duties.[28] Finally, NIR spectroscopy permits the assessment of physiological information from the tissue. Functional assessments are not possible with conventional

imaging devices unless contrast agents are utilized. Therefore, the NIR data can be collected continuously at the bedside.

To date, very little work has been performed using near infrared spectroscopy to determine burn depth. Afromowitz used a multispectral camera to evaluate burn depth using a real time video system or imaging burn depth indicator (IBDI).[184] This technology imaged patients through a filter that incorporated visible and near infrared light at four different wavelengths. The authors used a Kubelka-Munk model to attempt to describe the propagation of light through the tissue. The simplicity of the Kubelka-Munk model has made it a popular method for measuring the optical properties of a scattering sample by diffuse reflectance. Unfortunately, the assumptions of isotropic scattering, matched boundaries and diffuse irradiance are not typical of the interaction of light in tissue. Also, the Kubelka-Munk model cannot predict the spatial distribution of light due to scattering, because the model assumes scattered light occurs in only two directions. Moreover, the authors used ratios of reflected intensities to predict burn wound healing in a temporal fashion. Ratio techniques do not provide any information about the physiologic status of the tissue and are difficult to apply beyond a sample population.[28]

Eisenbeiss used a similar spectral technology to assess burn depth.[185] The data processing method used was a fuzzy c-means cluster algorithm, which is used to look for patterns within the spectra and the patterns used to classify the burn depth. A cluster approach to burn depth assessment of this type is difficult and prone to problems. The results obtained from the cluster analysis are not related to burn depth directly but the degree to which objects satisfy imprecisely defined observations. The initial optimization

of the classification is based on clinical evaluation of the burn, which in itself contains a high level of uncertainty. Cluster populations that are very different, as is the case with burn injuries, could influence the clustering results. A small cluster can be very important but it is often not found because the larger clusters determine the overall clustering result. The difficulty in applying a cluster approach lies in the interpretation of the results in relation to the physiological response.[28]

The technology utilized for this thesis differs significantly from the two previous studies, as the wavelengths of interest are predominantly in the near infrared region and consist of more sampled wavelengths (650–1050 nm). Using the Beer-Lambert relationship, the absorption and reflectance of light are used to determine the concentration of oxyhemoglobin and deoxyhemoglobin. These variables are then translated into tissue oxygen saturation and total hemoglobin parameters. This physiologic data obtained within the site of injury can provide valuable information about blood volume and oxygenation differences between viable and non-viable injuries.

1.8.1 **Pre-Clinical Experience**

NIR technology has been utilized in both a pre-clinical and clinical setting. The first *in vivo* application of NIR technology to assess burn depth was in a porcine contact burn wound model. From this study, superficial (1°), partial thickness (2°) and full thickness (3°) injuries could be distinguished as early as 10 minutes post-burn injury using the variables oxygen saturation and total hemoglobin as shown in Figure 1-12 and Figure 1-13. Partial thickness injuries could not be differentiated into viable and non-viable

injuries using one variable alone and required the combination of oxygen saturation, total hemoglobin and water content. This was necessary because the individual parameter differences that existed between the viable and non-viable partial thickness injuries were relatively small, but in combination the differences were large and statistically significant.[186]

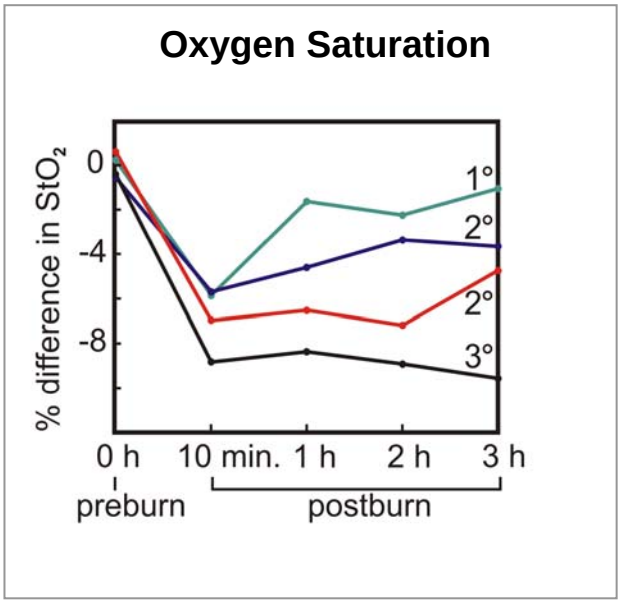

Figure 1-12: Oxygen Saturation as Measured with NIR in Porcine Burn Wounds[187]

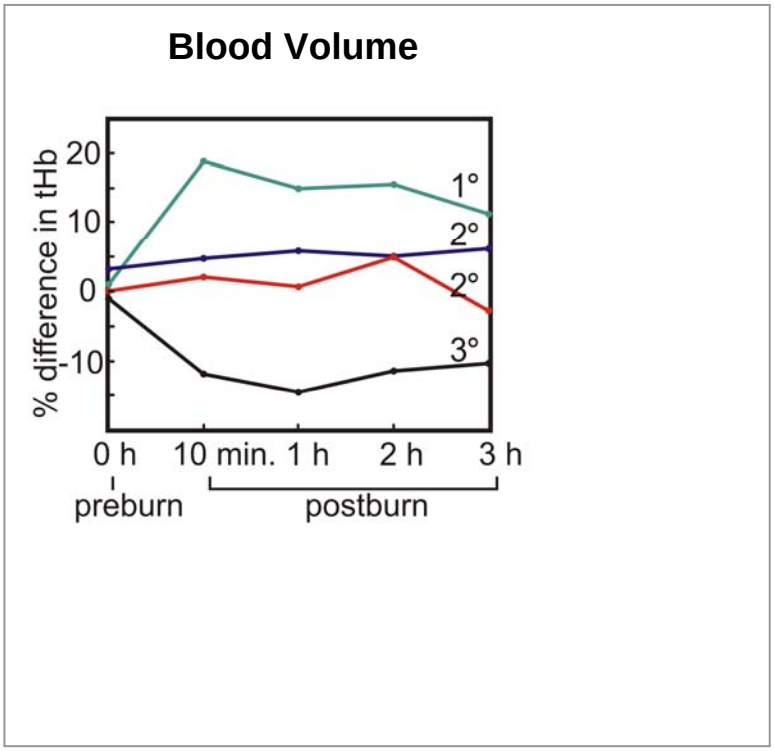

Figure 1-13: Perfusion as Measured with NIR in Porcine Burn Wounds[187]

NIR Imaging could also distinguish differences in burn depth using both oxygen saturation and total hemoglobin. NIR imaging is a separate technology that is camera-based and collects information over a larger surface area. The results for the NIR imaging device are shown only to highlight previous findings and will not be discussed in the thesis results. Results for oxygen saturation are shown in Figure 1-14. In this figure, it is difficult to determine the differences between the partial thickness and full thickness burn wounds using the digital image or a visual assessment. The NIR imaging oxygen saturation images show clear differences between the burn wounds. The full thickness injury (30 s) is black, which corresponds to no oxygenation. The superficial (3 s) injury has similar oxygen saturation as pre-burn levels. The partial thickness injuries (12 s and

20 s) have oxygen saturation that it is intermediate between the superficial and full thickness wounds.[186]

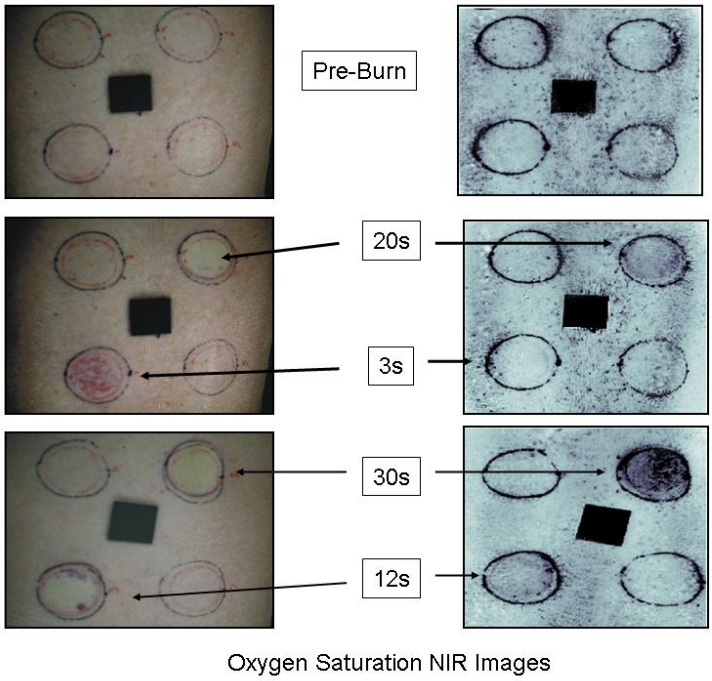

Figure 1-14: Oxygen Saturation NIR Images in Porcine Burn Wounds[188]

1.8.2 Clinical Experience: Superficial and Full Thickness Burns

NIR devices were developed for the clinical environment and first tested in superficial and full thickness burn injuries.[28] These injuries are easily distinguished using a clinical assessment and it was important to test the NIR devices on known clinical entities. NIR Point and imaging spectroscopy were utilized to assess superficial and full thickness injuries in 16 adult patients who were thermally injured and had less than 10% TBSA burn wounds. Superficial burns showed an increase in oxygen saturation and total

hemoglobin, unlike the full thickness injuries that showed a decline in both variables as shown in Figure 1-15.

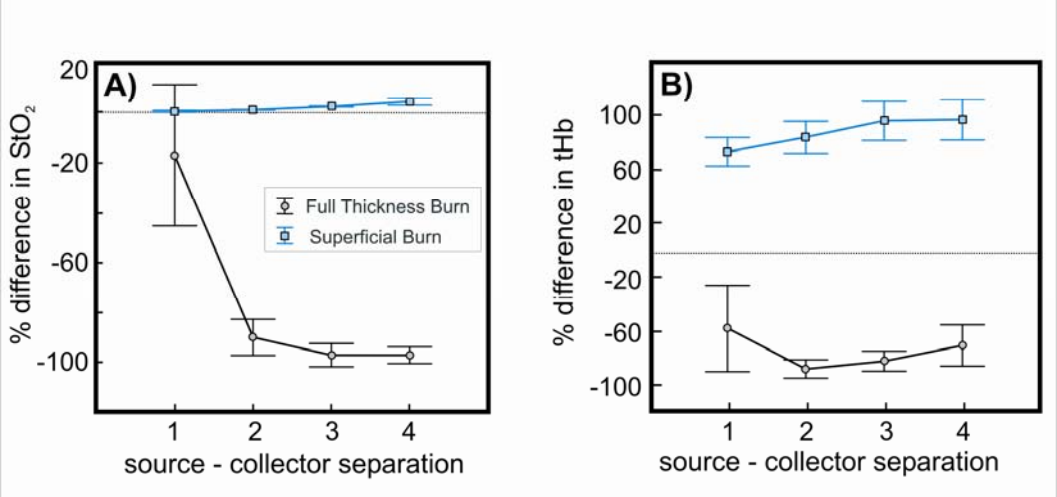

Figure 1-15: NIR Point Spectroscopy – Oxygen Saturation and Total Hemoglobin in Superficial and Full Thickness Clinical Burn Wounds[28]

NIR imaging could also distinguish superficial and full thickness injuries. Superficial injuries showed an increase in oxygenation as represented by white within the burn region (95% O_2 Saturation). Total hemoglobin increased within the superficial burn site as represented by grey-white areas (0.06 $mMcm^{-1}$). Results are shown in Figure 1-16.

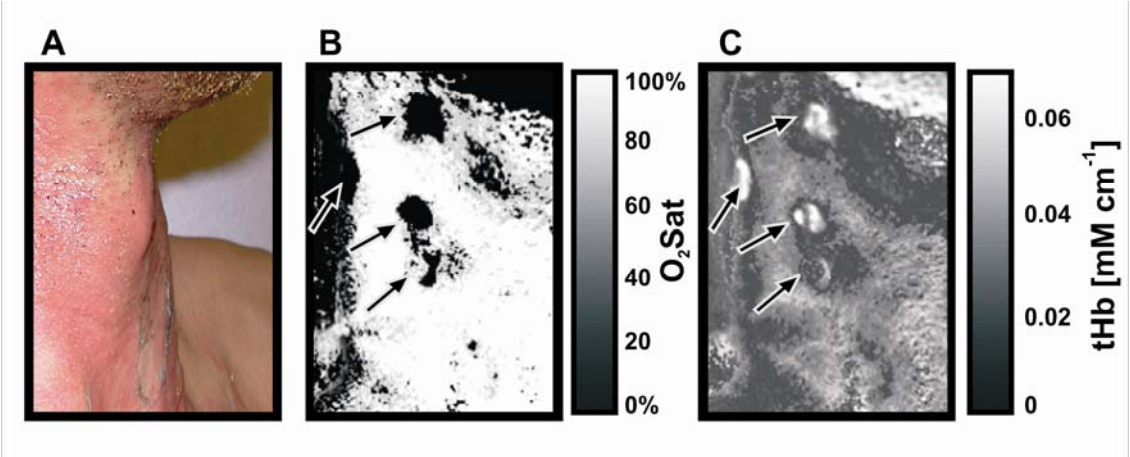

Figure 1-16: Near Infrared Imaging Spectroscopy: Superficial Burn A) Colour Digital Photograph of the Superficial Burn B) Oxygen Saturation Image and C) Total Hemoglobin Images[28]

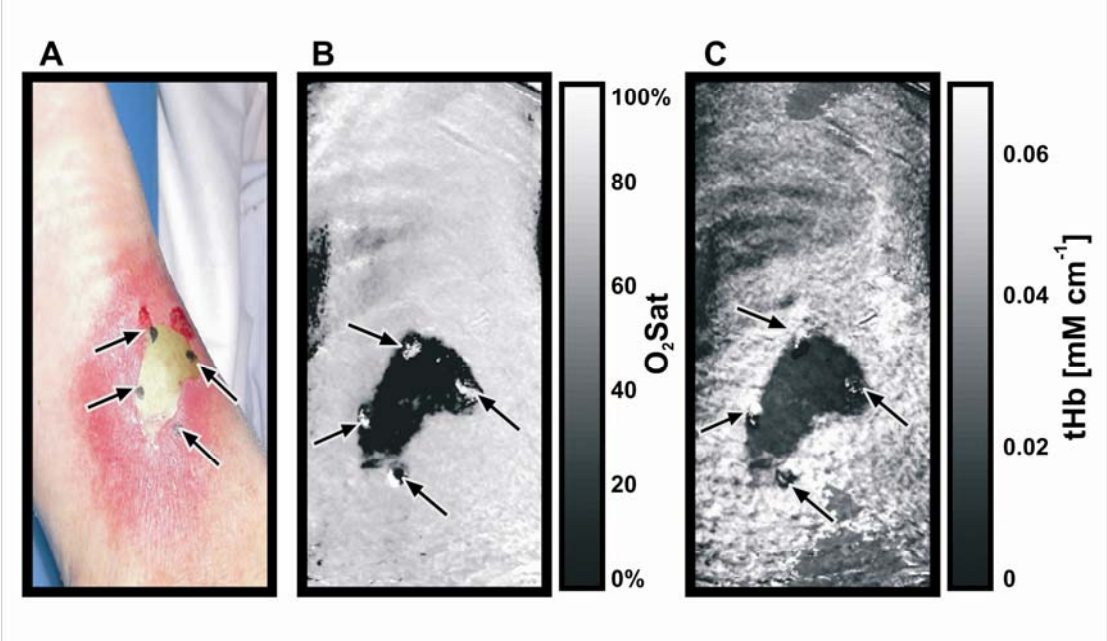

Figure 1-17: Near Infrared Imaging Spectroscopy: Full Thickness Burn A) Colour Digital Photograph B) Oxygen Saturation Image and C) Total Hemoglobin Images[28]

Full thickness injuries showed an absence of oxygenation as represented by black within the burn region (0% O_2 Saturation). There was a decrease in total hemoglobin within the burn region as represented by dark grey (0.01mMcm^{-1}). The total hemoglobin image also showed the zone of hyperemia that existed around the burn injury as shown in Figure 1-17.

1.8.3 **Clinical Experience: Partial Thickness Burns**

The first clinical study provided insight into the design and utilization of these devices within a clinical setting. However, the study did not address the real clinical dilemma of classifying partial thickness injuries as healing or non-healing wounds. The primary goal of the second clinical study was to investigate whether NIR devices could distinguish the clinically more difficult partial thickness burns in a small TBSA model (less than 10%). From this study, viable partial thickness wounds showed an increase in oxygen saturation compared to non-viable wounds as shown in Figure 1-18. It is difficult to tell if these statistically significant results are truly attributable to real alterations in hemodynamics as the error bars overlapped and the differences between the variables were small. NIR imaging for a superficial partial thickness injury is shown in Appendix A.

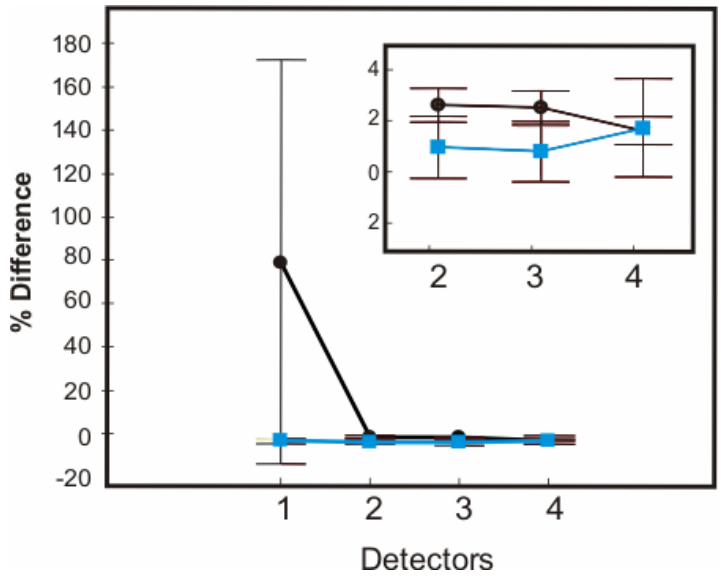

Figure 1-18: NIR Point Spectroscopy – Oxygen Saturation in Partial Thickness Clinical Burn Wounds

NIR Spectroscopy was also used to assess the water content within the superficial and deep partial thickness injuries in this same clinical study. The deep partial thickness burns showed a statistically significant increase in water content compared to superficial partial thickness burns at detectors 2 and 3 as depicted in Figure 1-19. However, no significant differences were noted at detector 4.[189] NIR imaging of a superficial and deep partial thickness injury are shown in Appendix D.

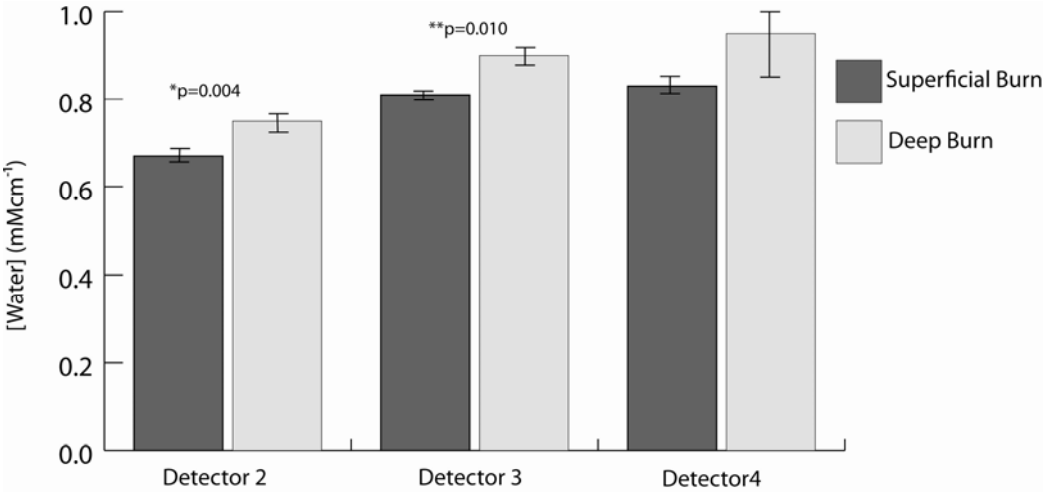

Figure 1-19: NIR Point – Water Content in Superficial and Deep Partial Thickness Clinical Burn Wounds[190]

1.9 Swine as a Model for Burn Depth Determination

A porcine burn wound model was chosen for this study as swine wound healing and histology is very similar to human skin. Like humans, swine heal primarily by reepithelialization, compared to other smaller animal wound healing models that rely on wound contraction (e.g., rodent, guinea pig, mice).[191]

Burn wounds heal primarily via reepithelialization of the burn wound via the hair follicle epithelium and viable epidermis. A model that has multiple hair follicles could impact the potential and rate of wound healing within the burn wound. The smaller animal models available for burn wound studies have large amounts of body hair.[191] Humans have sparse hair follicles in the skin, therefore it is important to replicate the clinical situation using an animal model that has less hair follicles. Swine are the only mammals that have

a sparse coat of hair that is similar to humans.[192] Swine hair follicles also progress through their hair cycle independent of the other hair follicles.[191] Arrector pilae muscles attach to the cortex of the hair follicle in both species.[193, 194] The arrector pilae muscle is an important landmark in the criteria developed to assess clinical burn depth as it is used to divide the dermis into halves. The major difference in the hair follicle of the swine is that they have a thin outer root sheath and thick inner root sheath.[193]

The degree of thermal injury to the tissue is dependent on the thickness of the skin, making it important to use a model in which skin thickness is similar to human skin. The NIR technology used in this study is specifically designed to interrogate the full thickness of human skin. A porcine wound model is ideal as skin thickness is very similar to human skin thickness. The human epidermis ranges from 50–120 μm, which is comparable to swine epidermis, which measures from 30–140 μm.[195] The dermal-epidermal thickness ratio is 10:1 to 13:1 in swine, which is similar to human ratios. Smaller rodent models have a thin epidermis and dermis compared to human skin, making them unsuitable for assessment with this particular NIR device as their skin is too thin.[191] In addition, by using a larger animal there is increased surface area to create multiple wounds of varying depths. This is in contrast to smaller mammals where burns of only one depth would be feasible.

Blood vessel location and viability have been shown to be an independent predictor of burn wound depth in the clinical grading system. Porcine blood vessel anatomy has a similar arrangement to human skin as there is a superficial, middle and deep plexus.[191, 193, 195] The deep plexus is located at the dermal-hypodermal junction and ascends to

supply the apocrine glands and the hair bulbs. The deep plexus also descends to supply the hypodermis. The middle plexus supplies the pilosebaceous apparatus and the mid portions of the hair bulbs. The superficial plexus supplies the rete ridges via capillary loops and the upper portion of the hair follicle.[193] The superficial plexus of the porcine dermis is actually less dense than in humans.[192] Sebaceous glands, apocrine glands and the lower portions of the hair follicles are poorly vascularized compared to the highly perfused appendages in humans.[195] This has implications related to burn depth as the structures of the dermis may be more sensitive to the effects of heat secondary to a decreased blood supply of hair follicles and glands.

There are differences in swine skin that could potentially impact the results obtained with the NIR device and histology results. Pigs do not have eccrine glands in the dermis and instead have apocrine glands.[192] Eccrine glands have been shown to be a predictor of burn depth when used in combination with collagen and endothelial necrosis. Apocrine glands in the human are located at specific anatomic regions such as the axilla and genitalia. In swine, apocrine glands are present in a 1:1 ratio with hair follicles and are believed to have a thermoregulatory function, although their function has not been fully elucidated.[193, 195] Mast cells are abundant in the porcine dermis and are located perivascularly.[192–194] Swine have a rapid and marked response to injury and will have a higher mast cell content than humans.[192] This does not directly impact the histology grading system for burn depth. However, the NIR results may be affected as mast cells release histamine, which has been shown to be associated with the increase fluid leakage and protein permeability from capillaries and venules post-burn injury. Therefore, the increase in mast cells post-burn injury may affect the water content in the

wounds. There is an extensive amount of fat in the subcutis of swine compared to human skin.[195] The adipocytes are arranged in chambers separated by connective tissue from the deeper reticular dermis, which is similar to humans. Full thickness injuries are characterized by fat necrosis in the subcutaneous layer and the large quantity of fat in the skin could make it difficult to create a true full thickness injury. It also complicates the grading system, as swine have fat that penetrates into the dermis and is associated with hair follicles and glands. Therefore, the dilemma will be in the situation where there is fat necrosis in the dermis but not in the true subcutaneous layer.

In summary, a porcine burn model was utilized in this study as skin thickness, histology and wound healing are comparable to humans.

Chapter 2: Aims and Hypotheses

2.1 Purpose

The purpose of this study was to test Near Infrared Point Spectroscopy as a tool to non-invasively assess burn depth in a swine model.

2.2 Hypothesis

NIR technology can accurately assess burn wound depth non-invasively in a swine burn model using the variables of oxyhemoglobin, deoxyhemoglobin, methemoglobin and water.

Chapter 3: Methodology

3.1 Study Overview

Ethics approval for this chronic animal study was obtained from the National Research Council of Canada's Animal Care Committee. Adult Yorkshire swine weighing between 30–45 kg were obtained from a commercial supplier and acclimatized for 4 days prior to the start of the experiment. Animals were housed in individual cages with water and food *ad libitum*. Two animals were housed in each room, which contained 2 individual cages.

Twelve sites were chosen on the dorsal aspect of the animal and divided into seven burn sites and five local control sites. The local controls were considered to be the sham portion of the experiment. The sites were monitored pre-burn, post-burn and every 12 hours after burn injury up to 96 hours after the injury. Animals were euthanized at predefined endpoints, which included 4, 12, 24, 36, 48, 72 and 96 hours after burn injury. At the time of euthanasia, biopsies were acquired from all sites for histological correlation of burn depth.

Near infrared spectroscopy devices were used to assess the changing hemodynamics and physiology of the skin over the course of the experiment. Measurements were acquired with a non-invasive portable Near Infrared Point Spectroscopy device.

3.2 Pre-Experiment

The animals were fasted for a minimum of 12 hours before induction in order to minimize the risk of aspiration. Water was available to the animals throughout the fast period. The swine were pre-medicated by intramuscular injection (IM) with midazolam (0.3 mg/kg) and ketamine 20 mg/kg IM. Atropine 0.02 mg/kg IM was given to reduce secretions during intubation. These medications are effective in lowering the amount of inhalant anesthetic required during the procedure and also minimize stress during transport.

Animals were induced by mask at 4–5% isoflurane in 2–3 litres per minute of oxygen until the animal no longer displayed a swallowing reflex. Immediately following induction, xylocaine topical spray was applied to the larynx to prevent laryngospasm. Intubation occurred using a 7.0–7.5 French endotracheal tube. Isoflurane was delivered at 1.5–2.5% carried by 40–60% oxygen mixed with medical air, with a flow of 2.0–3.0 L/min via the anesthetic cart (Excel 210, Ohmeda, Mississauga, ON) for the duration of the experiment. Heart rate and oxygen saturation were monitored via a pulse oximeter (PM-9000 Vet by Mindray and 5250 RGM by Ohmeda) positioned on the ear. Body temperature was maintained at 39.0°C ± 0.5°C with a heating blanket placed underneath the animal and monitored via a rectal temperature probe. Petrolatum ophthalmic ointment (Puralube®) was applied to the eyes to prevent desiccation during anesthesia. Intravenous access was obtained by placing an 18-gauge intravenous (IV) in the swine's auricular vein. Intravenous fluids of 5% dextrose at 10 times the animal's body weight (in ml) were given during the surgical procedure between 350–450ml/h. A urinary absorbent pad was placed under the animal to collect urine throughout the experiment.

Animals were placed in a sternal recumbency for the duration of the experiment. The dorsal surface of the animal was shaved using an A5 professional clipper with a #40 blade (Oster®, McMinnville, Tennessee). The neck region was also shaved in animals receiving an indwelling carotid artery catheter.

3.3 Carotid Artery Cannulation

Animals (n=5) euthanized at 12, 24, 36, 48, and 72 hours after burn injury received a carotid artery cannulation once anesthetized. The purpose of this procedure was to provide central arterial access for the acquisition of blood gases at each near infrared measurement time point until euthanasia.

The animal was positioned in dorsal recumbency with the legs retracted caudally. The sternal region and neck were prepped with isopropyl alcohol followed by chlorhexidine and providone-iodine. A paramedian incision was made cranial to the manubrium sterni directly over the trachea. The sternohyoideus muscle was split and retracted laterally. The thymus gland, associated lymph nodes and the stenomastoideus muscle were retracted laterally to expose the carotid sheath. A pulse was palpated before proceeding to retract the muscle laterally to ensure the sheath was not caught in the retractor. With the carotid sheath identified, the fascia was dissected, exposing the carotid artery, internal jugular vein and the vagus nerve. The adventitia was dissected from the carotid artery and three 1.0 silk ties were placed around the circumference of the artery. Two ties were placed caudally and one cranially. The length of the tubing was established by measuring the distance from the carotid artery to the area behind the ear and the dorsal

aspect of the neck. Extra length was added to account for the tubing that would reside in the carotid artery, and this was marked with an indelible pen before the tubing was cut to size.

The animal's leg was released from its caudal position and rotated laterally to expose the dorsal aspect of the neck. Using a trocar, a tunnel was created from the skin incision site to the dorsal aspect of the neck. Care was given to ensure the trocar resided above the cutaneous colli muscle and below the subcutaneous tissue. There is a nice plane of advancement in this area as there is no risk of injury to the parotid gland or other structures. Advancement of the trocar occurred in two stages. In the first stage, the trocar was advanced from the ventral midline incision (first incision) to the mid-lateral neck region (second incision). This was considered to be the halfway point between the ventral midline incision and the final incision on the dorsal neck region of the animal. The trocar was then advanced from the second incision to the final incision. In both situations, in order for the trocar to exit the skin a small incision was made where the trocar tip was visualized. Alligator forceps were used to bring the tubing from the final incision to first incision. The tubing was then flushed to ensure patency using heparin sodium (10,000 USP units/mL) in normal saline. Adequate movement within the subcutaneous tunnel was tested by sliding the tubing back and forth.

Retention beads were added to the tubing before cannulating the carotid artery. The retention beads were made from silastic tubing (1/8" x 1/16") and did not impede flow when tested with the heparin normal saline mix. A clamp was placed on the caudal portion of the carotid and the proximal portion was tied off. A small hole was then made

in the carotid artery using iris scissors. The tubing, with a slightly beveled edge, was advanced to the hemostatic clamp and tied. The clamp was removed and the tubing advanced until the pen mark was not visible. The second silk tie was used to hold the tubing in its final residing place. The retention beads attached to the tubing were sutured to the sternomastoideus muscle. This was to prevent excessive movement around the cannula insertion site. Retractors were removed and the stenohyoideus muscle and the subcutaneous fat were closed with a 2.0 chromic suture in a horizontal pattern. The skin of the ventral incision, second and final incision was closed with disposable staples (Royal 35W, Tyco Healthcare, Norwalk, Connecticut). All incisions were sprayed with 8-hydroxyquinoline or New Skin Clear Spray (Medtech, Jackson, WY). The animal was then positioned in sternal recumbency and prepared for the next phase of the experiment.

3.4 Burn Wounds

Once anesthetized the animal was placed in a sternal recumbency position. Prevention of pressure wounds and nerve palsies was accomplished with sufficient padding underneath the limbs and abdomen. A prefabricated template was used to mark twelve sites, each 3 cm in diameter, on the dorsal surface of the pig with an indelible pen. Six of the sites were located on the right side of the dorsal midline while the other six were located on the left side. It was important to control for the local effects of the burn wounds and the sites were kept at least 4 cm away from each other. In the previous study using this template there were no hemodynamic changes within the control sites. The dorsal skin surface was prepped (sterile) in the same fashion as the carotid artery

cannulation. Providone-iodine was removed prior to NIR measurements as it could interfere with the results. Adherence to sterile technique occurred throughout the experiment. Once the sites were marked and the skin prepped, pre-burn measures were acquired using the NIR devices.

Burns were made on the dorsal surface of the animal using a heated brass metal rod. Burn depth depends on three parameters, the temperature of the metal rod, the pressure or force on the skin and the length of time the rod is applied to the skin. Two brass rods (3 cm diameter) were immersed in 100°C boiling water and one rod kept at body temperature (39°C). The pressure of the brass metal rod was kept constant by using a 5-pound weight fixed to the brass rod. Altering the length of time the brass rod is applied to the skin while keeping temperature and pressure constant will create burns that range from superficial to full thickness.

Seven burns sites were created by holding the brass rod heated to 100°C at constant pressure for 3, 12, 20, 30, 75, 90 and 120 seconds. The time intervals for the burn wounds were non-uniform and were chosen as they consistently created the burn depth of interest in a swine model. The model was tested in 5 animals prior to the study to evaluate histology and the length of time required to complete wound healing. The 3 s and 12 s burns are superficial partial thickness injuries and healed in 7–16 days post injury. The 20 s and 30 s burn wounds are deep partial thickness injuries and did not heal within 16 days post-burn. The 75–120 s burn injuries are full thickness burn wounds that also did not heal within 16 days post-burn injury. The control sites (n=5) were created using a brass rod kept at 39°C held *in situ* with constant pressure for 20, 30, 75,

90 and 120 seconds. Varying the time points for the control was important to show that increasing the length of time of brass rod placement did not produce a crush injury to the tissue and affect the values of oxy- and deoxyhemoglobin .

Once every site was created, NIR measurements were acquired immediately post-burn and 1 hour after the injury. Digital photographs and physical measurements of burn wound size were acquired. The 3-second burn site was treated with polysporin and the remaining six burns with silver sulfadiazine (Flamazine™, Smith and Nephew™, UK). Wet-to-dry dressings were placed on top of the burn sites. A large burn gauze was placed over the top of the individual dressings and sutured to the animal's skin laterally. The midline of the burn pad was cut, creating two flaps that could be opened and closed easily. A custom swine jacket was placed over the top to keep the dressings clean and prevent the animal from injuring the wounds.

Prior to reversing the anesthesia, buprenophrine (0.1mg/kg IV or IM) and carprophen (4.4 mg/kg IM) were given for post-operative pain. The dextrose/saline infusion was stopped and the needle hub covered with a needle free connector or Clave® system (ICU Medical Inc, San Clemento, CA). The Clave® system was felt to be a safer alternative for the technicians as the animals were receiving multiple drugs at multiple time points. The ear vein IV was sutured in place and covered with a transparent waterproof dressing (OpSite™, Smith and Nephew™, UK). The anesthesia was reversed by turning off the isoflurane. The swine recovered under a heating lamp and all vital signs were monitored. Once sternal and stable, pigs were returned to the animal facility

and individually housed to prevent damage to dressings. Water and food were provided *ad libitum*.

3.5 Near Infrared Point Spectroscopy (NIR Point)

The NIR Point Spectroscopy device is comprised of a fiber optic probe that delivers and collects light from the tissue. Collected light is dispersed into a spectrum via an imaging spectragraph and a CCD (charge coupled device) records the spectrum over 500 to 1100 nm wavelength range (Sciencetech Inc., London, On, Canada). The light source used was a 100 W quartz tungsten halogen white light source model 77501 (Oriel, Strattford, CT). The fiber optic bundle or probe (Fiberguide Industries, Stirling, NJ) consisted of one fiber to deliver the light and four fibers to detect the light returning to the system. The detector fibers were attached via an entrance slit to the imaging spectragraph. The detection fibers are displaced by regular intervals (1.5 mm, 3 mm, 4.5 mm and 6 mm) from the light delivery fiber. In this configuration, light gathered by the sequence of detection fibers sample different volumes of tissue. The greater the separation or interval between the light delivery fiber and the collection fiber, the deeper the light penetrates into the tissue. Detector 1 is a surface wound detector, 2 and 3 are considered the dermal detectors and detector 4 is a deep tissue collector. The detectors are commonly called source collectors and are represented in the figures as “sd.” Raw reflectance measurements were converted to optical density units through a ratio of the tissue reflectance against a 99% Spectralon® reflectance standard (LabSphere Inc., North Sutton, NH) prior to data processing.

3.6 Data Collection

Each set of wound measurements consisted of data from the three near infrared devices. Digital photographs were used to document the clinical appearance of the wounds at each time point. Environmental and rectal temperatures were recorded at each time point. Data was collected in a temporal manner with “time” referring to time in relation to the burn injury. Prior to creating the burn injuries (pre-burn), a complete set of spectroscopic measurements was acquired. After burn injury, NIR measurements were acquired immediately post-burn (15 minutes) and 1 hour after the injury. These measurements occurred in the operating room with the animal under anesthesia.

Subsequent NIR measurements were acquired at 12, 24, 36, 48 and 96 hours after injury. Measurements were acquired with the animal under sedation and moved from its housing cage to a separate clean cage with no shavings. The equipment was kept in the clean cage and referenced prior to sedating the animal. Keeping the equipment in a separate room made it easier to calibrate the measurements. This limited the time of sedation required to collect all the NIR data. Burn wounds are at high risk for infection, therefore it was important to maintain a clean environment for data collection. In addition, prophylactic antibiotics, Enrofloxacin 5mg/kg IM (Baytril®, Bayer), were given once daily to the swine for the duration of the experiment except on the day of euthanasia. Pain control was maintained throughout the study by a daily dose of carprophen IM (4.4mg/kg IM).

Sedation of the swine occurred using a combination of ketamine (dose) given IV or IM. This was followed by medetomidine (Domitor®, Pfizer, London, ON) through the ear

vein. The advantage of using the Clave system was that the syringe screws onto the cannula, making it easier to deliver the medication and avoiding a second IM injection for the animal. In situations where there was no IV access, medetomidine was given 0.1mg/kg IM with an additional 0.5 ml to account for losses in the butterfly tubing. In addition, a new IV site was placed in the opposite once the medetomidine had its effects. With the animal sedated, the custom swine jacket was opened, the burn quilt folded backwards and dressings removed. Any excess ointment or cream was removed gently with dry gauze, as silver may interfere with the near infrared results. Silver acts like a mirror and reflects light directly from its surface, which means it prevents light from entering the tissue. This process is known as specular reflectance. Once the NIR data was collected, the dressings were replaced, the burn quilt folded and tied, and the jacket closed. The animal was placed back in its cage and reversal of the medetomidine sedation occurred with atipamezole hydrochloride IV or IM 0.1mg/kg (Antisedan®, Pfizer, London, ON).

Animals euthanized at 12, 24, 36, 48 and 72 hours after burn injury had indwelling carotid artery access. Blood gases were acquired every 12 hours after burn injury at the time of the NIR data collection. Blood, approximately 3 ml, was collected using a 5 ml syringe attached to the IV hub. The syringe was capped and placed on ice for transport to the blood gas analyzer (Stat Profile Critical Care Xpress, Nova Biomedical, Mississauga, ON). The intra-arterial access cannula patency was maintained by flushing the catheter with 0.02 cc of heparin sodium (10,000 USP units/mL) in 20 ml of normal saline. This was performed at each time point after the arterial blood gas was collected.

Euthanasia was considered to be the endpoint of the study. At the time of euthanasia, the animal was sedated using the pre-experiment medications that were administered for transport and brought to the operating room. The animal was anesthetized and ventilated as described. After a complete set of spectroscopic measures were acquired, biopsies were acquired from each site for histology. Euthanasia time points included 12 hours (n=1), 24 hours (n=1), 36 hours (n=1), 48 hours (n=1), 72 hours (n=1) and 96 hours (n=11). One animal was euthanized at each specific time point after burn injury to correlate the histology with the NIR findings. Once the experiment was completed, animals were euthanized by an intra-venous injection of potassium chloride (149mg/ml, 1–10ml per animal) or euthanyl (125mg/kg IV) while under anesthesia.

3.7 Histology

Biopsies were acquired from the burn and control sites at the time of euthanasia using a 6 mm disposable punch biopsy (Miltex, Germany). Four specimens were acquired from the burn or control site in the pattern outlined in Figure 3-1. All specimens were placed in individual specimen bottles containing 10% formalin. The specimen was bisected in a coronal fashion and fixed in formalin for a minimum of 72 hours. Specimens were then transferred to 95% ethanol and placed in a tissue processor (Leica TP 1020, Wetzlar, Germany). Paraffin blocks were sectioned using a cryotome set at 4 microns and each slide was stained with hematoxylin and eosin (H&E).

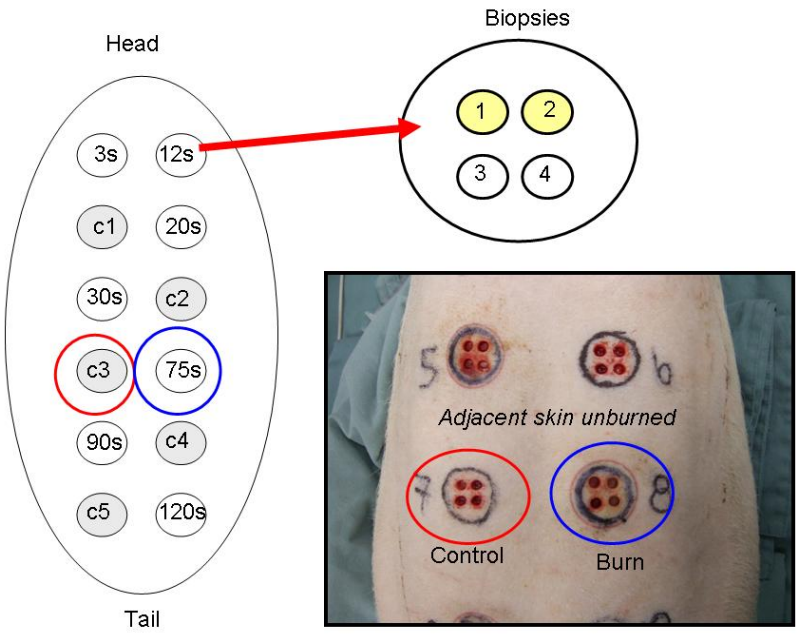

Figure 3-1: Histology Sampling Plan

Paraffin sections were dewaxed in 5 changes of xylene and brought down water through graded alcohols. Sections were then pretreated with 1% pepsin in 0.01N HCl (pH2.0) for 15 minutes at 37°C. Endogenous peroxidase and biotin activities were blocked respectively using 3% hydrogen peroxide and Lab Vision's avidin/biotin blocking kit (cat.# TA-015-BB). After blocking for 10 minutes with 5% normal goat serum (Vector Labs), sections were stained for 1 hour with mouse monoclonal antibody against vimentin (ARP: clone 3B4) at 1/500 in a moist chamber. This was followed by 30 minutes each with biotinylated horse anti-mouse IgG or biotinylated goat anti-rabbit IgG (Vector Labs.) and HRP-conjugated Ultra Streptavidin (ID Labs. Inc. cat.#BP2378). Colour development was done with freshly prepared NovaRed solution (Vector Labs. Inc:cat# SK-4800) and counterstained with Mayer's hematoxylin. Finally, sections were

dehydrated through graded alcohols, cleared in xylene and mounted in Permount (Fisher: cat.# SP15-500).

Two specimens (as highlighted in Figure 3-1) were evaluated by a physician specialized in the area of burn depth pathology. The other two specimens were placed in the histology database for future histology studies. The entire microscopic field of the burn and control wound were evaluated. Specimens were evaluated according to the viability of the collagen, blood vessel endothelium, epithelium of the appendages and fat necrosis. The criteria for the histological determination of burn depth has been established and evaluated over the past 5 years in a clinical setting (Appendix B and Appendix C) Based on the histological objective criteria, the biopsies will be graded as superficial, superficial partial thickness, deep partial thickness or full thickness burn wounds.

3.8 Data Processing

NIR Point technology data is processed using a modified Beer-Lambert relationship as described in section 1.9. Spectra are initially converted from raw reflectance spectra to absorption using the reflectance standard. The relative concentrations of the chromophores are derived over a spectral range of by a least squares estimate of the extinction coefficients to the measured spectrum. The spectral range for deoxyhemoglobin and oxyhemoglobin was 680–820 nm, and was 940–1040 nm for water and 610–840 nm for methemoglobin.

To account for tissue scatter variations in the measured spectrum, a linear scatter term (mλ +offset) was added to the Beer-Lambert relationship. All computations were performed using MATLAB Version 6 (The Mathworks Inc., South Natick, MA).

The NIR Point Spectroscopy provides oxy- and deoxyhemoglobin , methemoglobin and water content at four source collector separations. Detector 1 is 1.5 mm, detector 2 is 3 mm, detector 3 is 4.5 mm and detector 4 is 6 mm away from the light source. Data from detector 1 will not be shown in this thesis as this detector's position is greatly affected by the surface irregularities of the epidermis. Over the past 5 years, the data within this detector is variable and represents light interrogating only the very superficial portion of the epidermis.[196] As this region is necrotic in burn injuries, the data from this detector does not yield valuable information about the degree of burn injury.

3.9 Statistical Analysis

The following is a synopsis of the statistical analysis and how the results will be presented in each chapter. Statistics are presented for the histology chapter separately, as the large majority of the data are non-parametric. The NIR data statistics deal with parametric data and are described in section 3.9.2 to 3.9.5. All statistical computations were performed using SPSS v. 17 (Chicago, IL).

3.9.1 Statistics for Histology Chapter

Objective criteria used to assess differences in burn depth included the level of collagen and endothelial necrosis along with the degree of injury to the hair follicles, apocrine

glands and fat. The level of collagen necrosis was defined as less than the upper 1/3 of the dermis, between the upper and middle 1/3 of the dermis and the lower 1/3 of the dermis. Endothelial necrosis was defined in the same way as the collagen, with the added category of endothelial necrosis presence in the subcutaneous tissue. Hair follicles, apocrine glands and fat necrosis were defined as absent, partially necrotic or fully necrotic.

The objective categories to describe vimentin immunostaining include the upper ½, lower ½, subcutaneous tissue and absent. The designation “all” means the entire dermis and subcutaneous tissue showed positive vimentin staining. The upper ½ describes the presence of vimentin immunostaining in the majority of the dermis except for a small portion within the upper ½ of the dermis. The lower ½ means that only the lower ½ of the tissue and the subcutaneous tissue has positive immunostaining but that there is an absence of positive cells in the upper ½. The designation subcutaneous tissue means that there are only positive cells in the hypodermis and the dermis above shows an absence of staining. Absent immunostaining was defined as no positive cells present within the specimen.

Non-parametric data was analyzed using a chi-square analysis. If the expected frequency of the cell was less than 5 then Fischer’s exact test was performed.

3.9.2 **NIR Data – ANOVA**

To evaluate the differences that occur at each time point, an ANOVA was utilized as described in sections 3.9.3 to 3.9.5.

3.9.3 **NIR data – ANOVA: Raw Values for the Variable**

Raw methemoglobin values are the mean values of the variable measured within the sites using NIR technology. The chromophore results obtained from detectors 2 to 4 were evaluated.

3.9.4 **NIR data – ANOVA: Change from Baseline**

This section shows the variable data as a change from baseline or the pre-burn measure (e.g., Burn-preburn/preburn). These results are presented as a magnitude change from the pre-burn period. Data for source collectors 2–4 are evaluated.

3.9.5 **NIR data – ANOVA: Hemoglobin as a Ratio of Total Hemoglobin**

This section presents oxy-, deoxy- or methemoglobin as a ratio of the total hemoglobin in the burn and control sites (e.g., mean methemoglobin/mean total hemoglobin).

Chapter 4: Results – Inclusion and Exclusion of Data

All animals (n=16) were included in the study. Animals were euthanized at specific time points from 1 hour to 96 hours post-burn injury as indicated in Table 4-1. At the time of euthanasia, 4 biopsies were acquired from each of the 12 sites located on the dorsum of the animal.

Number of Animals/Sites per Group								
Time (hours)	**1**	**12**	**24**	**36**	**48**	**72**	**96**	**Total**
Number of Animals	1	1	1	1	1	1	10	16
Number of Sites	12	12	12	12	12	12	120	192

Table 4-1: Number of Animals/Sites Included at Each Time Point

Of the four collected, two biopsies were utilized for the histological determination of burn depth. The specimens were from the same location for all the biopsies. There were no histological differences between the two biopsies evaluated. Therefore, the results were reported as a combined measurement or one sample for each burn or control wound. The two remaining specimens from each site were placed in the histology database for future investigations.

There were 7 burn sites and 5 control sites as shown in Figure 4-1 and Table 4-2. There were a total of 112 burn specimens and 80 control specimens for histological review. The control site specimens had normal collagen, blood vessels, hair follicles, apocrine glands, sebaceous glands and fat. There was no evidence of a crush injury to the tissue

from brass rod placement. There was no evidence of an inflammatory reaction as the mast cell content or polymorphonuclear leucocytes in the tissue was normal.

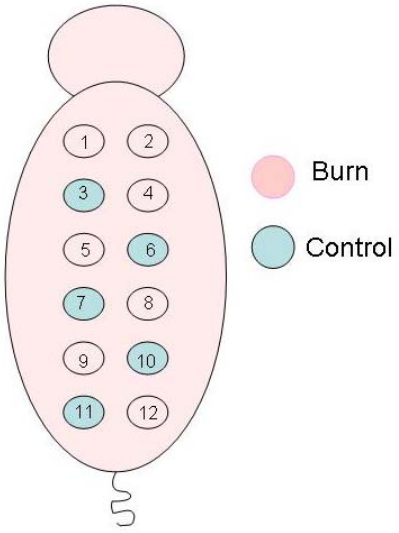

Figure 4-1: Location of Burn and Control Sites

Site Location	Contact Time (seconds)	Burn vs. Control
1	3	Burn
2	12	Burn
3	20	Control 1
4	20	Burn
5	30	Burn
6	30	Control 2
7	75	Control 3
8	75	Burn
9	90	Burn
10	90	Control 4
11	120	Control 5
12	120	Burn

Table 4-2: Site Location and Contact Time with Brass Rod

The 3 s, 12 s, 20 s and 30 s injuries all had varying degrees of injury to the tissue as will be described in Chapter 5. The 75 s, 90 s, and 120 s burn wounds were identical in terms of the degree of injury to the collagen, blood vessels, hair follicles and apocrine glands as shown in Figure 4-2 . The only difference between the injuries was the physical level of fat necrosis, as the 75 s burn injury had more viable fat compared to the 120 s burn. The only difference between these three burns was the level of fat necrosis, with the 120 s showing complete necrosis of the entire thickness of the subcutaneous tissue. As there were only minor morphological differences between these burn injuries, only the 90 s burn injury was utilized in the data analysis as the full thickness burn injury. The 75 s and 120 s burn wounds were eliminated from further statistical analysis.

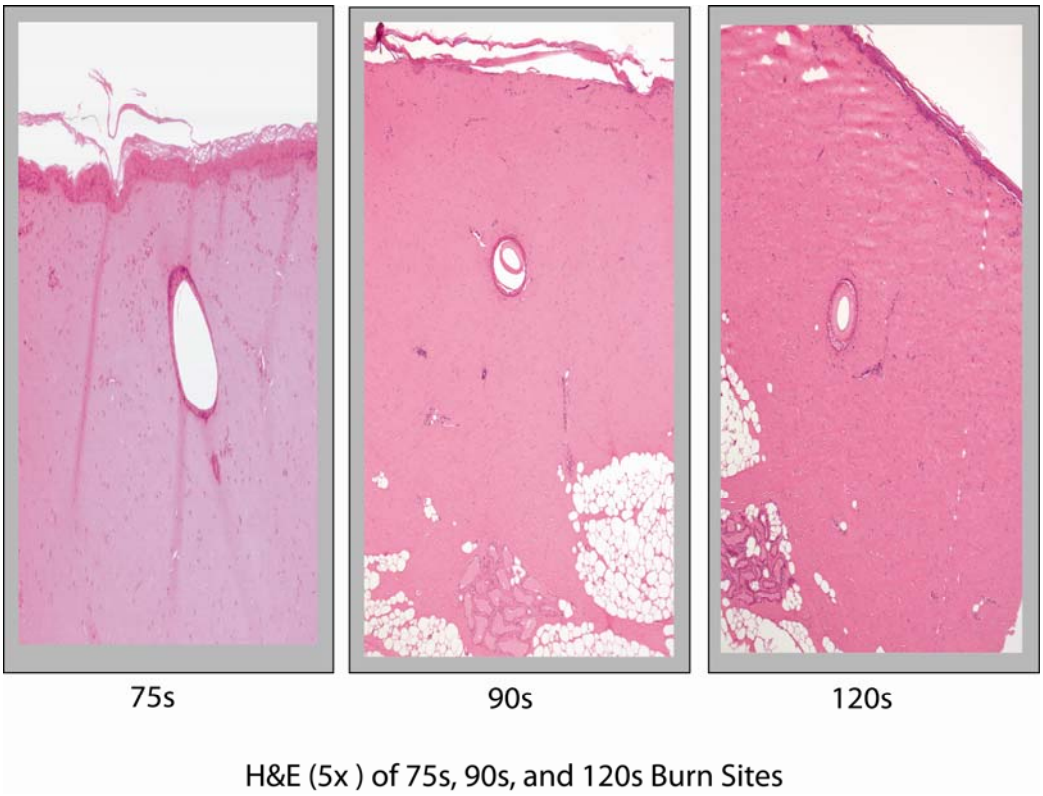

Figure 4-2: H&E of 75 s, 90 s and 120 s Burns Showing Similarities

The final number of animals and sites per group are shown in Table 4-3. There were 5 burn sites and 5 control sites used for each animal for the statistical analysis.

Number of Animals per Biopsy Group								
Time (hours)	**1**	**12**	**24**	**36**	**48**	**72**	**96**	**Total**
Number of Animals	1	1	1	1	1	1	10	16
Number of Sites	10	10	10	10	10	10	100	160

Table 4-3: Number of Animals per Histology Group

NIR spectroscopy data was collected pre-burn, post-burn, and 1 hour, 12, 24, 36, 48, 60, 72 and 96 hours after burn injury. The number of animals included for NIR data analysis is shown in Table 4-4.

Time (hours)	**Pre-Burn**	**Post-Burn**	**1**	**12**	**24**	**36**	**48**	**60**	**72**	**96**
Number of Animals	16	16	16	14	14	13	12	9	11	10

Table 4-4: Number of Animals per Time Group for NIR Data Analysis

Data from one animal was excluded at the 12-hour time point because the animal was hyperthermic and had a bradycardic event post-medetomidine administration. The bradycardia was reversed immediately with the atipamezole hydrochloride and the burn

dressings were removed to address the hyperthermia. Data from two animals were excluded at the 60-hour time point as both animals could not be sedated with the medetomidine. The 60-hour time point was difficult for the majority of the animals as a new IV site had to be obtained. Consequently, IM medetomidine was used for sedation and there was variability in the response to the intramuscular injection compared to an intravenous injection.

Finally, the 60-hour and 72-hour time point were excluded from the data analysis to reduce the number of data points analyzed statistically. These time points were chosen as the results obtained for oxyhemoglobin , total hemoglobin, methemoglobin and water content did not experience large changes within this time point.

Chapter 5: Histology

5.1 Results

5.1.1 Hematoxylin and Eosin

The biopsies acquired at the 96-hour time point were compared (n=10 animals) in order to limit the variability that can occur due to the dynamic nature of a burn wound. Therefore, there were 10 specimens in each burn depth category of 3, 12, 20, 30 and 90-second burns for an overall total of 50 specimens. H&E images are shown in Figure 5-1 for control and burn sites.

The 3 s burn wound collagen necrosis was present only in the upper portion of the dermis. The area of necrosis was immediately below the epidermis and extending into a small portion of the reticular dermis. The 12 s injury collagen necrosis was more extensive than the 3 s burn but the majority of cases were still limited to the upper 1/3 of the dermis. Two specimens from the 12 s burn site had collagen necrosis that extended into the mid portion of the dermis. Collagen necrosis extended to the mid portion of the dermis for the 20 s and 30 s burn wounds. The majority (8/10) of the 90 s burns wounds had collagen necrosis that extended the entire thickness of the dermis. The burn sites differed in terms of the degree of injury to the collagen [χ^2= 52.6, df=8, p<0.0001] as shown in Figure 5-2.

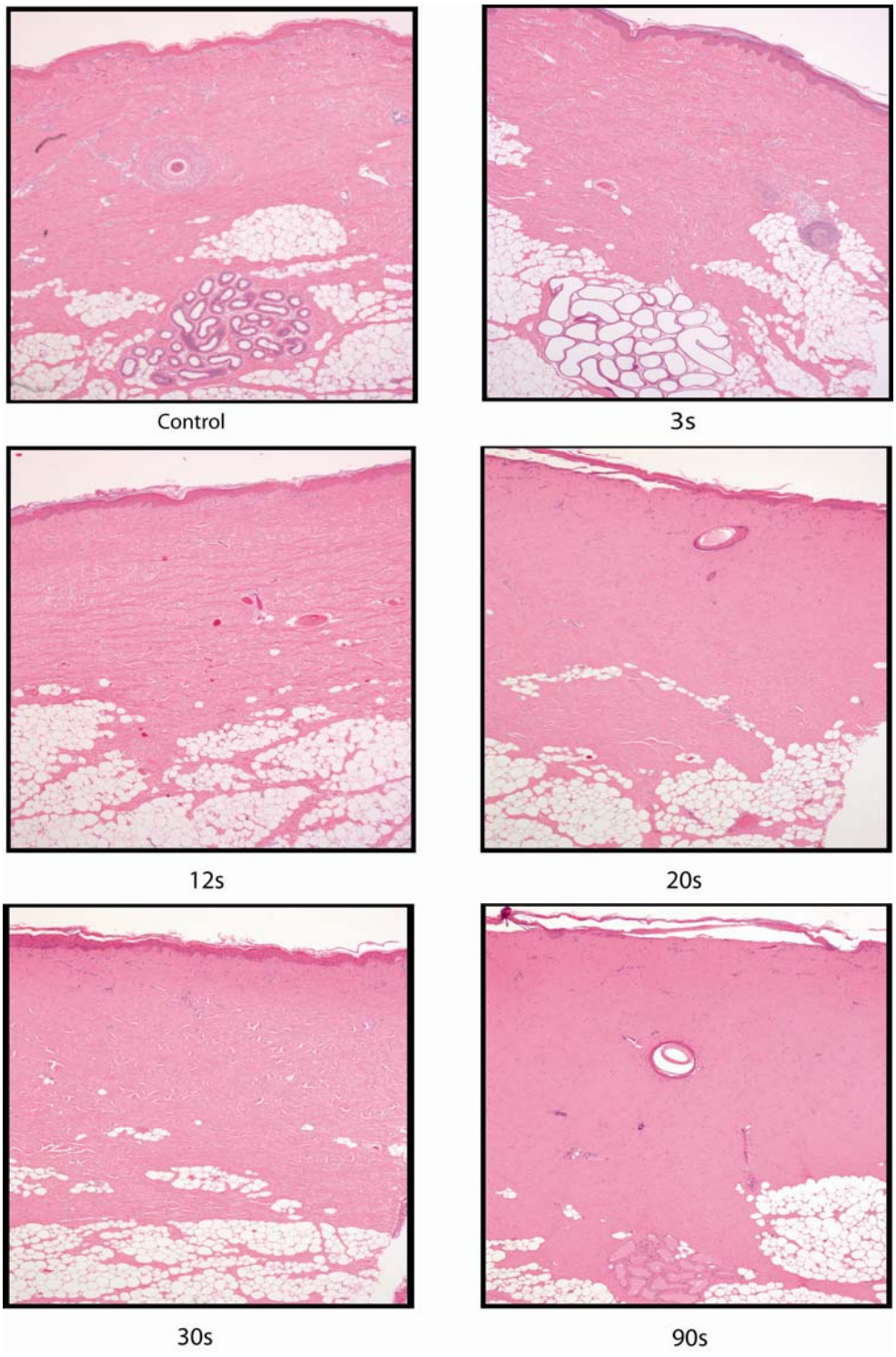

Figure 5-1: H&E of Burn and Control Sites (*5x* magnification)

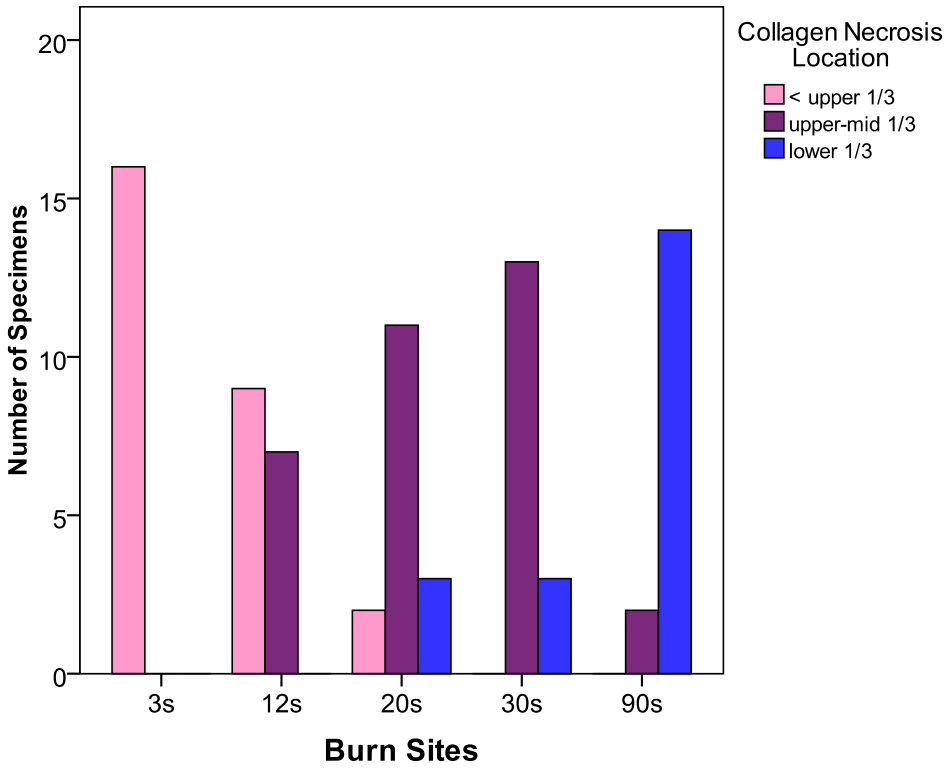

Figure 5-2: Location of Collagen Necrosis within the Burn Sites

The 3 s burn injury showed minimal injury to the endothelium located in the superficial capillary plexus. The mid plexus and deep plexus endothelium was intact and the vessels patent. The 12 s, 20 s and 30 s injuries all showed endothelial necrosis and vessel occlusion that extended into the lower portion of the dermis and encompassed the deep capillary plexus. The 12 s, 20 s and 30 s injuries all showed progressive injury to the endothelium as the degree of injury increased. The current classification system did not capture the progression of tissue injury. The 90 s burn vessel injury extended into the subcutaneous tissue for the majority (8/10) of specimens. The burn sites showed

progressive endothelial necrosis as burn depth increased [χ^2= 58.7, df=8, p<0.0001] as shown in Figure 5-3: Blood Vessel Necrosis by Burn Site

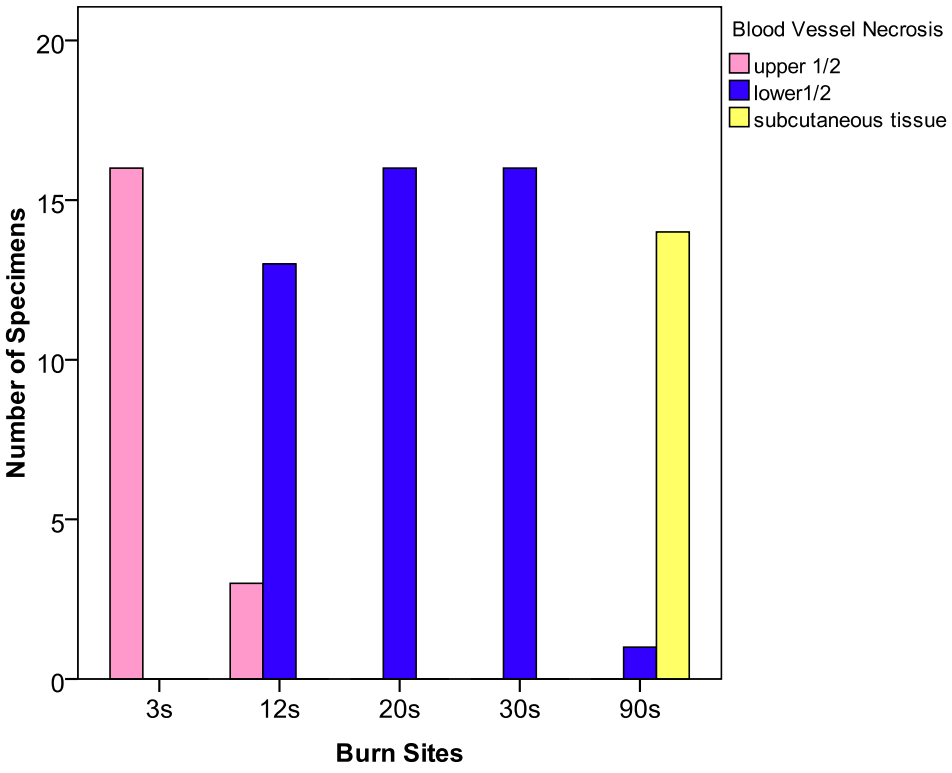

Figure 5-3: Blood Vessel Necrosis by Burn Site

Hair follicle necrosis was absent from the 3 s burn in 4 specimens. Partial necrosis of the hair follicle was present in the other 6 cases. The location of the partially necrotic hair follicles was present in the upper portions of the dermis. The 12 s injury showed full necrosis of the hair follicle in 5 of 10 cases. The hair follicles showed full necrosis for all

of the specimens from the 20 s, 30 s and 90 s sites. The burn sites differed in terms of the degree of necrosis to the hair follicle [χ^2= 39.9, df=12, p<0.0001].

The apocrine glands were normal in all 10 specimens from the 3 s burn. The 12 s injury showed full necrosis of the glands in 7 of 10 cases. The 20 s (9/10), 30 s (9/10) and 90 s (9/10) burn injuries all had apocrine glands that were fully necrotic [χ^2= 45.1, df=12, p<0.0001].

The subcutaneous tissue was normal for all the specimens in the 3 s, 12 s and 20 s burn injuries. In 1 case, the fat showed evidence of necrosis in the 30 s burn injuries. In porcine skin fat can be present in the dermis and is generally associated with the hair follicles or apocrine glands. The location of the fat necrosis for the 30 s injuries was located within the fat surrounding the glands or the hair follicles. The 90 s burn injuries had fat necrosis that extended beyond the fat located in the dermis. The burn wounds differed in terms of the location of fat necrosis [χ^2= 8.5, df=4, p<0.001]. A summary of the major findings of the histology for the burn sites and the depth classification is shown in the table below (Table 5-1).

Brass Rod Contact Time	Collagen Necrosis Location	BV Necrosis Location	Hair Follicle Necrosis	Fat Necrosis	Burn Depth Classification
3 s	Less than Upper 1/3	Upper 1/3	None	None	Superficial Partial
12 s	Upper 1/3	Lower 1/3	None or Partial	None	Superficial Partial
20 s	Upper 1/3 to Lower 1/3	Lower 1/3	Full	None	Deep Partial
30 s	Upper 1/3 to Lower 1/3	Lower 1/3	Full	None	Deep Partial
90 s	Lower 1/3	Subcutaneous Tissue	Full	Yes	Full Thickness

Table 5-1: Summary of Histology Criteria for Burn Sites

5.1.2 **Vimentin Immunostaining**

A total of 60 specimens from 10 swine were evaluated for the presence of positive vimentin immunostaining. There were 10 specimens in each burn depth category of 3, 12, 20, 30 and 90-second burns along with 10 specimens from the control sites. Vimentin staining was present in 50 of 60 cases and absent in 10 of 60 cases. The 3, 12, 20, 30 s and control sites all had positive vimentin immunostaining. The 90 s injuries showed an absence of vimentin staining. The burn and control sites differed in terms of the presence or absence of staining [χ^2= 41.1, df=5, p<0.0001].

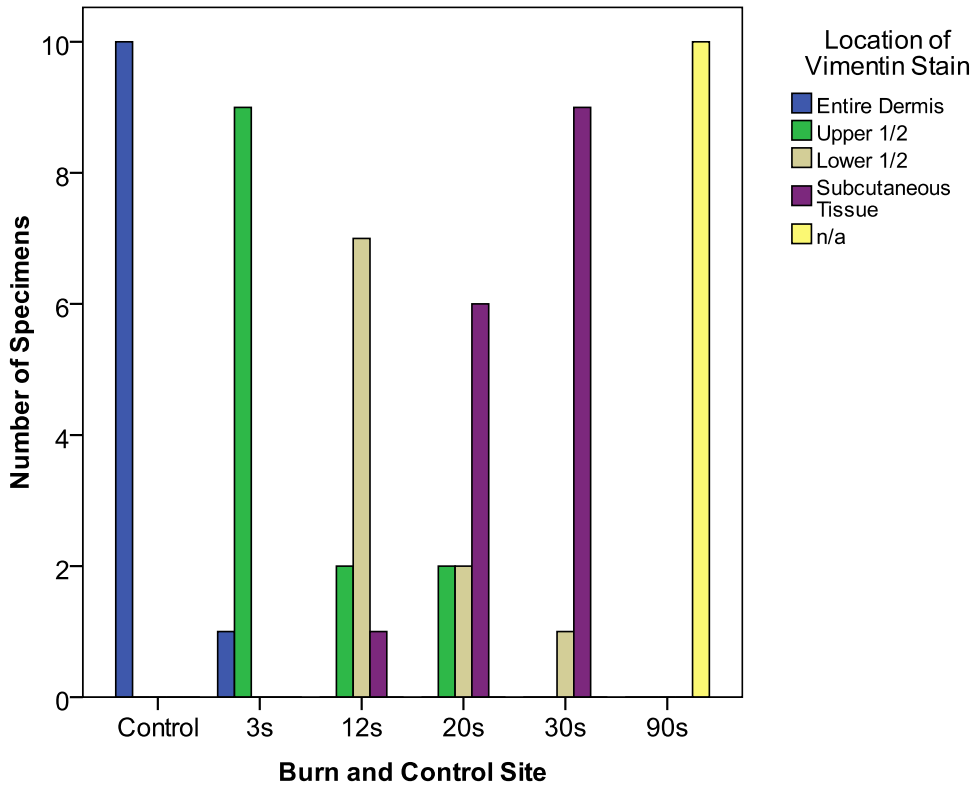

Figure 5-4: Location of Vimentin Immunostaining

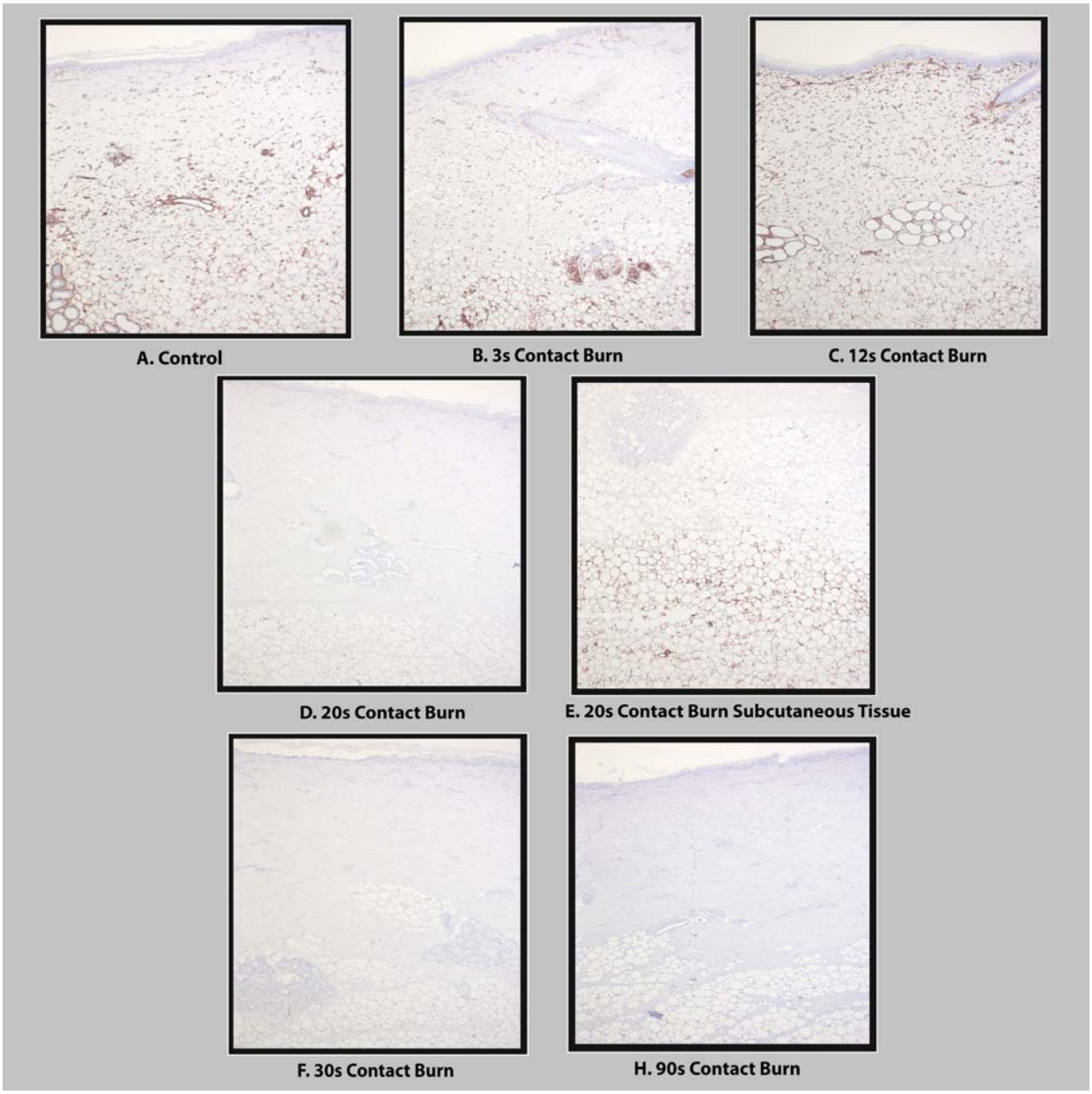

Figure 5-5: Vimentin Immunostaining of Control and Burn Sites (*5x* magnification)

Vimentin immunostaining was present in the entire dermis and subcutaneous tissue for the control site as shown in Figure 5-5 panel A. The 3 s burn showed a small absence of staining in the upper portion of the dermis for the majority (9/10) of cases as shown in Figure 5-5 panel B. The 12 s burn had an absence of staining in the upper portion of the dermis in 70% of cases (7/10) Figure 5-5 panel C. The other 2 specimens were similar to the 3 s injury as there was only a small absence of staining in the upper dermis. The 20 s burn showed more variability with positive vimentin staining in the upper ½ (2/10), lower ½ (2/10) and subcutaneous tissue (6/10) as shown in Figure 5-5 panel D and E. The 90 s injury showed an absence of positive vimentin cells in all cases. The sites differed statistically in terms of the location of the stain [χ^2= 105.1, df=20, p<0.0001] as shown in Figure 5-4.

5.2 Discussion

5.2.1 Challenges Associated with Histology

Creating a reference standard in the area of burn depth determination is a challenging and multifaceted problem. These challenges are related to the inherent nature of histopathology and the inherent variability of burn wounds. Biopsies are rarely acquired clinically, which translates to a lack of expertise in the histopathology of burn depth determination. Pathologists who do not routinely view specific types of tissue have a greater chance of producing an error in their reports. Biopsies are invasive and histology results require too much time to be of benefit in the clinical environment, and consequently histology has been relegated mainly to the research environment.

However, with the advent of new tools to assess burn depth a reference standard is critical and has to be well-defined. A histopathology report is based on the experience and judgment of the pathologist, which adds an element of bias or subjectivity to the diagnosis. In addition, like other areas of pathology the correct diagnosis is not well-defined. This is felt to be secondary to inadequate diagnostic criteria, inappropriate classification methods and limitations of the morphological diagnosis.[122] This last statement accurately summarizes the current state of affairs with burn depth histopathology. There have been no revisions in over 50 years and there are no consensus criteria to classify tissue injury.

Insight into the limitation of the reference standard was the impetus for establishing a burn wound histology database at the onset of the thesis work. The database was initially started as a clinical database but has since expanded to include porcine burn specimens. Currently, there are over 300 human specimens and 500 porcine burn wound biopsies. The information contained in the database has been used to develop objective grading criteria for burn depth determination and to investigate the utilization of adjunctive staining techniques.

In order to reduce the subjectivity of slide assessment, objective criteria were predefined and placed in a proforma document to use while viewing the slides. Proforma documents have been shown to improve the quality and completeness of reports for colorectal carcinoma resections, cervical loop excision biopsies and breast carcinoma.[197–199] Criteria used to evaluate burn depth include the level of collagen and endothelial necrosis in the dermis. The epidermis, hair follicle, sebaceous glands, eccrine glands

and fat were evaluated according to the degree of necrosis to the structure. The proforma document utilized to assess clinical burn depth is shown in Appendix B.

5.2.2 **Burn Depth Classification**

The challenges of classifying burn wounds extend beyond the limitations of histology. Burn wounds have inherent variability, which means biopsies taken from one region of the tissue may not fully represent the global physiology of the wound. Jackson described the zones of injury within the burned tissue, but this is not always easy to visualize when assessing clinical wounds. Burns change rapidly over time and can progress in terms of the level of injury. The dynamic nature of the injury means the timing of the biopsies can affect the results, as a wound may be superficial at the early time points (e.g., 1 hour post-burn) but be dramatically different at 5 days post-burn.

The degree of thermal injury to the tissue progressed as the length of the brass rod contact time increased. This depth progression ranged from a 3 s superficial partial thickness injury to a full thickness 90 s burn wound as shown in Table 5-1. The time for complete wound healing also supports the histology diagnosis as the shorter times corresponded with the minimal injuries to the collagen, endothelium and hair follicles. The inability to heal the wound corresponded to the deep partial and full thickness injuries.

Burn depth has classically been viewed as a physical measurement of injury to the tissue and this has been reflected in histology studies. However, the viability of a burn

wound is determined not only from the level of injury to the tissue but more specifically to the structures that are injured. This is reflected in histology reports that have focused on either the status of collagen, intermediate filament proteins, the viability of appendages, the presence of infection or the vascular nature of the burn wound.[25, 200–204] There are few reported studies to date that look at all of these variables in combination or provide objective criteria for pathologists to use when defining burn injury.

In the clinical environment, the histology of superficial and full thickness injuries is relatively easy to define. The partial thickness injuries, however, are much more difficult to classify as there is increased variability within the specimens. Grading criteria were created over the course of this work in order to objectively define burn depth in the clinical environment. A multifactorial approach using a combination of variables was used to classify the burn into viable and non-viable injuries. These variables included the epithelium of eccrine glands and hair follicles, endothelium and collagen. The health of the tissue is defined by the degree of injury to these various structures instead of a physical measurement or the location of tissue injury. The variables used to define burn depth in swine included collagen necrosis, blood vessel necrosis, necrosis of the hair follicles and fat.

The 3 s burn injury showed minimal damage to the structures of the skin. The necrosis of the collagen was barely perceptible and there was no fat necrosis. The endothelial injury was present in the upper 1/3 of the dermis but did not span the entire region. In 6 of 16 cases the hair follicles showed some necrosis of the epithelium. These hair follicle shafts were located in the upper portion of the dermis and epidermis and the injury was

found at the most superficial portion of the hair follicle. In human specimens, the presence of hair follicles is not as predominant as in swine specimens. Hair follicles were present in 70% (234/336 specimens) of the clinical cases and in most specimens only one cross-section of the shaft was visible. In addition, hair follicle necrosis was not an independent predictor of depth in the clinical situation. However, hair follicles are present and the epithelium can be evaluated for injury in the large majority of swine specimens. Also, entire hair follicles can be evaluated in various levels of the skin if the specimens are cut in levels or repeat sections. This means that the location of hair follicle necrosis can be defined. Therefore, the location of hair follicle necrosis might be an important predictor of outcome in a swine model.

The 20 s and 30 s burn wounds were easily classified as deep partial thickness injuries as the collagen necrosis extended into the lower 1/3 of the dermis. The endothelium and epithelium were not viable and the only normal structure in the wounds was the subcutaneous tissue. The 30 s injury showed a greater degree of necrosis to the collagen, hair follicles and endothelium when compared to the 20 s burn injury.

Full thickness injuries could be distinguished from partial thickness injuries by the presence of fat necrosis, which is considered to be the hallmark of this injury. The 90 s burn wound is a full thickness burn wound secondary to the presence of fat necrosis.

The only burn site that was difficult to evaluate was the 12 s burn wound. The 12 s burn wound showed minimal damage to the dermal collagen and no fat necrosis present in the wound. However, the endothelial necrosis spanned the entire thickness of the dermis

and the hair follicles were necrotic in 11 of 16 cases. In the 11 cases identified, the upper portion of the hair shaft was present in the specimen and the status of the hair bulb was unknown. Previous histology clinical experience suggests that these injuries should be classified as non-healing wounds based on the degree of injury to the endothelium and epithelium. However, the 12 s burn healed within 16 days of burn injury, which means that this wound is a healing or viable wound. The rationale for the 12 s burn injury's ability to heal may be related to the small size of the injury and the intact epithelium at the wound edges. The deep hair bulbs were not visualized in these specimens, as levels were not cut to view the entirety of the hair follicle. The lower portion of the hair follicle could have provided viable epithelium for wound healing.

The deep vascular plexus at the dermal-fat interface was patent with non-necrotic endothelium. The deep plexus supplies the bulb and lower shaft of the hair follicle, which suggests that the hair may have been adequately perfused in this region. Finally, collagen necrosis has been shown to be an independent predictor of tissue viability in the clinical setting. There was minimal injury to the collagen in the 12 s swine burn injury despite the deep level of blood vessel necrosis. This would be an unusual finding in clinical biopsies, as the level of collagen necrosis and the endothelial necrosis are similar in the majority of cases.

5.2.3 **Histology Versus Wound Healing Time**

Investigators working to develop new technologies to assess burn depth have debated the use of histology versus wound healing time as the reference standard. Wound

healing time is non-invasive, cheap and does provide the true answer to the ability of an injury to heal. However, the measurement of wound healing time requires the investigator to wait for the wounds to granulate. This is not ethical in a clinical situation, as prolonging treatment for deep partial thickness injuries has a direct impact on patient outcome. Operative decisions are made quickly in the current climate of early tangential excision and grafting, which makes it difficult to determine the true wound healing time of the injury and consequently the depth of injury. The advantage of the laboratory environment is that wound healing time can be evaluated, and in this study the 3 s burn injury was 100% granulated by 7 days post-injury and the 12 s burn by 16 days. The other burn sites did not heal by the 16-day time period and these wounds were considered non-viable injuries.

The histological assessment of burn injury is based on the visible features within the biopsy but may not truly reflect the entire surface of the burn wound. Histology is expensive, can be subjective and viability determinations are difficult for indeterminate burn injuries. The advantage of histology over wound healing time in the clinical environment is that biopsies can be acquired at any time. The laboratory environment represents the best of both environments as biopsies and wound healing time can be evaluated. In this study, wound healing time in conjunction with histology was important to accurately identify burn wound depth, especially with the 12 s burn injuries.
From this study, utilizing wound healing time and histology in combination improved the robustness of the reference standard. The real challenge in the clinical environment is developing a method to calculate wound healing time in a climate of early excision. As

an outcome measure, wound healing time is critical for the next phase of validating the clinical histological grading system.

5.2.4 **Objective Criteria for Burn Depth Determination**

Separating partial thickness injuries into viable and non-viable injuries is difficult and not clear-cut. In the past, burn wound histology studies have focused on the status of collagen, intermediate filament proteins (vimentin), the viability of adnexal structures, the presence of infection or the vascular nature of the burn wound as independent entities.[25, 200–202, 204] However, the viability of the burn wound is dependent on multiple factors such as adequate blood supply, proliferating epithelium and a structural framework. Therefore, a viability determination should include more than one histology feature.

Singer et al. evaluated several criteria for burn depth determination in a partial thickness burn porcine model. From this study, it was reported that the structures of the skin have varying sensitivity to thermal insult. The endothelial cells appear to be injured by the lowest temperature and shortest duration of heat exposure, followed by mesenchymal cells, hair follicles and collagen. Because the structures respond differently to the thermal injury it may be of value to weight the variables accordingly. The Singer study was small (n=2) and was performed in a porcine model, which makes it difficult to evaluate the effects of heat on the eccrine glands, as they are absent in swine. In addition, the biopsies in the Singer study were acquired early after burn injury (30 minutes) and there was no correlation to wound healing time.[205] As there is still no

evidence that one variable may be more important than another, the variables in all of the histology work to date considers each variable to have equal weight.

In clinical studies, the combination of dermal collagen, endothelial and eccrine gland necrosis are predictors of partial thickness wound viability. The combination of collagen necrosis, endothelial necrosis and eccrine necrosis produced a sensitivity of 94% (95% CI 78–99%) and a specificity of 88% (95% CI 70–96%). The area under the ROC was 0.96 ± (95% CI 0.91–1.00).

Collagen and endothelial necrosis were defined according to their location in the dermis. In the clinical specimens, the dermis is divided into halves based on the position of the erector pilae muscle or hair follicle. This is a preferred method over the use of a microtome. A microtome is used to assess the physical measurement of the degree of injury to the tissue and is expressed in relation to total dermal thickness. The reference point for the microtome measurement is the basement membrane. Experience with the specimens during this thesis showed that the basement membrane is difficult to identify within the necrotic eschar and is not a reliable anatomic landmark in clinical specimens. The technique of dividing the dermis into halves worked well in the clinical situation and can still account for the differences in skin thickness. However, this may not be true for swine burns as the basement membrane was visible and it would be possible to utilize a microtome to measure the depth of injury. In this swine model, it may be a more objective way to evaluate burn depth than the anatomic divisions used in this study.

There have been a variety of techniques used to assess the degree of injury to the dermal collagen. The bifringence of collagen, Verhoeff's stain and Masson's trichrome stain can all document the level of injury to the tissue.[201, 206–208] The level of injury to the collagen is easy to evaluate with an H&E and does not require special staining techniques. Human and swine differ in terms of the degree of injury to the collagen and endothelium. In swine, the degree of injury to collagen lags behind the more severe damage to the hair follicles, glandular structures and endothelium. In humans, there is also a lag but the injury to the collagen and the blood vessels is in alignment.

The classification of patent and occluded vessels in this work is based on the study by Watts et al.[204] The only difference between this swine study and the Watts study is that endothelial necrosis and vessel occlusion are treated as two separate entities. The rationale for the separate entities was in line with the proforma document so that all features of the burn wound biopsy were reported. It was also used to evaluate if there were circumstances in which the vessel occlusion and endothelial necrosis may not be associated. In the majority of swine cases, if the vessels were occluded then the endothelium was necrotic. However, the two should still be evaluated separately to ensure that a vessel with tightly packed red blood cells is not mistaken for a vessel with debris and interpreted as a necrotic occluded blood vessel. Papp also successfully used the Watts classification to document the progression of burn injury up to 48 hours after injury in a porcine burn wound mode.l[24]

Endothelial damage has also been shown to be a valuable indicator of burn depth when differentiating partial thickness injuries in the clinical grading system. The importance of

vascular patency is also supported by Boykin's study, which uses a mouse ear chamber model where platelet microthrombi occluded the post-capillary venules and arteriovenous shunts 12–48 hours after injury.[26] Regas et al. developed a rat comb burn model to examine the vascular changes in the zone of stasis. Vascular casts and occlusion were associated with decreased perfusion in the zone of coagulation and zone of stasis at 24 hours post-injury.[209] In all of these studies, vascular occlusion was associated with necrosis of the tissue, which makes it important to evaluate the status of blood vessels.

The epithelium surrounding the hair follicle is important as it represents the regenerative capacity of the burn tissue.[210] Hinshaw described the progressive injury that occurs to the hair follicle in the first 24 hours post-injury.[211] Foley used the injury to the hair follicle to differentiate superficial and deep partial thickness burn wounds. Superficial injuries were described as having necrosis of the upper hair follicle shafts and deep partial thickness injuries as complete destruction of the follicle.[212] Ho-Asjoe et al. was one of the first groups to utilize immunohistochemistry to show the degree of thermal injury to hair follicles in human skin. Collagen IV antibodies demonstrated a gradual loss in staining in the hair follicle shaft as burn depth increased.[202] Unfortunately, the hair follicle is not always present in the clinical burn specimen secondary to the anatomic region of the biopsy or the section viewed by the pathologist. Eccrine glands are present in nearly every clinical slide and have been used as a tool to evaluate the viability of the burn. Swine do not have eccrine glands, therefore these structures could not be evaluated in this study.

The clinical model developed and tested during the thesis is a first attempt at creating a grading system for the histological determination of burn depth. However, the 95% CI associated with the specificity of the model was broad, which means that the capacity of the grading system to identify the true negatives or non-viable wounds has some variability. This may be a reflection of the imperfection of the grading system, which fails in the following clinical scenario. The burn wound is described as an upper 1/2 collagen and blood vessel necrosis with a partially necrotic epithelium of the hair follicle and eccrine glands. This scenario occurred in 11% (16/142) of partial thickness cases and 8% (16/194) of the overall clinical study population. This is common in pathology, as multiple stains are generally required to differentiate difficult lesions or wounds. Other techniques in combination with the H&E would serve to more clearly define the partial thickness injuries and address the small number of cases in which the diagnosis is not clear-cut.

5.2.5 **Vimentin Immunostaining**

Vimentin immunostaining was popularized by Nanney in 1996 as a tool to distinguish burn depth.[25] This represented a novel way to determine burn depth, but there are no published guidelines on how to interpret the stain. The burn sites created in this model were chosen to show the progression of thermal injury in terms of depth and time. This type of model was important in order to compare the previously published vimentin findings with the findings from this animal study.

The presence of vimentin immunostaining could accurately differentiate partial thickness and full thickness injuries. The 3–30 s burn wounds showed the presence of positive immunostaining and the 90 s injury showed an absence of staining. The location of the vimentin staining was important to differentiate the 3 s and 30 s injuries. The 3 s injury had a minimal absence of staining and the 30 s injury showed positive immunostaining only in the subcutaneous tissue. The 12 s and 20 s injuries, however, were difficult to differentiate as both had variable levels of vimentin staining. The 12 s and 20 s burn wounds represent the indeterminate injuries and are the most difficult to differentiate using histology. Vimentin as a single staining technique could not distinguish these injuries into viable and non-viable burns.

This was similar to the results obtained from the clinical studies that evaluated 174 human burn specimens. The objective criteria used to determine burn depth classified 75 specimens in the superficial partial thickness category, 59 as deep partial thickness injuries and 40 as full thickness burn wounds. Deep partial thickness injuries showed no demarcation line in 78% of cases and have weak immunostaining in 68% of cases. This is compared to a superficial partial thickness injury where 46% have no demarcation line and 33% have weak immunostaining. This suggests that the absence of staining may indicate non-viability of an injury, but this distinction is not clear-cut and is difficult to interpret. The results from the clinical study indicated that vimentin immunostaining should not be utilized in isolation. This is a situation where statistical significance does not translate to clinical use.

The progression of burn injury over time is well-documented using vimentin.[25] This indicates that the timing of vimentin immunostaining may impact the results of the technique. In the animal study, the progression of burn injuries over time was not observed using this stain. The results at 1 hour post-burn reflected what occurred at 96 hours after the injury. However, there was inherent variability in the results that can be seen in the 20 s burn injury, which vacillated between staining only in the subcutaneous fat to an absence of staining in the upper portions of the dermis.

In the clinical environment, the timing of the acquisition of the burn wound biopsy has been shown to be critical to the interpretation of vimentin results. For example, a superficial burn shows very little change in vimentin immunostaining at time points 1 and 3 days post-burn injury. A deeper injury resembles a superficial partial thickness on day 1 but progresses over time to either a mid-dermal or pan-dermal absence of vimentin immunostaining by day 3.[25] If a partial thickness burn wound is biopsied at day 1 then it would be difficult to determine its viability at this time point using vimentin, as the majority of the dermis will stain positive. In the clinical studies, biopsies occured at a mean of 3.5 days post-burn injury, with the majority of biopsies obtained between 3–4 days (65%) after injury. At this time point, burns should have been easily distinguished using vimentin according to previous published studies. However, this was not the case with the clinical studies performed during this thesis, and the results obtained for the partial thickness and full thickness injuries were difficult to utilize.

Vimentin is used by pathologists to identify neoplasms derived from mesenchymal cells such as sarcoma, lymphoma and melanoma. However, vimentin has limited diagnostic

value as a single entity and needs to be used in conjunction with other antibodies in order to classify the tumour.[125] For example, vimentin and keratin are used collectively in order to distinguish melanoma from undifferentiated carcinomas and large cell lymphomas.[213] If vimentin is used in combination with other techniques to provide a definitive diagnosis in other areas of pathology then it should not be used in isolation for burn depth determination.

5.2.6 **Limitations of Study**

The swine burn model was reproducible for the majority of burn sites as a similar depth burn was created on each of the 16 animals. The 12–30 s burn injuries, however, did show some variability in burn depth as the level of collagen necrosis was not the same at each site. For example, the 12 s burn injury collagen necrosis was less than the upper 1/3 of the dermis in 9 cases, with 7 cases in the upper to mid1/3 category. In the 3 s burn wound, 6 specimens showed partial necrosis of the hair follicle, unlike the other 10 specimens, which had an absence of hair follicle necrosis. The variance in the model is a representation of the inherent variability that exists within burn wounds.

The second limitation of the study was the fact that there was no superficial or first-degree burn injury. The space was limited on the dorsum of the animal and the priority was to include burn wounds that are normally seen clinically. First-degree injuries are easy to diagnose and do not require treatment at a specialized burn centre. However, scald burns can resemble first-degree injuries in the early phases of the injury and it would have been useful to assess the NIR results from these wounds.

The injuries created on the dorsum of the animal are considered contact thermal injuries. This type of animal model is a standard burn wound model but it may not truly replicate the clinical situation for all thermal injuries. Burn injuries do not always come in direct contact with a heated object and instead are exposed to high temperatures in the air or water. The rationale for using a contact burn model to create burn injuries is to protect the safety of the investigator. The ideal model for thermal injury evaluation is to heat the skin via hot water. Boiling water has been used in small animal models as chambers can be created where the animal resides. However, it is very difficult to create these chambers for larger animal models and hot water poses significant risk to the investigator creating the wounds.

In the animal study, only one animal was used for each of the specific histology time points, which means there was no baseline biopsy with which to compare the results. Progression of injury may have been shown more clearly with a baseline biopsy post-burn and serial biopsies over time from the same animal. It was not possible to perform serial biopsies in this study, however, as removing the tissue would remove the area of interest for the NIR Point data collection.

It is also important to consider that one animal may not truly reflect what occurs at that particular time point. For example, the 48-hour animal showed staining in the upper 1/3 of the dermis for the 12 s and 20 s injury when the large majority of the other animals showed a deeper injury to the tissue. In hindsight, it may have been more beneficial to acquire biopsies from the same animal at the specific time points post-burn injury. It is

important in the future to include more animals in the time groups. This would have eliminated the variability that may exist between the animals in terms of the depth of injury or response to injury. It has already been shown using H&E that the individual animals did show some variation in the tissue response to burn injury. Despite the limitations of the study, burn injuries were created on the dorsum of the animal that reflected the depth progression of thermal injury.

5.3 Summary and Conclusion

The results from the animal study showed that an H&E could easily differentiate partial thickness and full thickness injuries using fat necrosis as the hallmark of the injury. The 3 s, 20 s and 30 s burn wounds were easily categorized as superficial and deep partial thickness injuries using objective grading criteria. The 12 s burn was difficult to assess as the collagen showed minimal necrosis compared to the endothelium and epithelium. Wound healing time was used to classify the 12 s injury as a non-healing burn wound. The future of the reference standard relies on wound healing time as an outcome measure for the next phase of validating the clinical histology grading system.

Vimentin immunostaining could easily differentiate viable and non-viable injuries at the extremes of thermal injury. Vimentin as an individual technique is limited by its capability to distinguish indeterminate injuries. The recommendations for the utilization of vimentin include the following:

1) Vimentin should not be used in isolation but as an adjunct to H&E.

2) The timing of the biopsy may affect the vimentin immunostaining results and therefore it may be important to compare specimens acquired at the same time point. This is more important in the clinical environment, as there were no time differences in this current animal model.

In conclusion, vimentin immunostaining should not be considered the reference standard for burn depth determination. As an adjunctive tool with other staining methods it can provide useful information that collectively could be used to determine burn depth. However, it cannot fully elucidate the viability or non-viability of indeterminate burn wounds. Its utilization as an adjunctive tool to H&E still needs to be evaluated more carefully in the future. Defining the reference standard is an important part of advancing our ability to accurately determine burn depth and develop new diagnostic tools and treatments.

Chapter 6: Oxy- and Deoxyhemoglobin Content

6.1 Proportion of Deoxy- and Oxyhemoglobin to Total Hemoglobin

The figures and results in this section are presented as the ratio of oxy- and deoxy-hemoglobin to total hemoglobin. Significance values in the figures represent the differences between all sites shown on the x-axis in the figure at the particular time point.

6.1.1 **Pre-Burn**

The deoxy- and oxyhemoglobin levels in the burn and control sites are divided separately by the total hemoglobin to give the proportional amount oxy- and deoxyhemoglobin in the wounds. The sites located near the cranial region of the animal had a higher proportion of deoxyhemoglobin compared to its caudal counterparts. The proportion of oxyhemoglobin was low in the cranial region and increased caudally as shown in Figure 6-1. The approximate proportion of oxy- to deoxyhemoglobin levels is around 80:20, or 4:1. Statistical significance was achieved at source collectors 3 and 4 but not source collector 2.

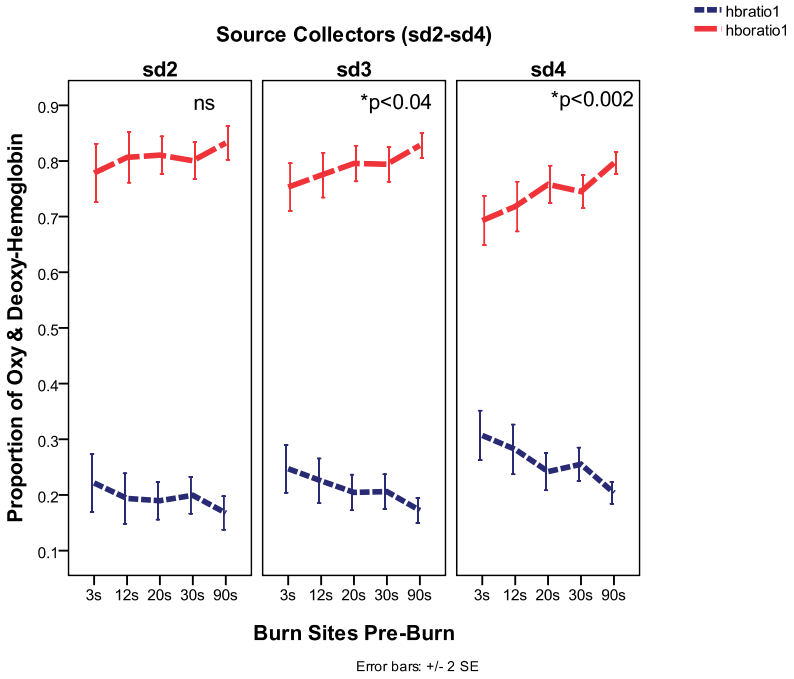

Figure 6-1: Proportion of Oxy- (hboratio1) and Deoxyhemoglobin (hbratio1) in the Burn and Control Sites Prior to Injury

6.1.2 **Burn Sites**

Immediately after burn injury and 1 hour post-burn, there were no differences in the proportion of oxyhemoglobin or deoxyhemoglobin between the burn sites at any of the source collector separations.

At the 12–96-hour time points, the ratio of deoxyhemoglobin to total hemoglobin is low in the superficial burns and increases as the depth of injury increases. The opposite was found with oxyhemoglobin, as high levels are found in the superficial wounds and decline as burn depth increases.

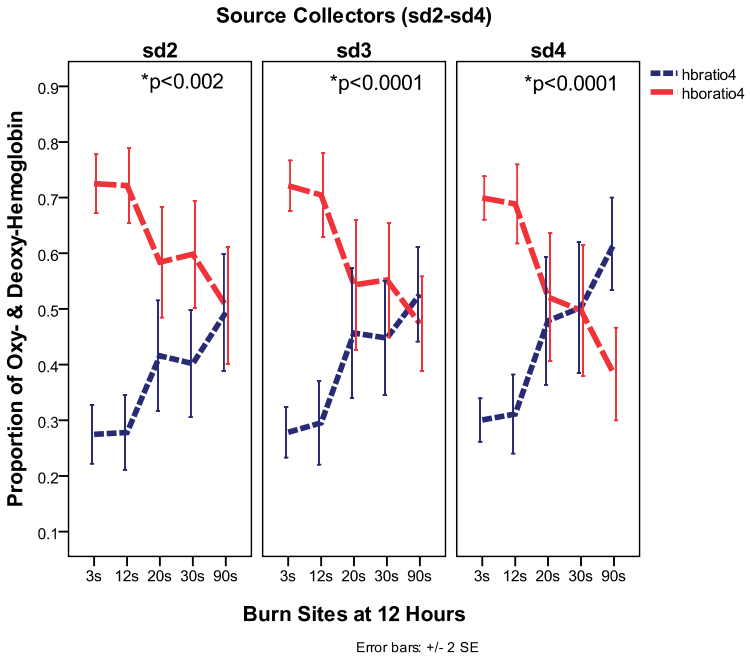

Figure 6-2: Proportion of Oxy- (hboratio4) and Deoxyhemoglobin (hbratio4) in the Burn Sites at 12 Hours Post-Injury

Twelve hours after burn injury, there is a clear demarcation between the burn sites. The the 3 s and 12 s injuries showing a 2:1 ratio of oxy: deoxyhemoglobin. The overlapping error bars for the 20 s and 30 s injuries indicate a 1:1 ratio of oxy- to deoxyhemoglobin. The same was true for the 90 s injury except in source collector 4, where the proportion of deoxyhemoglobin is higher. This was statistically significant at all source collectors as shown in Figure 6-2.

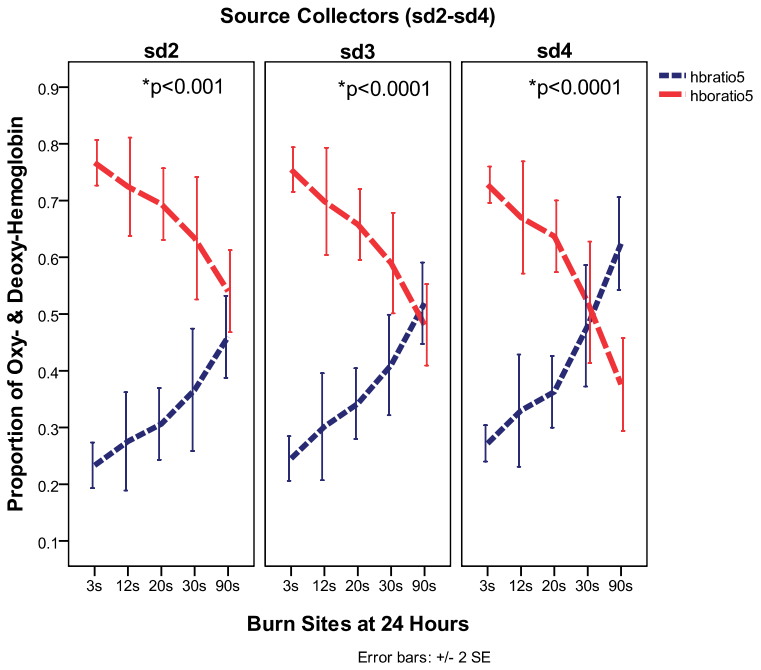

Figure 6-3: Proportion of Oxy- (hboratio5) and Deoxyhemoglobin (hbratio5) in the Burn Sites at 24 Hours Post-Injury

At 24 hours, the 3 s, 12 s and 20 s have a higher proportion of oxyhemoglobin in the wounds. The 30 s injury showed an increase in the oxy- to deoxy-hemoglobin ratio at source collector 2 and 3 but not at source collector 4. The 90 s burn shows a 1:1 ratio of oxy- to deoxyhemoglobin except in source collector 4, where the proportion of deoxyhemoglobin is higher than oxyhemoglobin. This was statistically significant for source collector 2, 3 and 4 as shown in Figure 6-3.

At 36 hours post-burn, for the majority of burns there is a higher proportion of oxyhemoglobin than deoxyhemoglobin as shown in Figure 6-4. The highest proportion of oxyhemoglobin remains within the 3–20 s burn injuries, which have a 3:1 ratio of oxy- to deoxyhemoglobin. The oxyhemoglobin proportion in the 30 s and 90 s burn wound

increases in source collectors 2 and 3. The 30 s and 90 s burn still show a 1:1 ratio of oxy to deoxyhemoglobin at source collector 4. This was statistically significant for source collectors 2, 3 and 4. The 48-hour time point results were very similar to the 36-hour time point as shown in Figure 6-5.

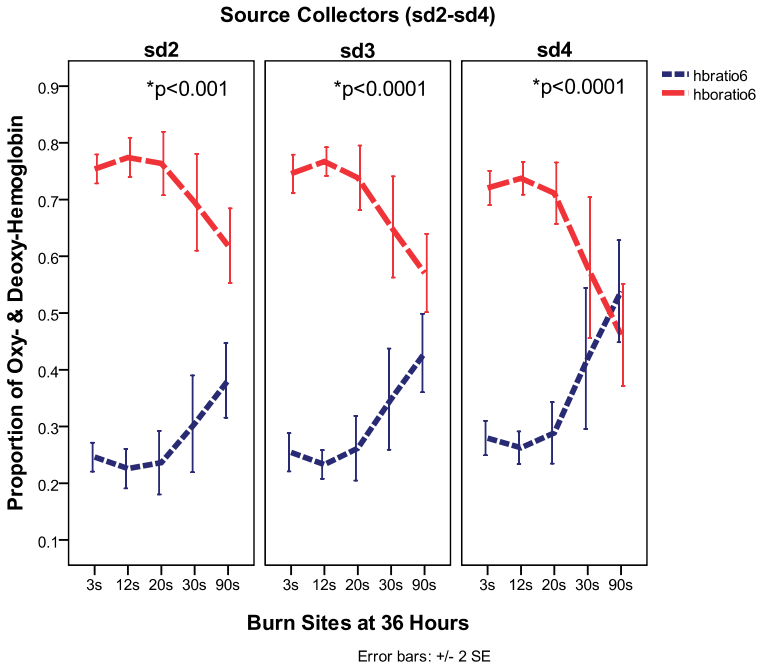

Figure 6-4: Proportion of Oxy- (hboratio6) and Deoxyhemoglobin (hbratio6) in the Burn Sites at 36 Hours Post-Injury

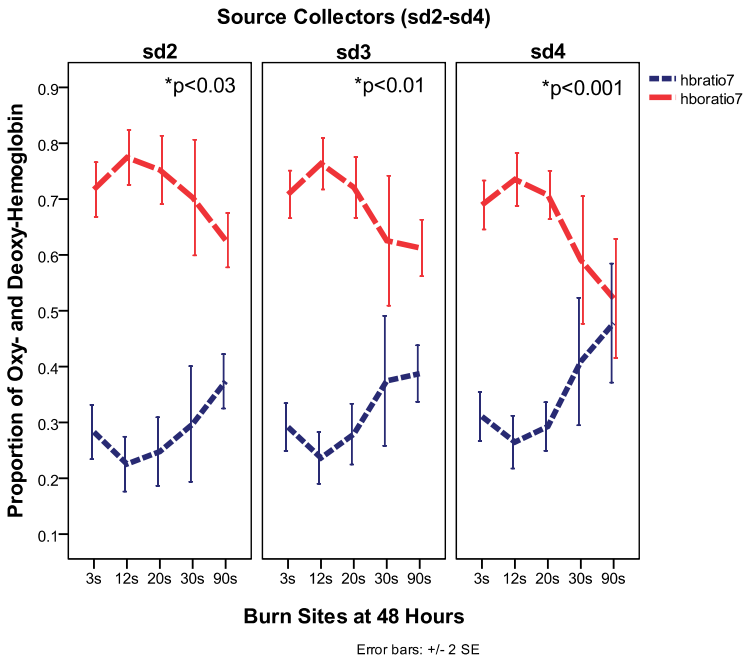

Figure 6-5: Proportion of Oxy- (hboratio7) and Deoxyhemoglobin (hbratio7) in the Burn Sites at 48 Hours Post-Injury

At 96 hours post-burn, the proportion of oxyhemoglobin to deoxyhemoglobin has exceeded pre-burn levels for the 3 s burn (6:1 ratio) as shown in Figure 6-6. The 12–30 s burns are closer to pre-burn proportions with a 3:1 ratio of oxy- to deoxyhemoglobin. The 90 s injury has a ratio of oxy- to deoxyhemoglobin that is less than 2:1. This was statistically significant at all 3 source collectors.

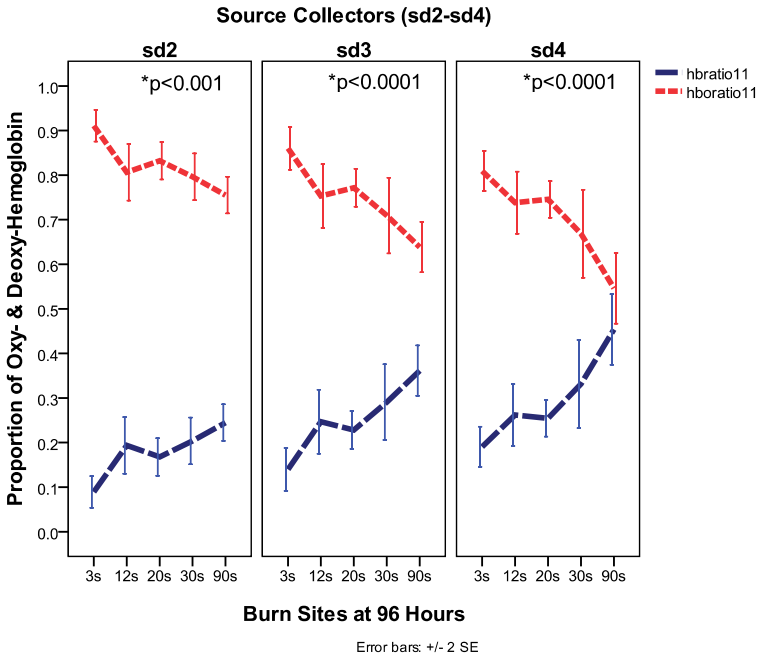

Figure 6-6: Proportion of Oxy- (hboratio11) and Deoxyhemoglobin (hbratio11) in the Burn Sites at 96 Hours Post-Injury

6.1.3 **Control Sites**

The proportion of oxy- to deoxyhemoglobin between the control sites did not change at the majority of time points and source collectors. The exception was at the 1-hour time point, as the proportion of oxyhemoglobin was lower in control site 1 (cranial) and increased up to control site 5 (caudal region) as shown in Figure 6-7.

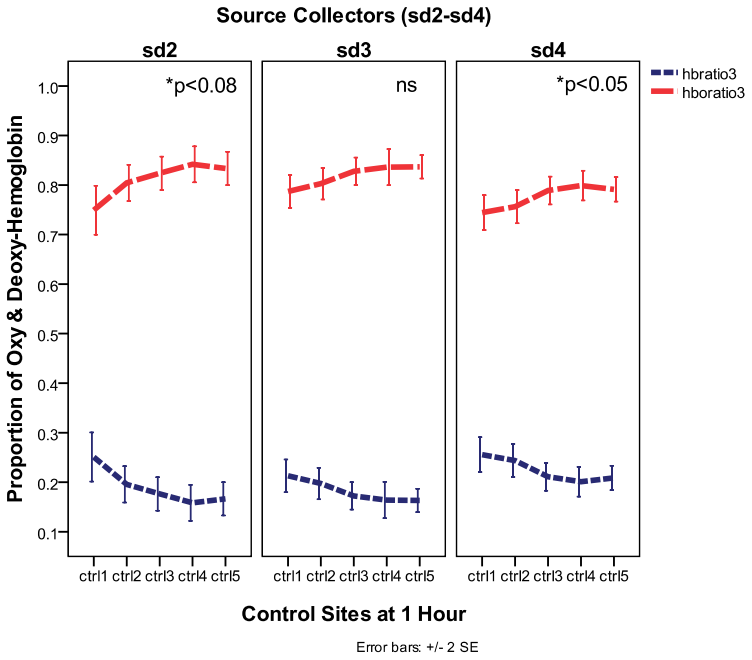

Figure 6-7: Proportion of Oxy- (hboratio3) and Deoxyhemoglobin (hbratio3) in the Control Sites at 1 Hour Post-Injury

6.2 Pre-burn

The figures and results in this section are presented as the mean values of oxy- and total hemoglobin. Significance values in the figures represent the differences between all sites shown on the x-axis in the figure at the pre-burn time point. Oxyhemoglobin and total hemoglobin levels increased from the cranial to the caudal sites at the pre-burn time point as shown in Figure 6-8 and Figure 6-9.

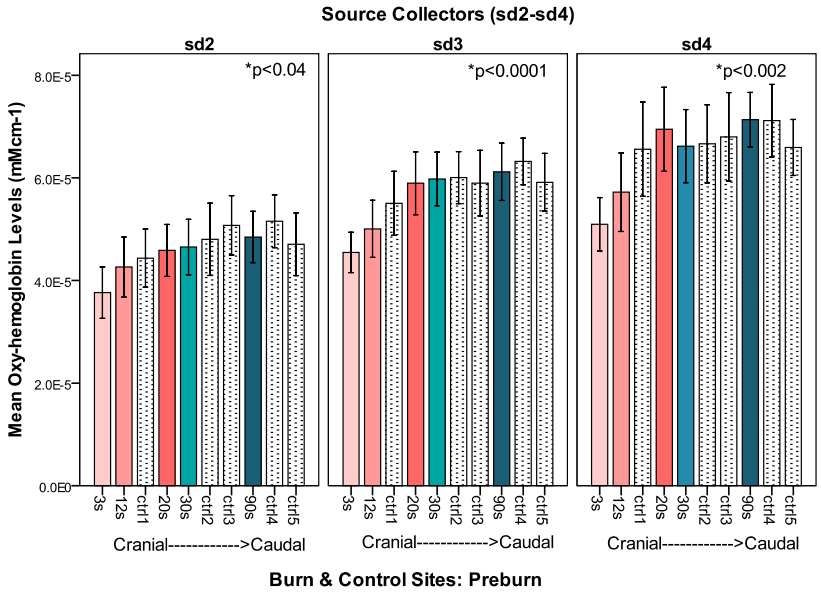

Figure 6-8: Mean Oxyhemoglobin Levels in the Control and Burn Sites Prior to Thermal Injury

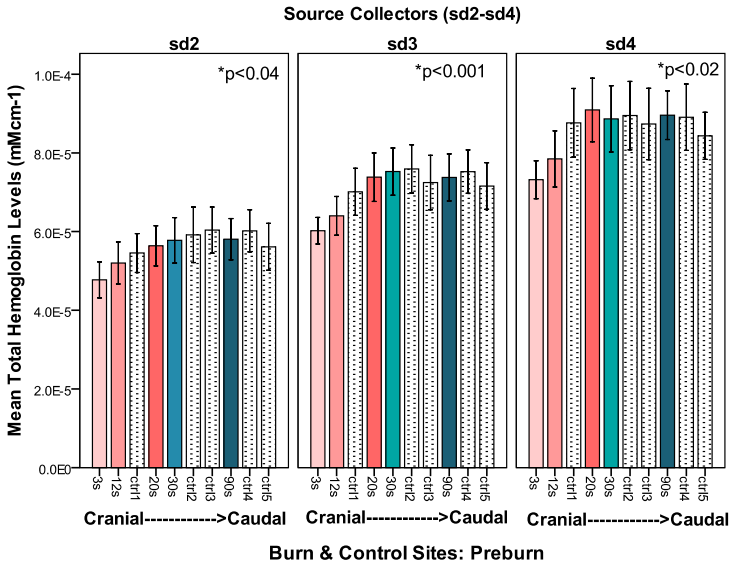

Figure 6-9: Mean Total Hemoglobin Levels in the Control and Burn Sites Prior to Thermal Injury

6.3 Change from Pre-Burn Values

The figures and results in this section are presented as the mean values of oxy- and total hemoglobin as a change from pre-burn values. In this statistical analysis, the burn sites were compared at each time point utilizing an ANOVA test. Therefore, the p-value the figures represent the largest p-value obtained from each analysis. For example, in Figure 6-10 for source collector 2 the p-value shown in the figure is less than 0.006. This p-value was obtained at 96 hours post-burn and for the rest of the time points the p-value was less than 0.0001. Therefore, p-values for each time point analysis were less than 0.006. All individual p-values were reported in accompanying ANOVA tables for each source collector separation.

6.3.1 Oxyhemoglobin

6.3.1.1 Burn Sites

Oxyhemoglobin levels differed between the burn sites at all of the time points and source collector separations as shown in Table 6-1, Table 6-2, Table 6-3 and Figure 6-10. Immediately after burn injury, the oxyhemoglobin levels in the 3-second burn (basehbo3s) experience a 63–79% increase compared to baseline levels at all source collectors. The 12-second burn (basehbo12s) experiences a 22–41% increase in oxyhemoglobin at source collectors 3 and 4 but only an 8% decrease at source collector 2. The remainder of the burn injuries showed an immediate decline in oxyhemoglobin ranging from 6–41% below pre-burn levels as measured by all detectors. Overall, the 90-

second burn (basehbo90s) showed the greatest decline in oxyhemoglobin levels at this time point.

At 12 hours after burn injury, the 3-second burn has a large increase (178–187%) above baseline. The 12-second injury shows the largest increase in oxyhemoglobin with values ranging from 99–166%. The 20 s (basehbo20s) and 30 s (basehbo30s) injuries have oxyhemoglobin levels above baseline. The 90-second burn experienced a 30% decrease in oxyhemoglobin levels.

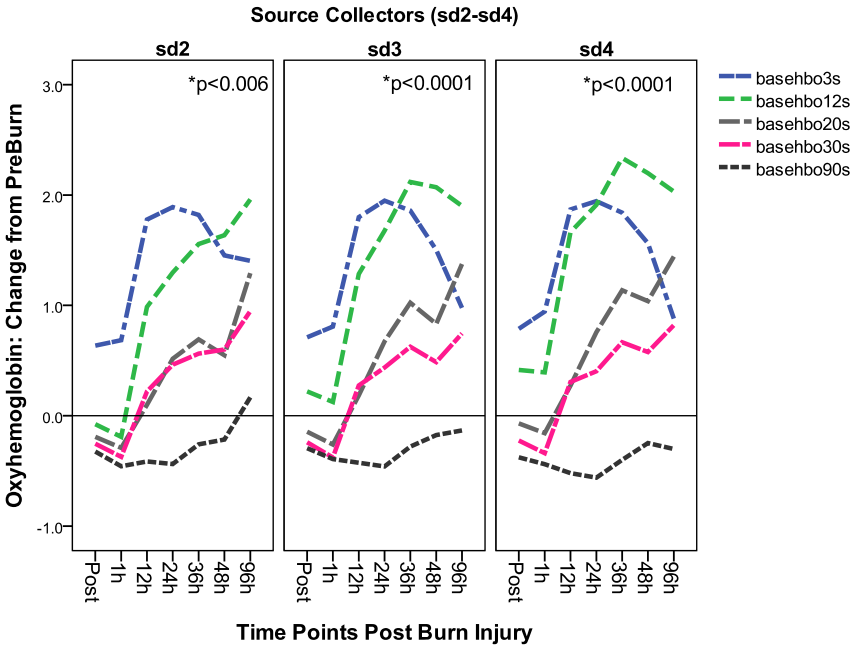

Figure 6-10: Burn Site Oxyhemoglobin Content as a Change from Pre-Burn Values over Time

Oxyhemoglobin as a Change from Baseline at SC 2: Mean Values (95% CI)								
Time	**3 s**	**12 s**	**20 s**	**30 s**	**90 s**	**df**	**F**	**p-value**
Post	0.63 (0.34-0.93)	-0.08 (-0.30-0.14)	-0.21 (-0.41-0.02)	-0.25 (-0.48--0.03)	-0.32 (-0.48 – -0.18)	4, 75	13.3	0.0001
1 h	0.69 (0.29-1.1)	-0.19 (-0.45-0.007)	-0.30 (-0.52--0.007)	-0.38 (-0.58--0.12)	-0.46 (-0.53--0.38)	4, 75	15.1	0.0001
12 h	1.8 (1.1-2.4)	1.0 (0.34 - 1.6)	0.12 (-0.16-0.36)	0.22 (-0.19-0.62)	-0.41 (-0.63 – -0.25)	4, 65	15.9	0.0001
24 h	1.9 (1.3-2.5)	1.3 (0.50-2.1)	0.52 (0.16-0.87)	0.46 (-0.49-0.97)	-0.44 (-0.62--0.25)	4, 65	13.0	0.0001
36 h	1.8 (1.3-2.3)	1.6 (0.80-2.3)	0.69 (0.44-0.94)	0.56 (0.16-0.96)	-0.26 (-0.51--0.005)	4, 60	14.7	0.0001
48 h	1.5 (1.0-1.9)	1.6 (0.80-2.5)	0.55 (0.23-0.87)	0.60 (0.07 -1.1)	-0.22 (-0.43-0.02)	4, 55	10.4	0.0001
96 h	1.4 (0.60-2.2)	2.0 (0.97-2.9)	1.3 (0.67-1.9)	0.95 (0.40-1.5)	0.17 (-0.43-0.76)	4, 45	4.2	0.006

Table 6-1: Oxyhemoglobin as a Change from Baseline for Source Collector 2

Oxy-Hemoglobin as a Change from Baseline at SC 3: Mean Values (95% CI)								
Time	**3 s**	**12 s**	**20 s**	**30 s**	**90 s**	**df**	**F**	**p-value**
Post	0.71 (0.46-1.0)	0.22 (0.04-0.39)	-0.14 (-0.32-0.04)	-0.24 (-0.46--0.02)	-0.30 (-0.41--0.18)	4, 75	21.6	0.0001
1 h	0.81 (0.52-1.1)	0.12 (-0.05 – 0.30)	-0.26 (-0.43--0.09)	-0.38 (-0.58--0.18)	-0.40 (-0.51--0.27)	4, 75	30.0	0.0001
12 h	1.8 (1.4-2.2)	1.3 (0.73-1.8)	0.18 (-0.13-0.5)	0.27 (-0.15-0.70)	-0.43 (-0.62--0.23)	4, 65	24.3	0.0001
24 h	1.9 (1.7-2.2)	1.7 (0.99 -2.4)	0.67 (0.30-1.0)	0.44 (0.002-0.87)	-0.46 (-0.63--0.29)	4, 65	24.3	0.0001
36 h	1.9 (1.5-2.2)	2.1 (1.5-2.8)	1.0 (0.68-1.4)	0.63 (0.25-1.0)	-0.28 (-0.5--0.05)	4, 60	26.7	0.0001
48 h	1.5 (1.2-1.8)	2.1 (1.4-2.7)	0.83 (0.5-1.2)	0.49 (0.03-0.95)	-0.17 (-0.39-0.04)	4, 55	19.5	0.0001
96 h	0.98 (0.44-1.5)	1.9 (1.1-2.7)	1.4 (0.82-1.93)	0.75 (0.26-1.23)	-0.13 (-0.53-0.27)	4, 45	8.6	0.0001

Table 6-2: Oxyhemoglobin as a Change from Baseline for Source Collector 3

Oxy-Hemoglobin as a Change from Baseline at SC 4: Mean Values (95% CI)								
Time	**3 s**	**12 s**	**20 s**	**30 s**	**90 s**	**df**	**F**	**p-value**
Post	0.78 (0.56-1.0)	0.41 (0.12-0.70)	-0.07 (-0.27-0.13)	-0.22 (-0.44--0.005)	-0.38 (-0.47--0.28)	4, 75	22.6	0.0001
1 h	0.94 (0.60-1.3)	0.39 (0.11-0.68)	-0.16 (-0.36-0.05)	-0.34 (-0.52--0.16)	-0.44 (-0.53--0.34)	4, 75	27.0	0.0001
12 h	1.9 (1.5-2.3)	1.7 (0.85-2.5)	0.27 (-0.08-0.63)	0.31 (-0.14-0.76)	-0.52 (-0.69--0.35)	4, 65	20.6	0.0001
24 h	1.9 (1.6-2.3)	1.9 (1.0-2.8)	0.76 (0.4-1.1)	0.40 (-0.06-0.87)	-0.56 (-0.74--0.38)	4, 65	19.6	0.0001
36 h	1.8 (1.5-2.2)	2.3 (1.5-3.2)	1.1 (0.80-1.5)	0.67 (0.20-1.1)	-0.40 (-0.65--0.14)	4, 60	21.1	0.0001
48 h	1.6 (1.2-1.9)	2.2 (1.4-3.0)	1.0 (0.62-1.5)	0.58 (0.11-1.0)	-0.25 (-0.53-0.03)	4, 55	17.5	0.0001
96 h	0.88 (0.29-1.5)	2.0 (0.9-3.2)	1.4 (0.8-2.0)	0.82 (0.31-1.3)	-0.30 (-0.58--0.02)	4, 45	8.2	0.0001

Table 6-3: Oxyhemoglobin as a Change from Baseline for Source Collector 4

Oxyhemoglobin levels continue to increase from baseline levels for the 3–30 s burn injuries. The 3 s experiences a 195% increase from pre-burn oxyhemoglobin levels at 24 hours and then declines towards baseline. The 12 s burn experiences a 156% increase above baseline at 36 hours before starting to decline towards baseline at the 48-hour and 96-hour time points for source collectors 3 and 4. However, oxyhemoglobin levels continue to increase in the 12 s burn at the second source collector. The 20 s and 30 s burn injuries have oxyhemoglobin levels that continue to increase up to 96 hours post-burn. The 90 s burn's oxyhemoglobin remains below pre-burn levels for the duration of the experiment.

6.3.1.2 Control Sites

There were no differences in oxyhemoglobin content between the control sites when the pre-burn measurement was taken into account.

6.3.2 Total Hemoglobin

6.3.2.1 Burn Sites

Total hemoglobin levels differed between the burn sites at each time point and source collector separations as shown in Table 6-4, Table 6-5, Table 6-6 and Figure 6-11. Immediately, after burn injury the 3 s burn has the highest increase (103–108%) in total hemoglobin from baseline levels. As burn depth increased the percentage increase in total hemoglobin in the wound declined. The 90 s burns showed a 13–16% decrease in total hemoglobin from baseline levels.

The 3 s burn (basethb3s) injuries experience a 192% increase in total hemoglobin at their peak levels at 12 hours. Levels plateau for the 24–36-hour time period before declining towards baseline at 96 hours.

The 12 s burn injury's (basethb12s) total hemoglobin levels remain lower than the 3 s burn injury up to 36 hours post-burn. At 36 hours, the 12 s burn injury experiences a peak increase in total hemoglobin levels of 205% above pre-burn levels. The total hemoglobin levels in the 12 s burn injury surpasses the 3 s total hemoglobin levels at this time point. At 48 hours post-burn, source collectors 3 and 4 show a decline in total

hemoglobin within the 12 s burn. However, source collector 2 shows a continued increase in total hemoglobin from pre-burn levels.

The 20 s (basethb20s) and 30 s (basethb30s) burn injuries have total hemoglobin values that increase above baseline for the duration of the experiment. The 20 s values are higher than the 30 s total hemoglobin values at the 24–96-hour time period for source collectors 3 and 4. Both the 20 and 30 s burn injuries do not attain the same total hemoglobin levels as the 3 and 12 s burn injuries. The 90 s (basethb90s) burn injury's total hemoglobin levels remain below or near baseline levels for the duration of the study.

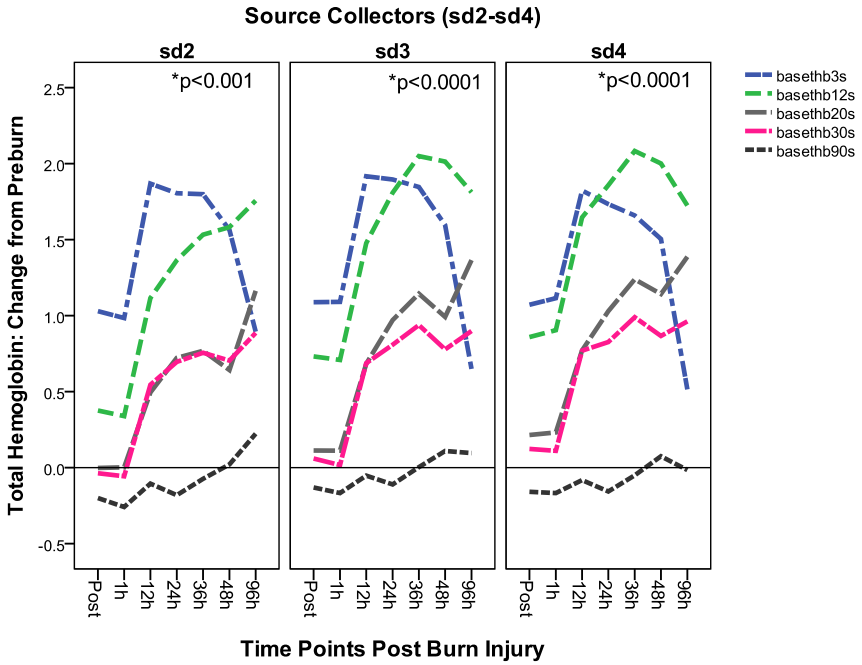

Figure 6-11: Burn Site Total Hemoglobin Content as a Change from Pre-Burn Values over Time

Total Hemoglobin as a Change from Baseline at SC 2: Mean Values (95% CI)								
Time	**3 s**	**12 s**	**20 s**	**30 s**	**90 s**	**df**	**F**	**p-value**
Post	1.0 (0.76-1.3)	0.38 (0.16- 0.59)	-0.002 (-0.14 -0.13)	-0.04 (-0.19 - 0.2)	-0.20 (-0.33 – -0.007)	4, 75	31.1	0.0001
1 h	0.98 (0.7-1.3)	0.34 (0.009 – 0.59)	0.002 (-0.17- 0.17)	-0.06 (-0.19- 0.080)	-0.26 (-034- -0.18)	4, 75	27.5	0.0001
12 h	1.9 (1.5-2.3)	1.1 (0.65-1.6)	0.49 (0.25-0.74)	0.55 (0.23-0.86)	-0.10 (-0.32 -0.11)	4, 65	22	0.0001
24 h	1.8 (1.4-2.2)	1.4 (0.84 -1.9)	0.72 (0.42-1.0)	0.70 (0.29-1.1)	-0.18 (-0.36-0.002)	4, 65	18.9	0.0001
36 h	1.8 (1.5-2.1)	1.5 (1.0-2.1)	0.77 (0.58-0.95)	0.76 (0.43-1.1)	-0.07 (-0.31-0.17)	4, 60	22.0	0.0001
48 h	1.6 (1.3-1.9)	1.6 (1.0-2.2)	0.64 (0.36-0.93)	0.70 (0.30-1.1)	0.002 (-0.27-3.1)	4, 55	14.3	0.0001
96 h	0.90 (0.48-1.3)	1.8 (1.0-2.5)	1.2 (0.75-1.6)	0.89 (0.48-1.3)	0.22 (-0.31-0.75)	4, 45	6.0	0.001

Table 6-4: Total Hemoglobin as a Change from Baseline for Source Collector 2

Total Hemoglobin as a Change from Baseline at SC 3: Mean Values (95% CI)								
Time	**3 s**	**12 s**	**20 s**	**30 s**	**90 s**	**df**	**F**	**p-value**
Post	1.1 (0.86-1.3)	0.73 0.51- 0.95)	0.11 (0.0005-0.22)	0.006 (-0.11 - 0.23)	-0.13 (-0.23 – -0.003)	4, 75	39.6	0.0001
1 h	1.1 (0.9-1.3)	0.71 (0.52 – 0.90)	0.11 (-0.015- 0.24)	0.002 (-0.12-0.15)	-0.17 (-0.28- -0.006)	4, 75	53.2	0.0001
12 h	1.9 (1.5-2.3)	1.5 (0.65-1.6)	0.68 (0.25-0.74)	0.69 (0.23-0.86)	-0.05 (-0.32 -0.11)	4, 65	27.2	0.0001
24 h	1.9 (1.6-2.2)	1.8 (1.3 -2.3)	0.97 (0.61-1.3)	0.81 (0.45-1.2)	-0.11 (-0.29-0.007)	4, 65	27.0	0.0001
36 h	1.8 (1.6-2.1)	2.0 (1.6-2.5)	1.1 (0.86-1.4)	0.94 (0.65-1.2)	0.0003 (-0.23-0.23)	4, 60	30.8	0.0001
48 h	1.6 (1.4-1.8)	2.0 (1.5-2.5)	1.0 (0.63-1.4)	0.78 (0.44-1.1)	0.10 (-0.17-0.40)	4, 55	20.0	0.0001
96 h	0.65 (0.27-1.0)	1.8 (1.1-2.5)	1.4 (0.97-1.8)	0.90 (0.53-1.3)	0.10 (-0.32-0.52)	4, 45	10.4	0.0001

Table 6-5: Total Hemoglobin as a Change from Baseline for Source Collector 3

Total Hemoglobin as a Change from Baseline at SC 4: Mean Values (95% CI)								
Time	**3 s**	**12 s**	**20 s**	**30 s**	**90 s**	**df**	**F**	**p-value**
Post	1.1 (0.90-1.2)	0.86 (0.56 -1.2)	0.21 (0.08 -0.35)	0.12 (-0.03 - 0.3)	-0.16 (-0.24 – -0.07)	4, 75	35.8	0.0001
1 h	1.1 (0.91-1.3)	0.90 (0.63 – 1.2)	0.23 (0.08-0.39)	0.11 (-0.01-0.23)	-0.17 (-0.24- -0.93)	4, 75	42.7	0.0001
12 h	1.8 (1.5-2.1)	1.6 (1.1-2.2)	0.77 (0.48-1.1)	0.77 (0.42-1.1)	-0.08 (-0.28 -0.11)	4, 65	23.4	0.0001
24 h	1.7 (1.4-2.2)	1.9 (0.84 -1.9)	1.0 (0.42-1.0)	0.83 (0.29-1.1)	-0.16 (-0.36-0.002)	4, 65	23.9	0.0001
36 h	1.7 (1.5-2.0)	2.1 (1.3-2.4)	1.2 (0.73-1.3)	0.99 (0.45-1.2)	-0.05 (-0.35-0.03)	4, 60	26.5	0.0001
48 h	1.5 (1.3-1.7)	2.0 (1.4-2.6)	1.1 (0.76-1.5)	0.87 (0.53-1.2)	0.08 (-0.25-0.40)	4, 55	17.0	0.0001
96 h	0.51 (0.15-0.89)	1.7 (1.0-2.5)	1.4 (0.97-1.8)	0.96 (0.61-1.3)	-0.02 (-0.30-0.26)	4, 45	11.7	0.0001

Table 6-6: Total Hemoglobin as a Change from Baseline for Source Collector 4

6.3.2.2 Control Sites

There was no change in total hemoglobin compared to baseline for the control sites at any of the time points or source collector separations.

6.4 Discussion

6.4.1 Proportion of Deoxyhemoglobin and Oxyhemoglobin

NIR has been used to monitor changes in oxygenation and perfusion of tissue in areas other than burn injuries. Studies manipulating the arterial or venous supply of a flap or limb have been used to track changes in oxy-, deoxy- and total hemoglobin as described in section 1.2.4 of the introduction. The vascular supply to the burn wound was not

manipulated directly in this study but thermal injuries institute varying degrees of damage to the microcirculation.

The ratio of oxy- to deoxyhemoglobin provides information about proportion of oxyhemoglobin in the burn wound. Figure 6-2 and Figure 6-6 clearly illustrate that as burn depth increased the proportion of deoxyhemoglobin increased and the proportion of oxyhemoglobin decreased. These differences were clear-cut between 12–24 hours post-burn, but at 36 hours post-injury the differences between the 12 s and 20 s are not as distinct. The 12 s burn is the true “indeterminate burn wound” and the inability to fully differentiate it from the 20 s burn may explain why it has been difficult to separate partial thickness indeterminate burn wounds at 36 hours after injury.

The proportion of oxyhemoglobin to total hemoglobin has been used in previous studies, as it represents oxygen saturation. However, the proportion of deoxyhemoglobin has never been assessed in any of the previous studies using the NIR Point technology.

The NIR Point technology was initially investigated as a tool to assess burn depth in an animal model. The current animal study and the previous study are both thermal contact swine burn models, and the major difference is that the previous study measured oxygen saturation and total hemoglobin for only 3 hours post-burn injury. In addition, the results obtained for the burn sites from the previous work were published as a change from control values.[187]

The previous animal study showed that oxygen saturation decreased in the 3 s injuries and total hemoglobin (blood volume) increased compared to the other injuries.
In the current animal study, there was no decrease in oxyhemoglobin detected post-burn, and oxyhemoglobin levels continued to increase over time. Oxygen saturation in the 3 s burn wound also increased over the study period. Total hemoglobin also increased in the 3 s burn wound in the current study, with high levels observed as early as 30 minutes post-injury. The findings from the current laboratory experiment also correlate with the clinical NIR findings as superficial injuries show increased perfusion and oxygenation.[28]

In the previous study, the 12 s burn wound experienced a decline in oxygen saturation with no real changes in total hemoglobin over the 3-hour time period. The findings from the current study differed as the 12 s burn wound showed an increase in oxyhemoglobin and oxygen saturation immediately post-burn and 1 hour after injury. Total hemoglobin in the 12 s burn wound also increased well above control values.

In the previous study, the 20 s and 30 s burn injuries showed a decrease in oxygen saturation compared to control values. The 20 s and 30 s burn injuries in the current laboratory experiment also showed a decline in oxyhemoglobin at the post-burn and 1-hour time point. Total hemoglobin values experienced a greater decline in the 30 s burn wound compared to the 20 s injury in the first porcine burn study, but in the current experiment there was an increase in total hemoglobin at both of these sites.

A 90 s burn wound was created in the current animal experiment and represented a full thickness burn wound. This burn injury showed a decrease in oxyhemoglobin, oxygen saturation and total hemoglobin. Results from the clinical setting also showed similar results using both Near Infrared Point Spectroscopy and Imaging as shown in figures Figure 1-15 and Figure 1-17.

The previous animal study was performed over 7 years ago using a different NIR spectroscopy device. The NIRSystems 6500 (Foss, Silver Springs. MA) device utilizes wavelength regions between 650–2500 nm and a bifurcated fiber bundle. The major difference in the NIRSystems device compared to the NIR Point device used in this study is related to the geometry of the probe. The NIR Point device has a separate light delivery fiber and source collectors that are spaced at particular distances from the light source. The conformation of the probe head was designed to specifically interrogate the various layers of the skin and provide deep penetration into the subcutaneous tissue. The NIRSystems device is designed so that the light source is centrally placed and there are a series of randomly organized detectors encircling the light source. The randomly organized detectors mean that light is collected by all the detectors at the same time. Detectors closer to the light source will receive the majority of light from the tissue because light has less distance to travel in the tissue. Also, the intensity of the light will be greater at the short source collector separations as there is less attenuation for a shorter pathlength. Therefore, the probe design of the NIRSystems device will primarily receive a signal from the very superficial portions of the skin. This is similar to detector position one for the NIR Point device as it primarily interrogates the epidermis. Detector 1 has been eliminated from the majority of the data analysis in the clinical environment

and in this current study as it provides variable results from a layer of the skin that does not provide useful information about the viability of a burn wound.[196]

The discrepancies between the previous animal study and the current animal experiment can be explained by a change in the NIR technology. The results from the current laboratory experiment are also supported by the hemodynamic changes seen in the clinical setting.

6.4.2 **Progression of Burn Injury**

NIR technology detected changes in oxy- and deoxyhemoglobin over time. Burn wounds could be differentiated statistically as early as a few minutes after injury with the clinical significance of the data becoming apparent at 12 hours post-injury. In the clinical setting, patients are rarely seen within an hour after injury with typical presentation around 12–24 hours post-burn.

The results for oxyhemoglobin and total hemoglobin obtained in the burn wounds over time can be described according to the degree of thermal injury. Overall, oxyhemoglobin and total hemoglobin values decreased with increasing burn injury.

Full thickness injuries oxy- and total hemoglobin remained below pre-burn levels for the majority of the experiment. This was expected, as full thickness injuries are necrotic with no viable blood supply and there is no perfusion to the wound.

Partial thickness injuries' (3–30 s) oxyhemoglobin levels were elevated above pre-burn values for the majority of the experiment. The most superficial injury (3 s) experiences the largest increase in oxyhemoglobin in the early period (up to 24 hours), peaks and declines towards baseline. The 12 s injury follows the same pattern as the 3 s burn wound with high levels of oxyhemoglobin (lower than for the 3 s burn) but peaks twelve hours later at 36 hours post-injury. Total hemoglobin followed the same pattern over time for the 3 s and 12 s burn with the exception that peak total hemoglobin levels were seen between 12–24 hours post-burn.

The 20 s and 30 s injuries showed an initial decrease in oxyhemoglobin below baseline but levels increased at 12 hours to 96 hours post-burn. The 20 s and 30 s burn sites did not show a decline towards baseline within the study period. Total hemoglobin levels were low post-burn but increased over time, reaching 3 s burn wound values by 96 hours.

The partial thickness burn sites resemble Jackson's zone of stasis where there is a mixed perfusion and oxygenation. This explains why the levels of oxy-, deoxy- and total hemoglobin are higher in the more superficial injuries than in the deeper partial thickness injuries. The differences in oxygenation and perfusion over time in the partial thickness burn wounds can be explained by the changes that occur in the microcirculation in the zone of stasis as documented by Boykin's mouse ear chamber scald burn model. Ninety minutes after the injury, platelet microthrombi cause a partial occlusion of the blood vessels in the zone of stasis with no ischemia. At 8–24 hours, leukocyte adherence to the endothelium affects the patency of the blood vessels with only 33–50% of the

capillaries open.[26] This variability in the number of patent versus occluded vessels could explain why there were variations in oxy- and total hemoglobin content in the 3–30 s burn wounds. The 30 s burn wound has less patent blood vessels and therefore less perfusion compared to the 3 s burn wound. Biopsy results from the sites also support this conclusion.

Total hemoglobin reflected the changes in oxyhemoglobin as values decreased with increasing thermal injury. The changes seen in the burn wounds over time are related to the perfusion of the injury. Laser Doppler has been used to monitor perfusion of various burn depths over time in a rat scald burn model. The results showed that average perfusion levels are inversely related to the depth of injury .[214] Similar findings were detected in the current study, as total hemoglobin decreased with increasing thermal injury.

Laser Doppler has also been used to categorize burn injuries into response patterns in a rat scald burn model. Full thickness injuries showed no change in perfusion over the time period. The partial thickness injuries showed an initial drop in perfusion levels, which increased by 24–72 hours post-injury. The NIR results from this study were similar to Green's study, except the partial thickness injuries showed an improvement in oxygenation and perfusion at 12–24 hours post-injury. The timing differences between the two studies are related to model differences. Green used a large TBSA rat scald burn model and the model used in this study is a small TBSA contact burn in swine. The size of the burn injury has a dramatic impact on perfusion and oxygenation of the burn wounds.

6.4.3 **NIR Spectroscopy and Mathematical Algorithms**

Near infrared spectroscopy is an innovative tool to assess the regional differences in oxygenation and perfusion. There are several commercial NIR devices available but none have received widespread acceptance or use.[4] This is partially related to the fact that researchers and manufacturers use different mathematical algorithms to convert the changes in light attenuation into chromophore measurements. Investigators infrequently report how the chromophores were extracted from the spectra or even which extinction coefficients were used. Consequently, NIR technology has been criticized for its lack of standardized software algorithms, wavelength selection and spacing between the light source and the detectors.[215] Without standardization or full disclosure of mathematical algorithms, it is difficult to compare the results of other studies using NIR technology. In addition, the mathematical algorithms applied to one NIR system may not provide accurate information if applied to another different NIR system.

Matcher et al. tested six published mathematical algorithms used to extract oxy- and deoxyhemoglobin and cytochrome aa_3. They found that all six algorithms performed differently when used with one standard NIR system. Certain algorithms produced similar results but the magnitude of the variables measured differed. For example, the hemoglobin extracted by two different algorithms yielded a magnitude difference of approximately 30%. Cytochrome aa_3 was very sensitive to algorithm changes and in certain models yielded results that did not fit with the physiologic picture. This paper identified the challenges associated with standardizing the mathematical equations, also

highlighting the importance of tailoring the math to the geometry of the NIR device. For example, the use of mathematical algorithms in transmission mode cannot be compared to their use in reflectance mode due to the differences in the pathlength and scattering properties of tissue. Also, the wavelength-dependent pathlength factors are not sensitive to geometry in large tissue models such as the human forearm, but are very important when assessing small tissue samples such as the rat brain. Finally, the extinction coefficients utilized by the algorithm can impact the magnitude of the variable extracted from the spectra. The two algorithms compared that produced magnitude changes with hemoglobin used extinction coefficients from whole intact blood versus lysed blood. The intact whole blood will contain scattering features from the red blood cells, which is not seen with the lysed blood and in this example affected the results obtained with the NIR device.[215]

6.4.4 **Limitations of the Study**

In hindsight, it would have been interesting to determine the changes in oxy-, deoxy- and total hemoglobin in a first-degree or superficial injury. This would have completed the spectrum of injury to the tissue and provided insight into burn wounds that initially present themselves as first-degree injuries but progress over time into partial thickness burn wounds. The results from this study suggest that burn wounds can be placed into discrete categories, but it is important to consider the wounds on a continuum in order to fully understand the pathophysiology of these injuries.

There were differences in total hemoglobin and oxyhemoglobin at all sites at the pre-burn time period. This is likely due to the non-randomization of the burn and control sites on the dorsum of the animal. There were several reasons for standardizing the location of the sites. The NIR technology used in this study is a depth-dependent device and the fibers are oriented in a particular fashion to collect light from various regions of the tissue. Skin thickness varies according to anatomic region and was held constant to ensure a consistent photon pathlength. Creating thermal injuries is a time- and temperature-dependent process. It is dependent on the skin's thickness, as thicker skin is more resistant to thermal damage.[17, 216, 217] To ensure that the same burn depth was created in each animal, the burns were instituted in the same anatomical position each time using the same temperature and pressure. In the initial pilot studies in 2001, there was some uncertainty surrounding the histological definition of burn depth, which may have impacted the ability to differentiate the partial thickness injuries using individual variables. Overall, the differences in pre-burn oxy- and total hemoglobin may not have been present if the sites were randomized. However, randomization would not have permitted the assessment of the depth-dependent nature of the thermal injury in terms of histology and NIR technology.

Oxyhemoglobin and total hemoglobin levels decreased at the cranial sites versus the caudal sites at the pre-burn time point. These differences can be attributed to the large musculocutaneous perforators that exist in the caudal end of the animal. The deep circumflex iliac artery and paired venae comitantes supply an 18 x 10 cm buttock flap in the cephalodorsal corner of the anterior superior iliac spine. Near the cranial region there is a 24 x 6 cm myocutaneous flap based on the thoracodorsal artery on the flank of the

pig, but it may have been far enough away from the experimental sites that it did not have the same impact on perfusion and oxygenation.[218] Although it can only be suggested that the proximity of the perforators impacted the pre-burn findings, it is a valuable lesson that may be important in the clinical environment. For example, understanding where the perforators are located in the skin would add greater insight into the oxygenation and perfusion differences seen at various anatomic sites.

Finally, one of the limitations of the NIR technology is determining in which vascular bed hemoglobin is found (arterial, capillary or venous). This makes it difficult to determine if an increase in oxygen saturation is due to increased perfusion or limited oxygen use.[151] In addition, hemoglobin may not be located in the vascular space in burn injuries and its presence in the interstitium has to be considered.

6.5 Major Findings and Conclusion

The purpose of this study was to test the capacity of NIR to non-invasively measure oxy-, deoxy- and total hemoglobin in burn wounds. NIR was capable of measuring oxy-, deoxy- and total hemoglobin non-invasively and a summary of the major findings include:

1) Oxyhemoglobin and total hemoglobin decreased as burn depth increased.
2) The ratio of oxy to deoxyhemoglobin was an accurate indicator of burn depth.
3) Hemodynamics changes over time in thermally injured tissue and can be accurately measured with NIR technology.

NIR technology could measure hemoglobin within the burn wounds and the proportion of hemoglobin could dichotomize burn wound depth into viable and non-viable injuries. Further work needs to be performed to determine the capacity of NIR technology to assess burn depth in a clinical setting and is discussed in Chapter 8: Summary and Future Directions.

Chapter 7: Methemoglobin Content

7.1 Results Overview

In this chapter, the methemoglobin results for source collectors 2, 3 and 4 will be combined to give a global assessment of methemoglobin content. Figure 7-1 shows the raw methemoglobin values for methemoglobin at 12 and 24 hours post-injury for the source collectors in combination. Figure 7-2 shows the methemoglobin values at the same time points when the source collectors are kept separate. The combination of the source collector separations improved the variability within the measurement as seen by smaller error bars in Figure 7-1 compared to keeping the source collectors separate in Figure 7-2. Stratifying methemoglobin into various tissue layers using the source collector separations may not make perfect physiologic sense. Free radicals formed in burn tissue do not form in just one small section of the wound. The activation of multiple biochemical pathways means that the response to injury will spread beyond the local boundaries of the initiating site. In theory, methemoglobin is a marker of the free radical load within the tissue and knowing the overall radical load may be more important than knowing what is happening in each individual layer of the tissue.

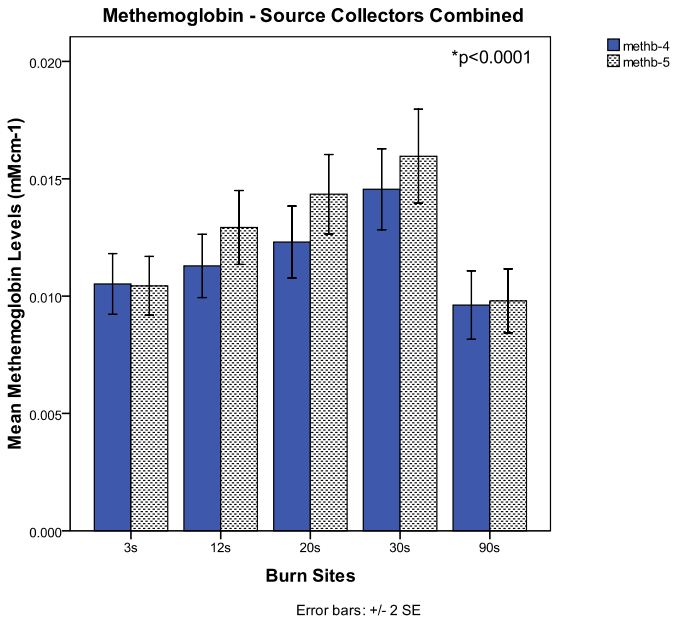

Figure 7-1: Mean Methemoglobin Levels in Burn Sites at 12 Hours (methb-4) and 24 Hours (methb-5) for Combined Source Collectors.

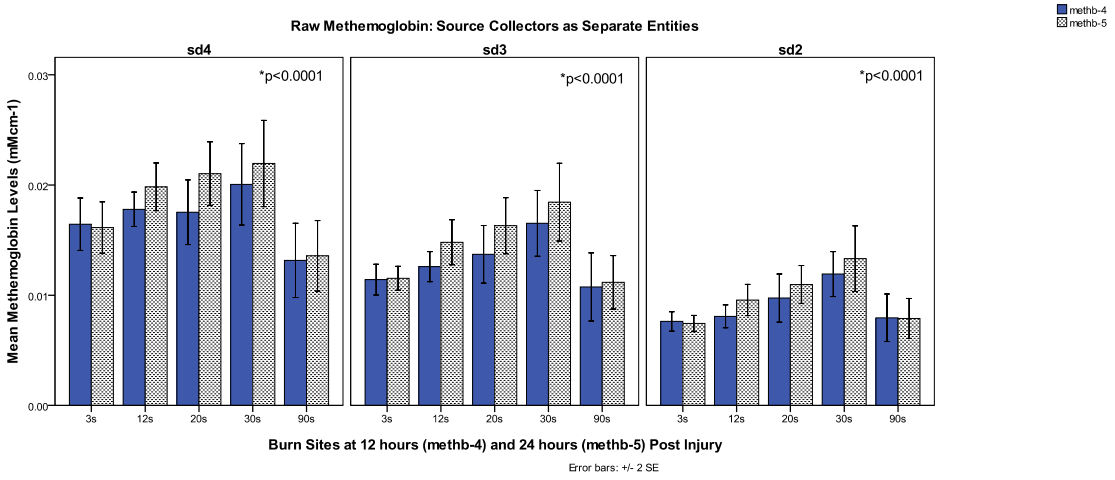

Figure 7-2: Mean Methemoglobin Levels in Burn Sites at 12 (methb-4) and 24 (methb-5) Hours Post-Burn for Source Collectors 2–4.

7.2 Methemoglobin as a Ratio of Total Hemoglobin

The figures and results in this section are presented as the ratio of methemoglobin to total hemoglobin. Significance values in the figures represent the differences between all sites shown on the x-axis in the figure at the particular time point.

The fraction of methemoglobin as a ratio of total hemoglobin was different at each time point post-burn injury as shown in Table 7-1. Immediately after the burn, the fraction of methemoglobin in the wounds increases with the degree of injury. The 90 s burn wounds' methemoglobin levels are double that of the other injuries as shown in Figure 7-3. The 1-hour time point results are similar to the post-burn time point and are not shown.

At 12 hours post-burn, the fraction of methemoglobin shows an elevation in the 12–30 s burn wounds. The 30 s fractions of methemoglobin are equivalent to the deeper injuries (90 s) as shown in Figure 7-4. The 24, 36 and 48-hour time point results are very similar to the 12-hour time point, with the fraction of methemoglobin the highest in the 30 and 90 s burn wounds. Results for 48 hours are shown in Figure 7-5.

At 96 hours post-burn injury, the highest fraction of methemoglobin is still within the deepest injuries. The fraction of methemoglobin in the 20 s burn is similar to the 30 s injury at this time point. The 3 and 12 s methemoglobin fraction still remain low as shown in Figure 7-6.

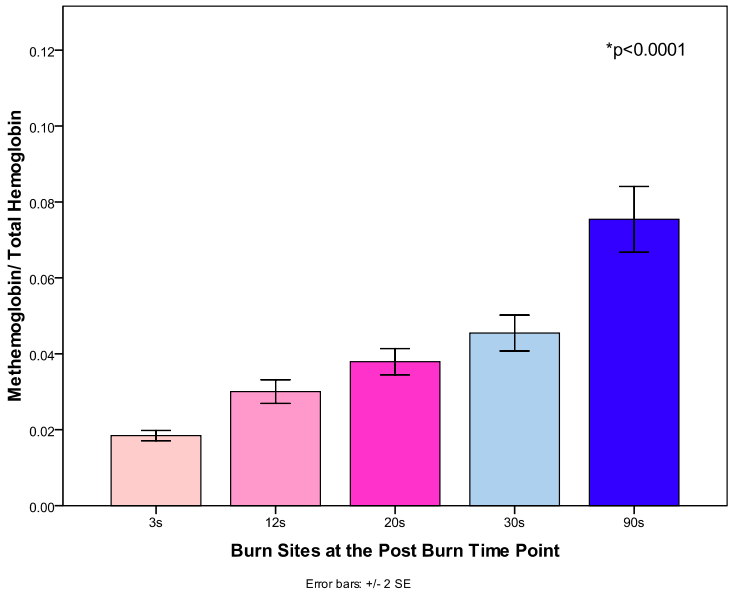

Figure 7-3: Proportion of Methemoglobin in the Burn Wounds at the Post-Burn Time Point

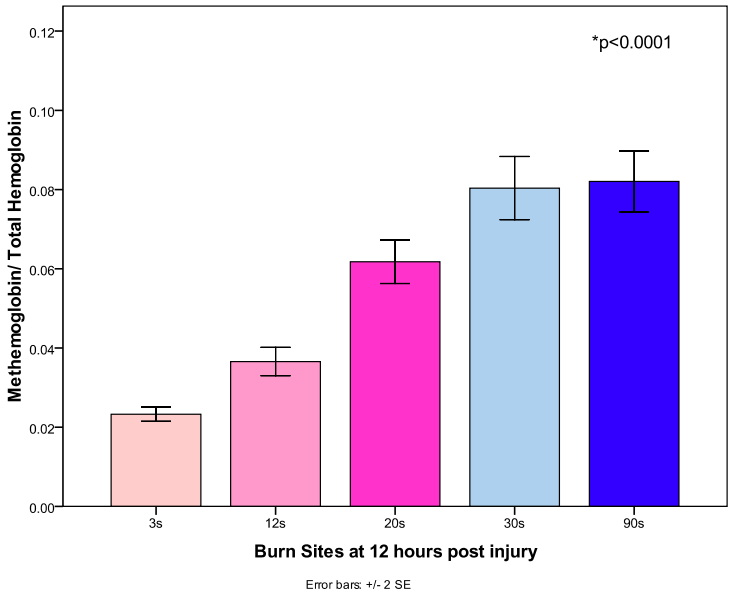

Figure 7-4: Proportion of Methemoglobin in the Burn Wounds at 12 Hours

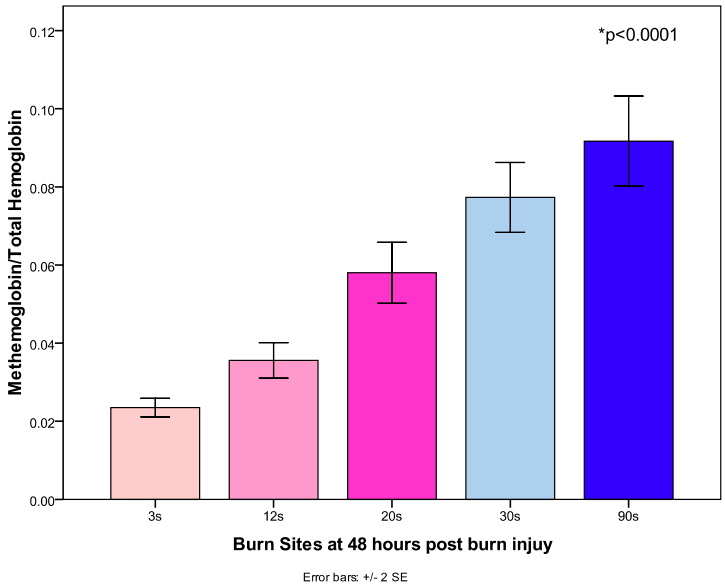

Figure 7-5: Proportion of Methemoglobin in the Burn Wounds at 48 Hours

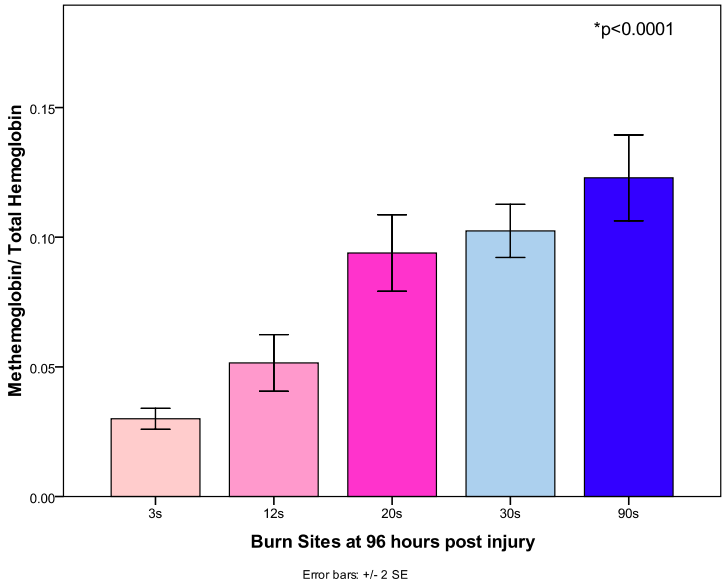

Figure 7-6: Proportion of Methemoglobin in the Burn Wounds at 96 Hours

Proportion of Methemoglobin: Mean Values (95% CI)								
Time	**3 s**	**12 s**	**20 s**	**30 s**	**90 s**	**df**	**F**	**p-value**
Pre	2.8×10^{-2} ($2.7\text{-}3.0 \times 10^{-2}$)	2.6×10^{-2} ($2.4\text{-}2.8 \times 10^{-2}$)	2.4×10^{-2} ($2.3\text{-}2.6 \times 10^{-2}$)	2.3×10^{-2} ($2.2\text{-}2.5 \times 10^{-2}$)	2.3×10^{-2} ($2.0\text{-}2.4 \times 10^{-2}$)	4, 235	9.6	0.0001
Post	1.7×10^{-2} ($1.6\text{-}1.9 \times 10^{-2}$)	2.9×10^{-2} ($2.5\text{-}3.3 \times 10^{-2}$)	3.7×10^{-2} ($3.3\text{-}4.1 \times 10^{-2}$)	4.5×10^{-2} ($3.9\text{-}5.0 \times 10^{-2}$)	7.6×10^{-2} ($6.5\text{-}8.6 \times 10^{-2}$)	4, 235	53.6	0.0001
1 h	2.0×10^{-2} ($1.8\text{-}2.2 \times 10^{-2}$)	3.1×10^{-2} ($2.7\text{-}3.5 \times 10^{-2}$)	3.9×10^{-2} ($3.4\text{-}4.2 \times 10^{-2}$)	4.6×10^{-2} ($4.1\text{-}5.1 \times 10^{-2}$)	7.1×10^{-2} ($6.2\text{-}8.0 \times 10^{-2}$)	4, 235	54.8	0.0001
12 h	2.1×10^{-2} ($2.0\text{-}2.3 \times 10^{-2}$)	3.5×10^{-2} ($3.1\text{-}3.9 \times 10^{-2}$)	5.8×10^{-2} ($5.3\text{-}6.4 \times 10^{-2}$)	7.7×10^{-2} ($6.8\text{-}8.6 \times 10^{-2}$)	7.9×10^{-2} ($7.1\text{-}8.8 \times 10^{-2}$)	4, 205	62.3	0.0001
24 h	2.1×10^{-2} ($2.0\text{-}2.2 \times 10^{-2}$)	3.6×10^{-2} ($3.2\text{-}4.0 \times 10^{-2}$)	5.7×10^{-2} ($5.3\text{-}6.2 \times 10^{-2}$)	8.7×10^{-2} ($7.5\text{-}9.9 \times 10^{-2}$)	8.3×10^{-2} ($7.1\text{-}9.4 \times 10^{-2}$)	4, 205	51.2	0.0001
36 h	2.1×10^{-2} ($1.9\text{-}2.2 \times 10^{-2}$)	3.5×10^{-2} ($3.0\text{-}3.9 \times 10^{-2}$)	4.8×10^{-2} ($4.5\text{-}5.2 \times 10^{-2}$)	7.2×10^{-2} ($6.4\text{-}8.1 \times 10^{-2}$)	8.3×10^{-2} ($7.2\text{-}9.3 \times 10^{-2}$)	4, 190	62.6	0.0001
48 h	2.1×10^{-2} ($1.9\text{-}2.3 \times 10^{-2}$)	3.4×10^{-2} ($2.8\text{-}3.6 \times 10^{-2}$)	5.4×10^{-2} ($4.4\text{-}6.0 \times 10^{-2}$)	7.3×10^{-2} ($6.1\text{-}7.9 \times 10^{-2}$)	8.7×10^{-2} ($7.4\text{-}9.9 \times 10^{-2}$)	4, 175	45.7	0.0001
96 h	2.9×10^{-2} ($2.4\text{-}3.4 \times 10^{-2}$)	4.7×10^{-2} ($3.7\text{-}5.7 \times 10^{-2}$)	8.4×10^{-2} ($7.0\text{-}9.9 \times 10^{-2}$)	9.3×10^{-2} ($8.3\text{ -}10 \times 10^{-2}$)	1.1×10^{-1} ($9.6\text{-}13 \times 10^{-2}$)	4, 145	34.0	0.0001

Table 7-1: Summary of ANOVA Results: Proportion of Methemoglobin to Total Hemoglobin at Each Time Point

7.3 Change from Baseline

There were no differences in methemoglobin content between the control sites pre-burn. This differs from the pre-burn values for the other variables of water, oxy- and deoxyhemoglobin values. As the levels of methemoglobin are not different pre-burn, it is not necessary to control for variability in the pre-experimental phase. However, representing the methemoglobin results as a change from baseline permits the demonstration of the magnitude change that occurs within the burn sites. The figures and results in this section are presented as the mean values of methemoglobin as a change from pre-burn values. In this statistical analysis, the burn sites were compared at

each time point utilizing an ANOVA test. Therefore, the p-value the figure represents the largest p-value obtained in the analysis (see Section 6.3). All p-values were reported in accompanying ANOVA tables for each source collector separation.

7.3.1 **Burn Sites**

The combination of the source collectors showed statistically significant differences between all the time points post-burn injury as shown in Table 7-2. Figure 7-7 represents the change in methemoglobin from pre-burn measurements over the study time period for the burn wounds.

Methemoglobin as a Change from Baseline: Mean Values (95% CI)								
Time	**3 s**	**12 s**	**20 s**	**30 s**	**90 s**	**df**	**F**	**p-value**
Post	0.07 (-7.5×10^{-3} - 1.4×10^{-1})	0.16 (5.3×10^{-2} - 2.7×10^{-1})	0.15 (4.1×10^{-2} - 2.6×10^{-1})	0.19 (8.1×10^{-2} - 2.9×10^{-1})	0.31 ($2.0 - 4.3 \times 10^{-1}$)	4, 235	2.9	0.02
1 h	0.20 ($1.2\text{-}2.7 \times 10^{-1}$)	0.13 (3.5×10^{-2} – 2.3×10^{-1})	0.10 (1.2×10^{-3} - 2.0×10^{-1})	0.14 (3.8×10^{-2} - 2.5×10^{-1})	0.21 (0.10-0.32)	4, 235	0.9	ns
12 h	0.70 (0.58-0.82)	0.86 (0.65 - 1.1)	1.2 (0.91 - 1.5)	1.5 (1.2-1.8)	0.76 (0.45 -1.1)	4, 205	7.5	0.0001
24 h	0.78 (0.67-0.89)	1.2 (0.94 -1.4)	1.7 (1.3-2.0)	2.0 (1.6-2.4)	0.77 (0.51-1.0)	4, 205	13.8	0.0001
36 h	0.80 (0.68-0.93)	1.4 (1.1-1.7)	1.6 (1.3-1.9)	2.0 (1.7-2.3)	1.0 (0.7-1.4)	4, 190	9.7	0.0001
48 h	0.76 (0.6-0.9)	1.4 (1.0-1.7)	1.5 (1.2-1.9)	1.8 (1.4 -2.2)	1.3 (0.91-1.7)	4, 175	5.5	0.0001
96 h	0.76 (0.49-1.0)	2.4 (1.7-3.0	2.9 (2.2-3.5)	2.3 (1.9-2.8)	1.8 (1.1-2.4)	4, 145	8.5	0.0001

Table 7-2: Summary of ANOVA Results: Comparison of Burn Sites Methemoglobin as a Change from Pre-Burn

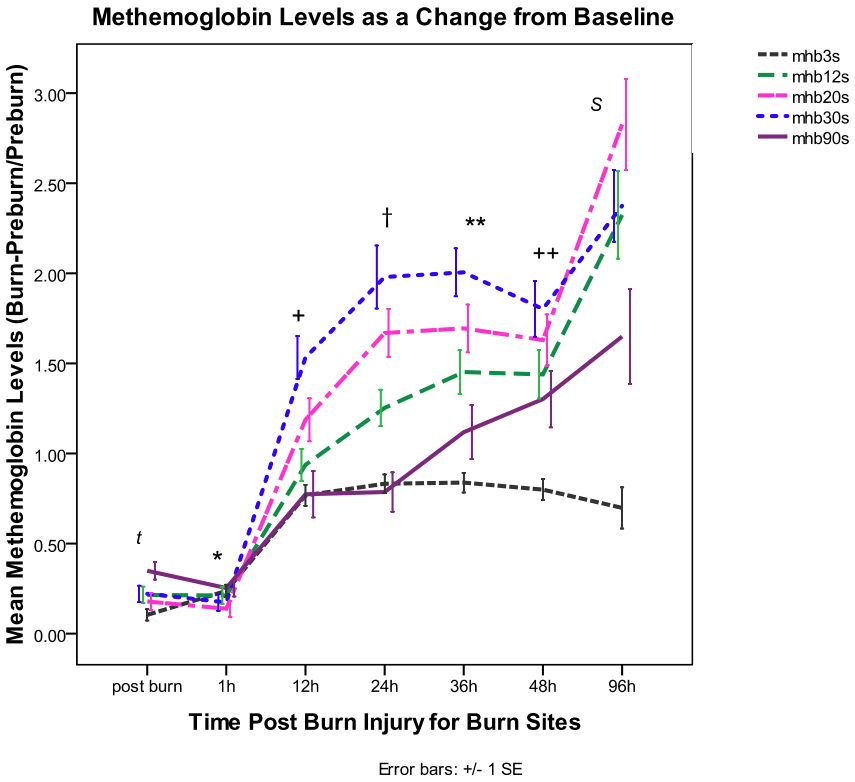

Figure 7-7: Change in Methemoglobin from Pre-Burn Levels within the Burn Sites (^{t} p<0.0001; *p<0.0001, $^{+}$ p<0.0001, † p<0.0001, **p<0.0001, $^{++}$p<0.0001, ^{s} p<0.0001)

Immediately after and 1 hour post-burn, methemoglobin levels are 25–50% higher in all burn injuries. The 90 s (mhb90s) burn has the highest values at both of these time points.

At 12 hours, the intermediate burn wounds' methemoglobin levels surpass the other injuries. The 30 s (mhb30s) injury had the highest increase of 170% above baseline. The 12 s (mhb12s) and 20 s (mhb20s) injuries experienced a 106% and 128% increase respectively. The lowest methemoglobin change was within the 3 s (mhb3s) and 90 s burn wound.

At 24–48 hours post-burn, all of the burn wounds show an even greater increase in methemoglobin levels over time. The greatest change is within the indeterminate injuries (12–30 s). The 30 s injury showed a 202-223% increase, the 20 s a 182–192% increase and the 12 s burn showed an increase of 141–192% over this time period. The 3 s burn showed very little change from baseline (86–92%) over this time period. The 90 s burn wound methemoglobin surpassed the 3 s level from 36–96 hours post-burn.

At 96 hours post-burn, the methemoglobin levels in the 3 s burn start to decline towards baseline (70%). The remainder of the injuries all showed a continued increase in methemoglobin. The 20 s burn injury's (314%) methemoglobin values surpass the 30 s injury's (272%) values at this time point.

7.3.2 **Control Sites**

Similar to the raw methemoglobin values, the control sites showed differences at 12 hours [$F(4, 205) = 3.9$, $p<0.004$], 24 hours [$F(4, 205) = 3.5$, $p<0.009$], 36 hours [$F(4, 190) = 3.1$, $p<0.02$] and 48 hours [$F(4, 175) = 2.5$, $p<0.04$] post-injury as shown in Figure 7-8. Control sites 2 and 3 both had the highest methemoglobin values compared to control sites 1, 4 and 5. These control sites are located between the indeterminate injuries or burn sites 12 to 30 s. The indeterminate burn injuries showed the highest levels of methemoglobin throughout the majority of the study.

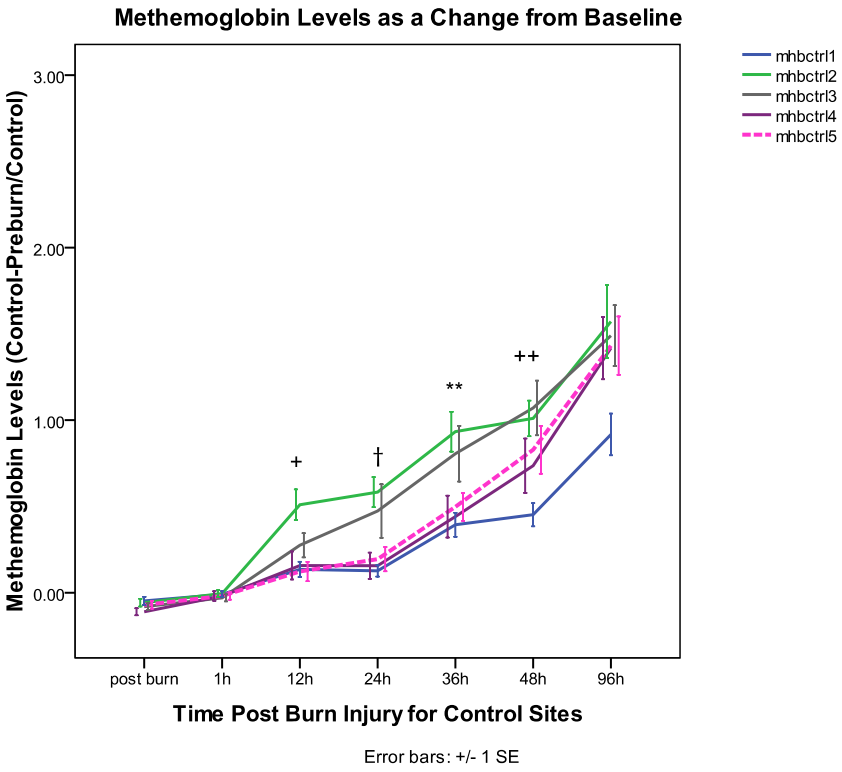

Figure 7-8: Change in Methemoglobin from Pre-Burn Levels within the Control Sites for Combined Source Collectors ($^{+}p<0.004$, $^{\dagger}p<0.009$, $^{**}p<0.02$, $^{++}p<0.04$)

7.4 Discussion

7.4.1 Methemoglobin Presence in Burn Wounds

This is the first time the presence of methemoglobin has been described in burn wounds. Methemoglobin was elevated above baseline or pre-burn levels for all of the burn wounds. The highest levels were consistently found in the indeterminate depth injuries at all time points. The presence of methemoglobin in the wound may be explained by the known presence of free radicals in a burn injury.[52] The presence of free radicals in the

burn wound would enable the oxidation of ferrous hemoglobin to methemoglobin. The generation of free radicals in the burn wound comes from several sources such as neutrophils, xanthine oxidase upregulation and hydrogen peroxide.[50, 51, 53] Neutrophils produce free radicals and hydrogen peroxide as a bacterial killing mechanism and are present in the wounds immediately after injury. Neutrophils are one of the major sources of toxic oxygen metabolites in burns.[53] The presence of neutrophils in the burn wound occurs as early as 4 hours post-burn.[50] Cetinkale showed a three-fold change in myeloperoxidase activity in the first hour post-burn in the lungs, kidney and liver after burn injury in a 25% TBSA burn in rats.[219] Myeloperoxidase activity of neutrophils remains high for 12–24 hours post-injury in animal models.[50, 220, 221] The superoxide radical and hydrogen peroxide have been implicated in the conversion of ferrous iron to ferric iron.[49] The influx of the neutrophils and subsequent release of oxidants into the burn wound could explain the increased presence of methemoglobin in the burn wounds in the acute period.

The ischemia reperfusion injury that occurs in burn injuries increases the amount of hypoxanthine, the substrate for xanthine oxidase, in the tissue. Xanthine oxidase produces the superoxide radical, which is a primary ROS involved in ferrous iron oxidation. Xanthine oxidase is also upregulated 15 minutes post-burn in rat burn model[53]. Xanthine oxidase activity is high in patients with 30% TBSA burn injuries.[55] Mast cells and histamine are known to be present in burn wounds and enhance xanthine oxidase activity.[53, 54]

The presence of hydrogen peroxide accelerates the formation of methemoglobin.[47] Hydrogen peroxide is produced by neutrophils, known to be present in a burn wound, and is produced by the conversion of the superoxide free radical by SOD. Hydrogen peroxide reacts with ferrous iron via a Fenton-like reaction to form methemoglobin.[56, 58] Intracellular H_2O_2 has been shown to be increased at 5 hours post-burn injury.[221]

Methemoglobin formation also occurs routinely in the tissue by nitric oxide. Nitric oxide interacts with oxy- and deoxyhemoglobin to form methemoglobin.[46] Nitric oxide levels increase 4 times above baseline in burn patients and remain high for at least 6 days post-injury.[55] Nitric oxide is scavenged by oxyhemoglobin to form nitrate and methemoglobin. Nitrate has been shown to be elevated for 1–8 days in large TBSA rat scald burns.[222] Patients have increased plasma nitrate at 24 hours post-burn with sustained nitrate levels up to 12 days post-injury.[223] Nitrate levels have also been measured in the skin and remain high for at least 24 hours post-burn.[224] In addition, the auto-oxidation of nitric oxide forms nitrite, which in turn reduces deoxyhemoglobin to methemoglobin and free nitric oxide.[46] The large quantity of NO in the burn wound along with the known interaction of NO with hemoglobin could also explain the high levels of methemoglobin in burn wounds.

Normally, when oxygen is offloaded from oxyhemoglobin to the tissue a superoxide free radical that auto-oxidizes the heme can be released, forming methemoglobin.[46, 47, 66] Auto-oxidation accounts for a lower proportion of methemoglobin formation, but increased offloading of oxygen in ischemic tissue could theoretically increase the auto-oxidation process and consequently methemoglobin formation.[48]

Hemolysis of the red blood cell occurs post-burn injury due to the presence of oxidants.[225] Hemolysis of the red cell decouples methemoglobin from its reductive mechanisms within the cell. Free methemoglobin can interact with hydrogen peroxide and peroxynitrite to form a more reactive ferryl intermediate.[45, 47, 48, 57, 58] Hemolysis of the red cell releases ferrous hemoglobin, which can be converted to methemoglobin in the presence of free radicals.[48] Therefore, hemolysis of the red blood cell is indirectly responsible for increased methemoglobin because of the loss of the reduction mechanisms and further exposure of hemoglobin to free radicals.

Finally, the effects of heat on the tissue could also play a role in methemoglobin formation. It has been shown in forensic studies and MRI ablation studies that an increase in temperature will convert ferrous to ferric hemoglobin.[62–64] Heat could also alter the red cell membrane structure and cause lysis independent of oxidant damage.[226]

The presence of neutrophils and the upregulation of xanthine oxidase produce known free radicals that could convert ferrous to ferric hemoglobin. Hydrogen peroxide, nitric oxide and the auto-oxidation of hemoglobin are involved in the formation of methemoglobin. The presence of these molecules or an increase in their activity in a burn wound are plausible explanations for methemoglobin formation in the wound. Hemolysis may be responsible for increased methemoglobin formation by decoupling hemoglobin from its reductive mechanisms and directly exposing the molecule to free radicals. Burn injuries involve the thermal destruction of the various structures within the skin and the effect of heat on methemoglobin formation or red cell destruction cannot be

eliminated. It is unknown which mechanism or combination of pathways is responsible for methemoglobin production in burn tissue. However, the presence of methemoglobin fits with our current knowledge of free radical formation post-burn injury.

7.4.2 **Methemoglobin Levels Increase Over Time**

Methemoglobin levels in the burn wounds increased over time. The largest increase occurred at 12 to 24 hours post-burn injury. There were day-to-day variations in methemoglobin levels with peak levels at the end of the study period for the majority of the burn wounds except the 3 s injury.

The large increase in methemoglobin content from the immediate post-burn period to 12 hours after injury could be related to the build-up of oxidants over this time period. Neutrophils are one of the major sources of toxic oxidants, are present as early as 4 hours post-burn and are high for 24 hours.[50] MPO activity is high at 12 and 24 hours, meaning the levels of oxidants generated are also high at these time points.[220, 221, 227] The high levels of methemoglobin at 12 hours could represent the over-production of ROS and the inability of the defence mechanisms to keep pace within this time frame.

Methemoglobin levels increased over time for the 12–90 s burn injury. The ongoing production of nitric oxide post-burn injury could be responsible for the increased levels of methemoglobin. NO is high for at least 12 days post-burn and levels are elevated at least 4 times above baseline values.[55, 60] In addition, the depletion of ATP and

upregulation of xanthine oxidase affects oxidant generation, especially when the burn wound is reperfused.[52]

Ischemia results in oxygen offloading from hemoglobin to the tissue and could explain the increased methemoglobin levels over time. Deoxyhemoglobin levels measured from burn wounds in this study showed peak levels at 12 hours with a high content for 48 hours after injury. At 96 hours, deoxyhemoglobin levels start to decline for all the burn wounds (data not shown). This finding does not support the hypothesis that auto-oxidation is involved in methemoglobin formation at the 96-hour time point. Methemoglobin values are actually increasing at 96 hours; if auto-oxidation was the prevalent pathway for methemoglobin formation then there should be a rise in the deoxyhemoglobin levels and not a decline. The ongoing free radical production is the more likely explanation for the continued increase in methemoglobin formation over time.

Free radicals are formed in normal physiologic processes but do not cause injury to the tissue. The very high levels of free radicals seen post-burn injury are explained by excess production and impairment of the defence mechanisms to scavenge the free radicals. The impairment of the defence mechanisms would explain why the production of free radicals is uninhibited over time.

The primary defence mechanism of the red blood cell is the NADH cytochrome b5/cytochrome b5 reductase system. This reduction system operates in normal individuals at a conversion rate of 15% per hour. This rate is slow when methemoglobin levels are high.[42] Methemoglobin dissociates more freely from the red cell, which

decouples it from the reductive mechanisms within the cell.[69] Hemolysis is know to occur immediately after injury and can decouple methemoglobin from its reductive mechanisms of the cell.[225] Ferritin, heme oxygenase-1, haptoglobin, and hemopexin are generally increased in the presence of methemoglobin.[56, 69, 74] However, it is unknown at this time if burn patients have higher levels of these proteins systemically or within their burn wounds. It is also unknown if these proteins are saturated.

The secondary defence mechanisms or antioxidant mechanisms are impaired post-burn injury. SOD is increased up to 4 days post-injury, which translates to increased superoxide radical formation. An increase in SOD activity is an indicator of high oxidant load[228]. Catalase, glutathione peroxidase, alpha-tocopherol and ascorbic acid are all reduced post-burn injury.[52, 67, 68, 229] Glutathione has been shown to be decreased at 1 hour post-burn with an even greater decline at 24 hours.[67, 220] The activity of glutathione peroxidase has also been shown to be 40% lower than baseline at 10 days post-injury.[228] Co-factors such as selenium used by the reducing enzymes are decreased post-burn injury.[228]

The defence mechanisms to neutralize free radical formation are impaired post-burn injury, which translates to free radical formation that is unchecked. The impairment of the defence mechanisms post-burn injury would explain the ongoing production and increase in methemoglobin over time. In addition, if the presence of methemoglobin is related to the level of free radicals in the tissue then methemoglobin could potentially be used as an indicator of the degree of burn injury.

7.4.3 **Methemoglobin and Burn Depth**

In theory, high methemoglobin levels should be an indicator of non-viability and low levels an indicator of viability. The 3 s burn is a viable wound and showed low levels of methemoglobin. The 30 s injury is a non-viable wound and had the highest levels of methemoglobin. However, the results from the 12–20 s burns do not fit with this theory using raw values of methemoglobin as shown in Appendix G. The 12 s and 20 s burn wounds are viable injuries yet had extremely high levels of methemoglobin. The 90 s are non-viable wounds and showed low levels of methemoglobin in the wound. Using the raw values for methemoglobin, it was difficult to dichotomize the injuries into viable and non-viable wounds.

Methemoglobin is formed from ferrous hemoglobin. Therefore, the methemoglobin levels are dependent on the total amount of substrate in the tissue. The fractional methemoglobin level was used to determine what proportion of hemoglobin within the sites was methemoglobin. The ratio of methemoglobin to total hemoglobin showed that as burn depth increased so did the fraction of methemoglobin. Therefore, high proportions of methemoglobin (30–120 s sites) are an indicator of non-viability as shown in Figure 7-3 to Figure 7-6.

Methemoglobin accumulation is secondary to increased formation or impaired reduction mechanisms or some combination of both. Methemoglobin at high levels is associated with endothelial and red cell membrane lipid peroxidation and levels above 60% carry an increased risk of mortality.[42] However, low levels of methemoglobin are normally found

in the circulation and represent 1% of the hemoglobin in circulation. This suggests that there may be two roles for methemoglobin:

1) Antioxidant role: Methemoglobin is a free radical scavenger as long as the defence mechanisms can keep pace with methemoglobin formation.
2) Pro-oxidant role: Increased production that exceeds methemoglobin removal results in lipid peroxidation of the endothelium and the red cell phospholipid membrane.

The 3 s burn is evidence for methemoglobin as an antioxidant. The 3 s injury had high methemoglobin levels at 12 hours post-burn, which plateaued for the majority of the experiment. The plateau means that methemoglobin production and removal were equivalent, suggesting that the reduction mechanisms were intact. The 3 s burn showed minimal injury to the tissue according to histology and was a healing burn wound. This suggests that methemoglobin in the 3 s burn may be beneficial and the levels are not high enough to cause tissue injury.

Support for methemoglobin as an antioxidant comes from *in vitro* endothelial cell experiments. Balla et al. incubated heme and endothelial cells together for varying times and then gave the endothelial cells an oxidant challenge such as activated neutrophils or hydrogen peroxide. If heme was incubated with the endothelial cells for at least 1 hour then the endothelial cell was highly sensitive to oxidation. If the endothelial cells were only briefly exposed to heme they were resistant to oxidant-mediated injury. This was felt to be related to the heme and methemoglobin upregulation of ferritin and heme

oxygenase-1.[56] Therefore, the presence of some heme in the wound may be of benefit in protecting the endothelium and cell membranes from future oxidant damage. Methemoglobin may be considered the end product of hemoglobin free radical scavenging. Ferrous hemoglobin scavenges peroxynitrite and hydrogen peroxide to form methemoglobin.[46]

Methemoglobin may play a pro-oxidant role in the 20–90 s burn wounds.
At high levels, methemoglobin can cause irreversible damage to the tissue and with systemic levels greater than 30% there is an increased risk of mortality. Ferrous iron scavenging of hydrogen peroxide or the superoxide anion generates not only methemoglobin but a hydroxyl radical. The hydroxyl radical is one of the most highly reactive and toxic oxidant molecules.[230] The toxicity of methemoglobin may also be related to its ferryl intermediate. Hydrogen peroxide and peroxynitrite interact with ferrous hemoglobin to produce a ferryl intermediate. The ferryl (Fe^{4+}) hemoglobin intermediate has been measured 60 minutes post-ischemia and re-oxygenation.[47] Burns experience an ischemia-reperfusion injury and it is plausible that the ferryl intermediate is present in the burn wound. The ferryl intermediate is extremely toxic because its formation also produces a reactive globin chain radical. The reactive globin chain radical cannot be reduced by the mechanisms that exist in the red blood cell.[59] The ferryl intermediate has been shown to abstract a hydrogen from unsaturated fatty acids, results in heme loss and is toxic to endothelial cells.[47] It can also further react with hydrogen peroxide to produce free iron and porphyrin degradation products.[46] Therefore, the formation of methemoglobin may exert damage through an intermediate that affects

the lipid cell membrane, resulting in the release of free methemoglobin and the subsequent release of iron.

The results from this study show that the higher fractions of methemoglobin were associated with the non-viable injuries compared to low levels in viable or superficial wounds. Determining the role of methemoglobin in the wound was beyond the scope of this particular study but is important to resolve in the future.

7.4.4 **Methemoglobin and Control Sites**

The methemoglobin changes that occurred in the burn wounds were not limited to the visible zone of injury. Control sites 2 and 3 showed elevated methemoglobin levels compared to the other control sites at 12, 24 and 36 hours post-burn. This is likely a reflection of the changes in the indeterminate injuries as the two controls are located between the 12–30 s burn wounds. This also explains why there were no differences in the burn sites when the control values were subtracted, as it made the differences between the burn sites very small as shown in Appendix H. It also suggests that the response to the injury is not contained within the burn region but extends at least 4 cm away from the sites in this swine burn model. The control site histology was reviewed and there was no detectable injury to the tissue nor were there changes in neutrophil or mast cell content.

The presence of methemoglobin in control sites represents the conversion of ferrous hemoglobin to ferric hemoglobin by oxidants formed near or within the control tissue.

This finding suggests that the inflammatory cascade occurring post-burn injury is not limited to the burn wound but extends to the surrounding regions even in a small TBSA burns. On the other hand, the methemoglobin present in the control sites could represent venous outflow from the burn wound. In either scenario, methemoglobin production at the control site or methemoglobin delivery to the control site exceeds removal, resulting in increased methemoglobin levels. This has direct implications for the control site utilized in the clinical environment. The visually normal-seeming skin next to a burn wound may not be physiologically normal. With their altered physiology, if these sites are utilized as controls then they are not true representations of baseline measures in burn patients. The results from this study suggest that controls should only be utilized as a guide but should not be incorporated into the final analysis when considering the degree of injury to the tissue. It also has implications for the choice of donor site, as high levels of methemoglobin may explain why some donor sites experience impaired wound healing.

7.4.5 **Methemoglobin and Near Infrared Spectroscopy**

The capacity of near infrared spectroscopy to measure methemoglobin non-invasively *in vivo* has only been described by one other group. Tromberg et al. described a broadband diffuse optical spectroscopy device that can measure methemoglobin non-invasively. To test the device, methemoglobin was induced by $NaNO_2$ injections and measurements acquired in a rabbit hind limb. The results of the NIR device were compared to the reference standard, co-oximetry, with a high correlation between the two devices (r^2=0.9). In addition, the broadband device could even assess the changes

that occur when methemoglobin was reduced back to ferrous hemoglobin post-methylene blue administration.[155]

The Tromberg device utilizes steady state spectroscopy, which is similar to the NIR device used in this study. The mathematical fitting routines and extinction coefficients are similar to the algorithms utilized in this study. This adds support for the results obtained in this animal burn model as another group has been able to successfully measure methemoglobin non-invasively *in vivo*.

In comparison to the device utilized in this study, the Tromberg device is a superior technology. Its superiority is related to the fact that it uses a combination of steady state spectroscopy and multifrequency domain photon migration techniques. Multifrequency domain photon migration uses laser diodes at specific wavelengths to measure the absorption and scattering of light. This permits the calculation of the absolute reflectance intensity and consequently the true pathlength of light. Therefore, as the pathlength of light is known the modified Beer-Lambert law is solved only for concentration, which permits a more quantitative approach to variable measurement. The NIR device used in this study cannot quantitate the pathlength of light and the Beer-Lambert law equation has to be solved for two unknowns, concentration and pathlength. This means the results obtained are a measure of the relative methemoglobin concentration, not the absolute concentration. The union of steady state and frequency domain spectroscopy represents a significant advancement for near infrared technology.

7.4.6 **Limitations of Study**

NIR spectroscopy could measure methemoglobin levels but was not correlated to the reference standard or co-oximetry values. The absorption spectra of methemoglobin show a signature peak at 630 nm, which is exploited by co-oximeters and NIR devices. However, despite its characteristic spectral signal the capacity of this NIR device to quantitate methemoglobin still needs to be correlated to the reference standard. A correlation between the two devices would also help validate the mathematical fitting routines required to extract methemoglobin from the overall burn wound spectrum.

The source collector separations may not be necessary when analyzing methemoglobin levels. The depth-dependent nature of the NIR spectroscopy device seemed appropriate for determining the degree of burn injury at the onset of this work five years ago. However, it is very difficult to precisely control or accurately determine the pathlength of light using steady state spectroscopy. Skin thickness varies anatomically and a depth-dependent device will interrogate different layers of the tissue depending on the region it is assessing. As the pathlength of light is unknown in steady state spectroscopy, it is likely that the variability in the measurement of methemoglobin occurs because different portions of the tissue are sampled. A global assessment of all tissue layers may be more appropriate given the inherent variability that exists in burned tissue. Combining source collectors 2–4 provided a global assessment of the tissue and was shown to decrease variability in the measurement. Future NIR designs will continue to use depth-dependent fibers as they are important when trying to resolve the issue of anatomic differences in skin thickness. However, modifications are required in order to improve our knowledge of light’s pathlength.

7.5 Major Findings and Conclusion

The purpose of this study was to test the capacity of NIR to non-invasively measure methemoglobin in burn wounds. NIR was capable of measuring methemoglobin non-invasively and a summary of the major findings include:

1) The proportion of methemoglobin increases with the severity of injury.
2) Methemoglobin levels increased over time for all the wounds except the 3 s injury.
3) Methemoglobin values within the control site increase over time, with high levels at 12–36 hours for the sites closest to the indeterminate injuries.

NIR technology could measure methemoglobin within the burn wounds and the proportion of methemoglobin could dichotomize burn wound depth into viable and non-viable injuries. The presence of methemoglobin in the burn wound raises many questions about its role in burn tissue. Further work needs to be performed to fully elucidate the true significance of methemoglobin in burn wounds.

Chapter 8: Water Content

8.1 Water Content: Raw Values

8.1.1 Raw Values: Pre-Burn

Water content increased from the cranial to caudal sites at the pre-burn time point for source collectors 2–4 as shown in Figure 8-1.

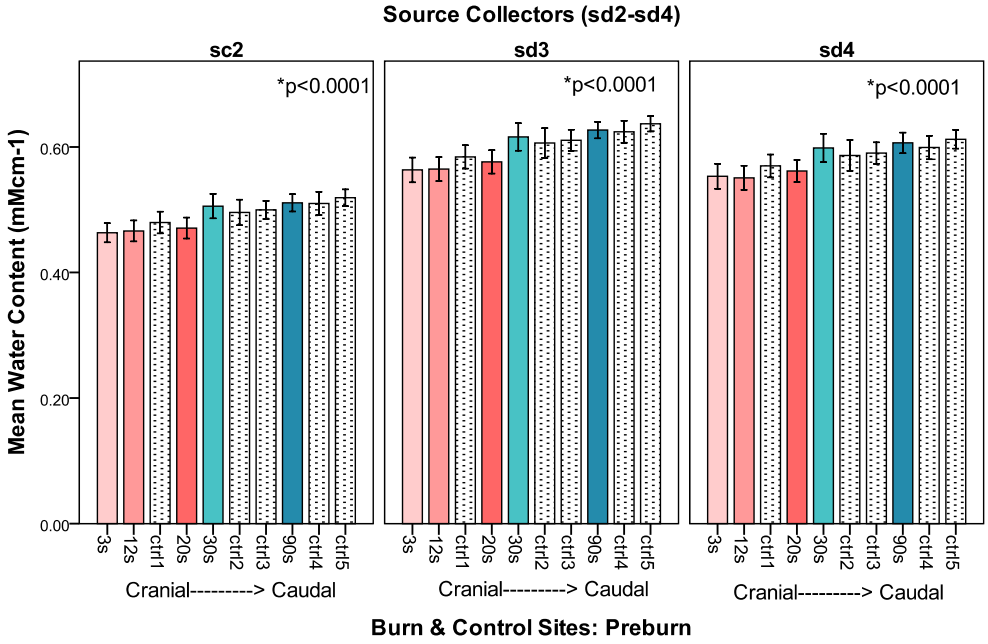

Figure 8-1: Mean Water Content for Burn and Control Sites Prior to Burn Injury for Source Collectors 2–4

8.2 Water Content: Change from Pre-Burn

8.2.1 Burns

The burn sites could be differentiated using a change in water content from pre-burn levels. Statistical significance was achieved at each time point post-burn and all source collectors 2–4 as shown in Table 8-1, Table 8-2, and Table 8-3. Figure 8-2 shows the results for all the burn wounds over time as a change in water content.

Water as a Change from Baseline at SC 2: Mean Values (95% CI)								
Time	**3 s**	**12 s**	**20 s**	**30 s**	**90 s**	**df**	**F**	**p-value**
Post	0.07 (0.04-0.09)	0.15 (0.10-0.19)	0.18 (0.15-0.21)	0.11 (0.08-0.14)	0.04 (0.007-0.07)	4, 75	13.6	0.0001
1 h	0.08 (0.04 - 0.12)	0.16 (0.13-0.20)	0.18 (0.15-0.21)	0.09 (0.05-0.14)	0.02 (-0.007-0.05)	4, 75	15.4	0.0001
12 h	0.17 (0.10-0.25)	0.30 (0.23-0.32)	0.23 (0.19-0.27)	0.12 (0.07-0.18)	0.04 (-0.01-0.08)	4, 65	14.4	0.0001
24 h	0.12 (0.07-0.18)	0.25 (0.19-0.31)	0.22 (0.17-0.26)	0.14 (0.09-0.18)	-0.01 (-0.06-0.03)	4, 65	19.4	0.0001
36 h	0.07 (0.02-0.12)	0.21 (0.14-0.29)	0.23 (0.18-0.28)	0.13 (0.09-0.18)	0.01 (-0.03-0.05)	4, 60	14.1	0.0001
48 h	0.09 (0.04-0.15)	0.18 (0.06-0.30)	0.21 (0.14-0.27)	0.12 (0.04-0.20)	-0.02 (-0.11-0.06)	4, 55	5.7	0.001
96 h	0.12 (0.06-0.16)	0.11 (0.03-0.19)	0.18 (0.11-0.24)	0.12 (0.03-0.22)	0.002 (-0.05-0.05)	4, 45	4.1	0.007

Table 8-1: Water as a Change from Baseline for Source Collector 2

Water as a Change from Baseline at SC 3: Mean Values (95% CI)								
Time	**3 s**	**12 s**	**20 s**	**30 s**	**90 s**	**df**	**F**	**p-value**
Post	0.10 (0.07-0.13)	0.16 (0.14-0.19)	0.17 (0.14-0.19)	0.10 (0.06-0.13)	0.02 (-0.01-0.06)	4, 75	16.4	0.0001
1 h	0.21 (0.08 - 0.16)	0.18 (0.15-0.20)	0.17 (0.14-0.20)	0.10 (0.08-0.13)	0.01 (-0.02-0.04)	4, 75	20.0	0.0001
12 h	0.21 (0.14-0.27)	0.30 (0.26-0.35)	0.23 (0.19-0.26)	0.14 (0.10-0.18)	0.008 (-0.04-0.06)	4, 65	24.2	0.0001
24 h	0.15 (0.11-0.20)	0.28 (0.22-0.34)	0.22 (0.19-0.26)	0.14 (0.11-0.18)	-0.007 (-0.06-0.03)	4, 65	26.1	0.0001
36 h	0.11 (0.07-0.14)	0.25 (0.17-0.32)	0.23 (0.19-0.28)	0.16 (0.12-0.19)	0.02 (-0.03-0.06)	4, 60	18.1	0.0001
48 h	0.11 (0.07-0.16)	0.19 (0.10-0.29)	0.20 (0.15-0.25)	0.13 (0.06-0.19)	-0.04 (-0.12-0.05)	4, 55	8.9	0.0001
96 h	0.13 (0.08-0.19)	0.11 (0.03-0.20)	0.16 (0.08-0.23)	0.11 (0.0001-0.22)	-0.02 (-0.07-0.03)	4, 45	4.0	0.007

Table 8-2: Water as a Change from Baseline for Source Collector 3

Water as a Change from Baseline at SC 4: Mean Values (95% CI)								
Time	**3 s**	**12 s**	**20 s**	**30 s**	**90 s**	**df**	**F**	**p-value**
Post	0.11 (0.08-0.14)	0.16 (0.12-0.19)	0.16 (0.13-0.19)	0.10 (0.06-0.13)	0.04 (0.0001-0.08)	4, 75	9.1	0.0001
1 h	0.12 (0.09-0.16)	0.18 (0.14-0.21)	0.16 (0.13-0.19)	0.11 (0.07-0.15)	0.04 (-0.002-0.08)	4, 75	11.2	0.0001
12 h	0.19 (0.13-0.25)	0.28 (0.23-0.33)	0.20 (0.16-0.24)	0.13 (0.08-0.17)	0.03 (-0.02-0.07)	4, 65	17.2	0.0001
24 h	0.12 (0.08-0.16)	0.22 (0.15-0.29)	0.18 (0.14-0.22)	0.11 (0.06-0.16)	-0.002 (-0.05-0.05)	4, 65	13.1	0.0001
36 h	0.09 (0.06-0.12)	0.21 (0.15-0.28)	0.19 (0.15-0.23)	0.13 (0.10-0.17)	0.02 (-0.02-0.06)	4, 60	15.4	0.0001
48 h	0.08 (0.04-0.12)	0.14 (0.07-0.21)	0.15 (0.11-0..18)	0.09 (0.03-0.15)	-0.03 (-0.10-0.11)	4, 55	8.1	0.0001
96 h	0.11 (0.04-0.18)	0.07 (-0.02-0.16)	0.09 (0.02-0.17)	0.07 (-0.05-0.19)	-0.02 (-0.09-0.04)	4, 45	1.7	ns

Table 8-3: Water as Change from Baseline at Source Collector 4

Figure 8-2: Burn Site Water Content as a Change from Pre-Burn Values over Time

The 3 s (basewater3s) and 12 s (basewater12s) burn have a large early peak in water content at 12 hours post-burn. The 12 s burn has the highest increase in water content at this time point. The 3 s burn water content declines rapidly towards baseline by 36 hours post-burn whereas the 12 s injury has a slower decline over the 24–96 hour time period. The 3 s burn does not show the same magnitude change in water content as the 12 s burn injury as shown in Figure 8-3.

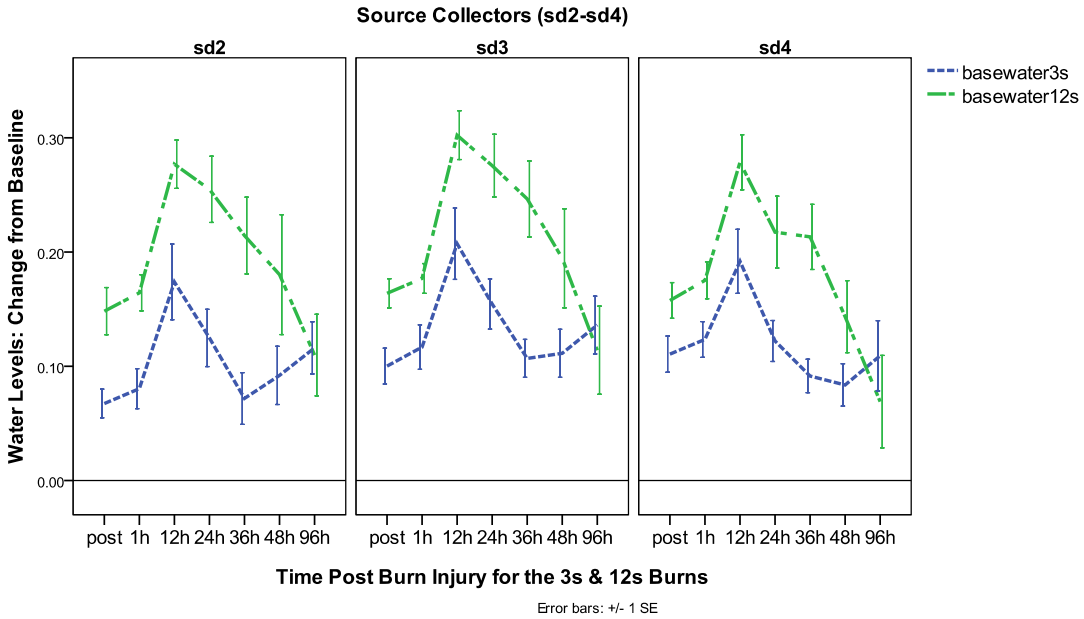

Figure 8-3: Water Levels as a Change from Pre- Burn within the 3 s and 12 s Burn Sites over Time

The 20 s (basewater20s) and 30 s (basewater30s) injuries do not show the same peak water content at 12 hours that is seen with the 3 s and 12 s burns. The water content is high for both injuries, and the 20 s injury has consistently higher levels than the 30 s burn wound over the time period. At 36 hours, the 20 s and 30 s injuries start to decline towards baseline levels as shown in Figure 8-4.

The 90 s (basewater90s) burn wound shows a small increase in water content immediately post-burn and at 12 hours. Levels hover near baseline for the majority of the time points as shown in Figure 8-5.

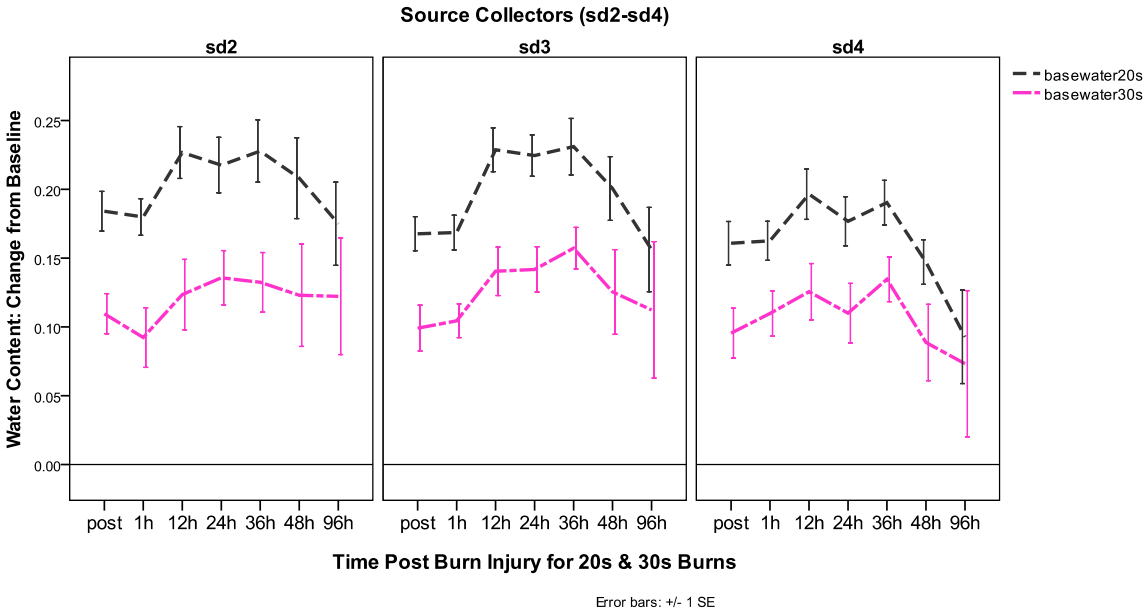

Figure 8-4: Water Levels as a Change from Pre-Burn within the 20 s and 30 s Burn Sites over Time

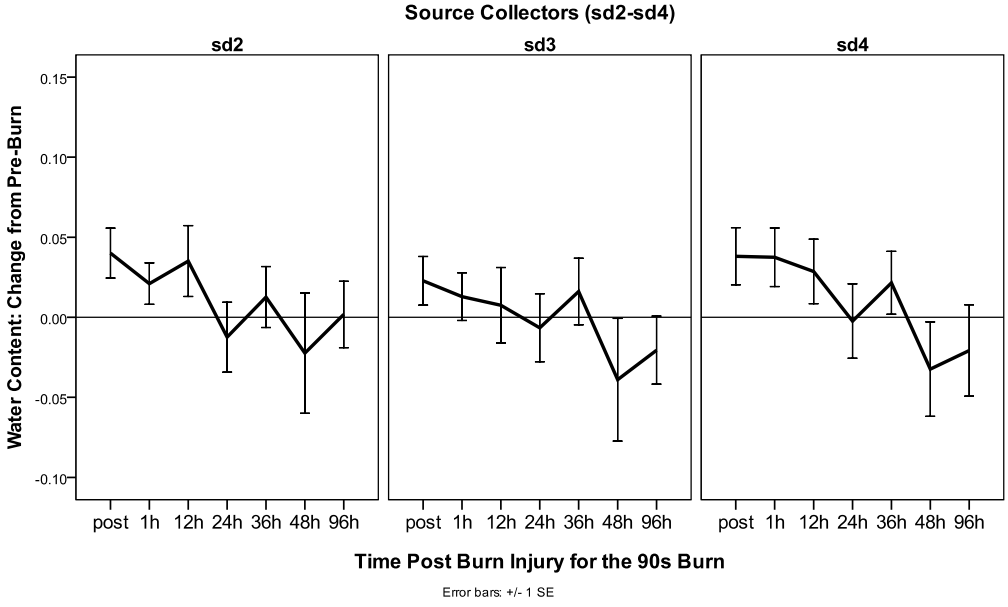

Figure 8-5: Water Levels as a Change from Pre-Burn within the 90 s Burn Sites over Time

8.2.2 **Controls**

At the majority of time points, there were no differences in water levels within the control sites. Differences were found at 1 hour post-injury at source collector 3 [$F(4, 75) = 3.2$, $p<0.02$]. Control site 1 experienced a 3% increase in water content compared to control sites 2 and 3, which experienced no change. Control sites 4 and 5 had a negative balance.

At 36 hours post-injury, the water content within the control sites showed a decline from pre-burn levels. The largest change was a 7% decrease in control site 1 and the smallest change at control 5 (0.5%). This was statistically significant at source collector 2 [$F(4, 60) = 2.6$, $p<0.0001$] and source collector 4 [$F(4, 60) = 3.4$, $p<0.01$].

8.3 Discussion

8.3.1 **Full Thickness Burn Wounds**

In this study, the water content was low within the full thickness burn wound at every time point. The water content of full thickness injuries showed minor changes from pre-burn levels and a paired control value (Appendix H).

Water content has been shown to be high in full thickness burn wounds in animal models. A rat contact burn showed an increase in water content in the subcutaneous tissue of a full thickness burn wound.[231] Sakurai et al. used a full thickness 40% TBSA burn model in sheep to investigate the water content of each anatomic layer using wet-to-dry measures. The highest increase in water content was found in the adipose tissue

(434%) versus the skin's water content, which only increased by 75%.[232] Studies utilizing the dielectric constant have measured high levels of water in full thickness injuries that remain high for 72 hours post-injury. This was in contrast to the low levels of water in the upper dermis at 24 hours post-burn in clinical full thickness burns. A full thickness injury has been reported to have peak water levels at 24 hours, with 25% of the edema remaining 1 week post-injury as measured in a 50% TBSA burn in rhesus monkeys.[233] In this study using NIR technology, there was no visible peak level of water at 24 hours or at any of the other time points. The findings using NIR technology differed from these studies, as the full thickness injuries' water levels either stayed close to pre-burn levels or had a water content that was below baseline. In addition, a large increase in water content was not found in the subcutaneous tissue compared to the dermis. In fact, water content remained close to baseline and the 90 s burn showed a decline in water content from pre-burn levels at 48 and 96 hours post-burn injury (Figure 8-5) This was an expected finding as technically a full thickness injury is defined as a burn that has complete necrosis of the dermis and all dermal structures along with fat necrosis. Fat necrosis can be secondary to the heating of tissues or from the progressive vascular thrombosis of the vessels, both of which cause an ischemic necrosis of the subcutaneous tissue. In either circumstance the blood vessels are destroyed, which terminates perfusion into the necrotic region and limits the possibility of the extravasation of fluids and proteins from the dead vessels. The biopsies of the histology of the burn wounds in this study support the NIR results as there was obvious fat necrosis, occluded blood vessels and necrotic endothelium in the subcutaneous tissue. The red cells in the blood vessels were coagulated and blocking perfusion of the fat. Fat necrosis

progressed over time and it was clear from the biopsies that this was secondary to ischemia as evidenced by a pseudomembranous change.

The Sakurai and Leape studies utilized large TBSA burns that produce a systemic response to injury, which directly impacts the degree of edema formation.[232, 233] It may be difficult to compare the results of a 2% TBSA burn to a 40–50% TBSA burn as there is a systemic response to a large TBSA burn. In this small TBSA burn study, the NIR results correlated with the histology findings and it was expected that a full thickness burn should have minimal edema. This reflects what is seen in the clinical environment, as full thickness injuries tend to be dry and leathery.[234, 235]

8.3.2 **Partial Thickness Burn Wounds**

The majority of studies designed to assess burn wound edema have investigated the changes occurring in one type of burn wound or a series of different depths of wounds. It is uncommon to find a study that includes the varying degrees of partial thickness injuries along with a measurement of edema. In general, burn edema pathophysiology studies have been performed in full thickness burn models until recently, when some investigators have compared superficial, partial and full thickness wounds.[113] There are very few studies that have investigated the water content in partial thickness burns of varying thermal injury.

The partial thickness injuries' (3–30 s) burn wounds all showed an increase in water content post-burn injury up to 96 hours post-burn. The partial thickness injuries also had

a higher water content than the 90 s burn wound. Other studies have also shown that partial thickness injury water content is high at 8 hours post-injury with increased levels up to 72 hours post-burn.[113] Partial thickness injuries also have the highest water content compared to superficial and full thickness injuries.[113] The results for the superficial partial injuries (3 s and 12 s) and the deep non-viable injuries (20 s and 30 s) were shown in separate figures in the results and will be discussed in their respective depth categories.

The 3 s and 12 s injuries show a similar pattern of water accumulation in the tissue. Water content experiences a large increase post-burn injury with peak levels at 12 hours post-burn. At 24 hours, there is a rapid decline towards baseline levels although neither reaches the pre-burn level or the control values by 96 hours. The major difference between the 3 s and 12 s burn injuries is the magnitude difference in water content. The 12 s burn injury had the highest water content of all the burn injuries at the majority of time points. The 3 s burn sites had the lowest water content of the partial thickness injuries.

The low levels of water in the 3 s burn wound may show that more superficial injuries do not experience the early “sucking” force of a strongly negative P_{if}.[85] The changes in capillary permeability (K_f) and the hypoproteinemia of the plasma all contribute to fluid flux out of the capillary and into the interstitium. In a more superficial burn, these changes in Starling’s forces may not be as dramatic as in deeper injuries. The large majority of the studies performed about edema pathophysiology have used full thickness burns as the model, so there is very little known about the changes that may occur in other injuries. The 3 s burn experienced the least amount of injury compared to the other

injuries. It is feasible that the safety mechanisms are still functioning to counteract the fluid efflux out of the tissue. The fractional exclusion of the interstitial matrix may change only enough to accommodate the increased protein and fluid content in order to restore the oncotic gradient limiting fluid movement out of the capillary. A counter-pressure is still being exerted by the interstitium as the compliance of the tissue is maintained. Finally, the lymphatics are intact and able to resorb fluid and protein more quickly than the deeper injuries. In has been documented that there is increased lymph flow for over 48 hours post-injury with full thickness injuries.[82, 92] In these studies, the lymph micropipettes were placed in the tissue next to the burn wound or zone of necrosis. This means that lymph measurements are technically from a zone of stasis or the area that is behaving like a partial thickness wound.

The 12 s burn injury experienced the highest increase in water content of all the burn sites. These high acute levels of water may be attributed to more dramatic changes in Starling's forces compared to the 3 s burn wound. A more negative P_{if} or an increase in the capillary permeability constant (K_f) with a greater decrease in plasma proteins could all contribute to fluid flux out of the capillary and into the interstitium. At 24 hours post-burn, the 12 s burn wound's water content begins to resolve and decline towards baseline levels. At 96 hours post-burn injury, the 3 s and 12 s raw water values do not differ. This means that the safety factors are intact in the 12 s injury and the water can be absorbed by the intact lymphatics.

The 20 s and 30 s burn injuries' water content increases immediately post-burn but does not experience peak water content like the 3 s and 12 s sites. The 20 s and 30 s actually

experience a plateau period from the 12–36-hour time point and then gradually decline towards baseline levels. The 20 s burn injury water content remains higher than the 30 s site when compared to pre-burn or control levels.

The high water content in the 20 s and 30 s injuries is likely related to dramatic changes in Starling's forces. The rapid accumulation of fluid in a burn wound is partially related to the degree of negativity of the interstitial hydrostatic pressure. P_{if} shows a rapid negative decline in the first 10–15 minutes after injury and could explain the rapid influx of water in the 12 s, 20 s and 30 s burn injuries immediately and at 1 hour post-injury compared to the other wounds. P_{if} has also been shown to be more negative in a deeper burn injury compared to a superficial wound.[85] This would explain why the 20 s and 30 s burns have a higher water content at 1 hour post-burn injury than the 12 s burn wound.

The 20 s and 30 s burn injuries do not show the same magnitude increase in water content as the 12 s burn injury. This may be partially related to the differences in perfusion of the wounds. The capillary endothelium sieving properties are impaired in the first 8 hours, allowing large proteins such as albumin to pass into the interstitium. After this time point, protein will accumulate in the interstitium because the lymphatics cannot keep pace with the initial influx of protein and fluid. For unknown reasons, proteins will not efflux from the capillary after 8 hours despite the enlarged pore radius.[77] A more superficial injury will have more patent blood vessels perfusing the injured region, which means there are more "leaky" vessels and an increased efflux of fluid and protein in these injuries. In a deeper injury, there are fewer patent blood vessels and therefore less fluid to move into the interstitium. Accordingly, the filtration coefficient (K_f) should

theoretically decrease with increasing thermal injury. This would serve to explain why the 12 s burn has the highest water values at 12–24 hours post-burn, as more fluid and protein has effluxed into the interstitium. The increase in the protein in the interstitium will change the colloid osmotic pressure, drawing more fluid into the matrix. The increase in fluid volume will also change the compliance of the tissue, permitting more fluid to enter the interstitium.[95, 96, 236]

Finally, the 20 s and 30 s injuries do not attain the same water levels as the 12 s burn and do not experience a rapid decline in water content. The gradual decline in water content represents an impairment of the lymphatics and safety factors. The more superficial injuries in this study were able to resorb fluid more rapidly than the deep partial thickness injuries. The differences in resorption may be explained by the degree of injury to the lymphatics. The lymphatics of the superficial injuries are likely intact and the deep injury lymphatics may be impaired or necrotic.

8.3.3 **NIR Versus Other Non-Invasive Edema Monitors**

Advances in edema pathophysiology have been limited because there are no validated clinical non-invasive tools. The majority of accurate and accepted techniques to assess edema are invasive. Wet-to-dry measures require a sample of tissue to be desiccated, lymph flow and protein content require the cannulation of lymphatic vessels, and fluorescent techniques requires the injection of tracers.[85, 237–239] All of these modalities are impractical in the clinical environment and are not conducive to repeated measures. Popular non-invasive tools include measurements of body weight changes, volumetry,

girth and limb circumference. Body weight changes are easy to measure but require a baseline measurement and do not provide information about edema pathophysiology.[103] The size and shape of a volumeter make it difficult to measure the entire limb and it can be difficult to transport because of the large volume of water required to fill the cylinder.[240] Volumetry is generally limited to the periphery and cannot be used in patients with open wounds. Limb or girth circumference is more practical in the clinical setting as it only requires a measuring tape. However, results are affected by the degree of tape tension, width and tape position.[241]

Non-invasive devices such as NMR spectroscopy, ultrasound, electrical impedance techniques, MRI and near infrared spectroscopy are non-invasive tools designed to assess the water content of the skin. The applications of these non-invasive devices to assess edema in burned tissue are limited to a small number of studies using electrical methods, MRI and NIR technology. All have shown promise in tissue water measurements but have limitations in terms of the capacity to assess edema in burn wounds.

Electrical methods assess water extremely rapidly (1–1.5 s), and the devices are portable and easy to use. There are commercial devices available and a number of studies have been published in the dermatology literature on its capacity to assess hydration of the skin. Electrical methods make the assumption that proton conduction dominates the *in vivo* environment and results are based on changes in conduction as a measure of water content.[180] However, with thermal injury and matrix changes conduction may not be completely proton based. Changes in temperature and humidity

affect the conduction properties of the tissue, necessitating measurements in a temperature-dependent, humidity-controlled environment. In fact, studies using these technologies have been performed only in the winter months for this reason. This affects this technology's ability to be used in the clinical setting, as the environmental temperature tends to vary depending on the systemic injury of the patient and the degree of hypothermia post-injury.[150]

Electrical methods also cannot provide a direct proportionality between total water content and the results obtained using these devices. As water can either be free or bound, anything that affects the bound water may interfere with conductance or the dielectric properties of tissue.[180] Ion concentration, sweating, emollients, dirt and body hair will all impact the dielectric constant and therefore change the conduction through the skin. In addition, penetration depth or the layer of skin under investigation is affected by the frequency delivered to the tissue and the geometry of the probe, which means the exact penetration depth of these devices has not been fully elucidated.[242–244] The degree of hydration of the skin affects the results obtained with the devices differently. There is variability in the reproducibility of repeat measures for some of the commercial devices.[180, 245, 246] Finally, the majority of these devices are designed to assess the stratum corneum and deeper measurements are required to assess the accumulation of edema in burn injuries.

Magnetic resonance imaging has used the physical state of water in the tissue to assess the degree of thermal injury according to T1 and T2 relaxation times. Partial thickness and full thickness injuries could be distinguished at 48 hours post-burn based on water

content.[13] However, in this particular study the burn tissue of the rat had to be excised and placed in optical density tubes for T1 and T2 time determinations. Nettlblad used magnetic resonance imaging to assess electrical burns in a few patients. T2 weighted images could localize the muscle necrosis that is not seen visually on the surface of the skin.[135] However, MRI is not practical in the burn clinical environment as the study period takes too long and there are specific ferromagnetic requirements to ensure the safety of the patients in the imaging suite. Large TBSA burns are hemodynamically unstable, which makes repeat transports to an imaging modality difficult. Spatial distortion is a problem with MRI as any involuntary movements decrease the signal to noise ratio. MRI is expensive and may not be cost effective in an already-expensive burn wound environment. Finally, the visualization of skin requires a specific skin gradient coil that currently has only been designed to assess extremities.

The strength of near infrared spectroscopy lies in its capacity to accurately measure water content from a simple reflectance of light. The spectrum of water has been well-elucidated for over 30 years and the wavelengths at which water absorbs light have little interference from the scattering properties of the tissue.[160] Water absorbs NIR light at specific wavelengths and in proportion to the amount of water that exists in the tissue. Between 900–1000 nm the measurement of water concentration receives little interference from other absorption molecules, making this a very accurate way to measure edema. Measuring hydration after surgery in a reverse McFarlane flap animal model, NIR technology water measurements were closely correlated with the clinical changes in edema formation.[160] In the clinical setting, water content could be used as a single variable to differentiate superficial and deep partial thickness injuries.[189]

8.3.4 **Limitations of the Study**

There are limitations when measuring edema in skin and using a device that is designed to interrogate the various layers of the tissue. The biggest challenge for any device used to assess skin is the non-uniformity of skin and the variability of skin thickness. Skin thickness varies with anatomic location and age, and there are even racial variations. Skin thickness is dynamic and affected by the degree of hydration. Hydration states are known to vary with age, gender, time of day, body position and disease states. The various hydration states influence skin thickness, which could potentially alter the tissue layer under assessment. The dielectric constant, ultrasound, MRI and MR spectroscopy, and near infrared spectroscopy are all devices that measure the hydration or water content of skin. Skin thickness has been a challenge for all of these technologies and the scientific community still needs to resolve these difficulties before this technology can be fully incorporated into the clinical environment. This is not an easy problem to resolve as the skin is dynamic and contains a variety of structures and cells that impacts electromagnetic radiation.

The second limitation of this study is that the water content results from the NIR Point technology were not correlated to a known standard for water determination. This limitation will be addressed in the future and is discussed in Chapter 9.

8.4 Major Findings and Conclusion

The purpose of this portion of the study was to test the capacity of NIR to non-invasively measure water content in burn wounds. NIR was capable of measuring water non-invasively and a summary of the major findings include:

1) The 12 s burn injury had the highest increase in water content compared to the other burn sites.
2) The 90 s injury's water content remained close to baseline levels for the experiment's time period.
3) The superficial partial thickness injuries (3 s and 12 s) showed peak water levels at 12 hours post-burn with a rapid decline in water content thereafter.
4) The deep partial thickness injuries (20 s and 30 s) had the highest water content at 1 hour post-burn, do not experience a peak in water content and show a gradual decline in water content.

NIR technology could assess water content *in vivo* and could demonstrate changes in water content over time. Burn depth could be classified based on the water content within the wound at each specific time point post-burn injury except 96 hours. Further research needs to be performed in order to validate the NIR technology's ability to assess edema in tissue and will be discussed in Chapter 9: Summary and Future Directions.

Chapter 9: Summary and Future Directions

9.1 Histology

In pathology, very rarely is one staining technique used alone to determine the diagnosis. H&E is a cheap and effective way to evaluate burn injuries, but in 4% of the clinical cases this staining technique does not yield enough information to make a definitive diagnosis. Other staining techniques are required as an adjunct to H&E in order to fully elucidate the diagnosis of the depth of injury using histology. Vimentin was not found to be useful in the clinical situation and should be reserved for tracking the progression of burn injury or as an adjunct to H&E. In this study, vimentin immunostaining was able to differentiate burn injuries using a vimentin demarcation line. Superficial partial thickness injuries had positive immunostaining in the dermis. Deep partial thickness and full thickness injuries had a demarcation line within the lower portion of the dermis or the subcutaneous tissue. It was difficult to determine differences between the 12 s and 20 s burn wounds, which are the true “indeterminate” injuries, using vimentin immunostaining.

Future goals in this area include looking for adjunctive stains to guide or aid pathologists with the diagnosis. Most importantly, as the hair follicle and endothelium are the most important features of a viable burn wound it is important to find other techniques that could help delineate their viability. CD31 has already been tested as a marker of endothelial cell integrity but it stains both necrotic and non-necrotic endothelium, which limits its utility in burn depth determination. An adjunctive stain that could assess

endothelium or epithelium viability would be extremely valuable as an adjunct to the H&E.

One of the most valuable findings from the histology portion of the thesis was the use of wound healing time to classify the depth of the 12 s burn wound as a superficial partial thickness injury or a viable wound. Wound healing time is difficult to assess in the clinical environment due to the practice of early excision and grafting in burn wounds. The reference standard, which is the objective histology criteria, cannot be fully defined until it has been compared to wound healing time or wound outcome. Future work in burn depth determination will require a combination of wound healing time and histology.

9.2 Hemoglobin

Oxyhemoglobin, total hemoglobin and the proportion of hemoglobin in the tissue were used to classify the injuries into viable and non-viable injuries. The proportion of hemoglobin in the wound clearly showed that as thermal injury progressed in depth the proportion of oxyhemoglobin decreased and deoxyhemoglobin increased.

The swine model in this study could be improved by creating shorter duration contact burns representing superficial burn wounds. At the control sites, there was no crush injury related to the longer duration of brass rod placement, therefore these additional control sites could be eliminated in future studies and replaced by burn sites.

The contact burn model is an accepted model for burn depth determination. However, in this study the depth of the injury using histology was well-defined within 12 hours post-burn, whereas other investigators have shown depth progression up to 3 days post-burn injury.[205, 247, 248] Contact burn wounds also produce a clear demarcation between viable and non-viable tissue.[205, 217, 248] Scald burns create a more variable pattern of damage to the collagen fibers and vasculature with depth progression over 72 hours.[217] It is important to investigate the differences that may exist between scald and contact thermal injuries. Scald burns are one of the most common types of thermal injuries presented to a burn centre and they are one of the most common injuries to children. Scald burns are extremely misleading as these wounds visually appear to be a first-degree burn injury. If scald burn wounds could be differentiated at early time points then management decisions could be made earlier.

This study was a small TBSA burn model but it is important in the future to perform studies in larger TBSA injuries. Large TBSA burns have a systemic response to the burn injury and this impacts burn wound progression and depth. It is important to determine if NIR technology can detect the changes that might occur in the burn wound in a larger TBSA burn. In addition, in a large TBSA burn wound the effects of varying resuscitation fluid volumes and the type of fluid delivered could be evaluated. NIR spectroscopy has been successfully used to determine the endpoints of resuscitation in trauma patients. However, burn patients were excluded from the studies due to their unique fluid requirements.

The zone of stasis is of great interest to investigators as it represents the area of the burn injury where the injury could potentially be reversed and the progression of injury inhibited. One of the major challenges in this area is the capacity to non-invasively monitor the changes that are occurring within this region. This makes it difficult to develop therapeutics designed to change the perfusion and oxygenation of the burn wounds, as the outcome measures are generally related to the visual appearance of the wound. A swine burn comb model could be used to generate the zone of stasis and near infrared technology could assess the hemodynamic changes within this region. Interventions such as prostaglandin inhibitors, histamine receptor agonists and antagonists, and bradykinin antagonists could be given and changes in the zone of stasis measured.

9.3 Methemoglobin

Methemoglobin was not detected in previous laboratory flap studies, normal clinical skin studies or the first acute porcine burn study that utilized the NIR devices. The impetus for examining the absorption spectra for methemoglobin came from one of the burn clinical studies, as methemoglobin was visualized in some of the spectra from the wounds. In the current animal study, as burn depth increased so did the proportion of methemoglobin to total hemoglobin in the wounds. Plausible but not proven explanations for the presence of methemoglobin in a burn wound include an antioxidant role in viable injuries and a pro-oxidant role in non-viable burn injuries.

There are no published studies utilizing *in vivo* near infrared spectroscopy to detect methemoglobin in burn wounds. However, near infrared technology is the reference standard for assessing methemoglobin *in vitro* and is used in the clinical laboratory routinely. Blood specimens sent to the laboratory are analyzed using a near infrared co-oximeter and the content of methemoglobin, carboxyhemoglobin and sulfinated hemoglobin can be measured. In order to validate the NIR device's capacity to measure methemoglobin *in vivo,* it is necessary to compare the NIR Point results with that of co-oximetry. The near infrared spectroscopy *in vivo* device could then be compared to the *in vitro* gold standard. This study may be challenging, as blood samples are required for the co-oximetry analysis and would limit the type of model that could be utilized. For example, a burn model could not be utilized, as it is difficult to cannulate partially necrotic blood vessels. A flap model would be ideal, as the perfusion to the flap could be controlled and therefore the formation of methemoglobin could be controlled. I have already attempted to utilize inspired gas ratios (oxygen, carbon dioxide, nitrogen) to produce methemoglobin *in vivo* but was unsuccessful at oxidizing hemoglobin to methemoglobin. The solution to this problem is the use of chemical compounds such as sodium nitrite to oxidize hemoglobin.

Overall, the experiments reported in this thesis show that methemoglobin is present in burn wounds. There are many questions surrounding the presence of methemoglobin in the wounds and its role in the tissue. Is methemoglobin a burn wound phenomenon only or do other types of wounds have high methemoglobin levels? Does the size of burn injury impact the levels of methemoglobin in the wound? At what time point in the first 12 hours post-burn does methemoglobin appear in the spectrum of burn injuries? Can the

timing of the presence of methemoglobin be tied to the presence of ROS or RNS in the wound? If methemoglobin could be reduced back to ferrous hemoglobin, would this change the viability of the burn wound?

As high levels are associated with non-viable injuries, the presence of methemoglobin in a burn wound is an exciting and interesting finding. Future work in this area is required to fully elucidate the role of methemoglobin in a burn wound.

9.4 Water

NIR technology was capable of measuring water content in varying burn depths over time. In general, as the depth of the burn increased the water content decreased. This was true for the 12–90 s burn injuries but does not apply to the 3 s burn injury as water content levels were low in the most superficial burn wound.

Near infrared spectroscopy is well-suited to determine water content in tissue. Water is the predominant signal within the NIR wavelength of interest and this is well-accepted by spectroscopists. However, in the area of edema pathophysiology, wet-to-dry measures, circumferential measures and lymph flow are considered accepted techniques to assess edema.

Introducing a new technology into this area requires that the technology be compared to what is currently accepted. Near infrared technology has to be validated for water measurements against an accepted practice of water content measurements. A series of

experiments are required in order to do this adequately. In the first experiment, NIR could measure the tissue water content in a swine model. The area of tissue could then be excised and wet-to-dry measures obtained. It is likely that this experiment may not be completely successful due to the nature of the NIR probe design. The light returning to the detector has some overlap in terms of its location in the skin. In addition, the light may detect some water in the tissue that is deeper or outside the biopsy specimen. This means that the NIR technology may detect more or less water than the wet-to-dry measures because it may be impossible to truly take a representative biopsy of the path of light.

The second experiment may yield more positive results as a flap model could be used to manipulate perfusion and therefore the water content of the tissue. NIR Point would assess the baseline levels of tissue water prior to raising the flap, post-flap elevation and after a series of fluid resuscitations. The saline infusions could be directly infused into the flap blood supply to ensure only the flap is receiving the fluid resuscitation. Near infrared spectroscopy would then be used to quantify the change in water content based on the volume of infusion. The ability of NIR to monitor the change in water content in the flap would serve to validate the technology. A non-invasive technology that can assess edema would be a significant advancement in furthering knowledge surrounding burn edema pathophysiology.

9.5 Overall Summary

In the future, it is important to determine which variables are critical for the determination of burn depth. This would serve to take the NIR devices from an offline data analysis technique to a device that can produce results for water, oxy-, deoxy-, met- and total hemoglobin at the bedside. The thesis does not address which variable or combination of variables are important for burn depth determination. Therefore, it is difficult to assign cut-off values that could classify a burn wound into viable or non-viable categories. In addition, the NIR Point device utilized in these studies measures the relative change in the variable content and therefore it is not the absolute number that determines depth but the variable deviation from a control or pre-burn site. At this moment in time, with respect to the development of the technology the frequency of false positive or false negative data is unknown. Also, without assigned cut-off values it is difficult to correlate the histology findings with the NIR Point results.

Developing *in vivo* mathematical algorithms is difficult because there are no current gold standards for measuring the hemoglobin or water content within the tissue. There are also no gold standards for the assessment of tissue viability, which makes validation of new devices challenging. Currently, determining how much of the tissue and which portions of the tissue are being interrogated has also not been fully elucidated.[151]

Overall, the knowledge obtained from this laboratory study in a porcine burn model will impact the clinical development of the NIR devices. Mathematical algorithms for the extraction of the chromophores have been modified and refined. The changes in water, oxy-, deoxy- and total hemoglobin over time and with increasing thermal injury have

been further elucidated using NIR technology. The discovery of methemoglobin in the burn wound adds a new variable that represents the degree of injury to the tissue, but its presence and purpose within a burn wound still needs to be fully investigated. NIR technology has shown promise as a non-invasive device to assess burn depth. A non-invasive monitor of hemodynamics has applications in the clinical setting that extend beyond the realm of burn wound depth determination and into other areas of medicine.

References

1. Heimbach DM, Afromowitz MA, Engrav LH, Marvin JA, Perry B. Burn depth estimation--man or machine. JTrauma 1984;24:373-8.
2. Heimbach D, Herndon D, Luterman A, et al. Early excision of thermal burns--an international round-table discussion, Geneva, June 22, 1987. JBurn Care Rehabil 1988;9:549-61.
3. Kamolz LP, Andel H, Haslik W, et al. Indocyanine green video angiographies help to identify burns requiring operation. Burns 2003;29:785-91.
4. Riordan CL, McDonough M, Davidson JM, et al. Noncontact laser Doppler imaging in burn depth analysis of the extremities. J Burn Care Rehabil 2003;24:177-86.
5. Kloppenberg FW, Beerthuizen GI, ten Duis HJ. Perfusion of burn wounds assessed by laser doppler imaging is related to burn depth and healing time. Burns 2001;27:359-63.
6. Jeng JC, Bridgeman A, Shivnan L, et al. Laser Doppler imaging determines need for excision and grafting in advance of clinical judgment: a prospective blinded trial. Burns 2003;29:665-70.
7. Arturson G. Forty years in burns research - the postburn inflammatory response. Burns 2000;26:599-604.
8. Sheridan RL, Schomaker KT, Lucchina LC, et al. Burn depth estimation by use of indocyanine green fluorescence: initial human trial. JBurn Care Rehabil 1995;16:602-4.
9. Green HA, Bua D, Anderson RR, Nishioka NS. Burn depth estimation using indocyanine green fluorescence. Arch Dermatol 1992;128:43-9.
10. Adams TS, Murphy JV, Gillespie PH, Roberts AH. The use of high frequency ultrasonography in the prediction of burn depth. JBurn Care Rehabil 2001;22:261-2.
11. Iraniha S, Cinat ME, VanderKam VM, et al. Determination of burn depth with noncontact ultrasonography. J Burn Care Rehabil 2000;21:333-8.
12. Cole RP, Shakespeare PG, Chissell HG, Jones SG. Thermographic assessment of burns using a nonpermeable membrane as wound covering. Burns 1991;17:117-22.
13. Koruda MJ, Zimbler A, Settle RG, et al. Assessing burn wound depth using in vitro nuclear magnetic resonance (NMR). JSurgRes 1986;40:475-81.
14. Park BH, Saxer C, Srinivas SM, Nelson JS, de Boer JF. In vivo burn depth determination by high-speed fiber-based polarization sensitive optical coherence tomography. JBiomedOpt 2001;6:474-9.
15. Srinivas SM, de Boer JF, Park H, et al. Determination of burn depth by polarization-sensitive optical coherence tomography. JBiomedOpt 2004;9:207-12.
16. Williams WG. Pathophysiology of the burn wound. In: Total Burn Care. London: Saunders; 2002:78-85.
17. Moritz AR, Henriques, F.C. II. The Relative Importance of Time and Surface Temperature in the Causation of Cutaneous Burns. American Journal of Pathology 1947;23:695-720.
18. Singer AJ, Berruti L, Thode HC, McClain SA. Standardized burn model using a multiparametric histologic analysis of burn depth. Academic Emergency Medicine 2000;7:1-6.
19. Lee RC, Astumian RD. The physicochemical basis for thermal and non-thermal 'burn' injuries. Burns 1996;22:509-19.

20. Despa F, Orgill DP, Neuwalder J, Lee RC. The relative thermal stability of tissue macromolecules and cellular structure in burn injury. Burns 2005;31:568-77.
21. Jackson DM. [The diagnosis of the depth of burning.]. BrJSurg 1953;40:588-96.
22. Zawacki B. The Natural History of Reversible Burn Injury. Surgery, Gynecology & Obstetrics 1974;139:867-72.
23. deCamara DL, Raine TJ, London MD, Robson MC, Heggers JP. Progression of thermal injury: a morphologic study. PlastReconstrSurg 1982;69:491-9.
24. Papp A, Kiraly K, Harma M, Lahtinen T, Uusaro A, Alhava E. The progression of burn depth in experimental burns: a histological and methodological study. Burns 2004;30:684-90.
25. Nanney LB, Wenczak BA, Lynch JB. Progressive burn injury documented with vimentin immunostaining. JBurn Care Rehabil 1996;17:191-8.
26. Boykin JV, Eriksson E, Pittman RN. In vivo microcirculation of a scald burn and the progression of postburn dermal ischemia. PlastReconstrSurg 1980;66:191-8.
27. Schiller WR, Garren RL, Bay RC, et al. Laser Doppler evaluation of burned hands predicts need for surgical grafting. JTrauma 1997;43:35-9.
28. Cross KM, Leonardi L, Payette JR, et al. Clinical utilization of near-infrared spectroscopy devices for burn depth assessment. WoundRepair Regen 2007;15:332-40.
29. Park DH, Hwang JW, Jang KS, Han DG, Ahn KY, Baik BS. Use of laser Doppler flowmetry for estimation of the depth of burns. Plast Reconstr Surg 1998;101:1516-23.
30. Atiles L, Mileski W, Purdue G, Hunt J, Baxter C. Laser Doppler flowmetry in burn wounds. J Burn Care Rehabil 1995;16:388-93.
31. Tandara AA, Mustoe TA. Oxygen in wound healing--more than a nutrient. World J Surg 2004;28:294-300.
32. Hunt TK, Niinikoski J, Zederfeldt B. Role of oxygen in repair processes. Acta Chir Scand 1972;138:109-10.
33. LaVan FB, Hunt TK. Oxygen and wound healing. Clin Plast Surg 1990;17:463-72.
34. Thorniley MS, Sinclair JS, Barnett NJ, Shurey CB, Green CJ. The use of near-infrared spectroscopy for assessing flap viability during reconstructive surgery. Br J Plast Surg 1998;51:218-26.
35. De Blasi RA, Ferrari M, Natali A, Conti G, Mega A, Gasparetto A. Noninvasive measurement of forearm blood flow and oxygen consumption by near-infrared spectroscopy. J Appl Physiol 1994;76:1388-93.
36. Hampson NB, Piantadosi CA. Near infrared monitoring of human skeletal muscle oxygenation during forearm ischemia. J Appl Physiol 1988;64:2449-57.
37. Irwin MS, Thorniley MS, Dore CJ, Green CJ. Near infra-red spectroscopy: a non-invasive monitor of perfusion and oxygenation within the microcirculation of limbs and flaps. Br J Plast Surg 1995;48:14-22.
38. Hoffman RS, Sauter D. Methemoglobinemia resulting from smoke inhalation. Vet Hum Toxicol 1989;31:168-70.
39. Percy MJ, McFerran NV, Lappin TR. Disorders of oxidised haemoglobin. Blood Rev 2005;19:61-8.
40. Mansouri A, Lurie AA. Concise review: methemoglobinemia. Am J Hematol 1993;42:7-12.
41. Bradberry SM. Occupational methaemoglobinaemia. Mechanisms of production, features, diagnosis and management including the use of methylene blue. Toxicol Rev 2003;22:13-27.

42. Wright RO, Lewander WJ, Woolf AD. Methemoglobinemia: etiology, pharmacology, and clinical management. Ann Emerg Med 1999;34:646-56.
43. Haymond S, Cariappa R, Eby CS, Scott MG. Laboratory assessment of oxygenation in methemoglobinemia. Clin Chem 2005;51:434-44.
44. Minetti M, Malorni W. Redox control of red blood cell biology: the red blood cell as a target and source of prooxidant species. Antioxid Redox Signal 2006;8:1165-9.
45. Buehler PW, Alayash, A.I. Oxidation of hemoglobin: mechanisms of control *in vitro* and *in vivo*. Transfusion Alternatives in Transfusion Medicine 2007;9:204-12.
46. Umbreit J. Methemoglobin--it's not just blue: a concise review. Am J Hematol 2006;82:134-44.
47. McLeod LL, Alayash AI. Detection of a ferrylhemoglobin intermediate in an endothelial cell model after hypoxia-reoxygenation. Am J Physiol 1999;277:H92-9.
48. Faivre B, Menu P, Labrude P, Vigneron C. Hemoglobin autooxidation/oxidation mechanisms and methemoglobin prevention or reduction processes in the bloodstream. Literature review and outline of autooxidation reaction. Artif Cells Blood Substit Immobil Biotechnol 1998;26:17-26.
49. Valko M, Leibfritz D, Moncol J, Cronin MT, Mazur M, Telser J. Free radicals and antioxidants in normal physiological functions and human disease. Int J Biochem Cell Biol 2007;39:44-84.
50. Mulligan MS, Till GO, Smith CW, et al. Role of leukocyte adhesion molecules in lung and dermal vascular injury after thermal trauma of skin. Am J Pathol 1994;144:1008-15.
51. Parihar A, Parihar MS, Milner S, Bhat S. Oxidative stress and anti-oxidative mobilization in burn injury. Burns 2008;34:6-17.
52. Horton JW. Free radicals and lipid peroxidation mediated injury in burn trauma: the role of antioxidant therapy. Toxicology 2003;189:75-88.
53. Till GO, Guilds LS, Mahrougui M, Friedl HP, Trentz O, Ward PA. Role of xanthine oxidase in thermal injury of skin. Am J Pathol 1989;135:195-202.
54. Friedl HP, Till GO, Trentz O, Ward PA. Roles of histamine, complement and xanthine oxidase in thermal injury of skin. Am J Pathol 1989;135:203-17.
55. Filippou D, Papadopoulos VP, Triga A, et al. Nitric oxide, antioxidant capacity, nitric oxide synthase and xanthine oxidase plasma levels in a cohort of burn patients. Burns 2007;33:1001-7.
56. Balla J, Vercellotti GM, Jeney V, et al. Heme, heme oxygenase, and ferritin: how the vascular endothelium survives (and dies) in an iron-rich environment. Antioxid Redox Signal 2007;9:2119-37.
57. Buehler PW, Alayash AI. Redox biology of blood revisited: the role of red blood cells in maintaining circulatory reductive capacity. Antioxid Redox Signal 2005;7:1755-60.
58. Patel RP, Svistunenko DA, Darley-Usmar VM, Symons MC, Wilson MT. Redox cycling of human methaemoglobin by H2O2 yields persistent ferryl iron and protein based radicals. Free Radic Res 1996;25:117-23.
59. Cooper CE, Torres J, Sharpe MA, Wilson MT, Svistunenko DA. Peroxynitrite reacts with methemoglobin to generate globin-bound free radical species. Implications for vascular injury. Adv Exp Med Biol 1998;454:195-202.
60. Rawlingson A. Nitric oxide, inflammation and acute burn injury. Burns 2003;29:631-40.

61. Szabo C, Ohshima H. DNA damage induced by peroxynitrite: subsequent biological effects. Nitric Oxide 1997;1:373-85.
62. Fechner GG, Gee DJ. Study on the effects of heat on blood and on the post-mortem estimation of carboxyhaemoglobin and methaemoglobin. Forensic Sci Int 1989;40:63-7.
63. Farahani K, Saxton RE, Yoon HC, De Salles AA, Black KL, Lufkin RB. MRI of thermally denatured blood: methemoglobin formation and relaxation effects. Magn Reson Imaging 1999;17:1489-94.
64. Bradley WG, Jr., Schmidt PG. Effect of methemoglobin formation on the MR appearance of subarachnoid hemorrhage. Radiology 1985;156:99-103.
65. Meyding-Lamade U, Forsting M, Albert F, Kunze S, Sartor K. Accelerated methaemoglobin formation: potential pitfall in early postoperative MRI. Neuroradiology 1993;35:178-80.
66. Kaufman T, Neuman RA, Weinberg A. Is postburn dermal ischaemia enhanced by oxygen free radicals? Burns 1989;15:291-4.
67. Konukoglu D, Cetinkale O, Bulan R. Effects of N-acetylcysteine on lung glutathione levels in rats after burn injury. Burns 1997;23:541-4.
68. Koizumi T, Goto H, Tanaka H, Yamaguchi Y, Shimazaki S. Lecithinized superoxide dismutase suppresses free radical substrates during the early phase of burn care in rats. J Burn Care Res 2009;30:321-8.
69. Liu X, Spolarics Z. Methemoglobin is a potent activator of endothelial cells by stimulating IL-6 and IL-8 production and E-selectin membrane expression. Am J Physiol Cell Physiol 2003;285:C1036-46.
70. Balla J, Vercellotti GM, Nath K, et al. Haem, haem oxygenase and ferritin in vascular endothelial cell injury. Nephrol Dial Transplant 2003;18 Suppl 5:v8-12.
71. Bunn HF, Jandl JH. Exchange of heme among hemoglobins and between hemoglobin and albumin. J Biol Chem 1968;243:465-75.
72. Balla J, Jacob HS, Balla G, Nath K, Vercellotti GM. Endothelial cell heme oxygenase and ferritin induction by heme proteins: a possible mechanism limiting shock damage. Trans Assoc Am Physicians 1992;105:1-6.
73. Balla G, Vercellotti GM, Eaton JW, Jacob HS. Iron loading of endothelial cells augments oxidant damage. J Lab Clin Med 1990;116:546-54.
74. Jeney V, Balla J, Yachie A, et al. Pro-oxidant and cytotoxic effects of circulating heme. Blood 2002;100:879-87.
75. Lund T, Onarheim H, Reed RK. Pathogenesis of edema formation in burn injuries. World J Surg 1992;16:2-9.
76. Demling RH. The burn edema process: current concepts. JBurn Care Rehabil 2005;26:207-27.
77. Pitt RM, Parker JC, Jurkovich GJ, Taylor AE, Curreri PW. Analysis of altered capillary pressure and permeability after thermal injury. J Surg Res 1987;42:693-702.
78. Leape LL. Initial changes in burns: tissue changes in burned and unburned skin of rhesus monkeys. JTrauma 1970;10:488-92.
79. Demling RH, Mazess RB, Witt RM, Wolberg WH. The study of burn wound edema using dichromatic absorptiometry. JTrauma 1978;18:124-8.
80. Onarheim H, Reed RK. Thermal skin injury: effect of fluid therapy on the transcapillary colloid osmotic gradient. J Surg Res 1991;50:272-8.
81. Harms BA, Kramer GC, Bodai BI, Demling RH. Effect of hypoproteinemia on pulmonary and soft tissue edema formation. Crit Care Med 1981;9:503-8.

82. Demling RH, Kramer G, Harms B. Role of thermal injury-induced hypoproteinemia on fluid flux and protein permeability in burned and nonburned tissue. Surgery 1984;95:136-44.
83. Kinsky MP, Guha SC, Button BM, Kramer GC. The role of interstitial starling forces in the pathogenesis of burn edema. JBurn Care Rehabil 1998;19:1-9.
84. Lund T, Wiig H, Reed RK. Acute postburn edema: role of strongly negative interstitial fluid pressure. AmJPhysiol 1988;255:H1069-H74.
85. Shimizu S, Tanaka H, Sakaki S, Yukioka T, Matsuda H, Shimazaki S. Burn depth affects dermal interstitial fluid pressure, free radical production, and serum histamine levels in rats. J Trauma 2002;52:683-7.
86. Lund T, Wiig H, Reed RK, Aukland K. A 'new' mechanism for oedema generation: strongly negative interstitial fluid pressure causes rapid fluid flow into thermally injured skin. Acta Physiol Scand 1987;129:433-5.
87. Wiederhielm CA, Fox JR, Lee DR. Ground substance mucopolysaccharides and plasma proteins: their role in capillary water balance. Am J Physiol 1976;230:1121-5.
88. Aukland K, Reed RK. Interstitial-lymphatic mechanisms in the control of extracellular fluid volume. Physiol Rev 1993;73:1-78.
89. Granger HJ. Role of the Interstitial Matrix and Lymphatic Pump in Regulation of Transcapillary Fluid Balance. Microvascular Research 1979;18:209-16.
90. Negrini D, Passi A, de Luca G, Miserocchi G. Pulmonary interstitial pressure and proteoglycans during development of pulmonary edema. Am J Physiol 1996;270:H2000-7.
91. Onarheim H, Reed RK, Laurent TC. Increased plasma concentrations of hyaluronan after major thermal injury in the rat. Circ Shock 1992;37:159-63.
92. Harms BA, Bodai BI, Kramer GC, Demling RH. Microvascular fluid and protein flux in pulmonary and systemic circulations after thermal injury. Microvasc Res 1982;23:77-86.
93. Brouhard BH, Carvajal HF, Linares HA. Burn edema and protein leakage in the rat. I. Relationship to time of injury. MicrovascRes 1978;15:221-8.
94. Guyton AC. Pressure-volume relationships in the interstitial spaces. Invest Ophthalmol 1965;4:1075-84.
95. Wiig H, Reed RK. Compliance of the interstitial space in rats. II. Studies on skin. Acta Physiol Scand 1981;113:307-15.
96. Guyton AC. Interstitial Fluid Presure. Ii. Pressure-Volume Curves of Interstitial Space. Circ Res 1965;16:452-60.
97. Demling RH, Lalonde C. Systemic lipid peroxidation and inflammation induced by thermal injury persists into the post-resuscitation period. J Trauma 1990;30:69-74.
98. Rantfors J, Cassuto J. Role of histamine receptors in the regulation of edema and circulation postburn. Burns 2003;29:769-77.
99. Papp A, Harma M, Harvima R, Lahtinen T, Uusaro A, Alhava E. Microdialysis for detection of dynamic changes in tissue histamine levels in experimental thermal injury. Burns 2005;31:476-81.
100. Tanaka H, Lund T, Wiig H, et al. High dose vitamin C counteracts the negative interstitial fluid hydrostatic pressure and early edema generation in thermally injured rats. Burns 1999;25:569-74.
101. Sakurai M, Tanaka H, Matsuda T, Goya T, Shimazaki S, Matsuda H. Reduced resuscitation fluid volume for second-degree experimental burns with delayed initiation of vitamin C therapy (beginning 6 h after injury). J Surg Res 1997;73:24-7.

102. Dubick MA, Williams C, Elgjo GI, Kramer GC. High-dose vitamin C infusion reduces fluid requirements in the resuscitation of burn-injured sheep. Shock 2005;24:139-44.
103. Tanaka H, Matsuda T, Miyagantani Y, Yukioka T, Matsuda H, Shimazaki S. Reduction of resuscitation fluid volumes in severely burned patients using ascorbic acid administration: a randomized, prospective study. Arch Surg 2000;135:326-31.
104. Arturson G. Microvascular permeability to macromolecules in thermal injury. Acta Physiol Scand Suppl 1979;463:111-22.
105. Barrow RE, Ramirez RJ, Zhang XJ. Ibuprofen modulates tissue perfusion in partial-thickness burns. Burns 2000;26:341-6.
106. Cetinkale O, Demir M, Sayman HB, Ayan F, Onsel C. Effects of allopurinol, ibuprofen and cyclosporin A on local microcirculatory disturbance due to burn injuries. Burns 1997;23:43-9.
107. Battal MN, Hata Y, Matsuka K, et al. Reduction of progressive burn injury by a stable prostaglandin I2 analogue, beraprost sodium (Procylin): an experimental study in rats. Burns 1996;22:531-8.
108. Nwariaku FE, Sikes PJ, Lightfoot E, Mileski WJ, Baxter C. Effect of a bradykinin antagonist on the local inflammatory response following thermal injury. Burns 1996;22:324-7.
109. Jonkam CC, Enkhbaatar P, Nakano Y, et al. Effects of the bradykinin B2 receptor antagonist icatibant on microvascular permeability after thermal injury in sheep. Shock 2007;28:704-9.
110. Tagami H, Ohi M, Iwatsuki K, Kanamaru Y, Yamada M, Ichijo B. Evaluation of the skin surface hydration in vivo by electrical measurement. J Invest Dermatol 1980;75:500-7.
111. Boyce ST, Supp AP, Harriger MD, Pickens WL, Wickett RR, Hoath SB. Surface electrical capacitance as a noninvasive index of epidermal barrier in cultured skin substitutes in athymic mice. J Invest Dermatol 1996;107:82-7.
112. Barel A, Clarys, P. Measurement of Epidermal Capacitance In: Serup J, Jemec, GBE, Grove, G, ed. Handbook of Non-Invasive Methods and the Skin: second edition. 2 ed. Boca Raton, Florida: CRC Press: Taylor & Francis Group; 2006:337-44.
113. Papp A, Lahtinen T, Harma M, Nuutinen J, Uusaro A, Alhava E. Dielectric measurement in experimental burns: a new tool for burn depth determination? Plast Reconstr Surg 2006;117:889-98; discussion 99-901.
114. Nuutinen J, Ikaheimo R, Lahtinen T. Validation of a new dielectric device to assess changes of tissue water in skin and subcutaneous fat. Physiol Meas 2004;25:447-54.
115. Nuutinen J, Lahtinen T, Turunen M, et al. A dielectric method for measuring early and late reactions in irradiated human skin. Radiother Oncol 1998;47:249-54.
116. Goretsky MJ, Supp AP, Greenhalgh DG, Warden GD, Boyce ST. Surface electrical capacitance as an index of epidermal barrier properties of composite skin substitutes and skin autografts. Wound Repair Regen 1995;3:419-25.
117. Petaja L, Nuutinen J, Uusaro A, Lahtinen T, Ruokonen E. Dielectric constant of skin and subcutaneous fat to assess fluid changes after cardiac surgery. Physiol Meas 2003;24:383-90.
118. Kao HP, Cardoso ER, Shwedyk E. Correlation of permittivity and water content during cerebral edema. IEEE Trans Biomed Eng 1999;46:1121-8.

119. Papp A, Lahtinen T, Harma M, Nuutinen J, Alhava E. Dielectric measurement in experimental burns: a new tool for burn depth determination. Plast Reconstr Surg 2007;119:1958-60.
120. Bossuyt PM, Reitsma JB, Bruns DE, et al. The STARD statement for reporting studies of diagnostic accuracy: explanation and elaboration. Ann Intern Med 2003;138:W1-12.
121. Petro A, Schwartz J, Johnson T. Current melanoma staging. Clin Dermatol 2004;22:223-7.
122. Ramsay AD. Errors in histopathology reporting: detection and avoidance. Histopathology 1999;34:481-90.
123. Oshima RG. Intermediate filaments: a historical perspective. Exp Cell Res 2007;313:1981-94.
124. Paramio JM, Jorcano JL. Beyond structure: do intermediate filaments modulate cell signalling? Bioessays 2002;24:836-44.
125. Nagle RB. A review of intermediate filament biology and their use in pathologic diagnosis. Mol Biol Rep 1994;19:3-21.
126. Steinert PM. Intermediate filaments in health and disease. Experimental and Molecular Medicine 1996;28:55-63.
127. Colucci-Guyon E, Portier MM, Dunia I, Paulin D, Pournin S, Babinet C. Mice lacking vimentin develop and reproduce without an obvious phenotype. Cell 1994;79:679-94.
128. Evans RM. Vimentin: the conundrum of the intermediate filament gene family. Bioessays 1998;20:79-86.
129. Lawson RN. Early Applications of Thermography. Ann N Y Acad Sci 1964;121:31-3.
130. Anselmo VJ, Zawacki BE. Effect of evaporative surface cooling on thermographic assessment of burn depth. Radiology 1977;123:331-2.
131. Black KS, Hewitt CW, Miller DM, et al. Burn depth evaluation with fluorometry: is it really definitive? J Burn Care Rehabil 1986;7:313-7.
132. Cantrell JH, Jr. Can ultrasound assist an experienced surgeon in estimating burn depth? J Trauma 1984;24:S64-70.
133. Pierce MC, Sheridan RL, Hyle Park B, Cense B, de Boer JF. Collagen denaturation can be quantified in burned human skin using polarization-sensitive optical coherence tomography. Burns 2004;30:511-7.
134. Milner SM, Bhat S, Gulati S, Gherardini G, Smith CE, Bick RJ. Observations on the microcirculation of the human burn wound using orthogonal polarization spectral imaging. Burns 2005;31:316-9.
135. Nettelblad H, Thuomas KA, Sjoberg F. Magnetic resonance imaging: a new diagnostic aid in the care of high-voltage electrical burns. Burns 1996;22:117-9.
136. Schweizer MP, Olsen JI, Shelby J, et al. NONINVASIVE ASSESSMENT OF METABOLISM IN WOUNDED SKIN BY P-31-NMR INVIVO. Journal of Trauma-Injury Infection and Critical Care 1992;33:828-34.
137. Pape SA, Skouras CA, Byrne PO. An audit of the use of laser Doppler imaging (LDI) in the assessment of burns of intermediate depth. Burns 2001;27:233-9.
138. Niazi ZB, Essex TJ, Papini R, Scott D, McLean NR, Black MJ. New laser Doppler scanner, a valuable adjunct in burn depth assessment. Burns 1993;19:485-9.
139. Reich G. Near-infrared spectroscopy and imaging: basic principles and pharmaceutical applications. Adv Drug Deliv Rev 2005;57:1109-43.

140. Jobsis FF. Noninvasive, infrared monitoring of cerebral and myocardial oxygen sufficiency and circulatory parameters. Science 1977;198:1264-7.
141. Cooper PG, Wilson GJ, Hardman DT, et al. Blood oxygen desaturation heterogeneity during muscle contraction recorded by near infrared spectroscopy. Adv Exp Med Biol 1997;428:285-92.
142. Cohn SM, Nathens AB, Moore FA, et al. Tissue oxygen saturation predicts the development of organ dysfunction during traumatic shock resuscitation. JTrauma 2007;62:44-54.
143. Crookes BA, Cohn SM, Bloch S, et al. Can near-infrared spectroscopy identify the severity of shock in trauma patients? JTrauma 2005;58:806-13.
144. Crookes BA, Cohn SM, Burton EA, Nelson J, Proctor KG. Noninvasive muscle oxygenation to guide fluid resuscitation after traumatic shock. Surgery 2004;135:662-70.
145. Kirkpatrick PJ, Smielewski P, Czosnyka M, Menon DK, Pickard JD. Near-infrared spectroscopy use in patients with head injury. JNeurosurg 1995;83:963-70.
146. Shibata S, Noriyuki T, Ohdan H, et al. Simultaneous estimation of pulmonary edema and tissue oxygenation by near-infrared spectroscopy. TransplantProc 1999;31:178-9.
147. Owen-Reece H, Smith M, Elwell CE, Goldstone JC. Near infrared spectroscopy. Br J Anaesth 1999;82:418-26.
148. Cohn SM. Near-infrared spectroscopy: potential clinical benefits in surgery. J Am Coll Surg 2007;205:322-32.
149. Reynolds KJ, Palayiwa E, Moyle JT, Sykes MK, Hahn CE. The effect of dyshemoglobins on pulse oximetry: Part I, Theoretical approach and Part II, Experimental results using an in vitro test system. J Clin Monit 1993;9:81-90.
150. Meyers RA, ed. Encylopedia of Analytical Chemistry. New Jersey: John Wiley and Sons; 2000.
151. Wahr JA, Tremper KK, Samra S, Delpy DT. Near-infrared spectroscopy: theory and applications. J Cardiothorac Vasc Anesth 1996;10:406-18.
152. Springsteen A. Standards for the measurement of diffuse reflectance - an overview of available materials and measurement laboratories. Anal Chim Acta 1999;380:379-90.
153. Rolfe P. In vivo near-infrared spectroscopy. Annu Rev Biomed Eng 2000;2:715-54.
154. Stranc MF, Sowa MG, Abdulrauf B, Mantsch HH. Assessment of tissue viability using near-infrared spectroscopy. BrJPlastSurg 1998;51:210-7.
155. Lee J, El-Abaddi N, Duke A, Cerussi AE, Brenner M, Tromberg BJ. Noninvasive in vivo monitoring of methemoglobin formation and reduction with broadband diffuse optical spectroscopy. J Appl Physiol 2006;100:615-22.
156. Prahl, Scott: Oregon Medical Laser Centre, 2007. (Accessed at http://omlc.ogi.edu/index.html.)
157. Zijlstra WG, Buursma, A., van Assendelft, O.W., ed. Absorption spectra of pig haemoglobin. Utrecht, The Netherlands: VSP BV; 2000.
158. Attas M, Hewko M, Payette J, Posthumus T, Sowa M, Mantsch H. Visualization of cutaneous hemoglobin oxygenation and skin hydration using near-infrared spectroscopic imaging. Skin ResTechnol 2001;7:238-45.
159. Jackson M, Sowa MG, Mantsch HH. Infrared spectroscopy: a new frontier in medicine. BiophysChem 1997;68:109-25.

160. Sowa MG, Payette JR, Mantsch HH. Near-infrared spectroscopic assessment of tissue hydration following surgery. JSurgRes 1999;86:62-9.
161. Wilson JR, Mancini DM, McCully K, Ferraro N, Lanoce V, Chance B. Noninvasive detection of skeletal muscle underperfusion with near-infrared spectroscopy in patients with heart failure. Circulation 1989;80:1668-74.
162. Sowa MG, Matas A, Schattka BJ, Mantsch HH. Spectroscopic assessment of cutaneous hemodynamics in the presence of high epidermal melanin concentration. ClinChimActa 2002;317:203-12.
163. Matas A, Sowa MG, Taylor V, Taylor G, Schattka BJ, Mantsch HH. Eliminating the issue of skin color in assessment of the blanch response. AdvSkin WoundCare 2001;14:180-8.
164. Dawson JB, Barker DJ, Ellis DJ, et al. A THEORETICAL AND EXPERIMENTAL-STUDY OF LIGHT-ABSORPTION AND SCATTERING BY INVIVO SKIN. Phys Med Biol 1980;25:695-709.
165. Kollias N, Baqer A. THE ABSORPTION CHARACTERISTICS OF HUMAN MELANIN IN THE VISIBLE. J Invest Dermatol 1986;87:446-.
166. Ferguson-Pell M, Hagisawa S. An empirical technique to compensate for melanin when monitoring skin microcirculation using reflectance spectrophotometry. Med Eng Phys 1995;17:104-10.
167. Cooper CE, Cope M, Quaresima V, et al. Measurement of cytochrome oxidase redox state by near infrared spectroscopy. Adv Exp Med Biol 1997;413:63-73.
168. Ward KR, Ivatury RR, Barbee RW, et al. Near infrared spectroscopy for evaluation of the trauma patient: a technology review. Resuscitation 2006;68:27-44.
169. Meyers RA, ed. Encyclopedia of Analytical Chemistry: Applications, Theory, and Instrumentation
Wiley & Sons; 2000.
170. van Veen R.L.P. SHJCM, Pifferi A., Torricelli A., Chikoidze E., Cubeddu R. Determination of visible near-IR absoprtion coefficients of mammalian fat using time- and spatially resolved diffuse reflectance and transmission spectroscopy. Journal of Biomedical Optics 2005;10:054004.
171. Goh CL. Seasonal Variations and Environmental Influences on the Skin. In: Serup J J, G.B.E, Grove, G.L. , ed. Handbook of Non-Invasive Methods and the Skin. Second ed. Boca Raton, FL: Taylor & Francis; 2006:33-6.
172. Mancini DM, Bolinger L, Li H, Kendrick K, Chance B, Wilson JR. Validation of near-infrared spectroscopy in humans. J Appl Physiol 1994;77:2740-7.
173. Davis SL, Fadel PJ, Cui J, Thomas GD, Crandall CG. Skin blood flow influences near-infrared spectroscopy-derived measurements of tissue oxygenation during heat stress. J Appl Physiol 2006;100:221-4.
174. Branchet MC, Boisnic S, Frances C, Robert AM. Skin thickness changes in normal aging skin. Gerontology 1990;36:28-35.
175. Tsukahara K, Takema Y, Moriwaki S, Fujimura T, Imokawa G. Diurnal variation affects age-related profile in skin thickness. J Cosmet Sci 2001;52:391-7.
176. Seidenari S, Pagnoni A, Di Nardo A, Giannetti A. Echographic evaluation with image analysis of normal skin: variations according to age and sex. Skin Pharmacol 1994;7:201-9.
177. Eisenbeiss C, Welzel J, Eichler W, Klotz K. Influence of body water distribution on skin thickness: measurements using high-frequency ultrasound. BrJDermatol 2001;144:947-51.

178. Lee Y, Hwang K. Skin thickness of Korean adults. Surg Radiol Anat 2002;24:183-9.
179. Nicander I, Nyren, M, Emtestam, L, Ollmar, S. Baseline electrical impedance measurements at various skin sites-related to age and sex. . Skin Res Technol 1997;3:252-8.
180. Berardesca E. EEMCO guidance for the assessment of the stratum corneum hydration: electrical methods. Skin Res Technol 1997;3:126-32.
181. Gniadecka M, Serup J, Sondergaard J. Age-related diurnal changes of dermal oedema: evaluation by high-frequency ultrasound. BrJDermatol 1994;131:849-55.
182. Eisenbeiss C, Welzel J, Schmeller W. The influence of female sex hormones on skin thickness: evaluation using 20 MHz sonography. Br J Dermatol 1998;139:462-7.
183. Kusano E, Yorifuji S, Okuno M, et al. Skin hemodynamics during change from supine to lateral position. J Neurosci Nurs 2000;32:164-8.
184. Afromowitz MA, Callis JB, Heimbach DM, DeSoto LA, Norton MK. Multispectral imaging of burn wounds: a new clinical instrument for evaluating burn depth. IEEE Trans Biomed Eng 1988;35:842-50.
185. Eisenbeiss W, Marotz J, Schrade JP. Reflection-optical multispectral imaging method for objective determination of burn depth. Burns 1999;25:697-704.
186. Sowa MG, Leonardi L, Payette JR, Fish JS, Mantsch HH. Near infrared spectroscopic assessment of hemodynamic changes in the early post-burn period. Burns 2001;27:241-9.
187. Sowa MG, Leonardi L, Payette JR, Fish JS, Mantsch HH. Near infrared spectroscopic assessment of hemodynamic changes in the early post-burn period. Burns 2001;27:241-9.
188. Attas EM, Sowa MG, Posthumus TB, Schattka BJ, Mantsch HH, Zhang SL. Near-IR spectroscopic imaging for skin hydration: the long and the short of it. Biopolymers 2002;67:96-106.
189. Cross KM, Leonardi, L, Gomez, M, Freissen JR, Levasseur, MA, Schattka, BJ, Sowa M, Fish JS. Quantification of water concentration (edema) in burn wounds using near infrared spectroscopy. J Burn Care Research 2009.
190. Cross KM, Leonardi L, Gomez M, et al. Noninvasive measurement of edema in partial thickness burn wounds. J Burn Care Res 2009;30:807-17.
191. Sullivan TP, Eaglstein WH, Davis SC, Mertz P. The pig as a model for human wound healing. Wound Repair Regen 2001;9:66-76.
192. Vardaxis NJ, Brans TA, Boon ME, Kreis RW, Marres LM. Confocal laser scanning microscopy of porcine skin: implications for human wound healing studies. J Anat 1997;190 (Pt 4):601-11.
193. Sims LD, Glastonbury, JRW, ed. Pathology of the Pig: A Diagnostic Guide; 1996.
194. Marcarian HQ, Calhoun ML. Microscopic anatomy of the integument of adult swine. Am J Vet Res 1966;27:765-72.
195. Meyer W, Schwarz R, Neurand K. The skin of domestic mammals as a model for the human skin, with special reference to the domestic pig. Curr Probl Dermatol 1978;7:39-52.
196. Cross KM, Leonardi L, Payette JR, et al. Clinical utilization of near-infrared spectroscopy devices for burn depth assessment. Wound Repair Regen 2007;15:332-40.
197. Mathers ME, Shrimankar J, Scott DJ, Charlton FG, Griffith CD, Angus B. The use of a standard proforma in breast cancer reporting. J Clin Pathol 2001;54:809-11.

198. Cross SS, Feeley KM, Angel CA. The effect of four interventions on the informational content of histopathology reports of resected colorectal carcinomas. J Clin Pathol 1998;51:481-2.
199. Reid WA, al-Nafussi AI, Rebello G, Williams AR. Effect of using templates on the information included in histopathology reports on specimens of uterine cervix taken by loop excision of the transformation zone. J Clin Pathol 1999;52:825-8.
200. Pruitt BA, Jr., Foley FD. The use of biopsies in burn patient care. Surgery 1973;73:887-97.
201. Chvapil M, Speer DP, Owen JA, Chvapil TA. Identification of the depth of burn injury by collagen stainability. Plast Reconstr Surg 1984;73:438-41.
202. Ho-Asjoe M, Chronnell CM, Frame JD, Leigh IM, Carver N. Immunohistochemical analysis of burn depth. J Burn Care Rehabil 1999;20:207-11.
203. Tyler MP, Watts AM, Perry ME, Roberts AH, McGrouther DA. Dermal cellular inflammation in burns. an insight into the function of dermal microvascular anatomy. Burns 2001;27:433-8.
204. Watts AM, Tyler MP, Perry ME, Roberts AH, McGrouther DA. Burn depth and its histological measurement. Burns 2001;27:154-60.
205. Singer AJ, Berruti L, Thode HC, Jr., McClain SA. Standardized burn model using a multiparametric histologic analysis of burn depth. Acad Emerg Med 2000;7:1-6.
206. Maitland DJ, Walsh JT, Jr. Quantitative measurements of linear birefringence during heating of native collagen. Lasers Surg Med 1997;20:310-8.
207. Flint MH, Lyons, M.F. The effect of heating and denaturation on the staining of collagen by the Masson Trichrome procedure. Histochemical Journal 1975;7:547-55.
208. Gursu KG. An experimental study for diagnosis of burn depth. Burns 1978;4:97-103.
209. Regas FC, Ehrlich HP. Elucidating the vascular response to burns with a new rat model. JTrauma 1992;32:557-63.
210. Monafo W, Bessey, P.Q. Wound Care. In: Herndon D, ed. Total Burn Care. London: Saunders; 2002:78-85.
211. Hinshaw JR. Early changes in the depth of burns. Ann N Y Acad Sci 1968;150:548-53.
212. Foley FD. Pathology of Cutaneous Burns. Surgical Clinics of North America 1970;50:1201-10.
213. Hendrix MJ, Seftor EA, Chu YW, Trevor KT, Seftor RE. Role of intermediate filaments in migration, invasion and metastasis. Cancer Metastasis Rev 1996;15:507-25.
214. Green M, Holloway GA, Heimbach DM. Laser Doppler monitoring of microcirculatory changes in acute burn wounds. J Burn Care Rehabil 1988;9:57-62.
215. Matcher SJ, Elwell CE, Cooper CE, Cope M, Delpy DT. Performance comparison of several published tissue near-infrared spectroscopy algorithms. Anal Biochem 1995;227:54-68.
216. Ngim RC. The burned ear (I): An experimental study with the rabbit model to evaluate scalding temperature, surface and histopathologic appearance, and healing responses with depth of injury. Ann Acad Med Singapore 1992;21:597-604.
217. Brans TA, Dutrieux RP, Hoekstra MJ, Kreis RW, du Pont JS. Histopathological evaluation of scalds and contact burns in the pig model. Burns 1994;20 Suppl 1:S48-51.
218. Kerrigan CL, Zelt RG, Thomson JG, Diano E. The pig as an experimental animal in plastic surgery research for the study of skin flaps, myocutaneous flaps and fasciocutaneous flaps. Lab Anim Sci 1986;36:408-12.

219. Cetinkale O, Senel O, Bulan R. The effect of antioxidant therapy on cell-mediated immunity following burn injury in an animal model. Burns 1999;25:113-8.
220. Sener G, Sehirli AO, Gedik N, Dulger GA. Rosiglitazone, a PPAR-gamma ligand, protects against burn-induced oxidative injury of remote organs. Burns 2007;33:587-93.
221. Hansbrough JF, Wikstrom T, Braide M, et al. Neutrophil activation and tissue neutrophil sequestration in a rat model of thermal injury. J Surg Res 1996;61:17-22.
222. Becker WK, Shippee RL, McManus AT, Mason AD, Jr., Pruitt BA, Jr. Kinetics of nitrogen oxide production following experimental thermal injury in rats. J Trauma 1993;34:855-62.
223. Gamelli RL, George M, Sharp-Pucci M, Dries DJ, Radisavljevic Z. Burn-induced nitric oxide release in humans. J Trauma 1995;39:869-77; discussion 77-8.
224. Sozumi T. The role of nitric oxide in vascular permeability after a thermal injury. Ann Plast Surg 1997;39:272-7.
225. Hatherill JR, Till GO, Bruner LH, Ward PA. Thermal injury, intravascular hemolysis, and toxic oxygen products. J Clin Invest 1986;78:629-36.
226. Cancio LC, Chavez S, Alvarado-Ortega M, et al. Predicting increased fluid requirements during the resuscitation of thermally injured patients. J Trauma 2004;56:404-13; discussion 13-4.
227. Cetinkale O, Konukoglu D, Senel O, Kemerli GD, Yazar S. Modulating the functions of neutrophils and lipid peroxidation by FK506 in a rat model of thermal injury. Burns 1999;25:105-12.
228. Agay D, Anderson RA, Sandre C, et al. Alterations of antioxidant trace elements (Zn, Se, Cu) and related metallo-enzymes in plasma and tissues following burn injury in rats. Burns 2005;31:366-71.
229. Horton JW. Oxygen free radicals contribute to postburn cardiac cell membrane dysfunction. J Surg Res 1996;61:97-102.
230. Till GO, Hatherill JR, Tourtellotte WW, Lutz MJ, Ward PA. Lipid peroxidation and acute lung injury after thermal trauma to skin. Evidence of a role for hydroxyl radical. Am J Pathol 1985;119:376-84.
231. Papp A, Romppanen E, Lahtinen T, Uusaro A, Harma M, Alhava E. Red blood cell and tissue water content in experimental thermal injury. Burns 2005;31:1003-6.
232. Sakurai H, Nozaki M, Traber LD, Hawkins HK, Traber DL. Microvascular changes in large flame burn wound in sheep. Burns 2002;28:3-9.
233. Leape IL. Kinetics of burn edema formation in primates. Ann Surg 1972;176:223-6.
234. Heimbach D, Engrav L, Grube B, Marvin J. Burn depth: a review. World JSurg 1992;16:10-5.
235. Heimbach D, Mann, R., Engrav, L. Evaluation of the burn wound management decisions. In: Herndon D, ed. Total Burn Care: Second Edition. 2 ed. London: Saunders; 2002:101-6.
236. Reed RK, Wiig H. Compliance of the interstitial space in rats. I. Studies on hindlimb skeletal muscle. Acta Physiol Scand 1981;113:297-305.
237. Mowlavi A, Neumeister MW, Wilhelmi BJ, Song YH, Suchy H, Russell RC. Local hypothermia during early reperfusion protects skeletal muscle from ischemia-reperfusion injury. Plast Reconstr Surg 2003;111:242-50.
238. Hedenstierna G, Lattuada M. Lymphatics and lymph in acute lung injury. Curr Opin Crit Care 2008;14:31-6.

239. Zaugg-Vesti B, Dorffler-Melly J, Spiegel M, Wen S, Franzeck UK, Bollinger A. Lymphatic capillary pressure in patients with primary lymphedema. Microvasc Res 1993;46:128-34.
240. Karges JR, Mark BE, Stikeleather SJ, Worrell TW. Concurrent validity of upper-extremity volume estimates: Comparison of calculated volume derived from girth measurements and water displacement volume. Phys Ther 2003;83:134-45.
241. Tewari N, Gill PG, Bochner MA, Kollias J. Comparison of volume displacement versus circumferential arm measurements for lymphoedema: implications for the SNAC trial. ANZ J Surg 2008;78:889-93.
242. Martinsen O, Grimnes, S, Haug, E. Measuring depth depends on frequency in electrical skin impedance measurements. Skin Res Technol 1999;5:179-81.
243. Fluhr J, Gloor M, Lazzerini, S, Kleesz P, Grieshaber, R, Berardesca, E. Comparative study of five instruments measuring stratum corneum hydration (Corneometer CM820 and CM 825, Skicon 200, Nova DPM 9003, Dermalab). Part II. In vivo. Skin Res Technol 1999;5:171-8.
244. Berardesca E. EEMCO guidance for the assessement of stratum corneum hydration: electrical methods. Skin Res Technol 1997;3:126-32.
245. Fluhr J, Gloor M, Lazzerini, S, Kleesz P, Grieshaber, R, Berardesca, E. Comparative study of five instruments measuring stratum corneum hydration (Corneometer CM 820 and CM 825, Skicon 200, Nova DPM 9003, DermaLab). Part II. In vivo. Skin Res Technol 1999;5:171-8.
246. Clarys P, Barel, AO, Gabard, B. Non-invasive electrical measurements for the evaluation of the hydration state of the skin: comparison between three conventional instruments-the Corneometer, the Skicon, and the Nova DPM. Skin Res Technol 1999;5:14-20.
247. Davis SC, Mertz PM, Bilevich ED, Cazzaniga AL, Eaglstein WH. Early debridement of second-degree burn wounds enhances the rate of epithelization--an animal model to evaluate burn wound therapies. J Burn Care Rehabil 1996;17:558-61.
248. Singer AJ, McClain S.A. A Porcine Burn Model. In: DiPietro LA, Burns, A.L., ed. Wound Healing: Methods and Protocols. Totowa, New Jersey: Humana Press Inc; 2003:107-19.
249. Field A. Repeated Measures Designs (GLM 4). In: Discovering Statisitcs using SPSS. London: Sage Publications; 2005:428-31.
250. Field A. Comparing Several Means: ANOVA (GLM 1). In: Discovering Statisitcs using SPSS. London: Sage Publications; 2005:339-41.

Appendices

Appendix A NIR Images of a Superficial Partial Thickness Burn Wound at Post-Burn Day 2 and 4.

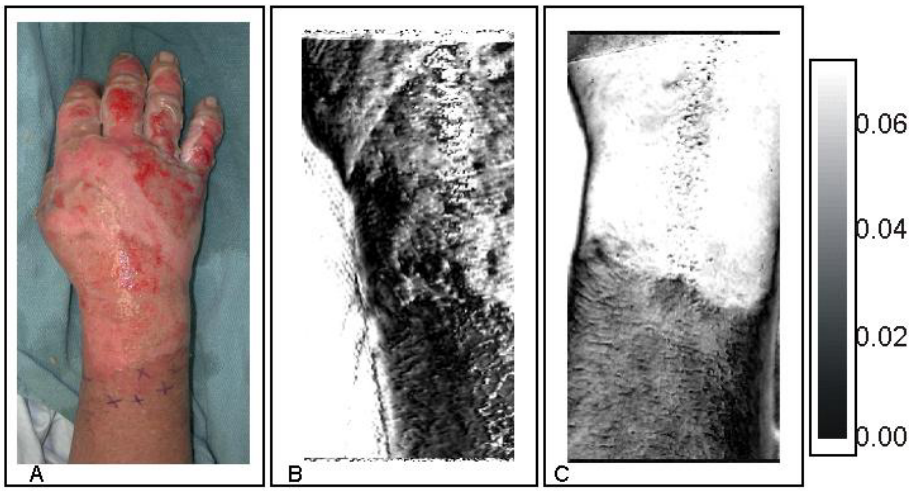

Figure A. NIR Total Hemoglobin Images of a Partial Thickness Burn Wound

A) Colour digital photograph of a superficial partial thickness hand burn. The photograph shows the burn on the hand and wrist. The proximal portion of the forearm is unburned skin and marked with Xs.

B) Post-burn day 2. There is mixed perfusion (total hemoglobin) within the burned region as represented by the combination of white and grey.

C) Post-burn day 4. There is increased perfusion within the burn wound as represented by the increase of white in the region. The burn and normal skin are easily delineated.

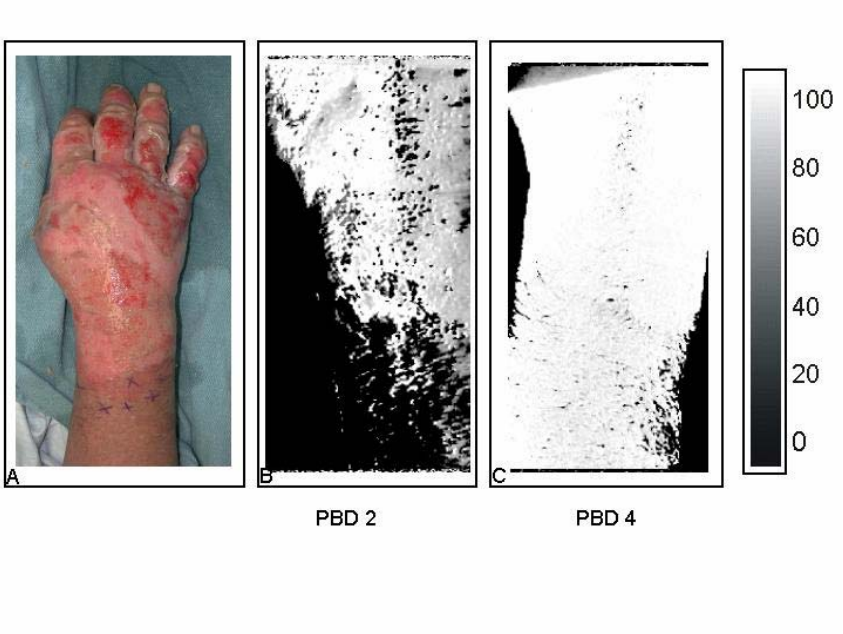

Figure B: NIR Oxygen Saturation Images of a Partial Thickness Burn

A) Colour digital photograph of a superficial partial thickness hand burn.

B) Post-burn day 2. There is increased oxygenation on day 2 post-burn as represented by the increase of white within the burn region.

C) Post-burn Day 4. There is increased oxygenation in both the burn and the normal skin at post-burn day 4 as represented by the increase of white in both areas.

Appendix B Proforma Document for Clinical Histology Database

Histopathology of Burn Wounds: Continuous Monitoring Study

Last Name: First Name: Patient Study ID: **Path Report ID:**

TBSA%: ☐ < 20% ☐ >20% PBD at OR: **Burn Visual Diagnosis:** ☐ Superficial ☐ PT-S ☐ PT-D ☐ Full

Pathology Specimen # **Biopsy Number:**

Reviewer: ☐ DG ☐ WH **Biopsy Anatomical Site:**

Epidermis & Dermis Findings

EPIDERMIS

Epidermis Present: ☐ Yes ☐ No ☐ Partial

Epidermis Necrosis: ☐ None ☐ Partial ☐ Full ☐ N/A

Comments:

DERMIS

Dermis Necrosis: ☐ Upper 1/3 ☐ Mid 1/3 ☐ Lower 1/3 ☐ N/A

Description: ☐ Fibrillar ☐ Non-Fibrillar ☐ Other

Vimentin Stain: ☐ Yes ☐ No

Comments:

Appendages Findings

HAIR FOLLICLES

Hair Follicles Present: ☐ Yes ☐ No ☐ Partial

Hair Follicles Necrosis: ☐ None ☐ Partial ☐ Full ☐ N/A

Erector Pilae Muscle:

Erector Pilae Present: ☐ Yes ☐ No ☐ N/A

Erector Pilae Necrosis: ☐ Yes ☐ No ☐ N/A

SWEAT DUCTS

Present:
☐ Yes ☐ No

Necrosis:
☐ None ☐ Partial ☐ Full ☐ N/A

Squamous Metaplasia:
☐ Mild ☐ Moderate ☐ Extensive

SEBACEOUS GLANDS

Present: ☐ Yes ☐ No

Necrosis: ☐ None ☐ Partial ☐ Full ☐ N/A

APPENDAGES COMMENTS

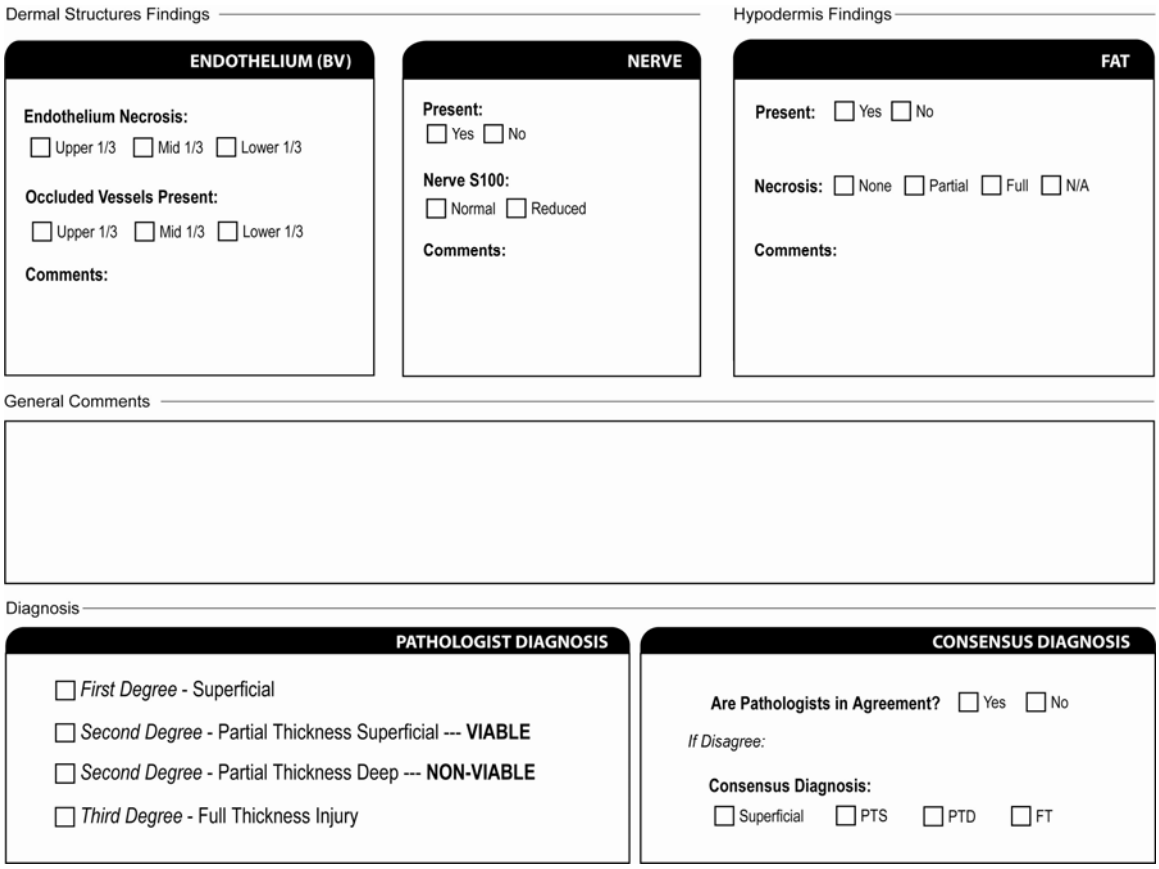

The proforma document contains the objective criteria used to determine burn depth histologically. This information is contained in the histology database.

Appendix C Histology Clinical Grading Criteria

Burn Category/ Criteria	Superficial	Superficial Partial Thickness	Deep Partial Thickness	Full Thickness
Dermal Collagen	Normal	Papillary dermal collagen necrosis (upper 1/2)	Papillary & reticular dermis necrosis (upper 1/2–lower 1/2)	Papillary & reticular dermis necrosis (upper 1/2–lower 1/2)
Dermal Blood Vessels Endothelium	Normal	Papillary dermal necrosis (upper 1/2)	Papillary & reticular dermal necrosis (upper 1/2–lower 1/2)	Papillary & reticular dermal necrosis (upper 1/2–lower 1/2)
Hair Follicle Epithelium	Normal	Normal-partial necrosis	Partial to full necrosis	Partial to full necrosis
Eccrine Gland Epithelium	Normal	Normal-partial necrosis	Partial to full necrosis	Partial to full necrosis
Subcutaneous Fat*	Normal	Normal	Normal	Any necrosis in the fat

**Septal edema may be present but is not an indicator of injury and without the loss of nuclei in the fat cell or irregularities in the shape this phenomenon was considered normal.*

Appendix D NIR Images of Water Content within a Superficial and Deep Partial Thickness Burn Wound

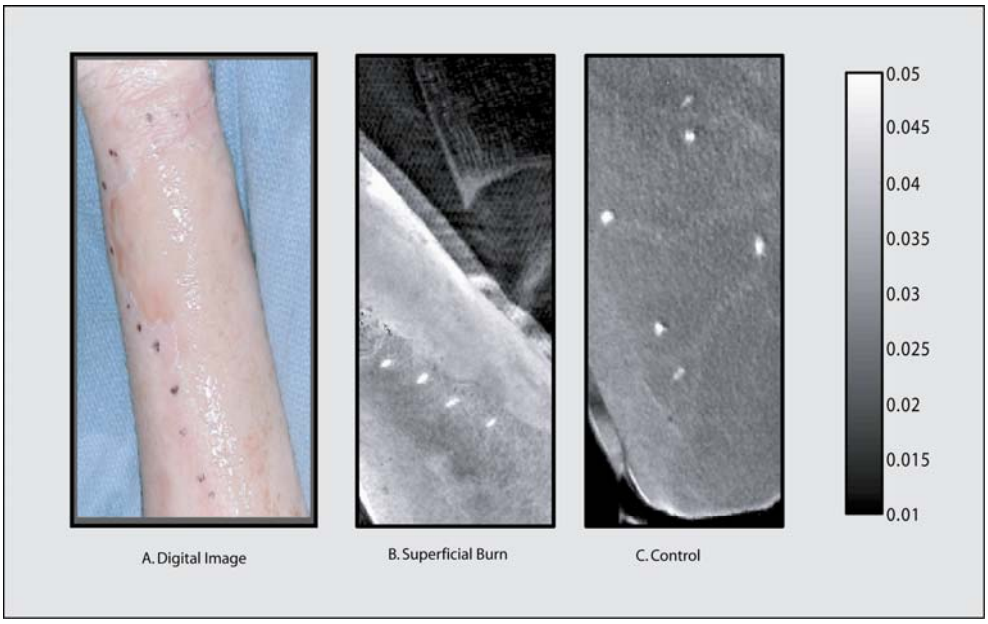

Superficial Partial Thickness Burn Wound of the Forearm

A. Digital image.

B. Burn site NIR image. Water content within the burn wound showing an increase in water compared to the control. The increase in water is represented by an increase of white within the burn. The region of interest is outlined by white dots.

C. Control site NIR image. Water content within the control site is less than the burn site as shown by the consistent grey within the region.

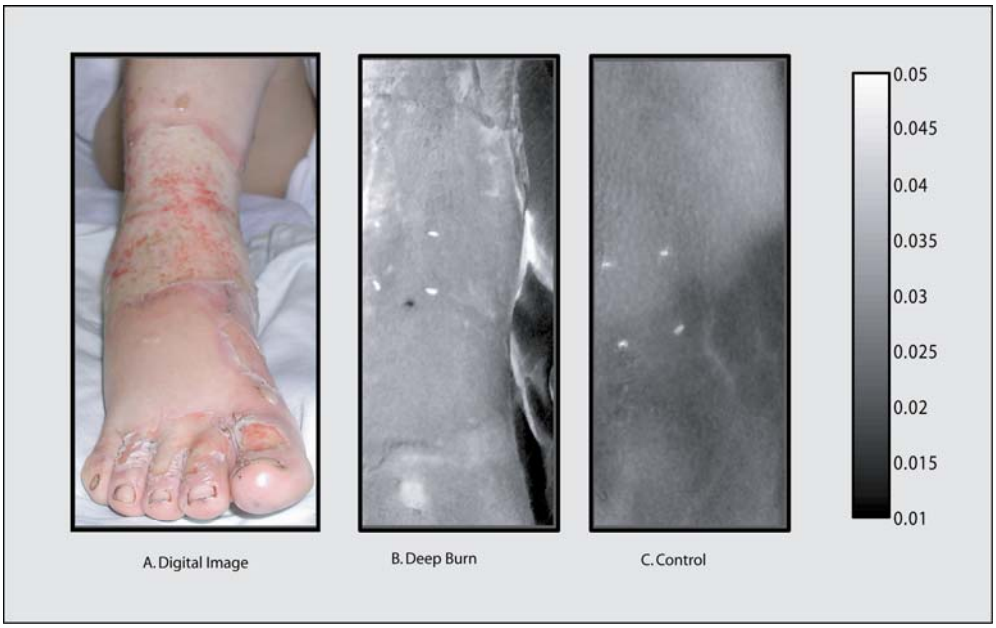

Deep Partial Thickness Burn Wound of the Leg

A. Digital image.

B. Burn site NIR image. Water content within the burn wound showing an increase in water. The increase in water is represented by an increase of white within the burn.

C. Control site NIR image. Water content within the control site is less than the burn site. However, the control site for this patient had a higher water content than for the superficial partial thickness hand burn as shown in the figure above.

Appendix E H&E of 75 s, 90 s and 120 s Burn Sites

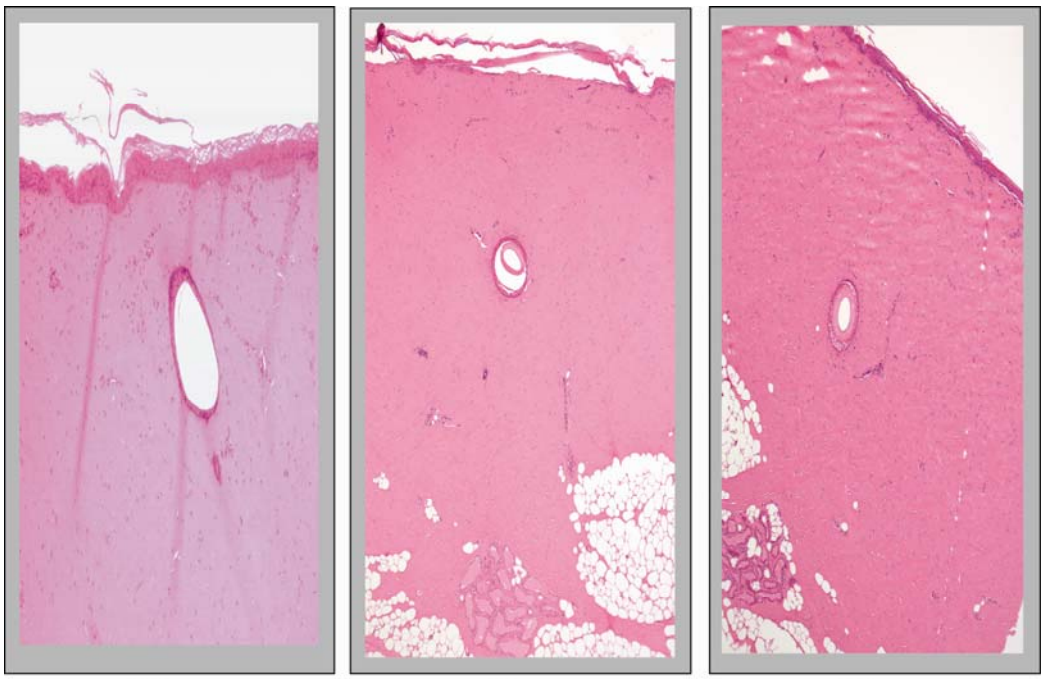

H&E (5x) of 75s, 90s, and 120s Burn Sites

The H&E of the 75 s, 90 s and 120 s burn sites showed no real differences in burn depth. All sites had complete dermal necrosis and hair follicle necrosis. Blood vessels were occluded and necrotic throughout the entire thickness of the dermis. Apocrine glands were fully necrotic in all specimens. The hallmark of a full thickness injury is fat necrosis which was present in all specimens. The only difference between these three burns was the level of fat necrosis with the 120s showing complete necrosis of the entire thickness of the subcutaneous tissue. As there were only minor morphological differences between these burn injuries, only the 90s burn injury was utilized in the data analysis as the full thickness burn injury.

Appendix F Repeated Measures

F.1 Methodology

The repeated measures ANOVA is a two-way factorial design in which the effect of time and burn depth is evaluated for methemoglobin content. In this design, the overall effect of time and degree of injury are evaluated over the whole time period. The between-subjects factor is burn site and the within-subjects factor is the variable at the particular time point. If Mauchly's test of the assumption of sphericity was violated, the degrees of freedom were corrected using the Greenhouse-Geisser estimate in order to produce a valid F-ratio. The Greenhouse-Geisser estimate varies between 1/k-1 (k, number of repeated measures) and 1. The closer ê is to 1.0 the more homogenous the variances of the differences and the closer the results are to being spherical. The Greenhouse-Geisser test is considered to be the most conservative in terms of rejecting the false null hypothesis.[249]

However, this repeated measures ANOVA does not provide specific information about how the injuries change over time. To evaluate these specific differences, multiple pairwise comparisons are made. The first set of comparisons evaluated differences that exist between each site (e.g., 3 s burn vs. 12–120 s burn) over the entire time period. The second set of comparisons evaluates the variable of time (e.g., time 1 vs. times 2–8). A Bonferroni correction was applied to the pairwise comparisons. A Bonferroni correction was used, as it is the most conservative in terms of the Type I error rate.[250] Statistical significance was achieved with a p-value less than 0.05 unless otherwise specified by the Bonferroni correction.

F.2 Oxyhemoglobin – Burn Sites

A repeated measures ANOVA was used to determine if there were changes in oxyhemoglobin over time. The within-subject effect of time was significant at source collector 2 [F (15.4, 154.2) = 6.2, p<0.0001], source collector 3 [F (14.4, 143.6) = 8.5, p<0.0001] and source collector 4 [F (16.1, 161.1) = 9.9, p<0.0001]. Differences existed between the burn sites at source collector 2 [F (4, 40) = 7.8, p<0.0001], source collector 3 [F (4, 40) = 9.1, p<0.0001] and source collector 4 [F (4, 40) = 10.8, p<0.0001].

The first pairwise analysis compared the oxyhemoglobin of each burn site to the other burn sites (3 s burn vs. 12–90 s). The 90 s burn had the lowest levels of oxyhemoglobin compared to the 3 s, 12 s, 20 s and 30 s burns as shown in Appendix Table F-1.

Mean Oxyhemoglobin Levels: Burn Sites		
Source Collector 3		
Burn Sites	**Mean ± SEM ($mMcm^{-1}$)**	**p-value 90 s vs. 3–30 s**
3 s	$9.6 \times 10^{-5} \pm 7.1 \times 10^{-6}$	0.0001
12 s	$1.0 \times 10^{-4} \pm 7.1 \times 10^{-6}$	0.0001
20 s	$8.3 \times 10^{-5} \pm 7.1 \times 10^{-6}$	0.001
30 s	$7.7 \times 10^{-5} \pm 7.1 \times 10^{-6}$	0.02
90 s	$4.7 \times 10^{-5} \pm 7.1 \times 10^{-6}$	

Appendix Table F-1: Pairwise Comparisons: 90 s Burn versus 3–30 s Burn Oxyhemoglobin Levels at Source Collector 3

The second pairwise analysis compared the values of oxyhemoglobin at each time point for the burn sites (time 1 vs. times 2–8). The pre-burn, post-burn and 1 hour post-injury did not differ from each other but were different from the 12–96-hour time points as shown in Appendix Table F-2.

Mean Oxyhemoglobin Levels: Burn Sites		
Source Collector 3		
Time	**Mean ± SEM ($mMcm^{-1}$)**	**p-value**
Pre-burn	$5.4 \times 10^{-5} \pm 1.7 \times 10^{-6}$	
Post-burn	$5.8 \times 10^{-5} \pm 3.2 \times 10^{-6}$	ns
1 hour	$5.1 \times 10^{-5} \pm 2.6 \times 10^{-6}$	ns
12 hours	$8.6 \times 10^{-5} \pm 4.2 \times 10^{-6}$	0.0001
24 hours	$9.6 \times 10^{-5} \pm 5.0 \times 10^{-6}$	0.0001
36 hours	$1.0 \times 10^{-4} \pm 5.1 \times 10^{-6}$	0.0001
48 hours	$1.0 \times 10^{-4} \pm 4.6 \times 10^{-6}$	0.0001
96 hours	$1.0 \times 10^{-4} \pm 6.0 \times 10^{-6}$	0.0001

Appendix Table F-2: Pairwise Comparisons: Pre-Burn versus Post-Burn Oxyhemoglobin Levels for Burn Sites at Source Collector 3

The oxyhemoglobin levels within the control site did not differ between the control sites or over the entire study time period. The first pairwise analysis compared the oxyhemoglobin of each control site to the other control sites (e.g., control 1 vs. controls 2–5). There were no differences in oxyhemoglobin when the controls were compared.

The second pairwise analysis compared the values of oxyhemoglobin at each time point for the control sites (time 1 vs. times 1–8). The time points post–burn differed from the pre-burn time point as shown in Appendix Table F-3.

Mean Oxyhemoglobin Levels: Control Sites		
Source Collector 3		
Time	**Mean ± SEM ($mMcm^{-1}$)**	**p-value**
Pre-burn	$6.6 \times 10^{-5} \pm 2.5 \times 10^{-6}$	
Post-burn	$6.5 \times 10^{-5} \pm 1.9 \times 10^{-6}$	ns
1 hour	$7.1 \times 10^{-5} \pm 2.3 \times 10^{-6}$	ns
12 hours	$9.6 \times 10^{-5} \pm 3.2 \times 10^{-6}$	0.0001
24 hours	$9.2 \times 10^{-5} \pm 3.9 \times 10^{-6}$	0.0001
36 hours	$1.0 \times 10^{-4} \pm 3.6 \times 10^{-6}$	0.0001
48 hours	$9.7 \times 10^{-5} \pm 3.6 \times 10^{-6}$	0.0001
96 hours	$9.7 \times 10^{-5} \pm 4.7 \times 10^{-6}$	0.0001

Appendix Table F-3: Pairwise Comparisons: Pre-Burn versus Post-Burn Oxyhemoglobin Levels for Control Sites at Source Collector 3

A repeated measures ANOVA was used to determine if there were changes in total hemoglobin over time for the burn sites at each source collector separation. The within-subject effect of time for the burn wounds' total hemoglobin content was significant at source collector 2 [$F(14.5, 144.6) = 8.0$, $p<0.0001$], source collector 3 [$F(13.3, 132.8) = 10.3$, $p<0.0001$] and source collector 4 [$F(14.8, 148.3) = 11.5$, $p<0.0001$]. Differences in total hemoglobin existed between the burn sites at source collector 2 [$F(4, 40) = 12.0$, $p<0.0001$], source collector 3 [$F(4, 40) = 12.8$, $p<0.0001$] and source collector 4 [$F(4, 40) = 14.7$, $p<0.0001$].

The first pairwise analysis compared the total hemoglobin of each burn site to the other burn sites (3 s burn vs. 12–120 s). The 90 s burn injury's total hemoglobin value was low in comparison to the other burn sites at all source collectors. The 3 s burn injury had the highest total hemoglobin over the experimental period and this differed from the 20 s, 30 s and 90 s burn injuries for source collector 2 as shown in Appendix Table F-4.

Mean Total Hemoglobin Levels: Burn Sites			
Source Collector 2			
Burn Site	**Mean ± SEM ($mMcm^{-1}$)**	**p-value 3 s vs. 12–90 s**	**p-value 90 s vs. 3–30 s**
3 s	$1.0 \times 10^{-4} \pm 5.6 \times 10^{-6}$		0.0001
12 s	$9.6 \times 10^{-5} \pm 5.6 \times 10^{-6}$	ns	0.0001
20 s	$8.1 \times 10^{-5} \pm 5.6 \times 10^{-6}$	0.05	0.02
30 s	$8.1 \times 10^{-5} \pm 5.6 \times 10^{-6}$	0.04	0.02
90 s	$5.4 \times 10^{-5} \pm 5.6 \times 10^{-6}$	0.0001	

Appendix Table F-4: Pairwise Comparisons: 90 s and 3 s Burns' Total Hemoglobin versus Other Sites at Source Collector 2

The second pairwise analysis compared the values of deoxyhemoglobin at each time point for the burn sites (time 1 vs. times 2–7). The post-burn time point's' total hemoglobin levels were higher than the pre-burn levels as shown in Appendix Table F-5.

Mean Total Hemoglobin Levels: Burn Sites		
Source Collector 3		
Time	**Mean ± SEM ($mMcm^{-1}$)**	**p-value**
Pre-burn	$6.8 \times 10^{-5} \pm 1.5 \times 10^{-6}$	
Post-burn	$9.3 \times 10^{-5} \pm 2.9 \times 10^{-6}$	0.0001
1 hour	$9.0 \times 10^{-5} \pm 2.5 \times 10^{-6}$	0.0001
12 hours	$1.3 \times 10^{-4} \pm 4.4 \times 10^{-6}$	0.0001
24 hours	$1.4 \times 10^{-4} \pm 5.3 \times 10^{-6}$	0.0001
36 hours	$1.5 \times 10^{-4} \pm 5.6 \times 10^{-6}$	0.0001
48 hours	$1.4 \times 10^{-4} \pm 5.4 \times 10^{-6}$	0.0001
96 hours	$1.2 \times 10^{-4} \pm 6.0 \times 10^{-6}$	0.0001

Appendix Table F-5: Pairwise Comparisons: Pre-Burn versus Post-Burn Total Hemoglobin Levels for Burn Sites at Source Collector 3

The total hemoglobin levels within the control site did not differ between the control sites or over the entire study time period. The first analysis compared the total hemoglobin of each control site to the other control sites (e.g., control 1 vs. controls 2–5). There were no differences in total hemoglobin when the controls were compared.

The second pairwise analysis compared the values of total hemoglobin at each time point for the control sites. The 12–96 hour post-burn time points differed from the pre-burn total hemoglobin values as shown in Appendix Table F-6.

Mean Total Hemoglobin: Control Sites		
Source Collector 3		
Time	**Mean ± SEM ($mMcm^{-1}$)**	**p-value**
Pre-burn	$7.2 \times 10^{-5} \pm 1.9 \times 10^{-6}$	
Post-burn	$7.6 \times 10^{-5} \pm 2.2 \times 10^{-6}$	ns
1 hour	$7.5 \times 10^{-5} \pm 1.7 \times 10^{-6}$	ns
12 hours	$1.0 \times 10^{-4} \pm 2.8 \times 10^{-6}$	0.0001
24 hours	$9.5 \times 10^{-5} \pm 3.3 \times 10^{-6}$	0.0001
36 hours	$1.0 \times 10^{-4} \pm 3.7 \times 10^{-6}$	0.0001
48 hours	$1.0 \times 10^{-4} \pm 3.4 \times 10^{-6}$	0.0001
96 hours	$9.8 \times 10^{-5} \pm 4.1 \times 10^{-6}$	0.0001

Appendix Table F-6: Pairwise Comparisons: Pre-Burn versus Post-Burn Total Hemoglobin Levels for Control Sites at Source Collector 3

F.3 Methemoglobin – Burn Sites

A repeated measures ANOVA was used to determine if the methemoglobin levels changed over time between the burn sites at each source collector separation. The within-subject effect of time for methemoglobin was significant for the combined source collectors [$F(15.9, 481.0) = 8.3$, $p<0.0001$]. Methemoglobin levels were different between the burn sites over the time period [$F(6, 182) = 4.9$, $p<0.0001$].

The first pairwise comparison evaluated the differences in methemoglobin content of one burn site to each of the other burn sites (e.g., 3 s vs. 12–120 s). There were no major differences in the overall methemoglobin content when the burns were compared.

The second pairwise analysis compared the values of methemoglobin within the burn sites at each time point (time 1 vs. times 2–8). This analysis showed that the levels of methemoglobin within the burns sites was lower pre-burn compared to the 12–96-hour time points as shown in Appendix Table F-7. At each time point, the overall methemoglobin content was different from the other time points ($p<0.0001$). The only exception was the comparison of methemoglobin levels at 36 hours versus 48 hours, which showed no statistically significant differences between these two time points.

Mean Methemoglobin Levels: Burn Sites		
Combined Source Collectors		
Time	**Mean ± SEM ($mMcm^{-1}$)**	**p-value**
Pre-burn	$6.0 \times 10^{-3} \pm 1.5 \times 10^{-4}$	
Post-burn	$8.0 \times 10^{-3} \pm 2.7 \times 10^{-4}$	0.0001
1 hour	$8.0 \times 10^{-3} \pm 2.7 \times 10^{-4}$	0.0001
12 hours	$1.2 \times 10^{-2} \pm 3.9 \times 10^{-4}$,	0.0001
24 hours	$1.4 \times 10^{-2} \pm 4.5 \times 10^{-4}$	0.0001
36 hours	$1.5 \times 10^{-2} \pm 4.8 \times 10^{-4}$	0.0001
48 hours	$1.6 \times 10^{-2} \pm 5.0 \times 10^{-4}$	0.0001
96 hours	$1.8 \times 10^{-2} \pm 6.9 \times 10^{-4}$	0.0001

Appendix Table F-7: Pairwise Comparison: Pre-Burn versus Post-Burn Deoxyhemoglobin Levels for Burn Sites

In summary, methemoglobin levels differed over the time period and between the burn sites. The specific paired tests showed that there was no difference between the

methemoglobin values in the burn wounds over the entire study period. However, the methemoglobin values measured post-burn were different than the baseline or pre-burn values. In addition, methemoglobin levels showed an overall increase at each time point post-burn injury.

F.4 Methemoglobin – Control Sites

A repeated measures ANOVA was used to determine if the methemoglobin levels changed over time between the control sites at each source collector separation. The control sites did change over time [$F(11.5, 372.7) = 2.5$, $p<0.004$] but the methemoglobin levels between the control sites did not vary.

The first pairwise analysis compared the methemoglobin content of each control site to the other control sites (e.g., control 1 vs. controls 2–5). There were no differences in methemoglobin content when the controls were compared.

The second pairwise analysis compared the values of methemoglobin at each time point for the control sites (time 1 vs. times 2–8). This analysis showed that the levels of methemoglobin within the control sites differed at the post-burn time points (except 1 hour) compared to the pre-burn measure as shown in Appendix Table F-8. Methemoglobin levels did not differ between 12 and 24 hours. There were also no differences between control methemoglobin values at 36 and 48 hours. All of the other time point comparisons showed statistically significant results.

Mean Methemoglobin Levels: Control Sites		
Combined Source Collectors		
Time	**Mean ± SEM ($mMcm^{-1}$)**	**p-value**
Pre-burn	$6.0 \times 10^{-3} \pm 1.6 \times 10^{-4}$	
Post-burn	$5.0 \times 10^{-3} \pm 1.7 \times 10^{-4}$	0.002
1 hour	$6.0 \times 10^{-3} \pm 1.8 \times 10^{-4}$	ns
12 hours	$8.0 \times 10^{-3} \pm 2.9 \times 10^{-4}$	0.0001
24 hours	$8.0 \times 10^{-3} \pm 3.7 \times 10^{-4}$	0.004
36 hours	$1.0 \times 10^{-2} \pm 4.3 \times 10^{-4}$	0.0001
48 hours	$1.1 \times 10^{-2} \pm 4.7 \times 10^{-4}$	0.0001
96 hours	$1.3 \times 10^{-2} \pm 4.7 \times 10^{-4}$	0.0001

Appendix Table F-8: Pairwise Comparisons: Pre-Burn versus Post-Burn Methemoglobin Levels for Control Sites

In summary, methemoglobin values differed over the time period but levels were not different between the control sites. The specific paired tests showed that the post-burn time points showed higher levels of methemoglobin in the control site compared to the pre-burn measurement.

F.5 Water Content – Burn Sites

A repeated measures ANOVA was used to determine if the water content changed over time between the burn sites at each source collector separation. The within-subject effect of time for water was significant at source collector 2 [$F(13.2, 131.5) = 3.6$, $p<0.0001$], source collector 3 [$F(13.1, 131.5) = 3.8$, $p<0.0001$] and source collector 4 [$F(12.4, 123.6) = 2.9$, $p<0.002$]. Water content differed between the burn sites over the

time period at source collector 2 [F (4, 40) = 9.3, p<0.0001], source collector 3 [F (6, 40) = 6.2, p<0.001] and source collector 4 [F (4, 40) = 4.8, p<0.003].

The first pairwise analysis evaluated the differences in water content of one burn site compared to each of the other burn sites (3 s burn vs. 12–90 s). The water values within the 3 s burn were lower than the 12 s, 20 s and 30 s injury. The 90 s burn wound differed from the 20 s and 30 s burn injury over the time period. Results for the pairwise comparisons between the burn sites over time are shown in Appendix Table F-9.

Pairwise Comparisons: Burn Sites Water Content			
Source Collector 3			
Burn Site	**Mean ± SEM ($mMcm^{-1}$)**	**3 s vs. 12–90 s p-value**	**90 s vs. 3–30 s p-value**
3 s	$6.2 \times 10^{-1} \pm 8.2 \times 10^{-3}$		ns
12 s	$6.7 \times 10^{-1} \pm 8.2 \times 10^{-3}$	0.003	ns
20 s	$6.7 \times 10^{-1} \pm 8.2 \times 10^{-3}$	0.007	0.05
30 s	$6.8 \times 10^{-1} \pm 8.2 \times 10^{-3}$	0.006	0.04
90 s	$6.3 \times 10^{-1} \pm 8.2 \times 10^{-3}$	ns	

Appendix Table F-9: Pairwise Comparisons of Water Content within the Burn Sites over the Study Time Period at Source Collector 3

The second pairwise analysis compared the mean water values at each time point for the control sites (pre-burn vs. post-burn to 96 hours). Mean water content at all the post-burn time points differed from the pre-burn time point for source collectors 2, 3 and 4. Results are shown in Appendix Table F-10 for source collector 3.

Pairwise Comparisons: Time Point Water Content		
Source Collector 3		
Time	**Mean ± SEM ($mMcm^{-1}$)**	**p-value**
Pre-burn	$5.9 \times 10^{-1} \pm 5.4 \times 10^{-3}$	
Post-burn	$6.5 \times 10^{-1} \pm 4.7 \times 10^{-3}$	0.0001
1 hour	$6.5 \times 10^{-1} \pm 5.2 \times 10^{-3}$	0.0001
12 hours	$6.9 \times 10^{-1} \pm 7.6 \times 10^{-3}$	0.0001
24 hours	$6.8 \times 10^{-1} \pm 7.5 \times 10^{-3}$	0.0001
36 hours	$6.7 \times 10^{-1} \pm 7.5 \times 10^{-3}$	0.0001
48 hours	$6.5 \times 10^{-1} \pm 9.4 \times 10^{-3}$	0.0001
96 hours	$6.4 \times 10^{-1} \pm 7.5 \times 10^{-3}$	0.0001

Appendix Table F-10: Pairwise Comparisons: Pre-Burn versus Post-Burn Water Levels for Burn Sites at Source Collector 3

F.6 Water Content – Control Sites

Water content within the control sites changed over time as measured with source collectors 2–4. The within-subject effect of time for water was significant at source collector 2 [$F(14.5, 145.2) = 1.9$, $p<0.03$], source collector 3 [$F(15.9, 158.6) = 2.0$, $p<0.02$] and source collector 4 [$F(15.8, 158.9) = 1.9$, $p<0.03$]. There were differences in the overall water content for the control sites at source collector 2 [$F(4, 40) = 10.1$, $p<0.0001$], source collector 3 [$F(4, 40) = 8.3$, $p<0.0001$] and source collector 4 [$F(4, 40) = 7.6$, $p<0.0001$].

The first pairwise analysis compared the water content of each control site to the other control sites (e.g.s control 1 vs. controls 2–5). Control site 5 had the highest water content and this level was statistically different than control sites 1–3. Control site 1 contained less water than site 4. The results are shown in Appendix Table F-11 for source collector 3. The results were similar for source collectors 2 and 4.

Pairwise Comparisons: Control Site Water Content			
Source Collector 3			
Control Site	**Mean ± SEM ($mMcm^{-1}$)**	**Control 5 vs. Control 1 p-value**	**Control 1 vs. Control 5 p-value**
1-cranial	$5.6 \times 10^{-1} \pm 9.2 \times 10^{-3}$	0.0001	
2	$5.8 \times 10^{-1} \pm 9.2 \times 10^{-3}$	0.003	ns
3	$5.9 \times 10^{-1} \pm 9.2 \times 10^{-3}$	0.03	ns
4	$6.1 \times 10^{-1} \pm 9.2 \times 10^{-3}$	ns	0.01
5-caudal	$6.3 \times 10^{-1} \pm 9.2 \times 10^{-3}$		0.001

Appendix Table F-11: Pairwise Comparisons of the Water Content within the Control Sites over the Study Time Period for Source Collector 3

The second pairwise analysis compared the values of water at each time point for the control sites (time 1 vs. times 2–8). The pre-burn water content was higher than the 12–96-hour time points at source collectors 2–4. Results are shown in Appendix Table F-12 for source collector 3.

Pairwise Comparisons: Time Point Water Content		
Source Collector 3		
Time	**Mean ± SEM ($mMcm^{-1}$)**	**p-value**
Pre-burn	$6.1 \times 10^{-1} \pm 5.1 \times 10^{-3}$	
Post-burn	$6.2 \times 10^{-1} \pm 4.3 \times 10^{-3}$	ns
1 hour	$6.1 \times 10^{-1} \pm 4.3 \times 10^{-3}$	ns
12 hours	$5.8 \times 10^{-1} \pm 7.1 \times 10^{-3}$	0.0001
24 hours	$5.8 \times 10^{-1} \pm 5.8 \times 10^{-3}$	0.0001
36 hours	$5.9 \times 10^{-1} \pm 5.0 \times 10^{-3}$	0.003
48 hours	$5.9 \times 10^{-1} \pm 5.5 \times 10^{-3}$	0.02
96 hours	$5.9 \times 10^{-1} \pm 5.4 \times 10^{-3}$	0.0001

Appendix Table F-12: Pairwise Comparisons: Pre-Burn versus Post-Burn Water Levels for Control Sites at Source Collector 3.

Appendix G Raw Values

G.1 Oxyhemoglobin – Burn Sites

Oxyhemoglobin levels between the burn sites differed for the majority of time points and source collectors separations as shown in Appendix Table G-1.

Immediately post-burn, only the 3 s (ohb3s) burn injury showed an increase in oxyhemoglobin levels at all the source collector separations. The 12 s (ohb12s) burn's oxyhemoglobin levels declined in source collector 2 but showed an increase in source collectors 3 and 4. The 20–90 s burn injuries all showed a decrease in oxyhemoglobin levels up to 1 hour post-injury as shown in Appendix Figure G-1.

Oxyhemoglobin: ANOVA Results for Burn Sites										
Time (hours)	**df**	**SC**	**F**	**p-value**	**SC**	**F**	**p-value**	**SC**	**F**	**p-value**
Post	**4, 75**	2	7.3	0.0001	3	7.1	0.0001	4	9.6	0.0001
1 h	**4, 75**	2	14.1	0.0001	3	17.5	0.0001	4	18.8	0.0001
12 h	**4, 65**	2	18.7	0.0001	3	19.6	0.0001	4	20.9	0.0001
24 h	**4, 65**	2	17.7	0.0001	3	17.0	0.0001	4	18.5	0.0001
36 h	**4, 60**	2	16.7	0.0001	3	20.8	0.0001	4	20.6	0.0001
48 h	**4, 55**	2	9.3	0.0001	3	14.3	0.0001	4	16.4	0.0001
96 h	**4, 45**	2	4.7	0.003	3	6.9	0.0001	4	11.3	0.0001

df = degrees of freedom
SC = source collector
F = F-statistic

Appendix Table G-1: Summary of ANOVA Results: Comparison of Burn Sites' Oxyhemoglobin at All Time Points and Source Collectors

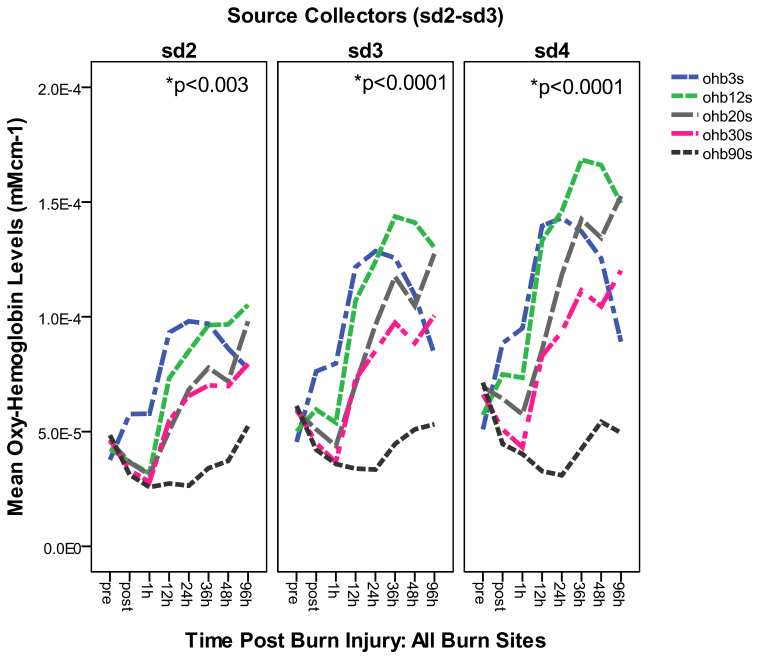

Appendix Figure G-1: Mean Oxyhemoglobin Levels within the Burn Sites over Time

At 12 hours, the oxyhemoglobin content within the 20 s (ohb20s) and 30 s (ohb30s) burns increases, unlike the 90 s (ohb90s) injury's oxyhemoglobin levels, which are lower than pre-burn levels. The 3 s burn's oxyhemoglobin levels peak at 12 hours as shown in Appendix Figure G-1.

At 36 hours, the 12 s, 20 s and 30 s burns show peak oxyhemoglobin levels. At this time point, the 12 s burn injury has the highest oxyhemoglobin levels compared to all the other burn injuries. The 3 s burn injury's oxyhemoglobin levels start to decline towards baseline at this time point.

At 48 hours, the oxyhemoglobin levels within the 12 s burn start to decline as shown in source collectors 3 and 4 but continue to increase in source collector 2. The 20–90 s burn injury's oxyhemoglobin levels continue to increase up to 96 hours post-burn. At 96 hours post-burn, the oxyhemoglobin levels remain high for the 3–30 s burn injury.

G.2 Oxyhemoglobin – Control Sites

There were no differences in oxyhemoglobin content at any of the time points or source collector separations. The only exception was at source collector 2 at the 1-hour time point. Control site 1 had less oxyhemoglobin than the other control sites [$F(4, 75) = 5.5$, $p<0.001$].

G.3 Total Hemoglobin – Burn Sites

Total hemoglobin levels differed between the burn sites at all of the time points and source collector separations as shown in Appendix Table G-2 and in Appendix Figure G-2.

Immediately post-burn, the 3 s (thb3s) and 12 s (thb12s) burn injuries show the highest levels of total hemoglobin of all the burn sites. The 20 s (thb20s) and 30 s (thb30s) burn injuries' total hemoglobin levels are slightly elevated above baseline. The 90 s (thb90s) burn has the lowest levels of total hemoglobin.

Total Hemoglobin: ANOVA Results for Burn Sites										
Time (hours)	**df**	**SC**	**F**	**p-value**	**SC**	**F**	**p-value**	**SC**	**F**	**p-value**
Post	**4, 75**	2	26.9	0.0001	3	25.0	0.0001	4	32	0.0001
1 h	**4, 75**	2	27.3	0.0001	3	39.4	0.0001	4	38.0	0.0001
12 h	**4, 65**	2	23.7	0.0001	3	22.2	0.0001	4	23.0	0.0001
24 h	**4, 65**	2	22.9	0.0001	3	22.3	0.0001	4	23.7	0.0001
36 h	**4, 60**	2	19.2	0.0001	3	22.8	0.0001	4	22.7	0.0001
48 h	**4, 55**	2	10.5	0.0001	3	14.6	0.0001	4	16.1	0.0001
96 h	**4, 45**	2	6.7	0.0001	3	10.4	0.0001	4	15.9	0.0001

df = degrees of freedom
SC = source collector
F = F-statistic

Appendix Table G-2: Summary of ANOVA Results: Comparison of Burn Sites Total Hemoglobin at All Time Points and Source Collectors

Total hemoglobin levels continue to rise in the 3–30 s burn injuries. The 3 s and 12 s burns show peak levels of total hemoglobin at 12 hours and 36 hours respectively. The 30 s burn's total hemoglobin peaks at 36 hours and levels remain high for the duration of the study period. The 20 s burn's peak total hemoglobin levels occur at 96 hours post-burn and are higher than the 30 s burn injury over the 24–96 hour time period. The 90 s burn injury's total hemoglobin levels are elevated slightly above baseline but remain low for the duration of the study.

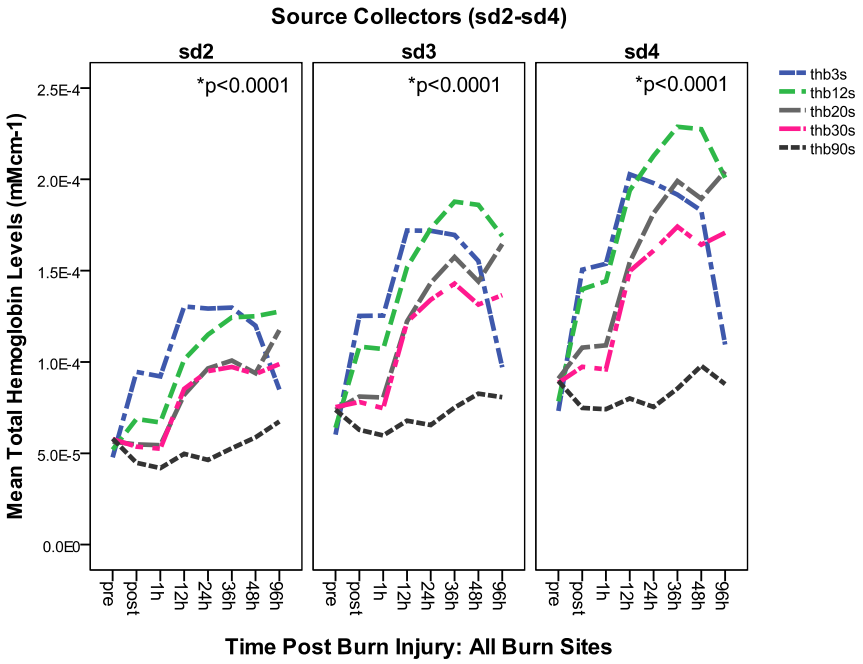

Appendix Figure G-2: Mean Total Hemoglobin Levels within the Burn Sites over Time

G.4 Total Hemoglobin – Control Sites

There were no differences in total hemoglobin between the control sites at the majority of time points and source collector separations. The only exception was at the 1-hour time point as total hemoglobin levels were low in control site 1 compared to the other control sites at source collector 2 [$F(4, 75) = 5.3$, $p<0.001$].

G.5 Methemoglobin – Burn Sites

The results obtained for methemoglobin using a combination of the source collectors showed differences between the burn wounds at all time points post-burn injury as shown in Appendix Table G-3. The changes in the raw methemoglobin content over time for the burn wounds are shown in Appendix Figure G-3.

Methemoglobin: ANOVA Results for Burn Sites				
Time	**Source Collector**	**df**	**F**	**p-value**
Pre-burn	2–4	6, 329	0.7	ns
Post-burn	2–4	6, 329	3.2	0.004
1 hour	2–4	6, 329	2.5	0.02
12 hours	2–4	6, 287	10.6	0.0001
24 hours	2–4	6, 287	12.7	0.0001
36 hours	2–4	6, 266	9.3	0.0001
48 hours	2–4	6, 245	4.6	0.0001
96 hours	2–4	6, 203	8.7	0.0001

df = degrees of freedom
SC = source collector
F = F-statistic

Appendix Table G-3: Summary of ANOVA Results: Comparison of Burn Sites Methemoglobin at All Time Points and Source Collectors

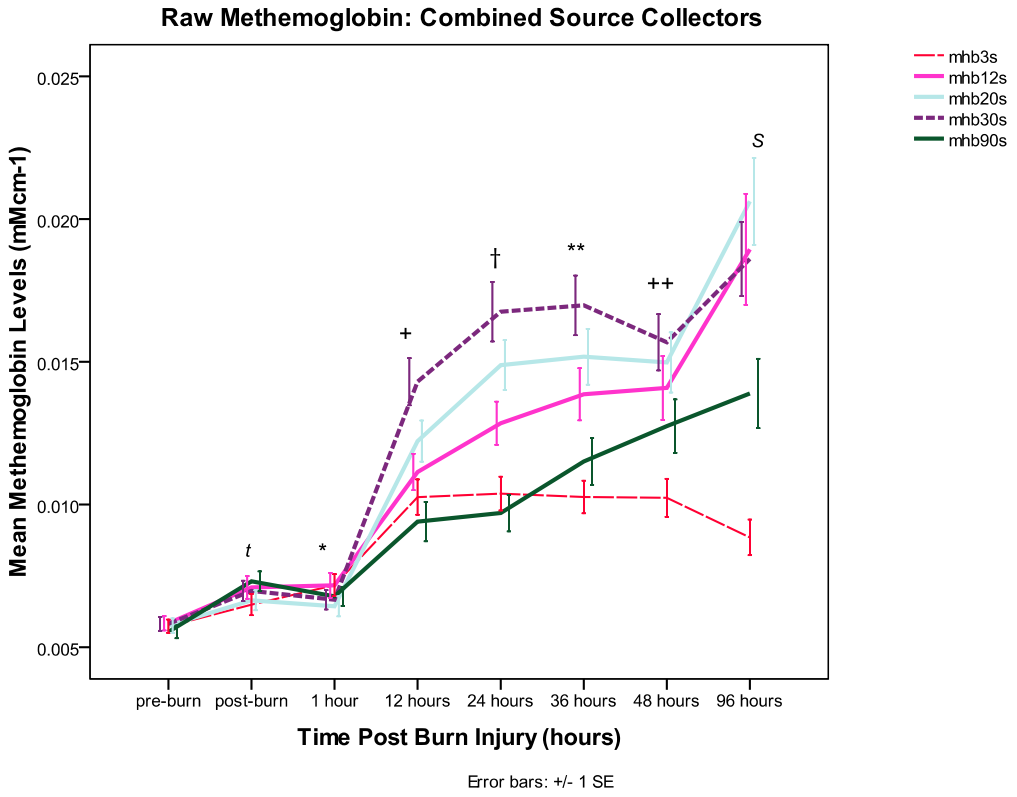

Appendix Figure G-3: Mean Methemoglobin Levels in Burn Sites over Time (^{t} p< 0.004; *p<0.02; $^{+}$, †, **, $^{++}$, ^{S}, p<0.0001)

All of the burn sites experienced a large increase in methemoglobin content at 12 hours post-burn injury. The highest methemoglobin levels were found in the 30 s burn wound (mhb30s). The 12 s (mhb12s) and 20 s (mhb20s) burns also had high methemoglobin levels while the 3 s (mhb3s) and 90 s (mhb90s) burn injuries had the lowest values.

The 30 s burn wound's methemoglobin values are the highest for the first 48 hours post-injury but are surpassed by the 12 s and 20 s burns at 96 hours. The 3 s burn's methemoglobin values experience an increase at 12 hours post-burn but levels plateau within the 122–448 hour time period. At 96 hours, the 3 s burn injury starts to decline

towards baseline. The deep injuries (90 s) show a gradual increase in methemoglobin values over the time period but never reach the same levels as the more superficial burns.

G.6 Methemoglobin – Control Sites

The control site values were significantly different at 12 hours [F (4, 205) = 3.5, p<0.009], 24 hours [F (4, 205) = 3.3, p<0.01] and 36 hours [F (4, 190) = 2.8, p<0.03] post-burn as shown in Appendix Figure G-4. Control sites 2 and 3 showed the highest levels of methemoglobin and were located between the indeterminate injuries (burn sites 12–30 s). The indeterminate burn injuries showed the highest levels of methemoglobin throughout the majority of the study.

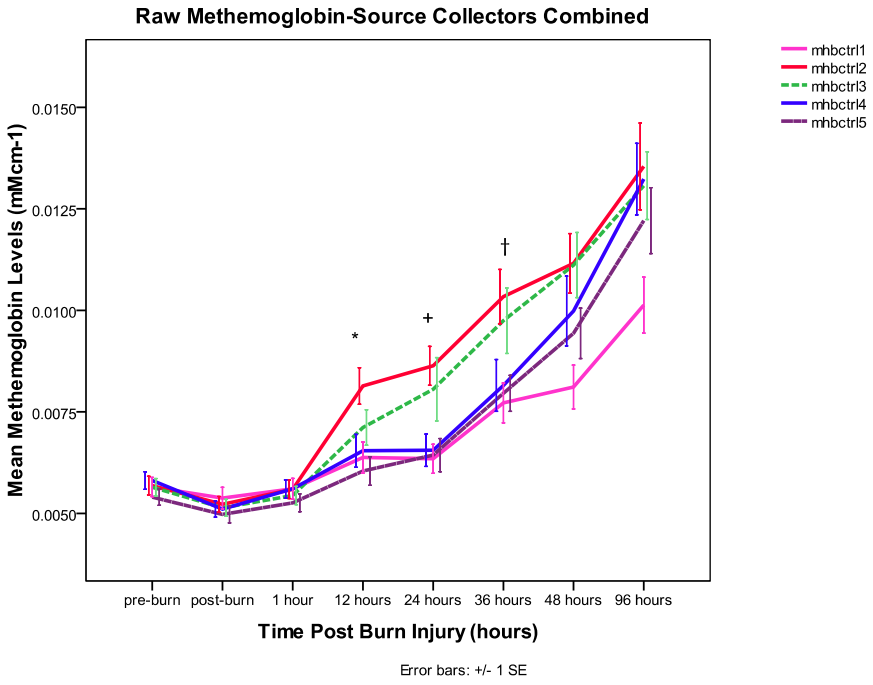

Appendix Figure G-4: Mean Methemoglobin Levels in Control Sites over Time (*p<0.009, $^{+}$p<0.01, †p<0.03)

G.7 Water – Burn Sites

The mean water content within the burn sites over time is shown in Appendix Figure G-5. p-values embedded in the figure indicate that differences existed between the burn sites at each time point for source collectors 2–4. There were no differences between the sites at 96 hours post-burn for source collectors 3 and 4. Appendix Table G-4 shows the results from the ANOVA for each time point and source collector separation.

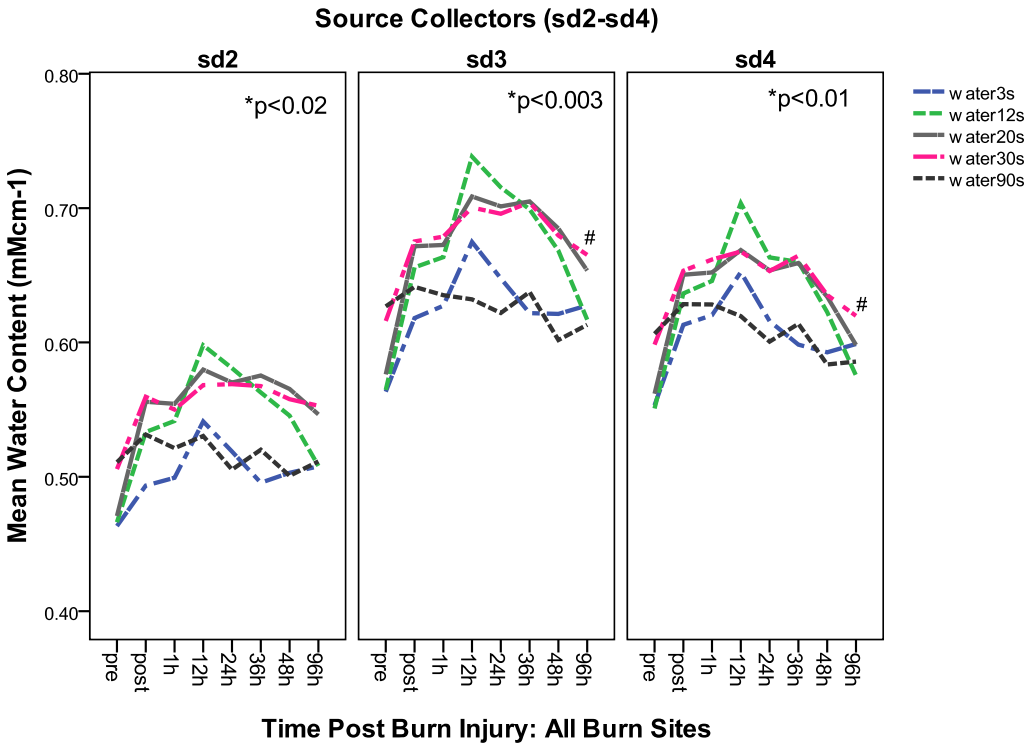

non-significant differences between burn sites at 96h for sd3 & 4

Appendix Figure G-5: Mean Water Levels within the Burn Sites over Time

The 3 s (water3s) and 12 s (water12s) burn injuries experience an increase in water content immediately after the burn injury. The water content within the wounds at the

post-burn and 1-hour time point is lower than the 20 s (water20s) and 30 s (water30s) burn wounds. At 12 hours post-burn, the water content in the 3 s and 12 s burns peaks before decreasing towards baseline. Only the 12 s burn injury's peak actually surpasses the 20 and 30 s burn injuryies' water content levels. The 3 s burn injury's water content remains low for the duration of the study in comparison to the 12–30 s burn wounds. Water content for the 3 s burn injury at the 36, 48 and 96-hour time point is similar to the 90 s (water90s) burn wound. The 3 s and 12 s burns' mean water content results are shown in Appendix Figure G-6.

Water Content: ANOVA Results for Burn Sites										
Time	**Df**	**SC**	**F**	**p-value**	**SC**	**F**	**p-value**	**SC**	**F**	**p-value**
Post-burn	**4, 75**	2	12.0	0.0001	3	6.4	0.0001	4	3.3	0.02
1 hour	**4, 75**	2	8.9	0.0001	3	5.5	0.001	4	2.5	0.01
12 hours	**4, 65**	2	6.9	0.0001	3	9.4	0.0001	4	10.6	0.0001
24 hours	**4, 65**	2	10.7	0.0001	3	9.3	0.0001	4	12.7	0.001
36 hours	**4, 60**	2	8.6	0.0001	3	7.3	0.0001	4	9.3	0.001
48 hours	**4, 55**	2	3.7	0.009	3	4.6	0.003	4	4.6	0.009
96 hours	**4, 45**	2	3.2	0.02	3	2.0	ns	4	8.7	ns

df = degrees of freedom
SC = source collector
F = F-statistic

Appendix Table G-4: Summary of ANOVA Results: Comparison of Burn Sites' Water Content at All Time Points and Source Collectors

The 20 s and 30 s burn wounds experience the largest increase in water content at the post-burn and 1-hour time point. Water levels peak at 12 hours post-burn but do not surpass the water content of the 12 s burn wound. Water levels begin to decline after 36 hours but do not return to pre-burn levels at 96 hours as shown in Appendix Figure G-7.

The 90 s burn injury initially experiences a small increase in water content. The 90 s burn injury water content is the lowest of all the burn injuries after the 12-hour time point. At 96 hours post-burn, the water content did not differ between the burn sites in source collectors 3 and 4 as shown in Appendix Figure G-7.

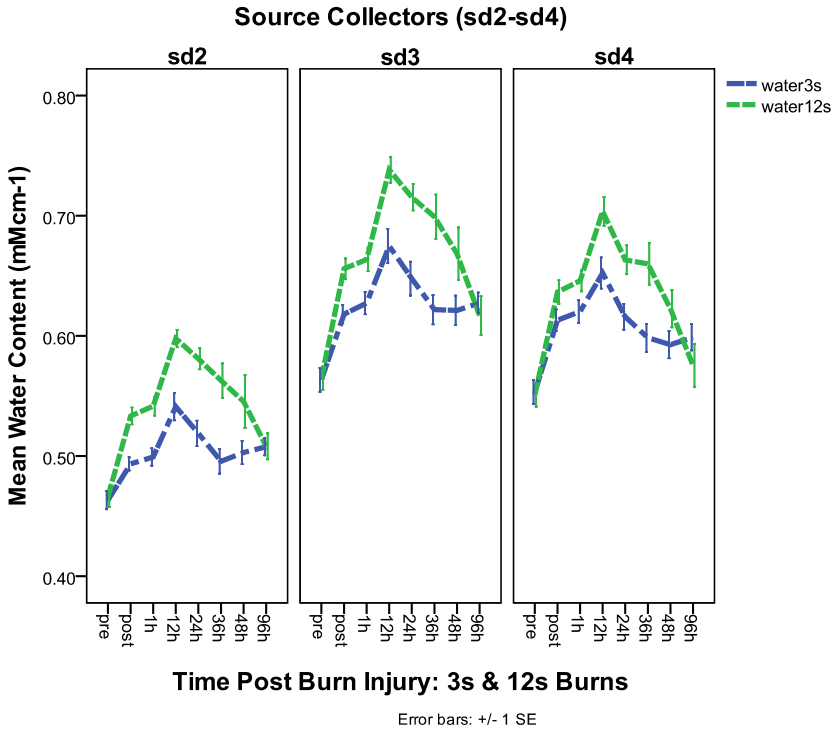

Appendix Figure G-6: Mean Water Levels within the 3 s and 12 s Burn Sites over Time

Appendix Figure G-7: Mean Water Levels within the 20 s-90 s Burn Sites over Time

G.8 Water – Control Sites

Water content within the control sites increased from control site 1 (cranial site) to control site 5 (caudal site) as shown in Appendix Figure G-8. This finding was statistically significant for the majority of time points and source collectors as shown in Appendix Table G-5. However, at source collector 2 there were no differences between the control sites at 1 hour and 48 hours post-injury. Source collector 3 did not show statistical differences between the sites at 1 hour and 12 hours post-injury. There were no differences in water content post-burn, 1 hour and 12 hours post-burn at source collector 4.

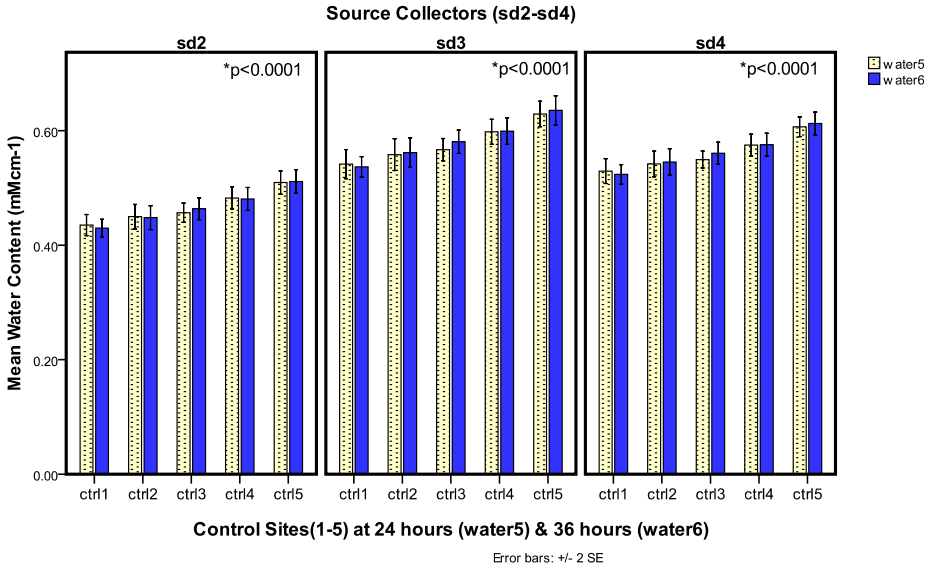

Appendix Figure G-8: Water Levels within the Control Sites at 24 and 36 Hours Post-Burn

Water Content: ANOVA Results for Control Sites										
Time	**df**	**SC**	**F**	**p-value**	**SC**	**F**	**p-value**	**SC**	**F**	**p-value**
Pre-burn	**4, 79**	2	3.1	0.02	3	4.8	0.002	4	2.7	0.04
Post-burn	**4, 79**	2	2.6	0.04	3	3.4	0.01	4	2.4	ns
1 hours	**4, 79**	2	1.8	ns	3	1.8	ns	4	1.2	ns
12 hours	**4, 65**	2	3.0	0.02	3	2.5	ns	4	2.3	ns
24 hours	**4, 65**	2	8.0	0.0001	3	7.7	0.0001	4	9.1	0.0001
36 hours	**4, 60**	2	10.5	0.0001	3	11	0.0001	4	11.3	0.0001
48 hours	**4, 55**	2	2.3	ns	3	2.7	0.04	4	3.1	0.02
96 hours	**4, 45**	2	3.1	0.02	3	4.2	0.006	4	4.1	0.007

df = degrees of freedom
SC = source collector
F = F-statistic

Appendix Table G-5: Summary of ANOVA Results: Comparison of Control Sites Water Content at All Time Points and Source Collectors

Appendix H Change from Control Values

H.1 NIR Data – ANOVA

This section shows the variable data from the burn site as a change from the control measure (e.g., Burn-control/ control). These results are presented as a magnitude change from the control and data for source collectors 2–4 are shown separately.

H.2 Oxyhemoglobin

Oxyhemoglobin levels differed between the burn sites at all of the time points and source collector separations as shown in Appendix Table H-1 and Appendix Figure H-1.

Oxyhemoglobin Change from Control: ANOVA Results for Burn Sites										
Time (hours)	**df**	**SC**	**F**	**p-value**	**SC**	**F**	**p-value**	**SC**	**F**	**p-value**
Post	**4, 75**	2	5.9	0.0001	3	7.6	0.0001	4	8.9	0.0001
1 h	**4, 75**	2	20.2	0.0001	3	26.0	0.0001	4	26.0	0.0001
12 h	**4, 65**	2	14.4	0.0001	3	23.0	0.0001	4	18.8	0.0001
24 h	**4, 65**	2	26.3	0.0001	3	16.7	0.0001	4	28.7	0.0001
36 h	**4, 60**	2	18.0	0.0001	3	22	0.0001	4	21.2	0.0001
48 h	**4, 55**	2	12.0	0.0001	3	12.4	0.0001	4	14.6	0.0001
96 h	**4, 45**	2	4.4	0.005	3	6.6	0.0001	4	8.5	0.0001

df = degrees of freedom
SC = source collector
F = F-statistic

Appendix Table H-1: Summary of ANOVA Results: Comparison of Burn Sites Oxyhemoglobin as a Change from Control

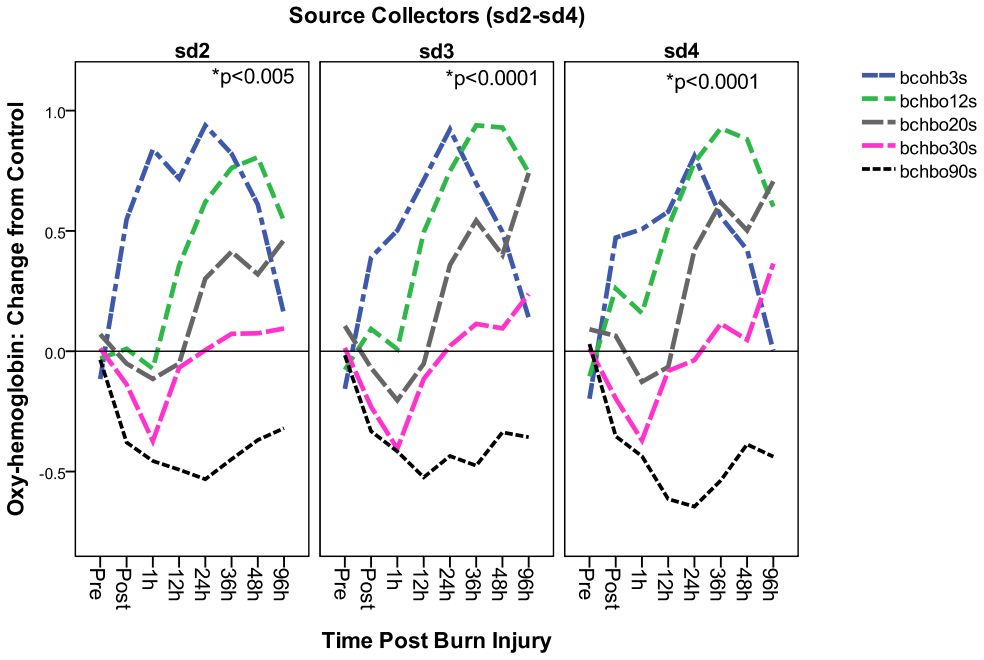

Appendix Figure H-1: Burn Site Oxyhemoglobin Content as a Change from Control Values from the Post-Burn to 96-Hour Time Point

The 3 s burn injury's (bcohb3s) oxyhemoglobin levels experience a 39–55% increase above control values immediately after injury. Oxyhemoglobin values remain high until 12 hours post-burn and then the 3 s values decline towards baseline. At 96 hours post-burn, the 3 s burn injury has reached control levels for source collector 4.

The 12 s burn (bchbo12s) experiences an increase in oxyhemoglobin at source collectors 3 (9%) and 4 (26%) but remains around baseline at source collector 2 immediately after burn injury. Oxyhemoglobin levels increase and peak at 48 hours post-

burn with an 88–101% increase above control values. After 48 hours, the oxyhemoglobin levels decline towards baseline.

The 20 s (bchbo20s) and 30 s (bchbo30s) burn injuries' oxyhemoglobin levels remain below baseline until 12 hours post-burn. At 24 hours post-burn, the 20 s burn shows a 30%–42% increase in oxyhemoglobin. Levels continue to increase up to 96 hours post-burn, when the 20 s burn injury has a 46–74% increase above controls. The 30 s burn increases to control values at 24 hours post-burn at source collectors 2 and 3. At 24 hours post-burn, source collector still shows a 4% decrease below control values. At 36 hours, the oxyhemoglobin levels increase above control values. The oxyhemoglobin levels in the 30 s burn only reach a high of 36% in source collector 4 at 96 hours post-burn.

The 90 s (bchbo90s) burn injury's oxyhemoglobin levels remain below control values for the 90 s burn injury for the study duration.

H.3 Total Hemoglobin

Total hemoglobin levels differed between the burn sites at all of the time points and source collector separations as shown in Appendix Table H-2 and Appendix Figure H-2.

Total Hemoglobin Change from Control: ANOVA Results for Burn Sites										
Time (hours)	**df**	**SC**	**F**	**p-value**	**SC**	**F**	**p-value**	**SC**	**F**	**p-value**
Post	**4, 75**	2	14.5	0.0001	3	18.1	0.0001	4	18.0	0.0001
1 h	**4, 75**	2	33.2	0.0001	3	42.5	0.0001	4	42.2	0.0001
12 h	**4, 65**	2	23.1	0.0001	3	26.2	0.0001	4	22.7	0.0001
24 h	**4, 65**	2	34.5	0.0001	3	22.7	0.0001	4	40.4	0.0001
36 h	**4, 60**	2	21.5	0.0001	3	22.8	0.0001	4	20.6	0.0001
48 h	**4, 55**	2	12.3	0.0001	3	10.9	0.0001	4	12.3	0.0001
96 h	**4, 45**	2	5.1	0.005	3	8.5	0.0001	4	10.0	0.0001

df = degrees of freedom
SC = source collector
F = F-statistic

Appendix Table H-2: Summary of ANOVA Results: Comparison of Burn Sites Total Hemoglobin as a Change from Control for All Time Points

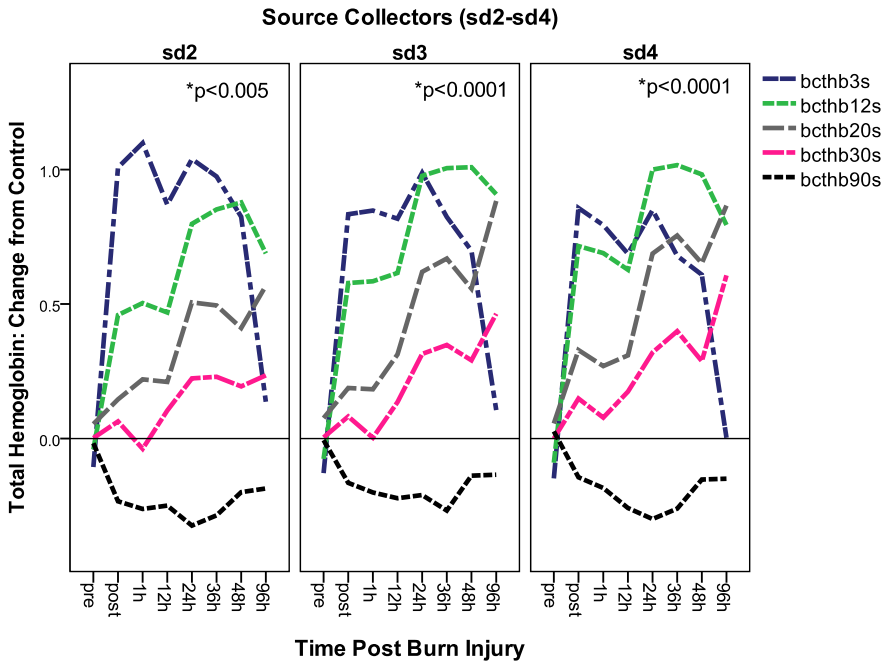

Appendix Figure H-2: Burn Sites' Total Hemoglobin Content as a Change from Control Values over Time

The 3 s burn (bcthb3s) experiences a large increase (83–100%) post-burn injury compared to control values. Values remain high up to 24 hours post-burn before declining back to control levels at 96 hours post-burn.

The 12 s burn injury (bcthb12s) experiences an increase (50–66%) in total hemoglobin post-burn injury but does not achieve the same values as the 3 s burn until 24–36 hours post-burn injury (80–100%). The 12 s burn surpasses the 3 s burn injury's total hemoglobin values at source collectors 3 and 4 at 48 and 96 hours post-burn. Total hemoglobin values start to decline at 48 hours post-injury but do not reach control levels at the end of the study time period.

The 20 s (23–33%) and 30 s (11–19%) burn wounds also experience an increase in total hemoglobin compared to control at 12 hours post-burn. Levels continue to rise and the 20 s (bcthb20s) burn injury's total hemoglobin values surpass the 3 s burn wound and attain the 12 s burn injury's values at 96 hours. The 30 s burn injury's (bcthb30s) increase above control values does not achieve the same magnitude as the 20 s burn injury.

The 90 s burn injury's (bcthb90s) total hemoglobin values do not reach control levels over the study period.

H.4 Methemoglobin

There were no differences between the burn sites for the majority of the time points and source collector separations when the control values were taken into account. The only statistically significant findings were for source collector 2 at 1 hour post-injury and source collector 3 at 36 hours post-burn injury. This data is not presented in the thesis because the overall findings are insignificant. The high values of methemoglobin within the control sites affected this measurement, as the differences between the burn sites were relatively small.

H.5 Water Content

The burn sites could be differentiated using the control as the baseline measure as shown in Appendix Figure H-3. Differences between the sites were found at all source collectors and time points. The only exception was the 96-hour time point for source collector 4 as shown in Appendix Table H-3.

Immediately post-burn, the 3, 12, 20, 30 and 90 s burn wounds show an increase above control values. Water values continue to increase post-burn injury with peak values at 12 hours for the 3 s burn. Water levels remain high in the 3 s burn at 24 hours before starting to decline towards control values. The 12 s injury's peak water levels occur between 12–36 hour post-burn. A rapid decline towards control values occurs at 48 hours. The 3 s and 12 s burn wounds do not reach control values by the 96-hour time

point. The results for the 3 s and 12 s burn wounds over time are shown in Appendix Figure H-4.

The 20 s and 30 s burn wounds show an initial increase in water content compared to control values. The peak water content occurs at 36 hours post-burn before there is a decline towards control values. The 90 s injury's water content is elevated above baseline but does not reach the same water levels as the other sites. The results for the 20, 30 and 90 s burn wounds over time are shown in Appendix Figure H-5.

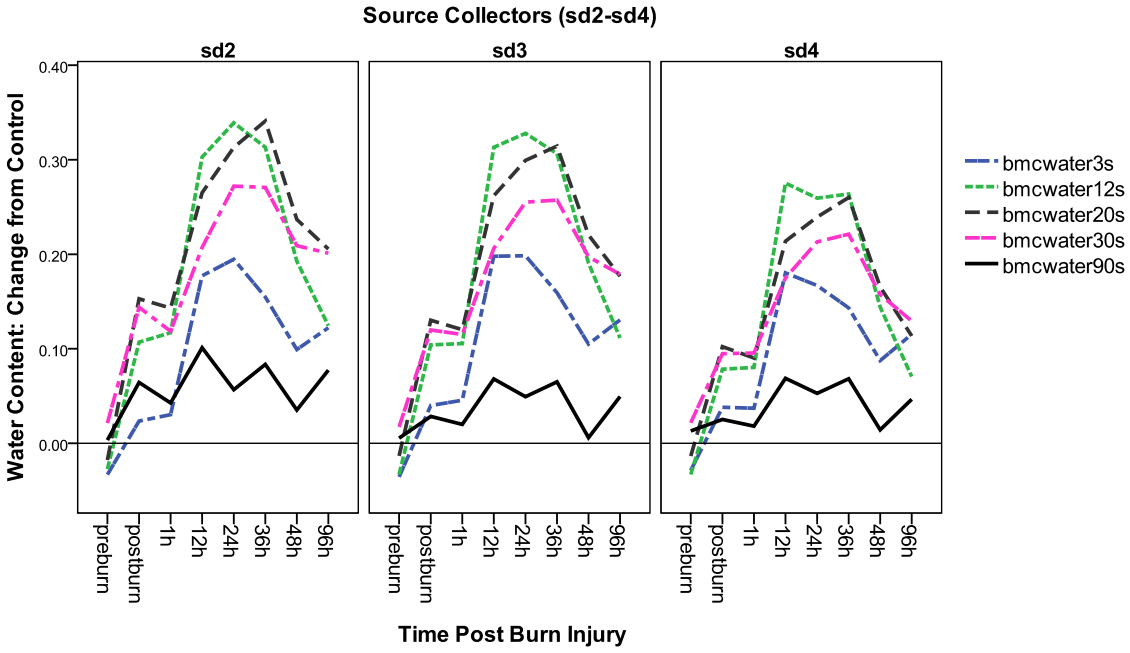

Appendix Figure H-3: Water Levels as a Change from Control within the Burn Sites over Time

Water Change from Control: ANOVA Results for Burn Sites										
Time	**df**	**SC**	**F**	**p-value**	**SC**	**F**	**p-value**	**SC**	**F**	**p-value**
Post-burn	**4, 75**	2	15.5	0.0001	3	11.6	0.0001	4	6.3	0.0001
1 hour	**4, 75**	2	12.2	0.0001	3	14.3	0.0001	4	9.3	0.0001
12 hours	**4, 65**	2	4.7	0.002	3	6.9	0.0001	4	6.3	0.0001
24 hours	**4, 65**	2	19.6	0.0001	3	16.3	0.0001	4	11.5	0.0001
36 hours	**4, 60**	2	17.4	0.0001	3	17.0	0.0001	4	12.0	0.0001
48 hours	**4, 55**	2	4.2	0.005	3	5.7	0.001	4	4.9	0.002
96 hours	**4, 45**	2	3.0	0.03	3	2.7	0.04	4	1.3	ns

df = degrees of freedom
SC = source collector
F = F-statistic

Appendix Table H-3: Summary of ANOVA Results: Comparison of Burn Sites' Water Content as a Change from Control for All Time Points and Source Collectors.

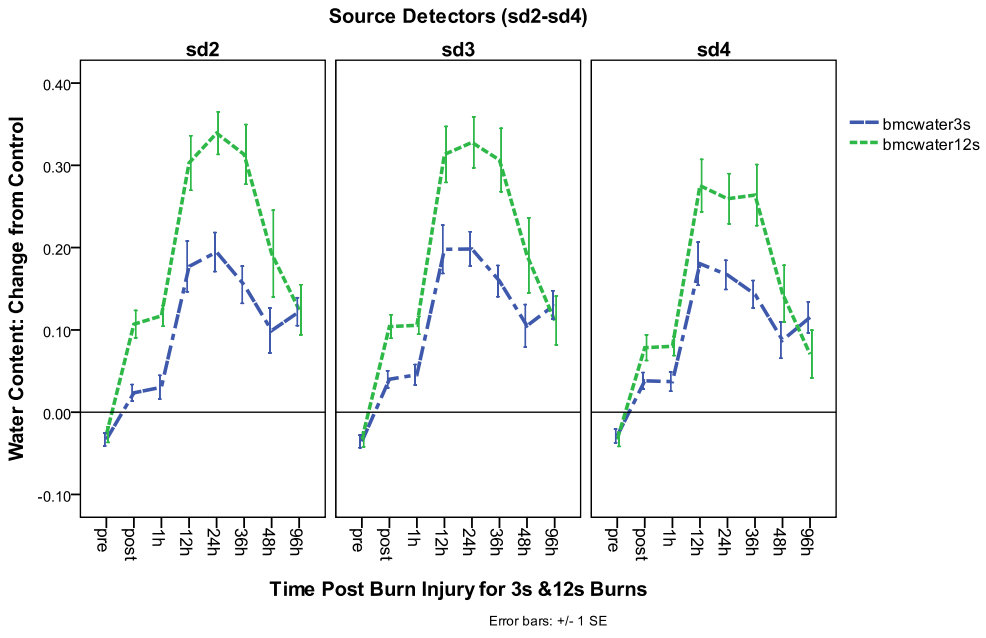

Appendix Figure H-4: Water Levels as a Change from Control within the 3 s and 12 s Burn Sites over Time

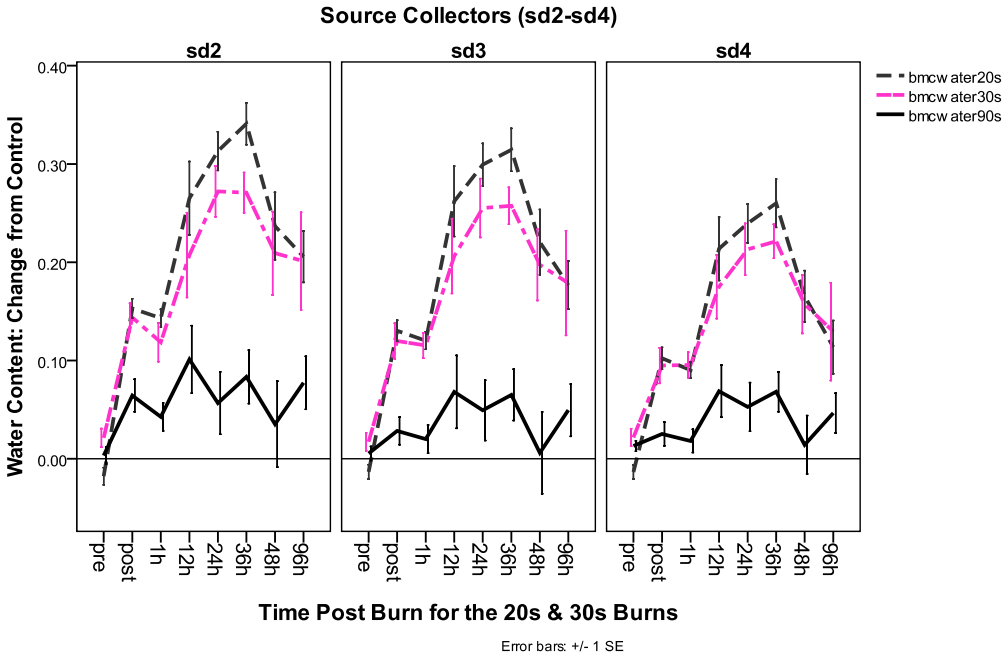

Appendix Figure H-5: Water Levels as a Change from Control within the 20 s, 30 s and 90 s Burn Sites over Time